Oligoglycerol Detergents for Native Mass Spectrometry of Membrane Proteins

Inaugural-Dissertation

to obtain the academic degree

Doctor rerum naturalium (Dr. rer. nat.)

Submitted to the Department

of Biology, Chemistry and Pharmacy

of Freie Universität Berlin

Submitted by

Leonhard Hagen Urner

From Berlin, Germany

2018

The work reported in this thesis was performed from Mai 2015 to July 2018, at the Freie Universität Berlin and the University of Oxford, under the supervision of Prof. Dr. Kevin Pagel.

1st Reviewer: Prof. Dr. Kevin Pagel

Freie Universität Berlin

2nd Reviewer: Prof. Dr. Rainer Haag

Freie Universität Berlin

Date of defense:

Danksagung

Die Zusammenarbeit mit Prof. Kevin Pagel und seiner Arbeitsgruppe haben mich motiviert zielgerichtet zu arbeiten und dazu inspiriert eigenständig neue Wege zu erkunden. Den Weg ins Unbekannte zu beschreiten kann dazu führen, dass man sich mit Dingen beschäftigt, die sich der Vorstellungskraft der gewohnten Umgebung entziehen. Für den Erfolg im Beruf reicht es daher nicht aus gute Ergebnisse zu haben, es erfordert auch viel Können sie entsprechend zu bewerten und angemessen zu präsentieren. Prof. Kevin Pagel hat mir Werkzeuge und Kontakte mit auf den Weg gegeben, um diese Herausforderungen bewältigen zu können. Er hat mir auch an entscheidenden Punkten meiner Laufbahn geholfen die Weichen für meine Zukunft zu stellen. Dafür möchte ich mich bei ihm bedanken und mit diesen Zeilen meine ehrliche und große Wertschätzung gegenüber seiner Persönlichkeit zum Ausdruck bringen.

Meine Karriere als Wissenschaftler hat weit vor meiner Doktorarbeit begonnen. Diesen Umstand habe ich unter anderem Prof. Rainer Haag zu verdanken, welcher mich schon vor meiner Bachelorarbeit mit offenen Armen in seiner Arbeitsgruppe aufgenommen hat. Seine Unterstützung als Mentor und Förderer hat mich motiviert mein berufliches Portfolio mit zusätzlichen Lehrtätigkeiten und ehrenamtlichen Aufgaben zu erweitern. Prof. Rainer Haag, Prof. Kevin Pagel, PhD Bala N. S. Thota, Dr. Olaf Nachtigall und Dr. Christian Kördel haben mir geholfen die ersten Erfolge meiner Karriere auf verhältnismäßig frühe Zeitpunkte zu datieren. Darüber hinaus haben mir die Labore und finanziellen Mittel von Prof. Rainer Haag meine präparativen Arbeiten erst ermöglicht. Ich vergleiche die Möglichkeiten, die sich aus seiner Infrastruktur ergeben haben, gerne mit denen des Garten Edens. Seine Großzügigkeit und Unterstützung habe ich nie als selbstverständlich betrachtet. Ich möchte auch seiner Persönlichkeit gegenüber meine große Wertschätzung und Dankbarkeit äußern.

Die alltägliche Arbeit im Labor und der Zusammenhalt in der Takustraße 3 waren wunderbar. Meine Kollegen im Labor 34.02 sind geniale Menschen und ich habe jeden Tag der Zusammenarbeit mit ihnen genossen. Katharina Goltsche, Marleen Selent, Marc-Philip Schweder und Dr. Monika Wyszogrodzka haben mich darin unterstützt alle Unklarheiten im Bezug zur Dendronsynthese zu bereinigen. Dank unserer Zusammenarbeit halten wir jetzt fundierte Grundlagen in den Händen, welche die Umsetzung künftiger Projekte auf der Basis von Triglycerol maßgeblich erleichtern werden. Dr. Carlo Fasting möchte ich für die unzähligen Stunden danken, in denen er mir geholfen hat die Vorteile der automatisierten Chromatographie für mich nutzbar zu machen. Mein Dank geht auch an alle Mitglieder vom Gerätezentrum BioSpuraMol, welche das Hauptrückgrat für meine erfolgreichen Synthesetätigkeiten bildeten. In den letzten drei Jahren meiner Arbeit wurden mehr als 800 NMRs und 300 Massenspektren reibungslos gemessen, mit der Hilfe von Dr. Andreas Schäfer, Anja Peuker, Gregor Dendel, H. Xuan Pham, Jana Sticht, Dr. Andreas Springer, Fabian Klautzsch, Thomas Kolrep und Maarika Bischoff. Prof. Kevin Pagel, Dr. Melanie Göth und Dr. Andreas Springer möchte ich danken für ihre Hilfe bei den Reparaturen am Ultima Massenspektrometer. Die Erfahrung in ein Massenspektrometer zu krabbeln, es zu reparieren und danach damit weiter zu messen, war legendär. Kersten Leo, Susanne Nitschke und Dirk Hauenstein aus der Materialverwaltung möchte ich für ihre Unterstützung bei der Materialbeschaffung und Entsorgung danken und die netten Small Talks beim täglichen Einkauf von Dichlormethan, Methanol und Bounty Küchenrollen.

Auch Katharina Tebel, Lydia Alnajjar, Achim Wiedekind, Jutta Hass, Dr. Wiebke Fischer, Eike Ziegler und Lisa Hummel möchte ich für die Unterstützung bei administrativen Vorgängen danken. Ohne eure Hilfe hätte es zeitweise sicherlich nicht so viel Butter auf meinen Broten gegeben. Für die Korrektur meiner schriftlichen Arbeit möchte ich mich bei Pam Winchester und Dr. Virginia Wycisk bedanken. Ich möchte auch allgemein der AG Haag, der AG Pagel und der Lunch Group für die tolle Unterstützung und Inspiration danken. Ohne das flüssige Zusammenspiel aller Mitarbeiter der Takustraße 3 wäre ich in der Kürze der Zeit nie so weit vorangekommen. Ich danke auch dem Fonds der Chemischen Industrie (FCI) und der Focus Area Nanoscale der Freien Universität Berlin für die finanzielle Förderung meiner Projekte.

Bei Prof. Carol V. Robinson möchte ich mich für die Gelegenheit bedanken ein Teil ihres Teams gewesen sein zu dürfen. PhD Idlir Liko und seine Kollegen haben mir geholfen meiner Arbeit einen Sinn zu geben. Einige eurer Leitsprüche hallen bei mir noch gut im Gedächtnis nach, z. B. *„Work hard, play hard!"* oder *"We are cowboys! Cowboys never plan! They succeed!"* Dank euch konnte ich mein serious-German-Dasein mit progressiver Gelassenheit vermischen. Durch diese Mischung erschließen sich mir heute noch neue Horizonte und ich bin besonders für die Unterstützung von PhD Idlir Liko von ganzem Herzen dankbar! Vielen Dank auch an Prof. Gert von Helden und Prof. Gerard Meijer, dass sie mir die Zusammenarbeit mit den Kollegen vom Fritz-Haber-Institut ermöglicht haben. Das waren unvergessliche und schöne Zeiten bei euch am Institut!

Mein ganz besonderer Dank richtet sich ebenfalls an alle Studenten, die ich während meiner Zeit betreuen durfte. Dabei mit inbegriffen sind Maiko Schulze, Christian Manz, Dorian Donath, Yasmine Maier, Marc-Philip Schweder, Alex Weikum und Armin Ariamajd. Ihr habt mir im Labor geholfen und dabei, sowohl euch als auch mich selbst kennenzulernen. Es war schön mitzuerleben, wie ihr über euch hinausgewachsen seid. Ihr habt eure eigenen Grenzen gefunden und überwunden. Das hat mich fortlaufend inspiriert weiterzumachen und wird auch in Zukunft eine starke Triebkraft für mich sein.

Darüber hinaus hat auch meine Familie zum erfolgreichen Verlauf meiner Doktorarbeit beigetragen. Ich möchte an dieser Stelle nun die Zühlsdorfer Gespräche am Kamin hervorheben, die mir geholfen haben die Herausforderungen von Berufsalltag und Freizeit zu relativieren und dadurch besser zu bewältigen. Gerne erinnere ich mich an ein Zitat, welches mein Stiefvater auf einem Zahnärztekongress meiner Mutter aufgeschnappt und ergänzt hat: *„Der Kopf ist oval, damit die Gedanken auch mal eine andere Richtung einnehmen können. Probleme kann man nicht mit der Denkweise lösen, mit der sie entstanden sind (Autor unbekannt)."* Ich kann diesen Sätzen nur wie folgt entgegnen: *„Als ich Sehen lernte, begriff ich erst, wie blind ich war."* Für unsere gemeinsame Zeit und eure Unterstützung danke ich euch von ganzem Herzen. Das gilt natürlich auch für den Rest meiner Familie und Gosener Gespräche sind damit auch inbegriffen.

Mein Dank richtet sich auch an alle Petes und Bobbies. Neben Ehrgeiz und Tatkraft, braucht es manchmal eben auch etwas Zerstreuung, um den Zug mit Volldampf rollen zu lassen. Der Weg der Nachhaltigkeit ist kurzfristig manchmal unbequem und zahlt sich oft erst auf lange Distanz aus. Dr. Olaf Nachtigall hat mich immer bestärkt in Sachen Nachhaltigkeit keine Abstriche zu machen. Ich hoffe wir werden auch in Zukunft noch den einen oder anderen Plausch abhalten. Ich darf mich zudem glücklich schätzen mit Dr. Virginia Wycisk eine starke Weggefährtin für mein Leben gefunden zu haben und ich bin gespannt was die Zukunft für uns bereithält.

Zusammenfassung

Membranproteine sind ein essentieller Bestandteil von biologischen Membranen. Sie tragen maßgeblich zur Regulierung von physiologischen Prozessen bei und bilden deshalb einen wichtigen Anhaltspunkt bei der Entwicklung von neuen Medikamenten. Verschiedene biophysikalische Methoden wurden entwickelt, um die dreidimensionale Struktur von Membranproteinen zu untersuchen. In diesem Zusammenhang haben Detergenzien eine besondere Bedeutung, denn sie können dabei helfen Membranproteine unter Erhalt ihrer nativen Struktur zu isolieren. In den vergangenen Jahren wuchs das Interesse an der Strukturuntersuchung von isolierten Membranproteinen mittels nativer Massenspektrometrie (MS). Diese Technik liefert Informationen über Masse und Zusammensetzung von komplexen Membranproteinen und ermöglicht die Untersuchung von Wechselwirkungen zu wichtigen Liganden, wie z. B. Medikamenten, Nukleotiden oder Lipiden. Die in diesem Zusammenhang bisher untersuchten Detergenzien bieten entweder vorteilhafte Eigenschaften für die Isolierung von Membranproteinen oder für deren Untersuchungen mittels nativer MS.

In der vorliegenden Arbeit wurde die Fragestellung adressiert, ob es möglich ist die molekulare Struktur von Detergenzien für beide Anwendungsgebiete zu optimieren. Dafür wurde erstmalig das Potential von dendritischen Oligoglycerol-Detergenzien (OGDs) evaluiert. Für diesen Zweck wurde eine Substanzbibliothek aufgebaut, indem einzelne Strukturparameter der OGDs systematisch variiert wurden. Um die generelle Anwendbarkeit von OGDs für die MS-Analyse von Proteinen zu evaluieren, wurden im nächsten Schritt Mischungen von löslichen Proteinen und OGDs mittels MS untersucht. Beobachtungen führten zu der Hypothese, dass sich Ladungszustände von Proteinen durch die Basizität der OGDs steuern lassen. Weiterführende Studien mit dem trimeren Membranprotein OmpF untermauerten diese Hypothese und bestätigten darüber hinaus die Anwendbarkeit von OGDs für die Analyse von Membranproteinen mittels nativer MS. In einer weiteren Studie wurde mit Hilfe von fünf verschiedenen OGDs und vier verschiedenen Membranproteinen gezeigt, wie sich durch Variationen in der OGD-Struktur wichtige Aspekte individuell steuern lassen, z. B. die Isolierung von Membranproteinen, Ladungsreduktion und die Möglichkeit Komplexe zwischen Membranproteinen und Lipiden zu detektieren. Darüber hinaus ermöglichten OGDs die einfache MS-Analyse von einem G-Protein-gekoppelten Rezeptor, welche derzeit eine der am schwierigsten zu untersuchenden Proteinfamilien ist und dessen Struktur von außerordentlicher pharmakologischer Bedeutung ist.

Die vorliegenden Ergebnisse zeigen, wie sich die molekulare Struktur von OGDs für die Isolierung von Membranproteinen und nativer MS-Anwendungen optimieren lässt. Darauf aufbauend lassen sich neue Detergenzien entwickeln, welche in Zukunft die Untersuchungen von Membranproteinen erleichtern können.

Abstract

Membrane proteins are associated with biological membranes and fulfill functions that are vital for all living organisms. They mediate many physiological processes and are therefore important targets for the development of new pharmaceutical drugs. Numerous biophysical approaches have been developed that address the elucidation of their three-dimensional structure upon isolation. In this context, detergents are important tools, because they can isolate and stabilize membrane proteins apart from their native host. In recent years there has been a growing interest in studying the structure and dynamics of isolated membrane protein complexes by native mass spectrometry (MS). This technique can provide information about the mass and composition of a membrane protein complex and allows one to study interactions with structurally relevant ligands, such as drugs, nucleotides, or lipids. Detergents that are suitable for native MS do not only require solution conditions appropriate for membrane protein isolation but also gas-phase properties that help to retain native protein structures and their non-covalent interactions in the vacuum of a MS instrument. However, detergent families that are currently available can facilitate either the isolation of membrane proteins or their analysis by native MS.

This thesis addresses the question, how one can optimize the molecular structure of a detergent family for membrane protein isolation and individual applications in native MS. With this regard, the utility of dendritic oligoglycerol detergents (OGDs) was evaluated, which have not yet been used in membrane protein research. For this purpose, a highly systematic OGD library was constructed by systematically changing the structure of these detergents. In order to prove their general utility for protein MS, mixtures between soluble proteins and OGDs were analyzed by native MS. Data obtained from the soluble protein ß-lactoglobulin (BLG) indicated that protein charge states can be manipulated by tuning the basicity of these detergents. A comparative study between BLG and the membrane protein OmpF revealed the validity of this design criterion and demonstrated for the first time the utility of OGDs for native MS of membrane proteins. Moreover, with a set of five different OGDs and four membrane proteins it was examined, how crucial aspects, such as membrane protein isolation, charge states, and the ability to detect binding with structurally relevant membrane lipids could be independently optimized by altering the OGDs' molecular structure. Furthermore, these detergents enabled the easy MS analysis of a G protein-coupled receptor protein (GPCR), which is one of the most challenging and most important protein families in pharmacology.

The obtained results open new avenues for the future development of detergents that cover optimal properties for membrane protein isolation and native MS applications.

Table of Contents

1. Introduction

Membrane proteins are one of the most fascinating classes of proteins in biology. They are located at the interface between two opposing environments, such as lipid membranes and their aqueous surrounding, and fulfill functions that are crucial for life of every organism.[1] Most membrane proteins function as communication gates or transport systems. In particular, they mediate signaling pathways across biological membranes and enable the interconversion between different forms of energy, which enables, for example, the provision of adenosine triphosphate (ATP) – the universal energy source in living cells.[2] Furthermore, membrane proteins are targets for more than 50% of all modern drugs.[3] Elucidating the membrane proteome is therefore of enormous interest in structural biology and medicinal chemistry.

Approximately 26% of human protein-coding genes correspond to membrane proteins and more than 800 unique membrane protein structures have been reported until today.[4, 5] Nuclear magnetic resonance (NMR),[6] X-ray crystallography,[7] small-angle neutron scattering (SANS),[8] electron microscopy (EM) techniques,[9] and gel-filtration techniques[10] are traditionally used for the structural investigation of membrane proteins and provide information about their three-dimensional structure and dynamics. All here-mentioned techniques require the use of membrane mimetica that keep the membrane protein ideally in a native and soluble state upon extraction from biological membranes. The isolation of membrane proteins is traditionally achieved with detergents, whose aggregates can preserve the native protein structure apart from its native host environment. The detergent's capability of preserving native protein structures remains protein specific and suitable detergents are identified empirically. Conventional condensed phase techniques, however, require comparatively large sample amounts, provide long measuring cycles and are not yet suitable for efficient high-throughput screenings.

An emerging technique that has the potential to overcome these limitations is native mass spectrometry (MS).[11] As such, MS techniques provide fast acquisition cycles, are very sensitive and therefore low sample consuming.[12] Protein-detergent mixtures can be ionized and transferred into the vacuum of a MS instrument, where the controlled removal of the detergent environment ideally leads to the release of intact membrane protein complexes.[13] The chemical nature of detergents influences the ease of the detergent removal and the charge states of the released protein ions.[14] Gentle activation conditions and low protein charge states are highly desired, because they reduce the impact of Coulomb-driven protein unfolding and support the preservation of natively folded states.[15-17] So-obtained mass spectra can provide information about the mass of a membrane protein complex, its subunit composition, or interactions with structurally relevant ligands, such as drugs, nucleotides, and lipids.[11, 13, 18] A more recent breakthrough came with the demonstration that the impact of co-purified membrane lipids on the structure and function of membrane proteins can be studied by MS techniques.[18, 19] The choice of the detergent alters the extent of lipid co-purification during protein isolation and can therefore dictate the success of the intended native MS application.[20] Furthermore, native MS allows one to estimate the compatibility between membrane proteins and detergents.[13] The valuable set of information, which can be gained from native MS experiments, can usefully complement the structural investigation of membrane proteins with other biophysical techniques.

1.1 Motivation

The emerging importance of native MS as a complementary tool for the structural elucidation of membrane proteins has raised the demand for new detergents.[21] Detergents that are suitable for native MS meet high expectations. They ideally need to provide not only favorable solution properties, which allow one to preserve native protein structures in solution, but also gas-phase properties that allow one to transfer and release native membrane proteins into the vacuum of a MS instrument. Favorable solution properties include the ability to extract membrane proteins from membranes under non-denaturing conditions and the ability to control lipid co-purification from biological membranes.[20] On the other hand, gas-phase properties that facilitate the structural analysis of membrane proteins include charge reduction and gentle release conditions for the detergent removal.[14-17] Available guidelines that help to estimate solution and gas-phase parameters of detergents regarding their molecular structure are kept very general.[14, 20] The ability to adjust the structure of a detergent to the scope of the experiment would clearly facilitate the investigation of the membrane proteome.

During the past 20 years, a new family of dendritic oligoglycerol detergents (OGDs) has been developed, which has not yet been considered for membrane protein research.[22] These detergents consist of a dendritic triglycerol head group and a variable hydrophobic tail, which are held together by a linker (Figure 1.1). The molecular architecture of OGDs is highly modular and today's available synthetic protocols allow one to systematically exchange individual detergent building blocks, which is a valuable perquisite for structure-property studies. The potential of OGDs for the application-oriented optimization of their molecular structure has been successfully demonstrated in the cases of surface coatings against bioadhesion,[23-25] dye labels for optical imaging on biological samples,[26, 27] and various drug delivery applications.[28, 29]

1.2 Outline

This thesis evaluates the potential of OGDs for the analysis of membrane proteins by native MS and if the modular architecture of these detergents can be optimized for the isolation and native MS analysis of membrane proteins. In particular, this thesis addresses the structural optimization of OGDs for membrane protein isolation, charge reduction and the ability to detect protein complexes formed with co-purified membrane lipids by MS.

The first part of **Chapter 2** gives an overview about the general utility of detergents for isolating membrane proteins. It summarizes the present knowledge about how the detergent's protein compatibility in solution can be estimated in relation to its molecular structure, different detergents classes, and alternative membrane mimetica. In the second part of this chapter, an introduction into native MS of membrane proteins is given and relevant detergent parameters are discussed. Finally, the family of OGDs is introduced, which has not yet been considered for membrane protein research and whose potential for membrane protein purification and individual native MS applications is evaluated throughout this thesis.

The utility of detergents for native MS experiments on membrane proteins depends on the chemical properties of the detergent's head group, hydrophobic tail, and linker. To explore if OGDs would allow one to adjust the detergent structure for a range of native MS experiments, a bottom-up strategy was applied. For this purpose, in **Chapter 3**, the synthesis of a new modular OGD library is presented, which covers systematic structural variations in head group, linker, and tail (Figure 1.1). Furthermore, a new synthesis concept is introduced that leads to the obtainment of OGD regioisomer mixtures.

Chapter 4 discusses the general utility of OGDs for the native MS analysis of proteins. With a set of six OGDs and four proteins, it is shown how the propensity of OGDs to promote protein charge reduction can be controlled by tuning the molecular structure of these detergents (Figure 1.1).

Chapter 5 evaluates whether OGDs can extract membrane proteins from biological membranes and control lipid co-purification. The results presented in this chapter show how protein isolation, charge reduction, and the ability to detect protein complexes formed with co-purified membrane lipids by native MS can be independently controlled by tuning the molecular structure of OGDs (Figure 1.1). Furthermore, the benefit of using OGD regioisomer mixtures over individual OGD regioisomers for membrane protein extraction is discussed. Furthermore, it is discussed if OGDs can enable the easy native MS analysis of G protein-coupled receptors (GPCRs) – a membrane protein family that accounts for nearly 40% of current drugs.[30] The data obtained during the last two chapters underline the enormous potential of OGDs for the isolation and native MS analysis of membrane proteins.

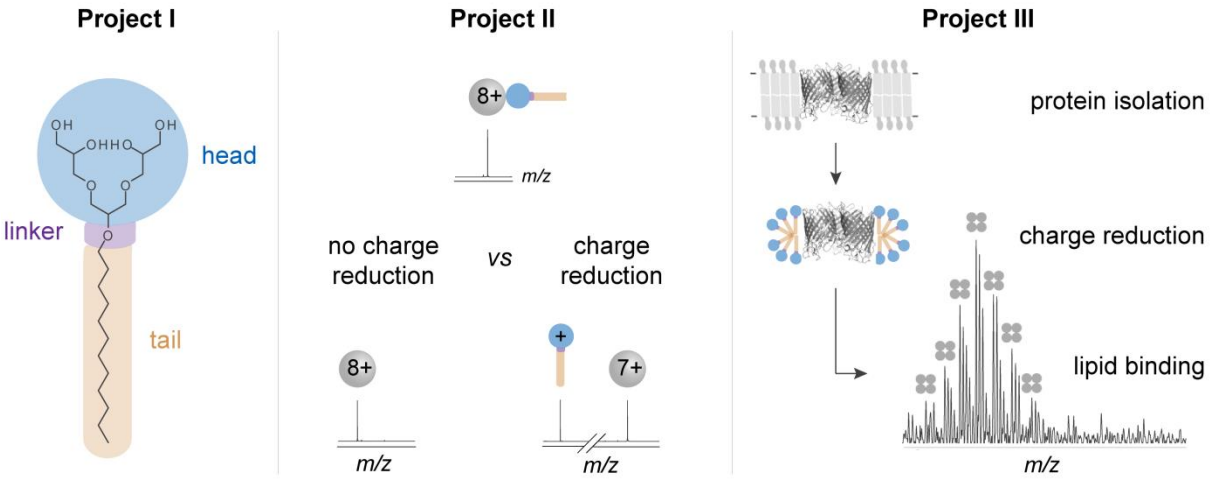

Figure 1.1: Evaluating the utility of OGDs for optimizing membrane protein purification and individual native MS applications. In the first project, the synthesis of a new OGD library is presented, which covers systematic structural variations with respect to the head group, linker and tail. In the other two projects, it is discussed how one can optimize protein isolation, charge reduction and lipid binding on-demand by tuning the molecular structure of these detergents.

2. Fundamentals

2.1. Detergents for Isolating Membrane Proteins

Detergents are indispensable tools for the structural investigation of membrane proteins and are traditionally used for their isolation from biological membranes. The general structure of detergents is reminiscent of lipids, which consist of a polar (water soluble) head group and a non-polar (water insoluble) tail that are held together by a linker group (Figure 2.1). In contrast to lipids, detergents have comparatively large hydrophilic head groups, small hydrophobic tails, and are therefore soluble in aqueous systems. Driven by the hydrophobic effect,[31, 32] detergents tend to aggregate in aqueous solution when a certain concentration threshold is exceeded – the so-called *critical aggregation concentration* (*cac*).[33] Depending on their molecular structure, concentration, solution environment, and temperature, detergents self-assemble into a variety of nanostructures, including micelles, rods, worm-like micelles, vesicles, tubes, and lamellae structures.[22, 34] Using this knowledge, Isrealachvili *et al.* developed a model-based theory that helps to explain the aggregate morphology by considering the geometrical considerations of the detergent's hydrophobic and hydrophilic building blocks.[35] The amphiphilic nature of detergent aggregates is reminiscent of self-assembled lipid bilayers, which is an important requirement for the detergent's utility to solubilize membrane proteins in the absence of biological membranes (Figure 2.1).[36]

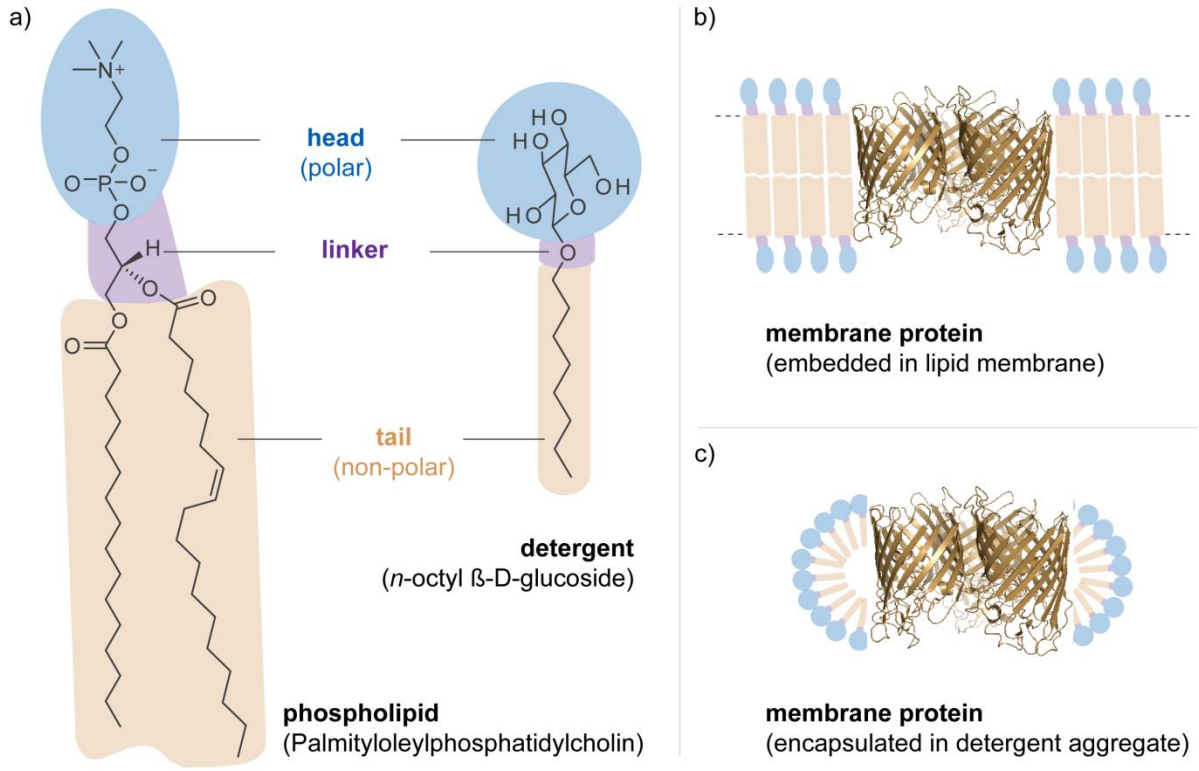

Figure 2.1: The structure of lipids, detergents, and their aggregates formed with membrane proteins. a) The molecular structure of lipids and detergents consist of a polar head group and a non-polar tail, which are hold together by a linker. b) – c) Membrane proteins are either embedded within water-insoluble cellular membranes or can be obtained in a water-soluble state upon encapsulation into detergent aggregates.

The transfer of membrane proteins from lipid membranes into detergent aggregates is generally referred to as protein extraction (Figure 2.2). Purified membrane proteins that are encapsulated in detergent aggregates are soluble in aqueous media and can be analyzed by common biophysical techniques, such as NMR spectroscopy, X-ray crystallography, SANS, EM, or native MS.[6-9, 13] However, no universal detergent is available that is capable to preserve the native structure of every membrane protein and that is compatible to every biophysical technique at once. This requires testing of different detergents, which can be readily achieved by gel-filtration experiments (Figure 2.2).[10] It is thereby important to mention that a detergent that is suitable to solubilize a protein upon detergent exchange must not be suitable for membrane protein extraction. The same is true for the detergent's compatibility to individual biophysical techniques. For example, a detergent that is suitable for X-ray crystallography must not be suitable for native MS applications. Therefore, when choosing a detergent one needs to consider not only the compatibility between membrane protein and detergent, but also the scope of the experiment (Figure 2.2).[37]

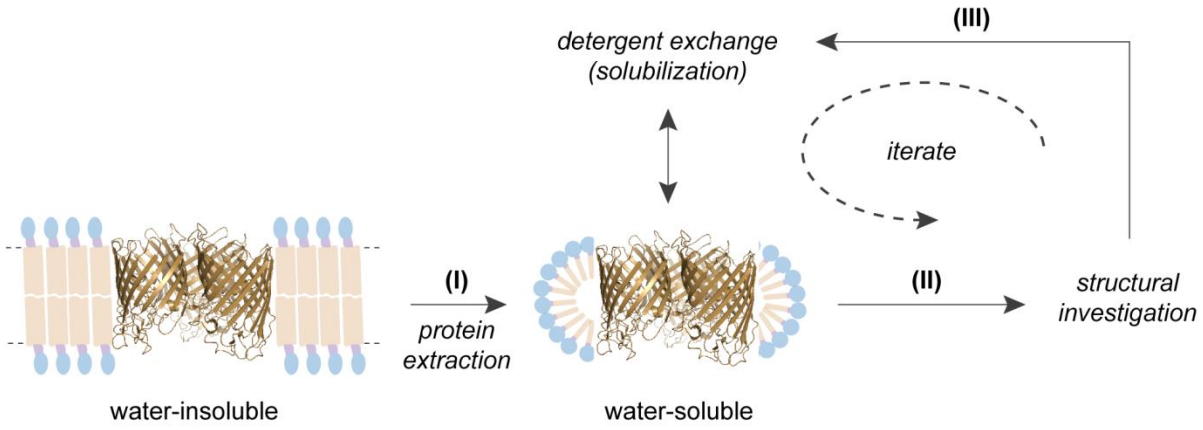

Figure 2.2: The utility of detergents for isolating and analyzing membrane proteins. (I) Detergents are used for dissolving membranes and extracting membrane proteins. The detergent environment increases the solubility of membrane proteins in aqueous solution. (II) The structure of solubilized membrane proteins can be analyzed by different biophysical techniques. (III) Unsuitable detergent environment is exchanged and the new sample is analyzed again.

2.2.1 Dissolution of Biological Membranes

Biological membranes are insoluble in water and comprise a diverse content of lipids and proteins. The heterogeneity of biological membranes usually hampers the structural investigation of membrane proteins within their native environment.[38, 39] Many biophysical tools are tailored for the investigation of purified membrane proteins.[21] In this context, detergents have significantly driven membrane protein research. They are used for membrane protein extraction and solubilization, which is a perquisite for the application of many biophysical techniques.[20, 40, 41] Many detergents effectively dissolve lipid membranes and solubilize membrane proteins during extraction; not all of them preserve the native structure of membrane proteins.[20, 40, 41] A detergent that can prevent a membrane protein from losing its structure and function is generally denoted as "non-denaturing" to a respective protein. The compatibility between a protein and a detergent, however, remains protein specific and needs to be evaluated for every detergent that has not been tested before.

Because detergents are important for the isolation of membrane proteins, the detailed mode of interaction with biological membranes has been extensively studied.[42-46] Primary work on this research area was focused on investigating the dissolution of lipid vesicles in solution as a function of the detergent concentration (Figure 2.3). For the detergent-induced dissolution of lipid vesicles a three-stage hypothesis was proposed:[42-45] First, detergent molecules are taken up at low concentrations by the lipid bilayer. Second, the saturation of the lipid bilayer with detergent molecules at higher concentrations creates a phase transition resulting in a transformation of lipid-detergent vesicles to lipid-detergent micelles. Third, the phase transition reaches an end point and the solubilization of the lipid vesicle is completed.

Kragh-Hansen *et al.* finally confirmed the validity of the three-stage hypothesis for describing the solubilization of protein-containing membranes.[46] The three-stage hypothesis was complemented by four transition phases (a – d, Figure 2.3): In the first phase (a), the protein-containing lipid bilayer takes up the detergent and they are randomly distributed across the membrane. In phase (b), the detergent concentration within the membrane reaches a critical point at which the detergents begin to interact cooperatively. As a consequence, large membrane fragments are formed, which are sealed at the edges by detergent assemblies, but no solubilization occurs at this point. In phase (c), above a detergent concentration which is called the *critical solubilization concentration* (*csc*), lipid- and protein-containing membrane units become solubilized in form of mixed aggregates, for example, micelles composed of lipids, proteins, and detergents. In phase (d), only mixed aggregates are present. Kragh-Hansen *et al.* confirmed that the solubilization of membrane proteins can be achieved at detergent concentrations below the detergent's *cac* (Figure 2.3).[46] Detergent concentrations that are nowadays practically applied for membrane protein extraction, however, lay typically above the detergent's *cac* and even higher detergent concentrations (~ 1w%) are used for the dissolution of biological membranes.[13, 14]

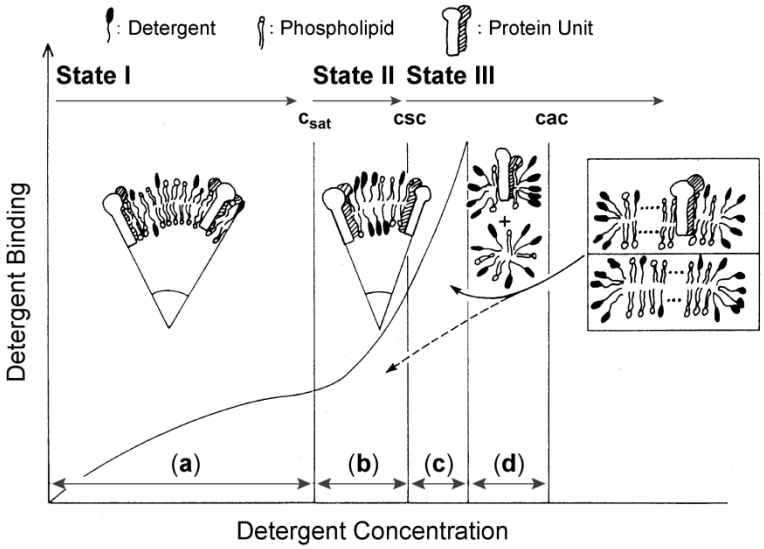

Figure 2.3: Overview of different states (I – III) and transition phases (a – d) that are encountered in solubilizing protein-containing membranes at different detergent concentrations. Further explanations can be found in the text above. The image was adapted from reference[46] with the permission of the American Chemical Society (Copyright 1993).

2.1.2 Classification of Detergents

Membrane proteins are prone to denaturation during the dissolution of biological membranes when high detergent concentrations are used. The perturbation of the native membrane protein structure has several causes: Detergents have a known propensity to substitute the natural lipid belt of membrane proteins, when high detergent concentrations are applied.[20, 40, 41] Lipids are key regulators for the oligomerization of membrane protein subunits. Furthermore, interactions between lipids and surface-exposed amino acids can significantly stabilize the three-dimensional structure of membrane protein complexes.[19, 47] The detergent's propensity to delipidate membrane proteins is therefore proposed as a major drawback for maintaining the native protein structure during extraction from biological membranes.[40, 41] Moreover, detergents can disturb hydrophobic and hydrophilic inter- and intramolecular protein interactions, which can destabilize the three-dimensional structure of a protein. In particular, ionic and zwitter-ionic detergents exhibit an enhanced propensity to disturb structurally relevant salt bridges.[48] Moreover, the lateral pressure, water content, and alkyl chain packing of native membranes are poorly duplicated in a detergent-solubilized state.[21]

Although it is generally well understood how the molecular structure of detergents causes protein denaturation, no precise design criteria are available yet that allow manipulating the detergent's protein compatibility on-demand. The number of different detergent structures published in literature is huge and overviews are given in different review articles.[20, 37, 40, 41] Throughout the following paragraphs, only a small selection of these detergents will be briefly introduced and discussed concerning their utility for membrane protein research.

Detergents can be generally classified according to the charge of their head group and are divided into four classes, such as non-ionic, cationic, anionic, and zwitterionic (Figure 2.4). Non-ionic detergents, such as saccharide or polyethylene glycol detergents, are most commonly used for protein purification (Figure 2.4).

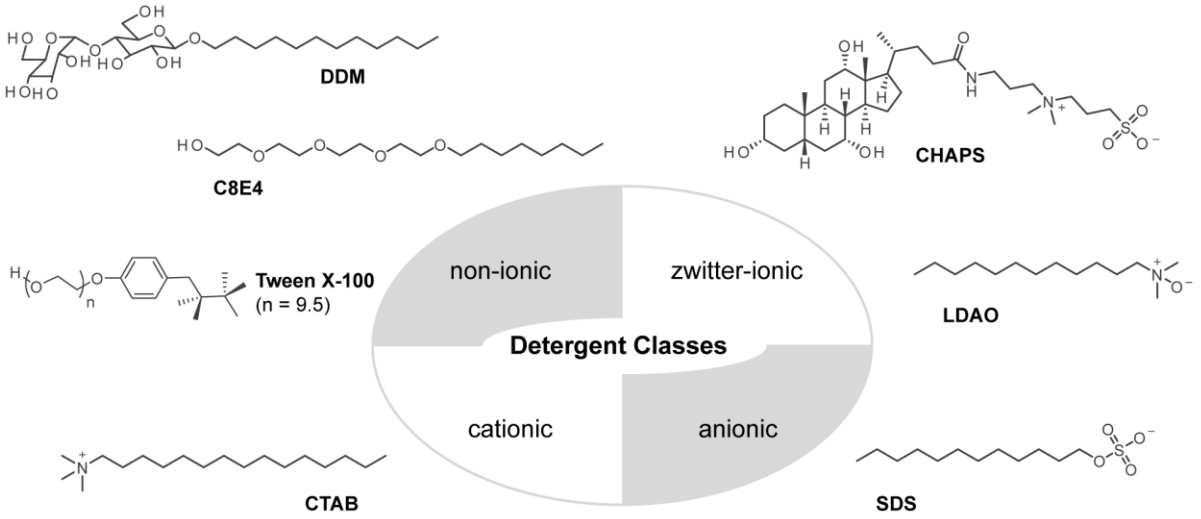

Figure 2.4: Overview of detergent classes that have been utilized for the purification and structural analysis of membrane proteins. The detergents are classified according to the charge of their head group as non-ionic, cationic, anionic, or zwitterionic detergents.

The popularity of saccharide detergents relies on the fact that they are effective in protein extraction and that they are non-denaturing enough to maintain functional states of many proteins.[20, 40, 41] Prominent examples are *n*-octyl ß-D-glucoside (OG) and *n*-dodecyl ß-D-maltoside (DDM). The majority of available membrane protein crystal structures has been solved with these detergents.[20] Other non-ionic polyethylene detergents, for example, C8E4, Brij®, Nonidet®, Triton®, or Tween X-100®, do not usually denature membrane proteins as well.[37, 49, 50] Except for C8E4, the main drawback of these detergents relies on their absorption properties in the UV range, which can interfere with protein concentration analysis by UV/VIS spectroscopy.[37] Furthermore, divalent cations, such as Fe^{2+}, Ca^{2+}, and Co^{2+}, can promote precipitation of these detergents.[37, 51]

Secondly, anionic and cationic detergents, for example, sodium dodecyl sulphate (SDS) and hexadecyltrimethylammonium bromide (CTAB), usually denature proteins (Figure 2.4). Their aggregation properties and solubility strongly depend on the salt content in solution and these detergents disturb salt bridges within the protein backbone that are crucial for membrane protein's structure and function.[48] Only a few membrane proteins have been successfully investigated with these detergents and they are less commonly used for the purification of membrane proteins.[52]

Thirdly, zwitterionic detergents, such as lauryldimethylamine oxide (LDAO), *n*-dodecyl phoscholine (Fos-Choline 12), or 3-[(3-cholamidopropyl)-dimethylammonio]-1-propanesulfonate (CHAPS), contain both a positive and a negative charge in their head group and exhibit intermediate denaturing properties (Figure 2.4).[37, 41] Michel *et al.* estimated that approximately 20% of all membrane proteins are stable enough to resist against the denaturing effects of LDAO.[20, 52] Phospholipid-like detergents, such as *n*-dodecylphoscholine (Fos-Cholin 12), have attracted much attention in recent years, because they can help to maintain functional states of GPCRs,[53-55] which is a challenging membrane protein family that accounts for nearly 40% of all current drugs.[30] Zwitterionic detergents are most successfully used for structural investigation of a few membrane proteins by NMR spectroscopy and X-ray crystallography.[20, 40, 41]

Gilbert G. Privé compared the protein compatibility behavior of the individual detergent classes and concluded general guidelines that help to estimate the denaturing properties of a particular detergent in relation to its molecular structure (Figure 2.5).[20] The general tendency of a detergent to denature membrane proteins can be understood by considering the structure of the polar head group and the length of the alkyl spacer.[20, 40] Non-ionic detergents, for example, that comprise a large head group and long alkyl spacers are non-denaturing (mild), while ionic detergents with a small head group and a short alkyl spacer are denaturing (harsh, Figure 2.5). The optimal length of linear alkyl spacers was thereby proposed to be 12 – 14 carbon atoms long.[20, 40] However, no general specifications for alternative hydrophobic motives, like cholesterol or branched chain architectures or specific head group structures, are available so far. The qualitative estimations made by Gilbert G. Privé fit very well to the behavior of detergent families that are most commonly applied in membrane protein research (Figure 2.5). He also stated that the estimations drawn from these detergent guidelines might not apply for all protein-detergent combinations and that exceptions to these estimations might be found in particular cases.[20]

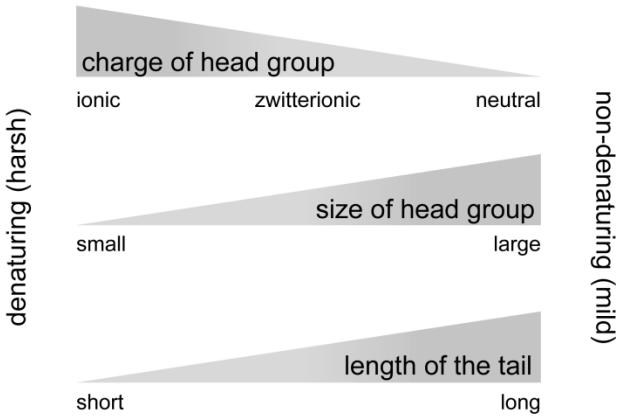

Figure 2.5: General design considerations proposed by Gilbert G. Privé that help to estimate the detergent's denaturing properties in relation to its molecular structure. The image was adapted from reference[20] with the permission of Elsevier (Copyright 2007).

2.1.3 Alternatives to Detergents

To overcome the general limitations that are associated with the use of detergents for the structural investigation of membrane proteins, many different alternative systems have been explored. An emerging class of molecules whose potential for membrane purification has been explored during the last decades are hemifluorinated surfactants (HFSs), which contain a hydrophilic head group and a (partially) fluorinated hydrophobic tail (Figure 2.6).[56] Fluorinated hydrocarbon chains exhibit a low miscibility with hydrocarbons, in line with their low propensity to dissolve biological membranes. However, HFSs are well suited for detergent exchange experiments and can be used as alternatives to classic detergents for the solubilization of membrane proteins, as confirmed for bacteriorhodopsin, cytochrome b_6f, and the bacterial outer membrane protein A (OmpA).[57-59] Compared to classic detergents, the use of HFSs can enhance the protein stability in solution. Cytochrome b_6f, for example, was found to be more stable when it was transferred from saccharide detergents to a HFS called C2-H5C6F12C2H4-S-poly-tris-(hydroxymethyl)-aminomethane (HF-TAC, Figure 2.6).[58] Due to the low miscibility between fluorinated chains and hydrocarbons, HFSs most likely exhibit a lower propensity to delipidate membrane proteins. They are therefore suggested to promote a better retention of structurally relevant lipids on protein surfaces, which in turn can stabilize the native structure of membrane proteins.[58] The synthesis of HFSs is very expensive. Their limited availability together with the high synthetic costs hampers the preparation of large HFS batches, which are required for detergent exchange experiments.[56, 60]

Another class of molecules that make it possible to handle membrane proteins in a detergent-free environment are amphipols (Figure 2.6).[60-62] These systems are hydrophilic polymers that are grafted with hydrophobic chains, which introduces amphiphilic character into their molecular structure. They can form stable complexes with a broad range of more than 30 different membrane proteins in solution.[60] Membrane protein that have been solubilized with amphipols comprise molecular masses of more than 1 MDa.[60-62]

Contrary to detergents, amphipols disperse membranes into large lipid-polymer aggregates.[63] Their propensity to delipidate membrane proteins is therefore lower than that of detergents, which can improve membrane protein stability upon isolation. They have been explored for NMR, EM, and native MS experiments, but are not well-suited yet for membrane protein crystallization.[60, 62]

Another alternative are lipopeptides (LPD), which were designed to mimic the lipid environment. LPDs consist of a 25-amino-acid-long alpha helical peptide monomer and their ends are functionalized with fatty acid moieties.[64, 65] The length of LPDs is akin to the thickness of biological membranes (Figure 2.6).[64] The alpha helix exhibits facial amphiphilic character, because it comprises a hydrophobic inner side consisting of alanines and a hydrophilic outer side made of polar amino acids.[64] Like HFSs, LPDs are expensive to produce and are not suitable for protein extraction.[65] They are effective in protein solubilization and their potential for NMR studies and X-ray crystallography is still under investigation.[65]

Another alternative system that has attracted attention for the structural investigation of membrane proteins are bicelles.[66] They consist of a lipid bilayer segment that is surrounded by a belt of detergents. Bicelles can be readily formed by adding detergents to protein-containing lipid bilayers. Their structure is similar to lipid membranes, which makes them to promising tools for studying lipid-protein interactions. However, not all proteins are able to self-assemble into stable bicelles. Therefore, membrane scaffold proteins (MSPs) were developed, which enable the reconstitution of membrane proteins into stable nanodiscs.[67, 68] Compared to bicelles, nanodiscs consist of a phospholipid bilayer core that is stabilized at its edges by a MSP. Bicelles and nanodiscs are used for studying membrane proteins by EM, NMR, X-ray crystallography, and native MS.[21, 66-71] However, they still require the use of detergents as they cannot be directly applied for extracting membrane proteins.

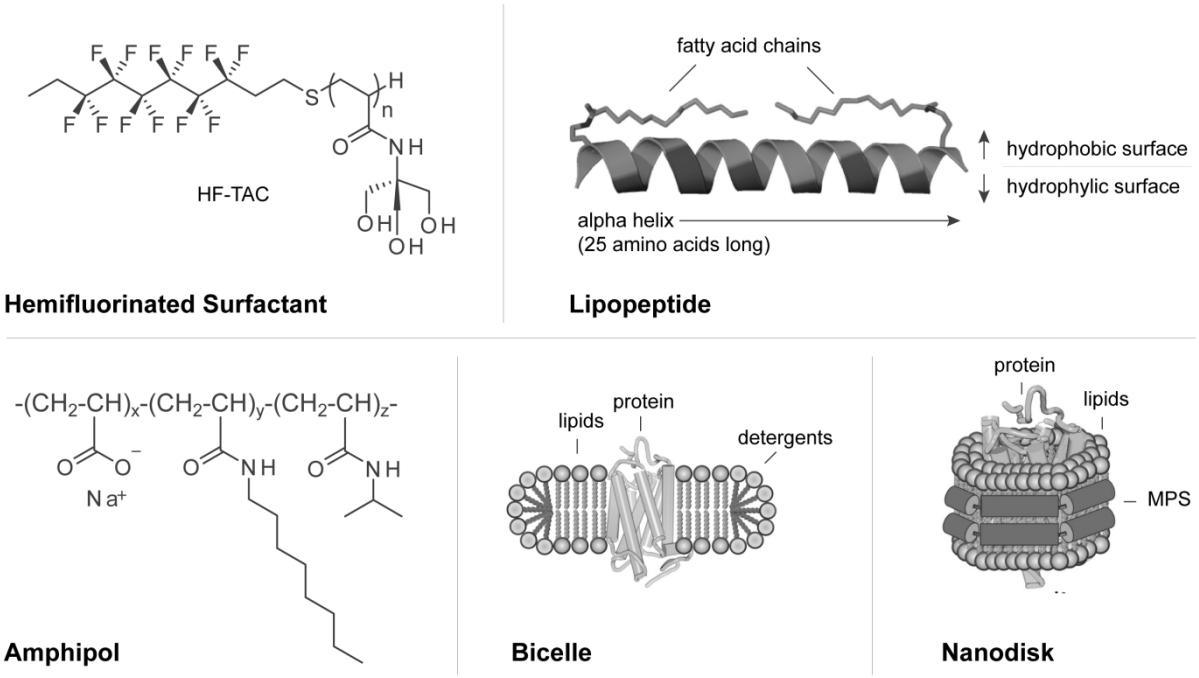

Figure 2.6: An overview about alternatives to detergents, which can be used for the structural investigation of membrane proteins.

2.2 Analysis of Membrane Proteins by Native Mass Spectrometry

Over the past 30 years, native mass spectrometry (MS) has contributed to the foundation of new research fields, including proteomics and metabolomics, and provided new tools that are complementary to condensed phase techniques. In native MS, molecules are ionized and transferred into the vacuum with the aim to maintain non-covalent interactions from native solution species. In particular, native MS on membrane proteins allows one not only to investigate the protein structure itself but also interactions with small molecules, such as drugs, nucleotides and lipids.[11] The dielectric constant of hydrophobic lipid bilayer compartments is close to that of vacuum. In the 1990s, it was therefore discussed if vacuum could be a good mimic for the native host environment of membrane proteins.[72] Experiments of Ilag *et al.* and Lengqvist *et al.* confirmed that membrane proteins can indeed be transferred and analyzed in the vacuum of a MS instrument.[73, 74] However, there was still a question if solution interactions between protein subunits or to small molecules can be maintained.

A breakthrough came in 2008 with the first demonstration that a heteromeric adenosine 5´-triphosphate (ATP)–binding cassette transporter ($BtuC_2D_2$) could be transferred intact into the vacuum of a MS instrument.[75] The results obtained by Barrera *et al.* revealed for the first time that interactions of transmembrane subunits, cytoplasmic subunits, and also non-covalent interactions of membrane proteins to small molecules, such as ATP or lipids, could be analyzed by MS. Mass spectra of membrane proteins report on molecular masses, oligomeric states, the composition of native subunits, and binding events to structurally relevant ligands,[13, 18] which make native MS a valuable and complementary technique for applications in proteomics and metabolomics. Amongst other factors, these first remarkable results were enabled by the use of detergents.[73-75] Their aggregates turned out to be able to protect the structure of membrane protein complexes not only in solution but also during their transport into the vacuum and ionization.[75] The following sub-chapters summarize instrumental backgrounds, opportunities, and limitations that arise from native MS on membrane proteins as well as the properties of detergents classes that have driven this emerging research field.

2.2.1 Electrospray Ionization

A typical MS instrument consists at least of three parts: (1) ion source, (2) mass analyzer, and (3) detector (Figure 2.7).[76] The transport of membrane proteins into the vacuum of a MS instrument is commonly achieved by an ionization source. Apart from less common methods, such as laser-induced liquid bead ion desorption (LILBID)[77] or desorption electrospray ionization (DESI),[78] techniques based on electrospray ionization (ESI) are today most commonly used for native MS experiments on membrane proteins.[11]

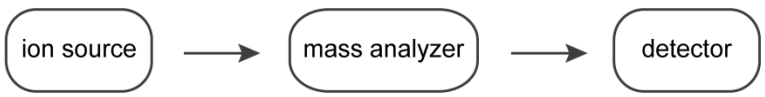

Figure 2.7: Schematic overview about the basic parts of a MS instrument.

An ESI source requires a conductive capillary with a diameter of 0.1 – 0.2 mm (Figure 2.8). The capillary is connected to a syringe that is loaded with liquid analyte. Driven by a syringe pump, the liquid is pressed through the capillary with flow rates of about 1 – 20 µL/min. The capillary exit is placed towards the entrance of the MS instrument and a high voltage of about 1 – 6 kV is applied. The strong electric field causes charge separation inside the liquid.[79] According to the polarity shown in Figure 2.8, negatively charged ions travel to the wall of the capillary, while positively charged ions travel to the exit of the capillary. Due to accumulation of charges at the capillary exit, a so-called Taylor cone is formed,[80] from which charged droplets with sizes in the micrometer range are emitted. They traverse to the entrance of the MS instrument, solvent evaporates until the surface charge density reaches the Rayleigh-limit, and the droplets undergo Coulomb fissions.[79] This leads to the formation of smaller electrospray (ES) droplets. The miniaturized version of ESI is nanoelectrospray ionization (nESI).[81] Instead of the above-described conductive capillaries, metal-coated borosilicate capillaries are used with tip openings of about 1 – 5 µm. As a result, smaller sample amounts of about 1 – 2 µL can be sufficient for sample analysis. Furthermore, smaller initial ES droplets are formed and as a consequence, nESI can be more tolerable to salt and buffer additives.[79]

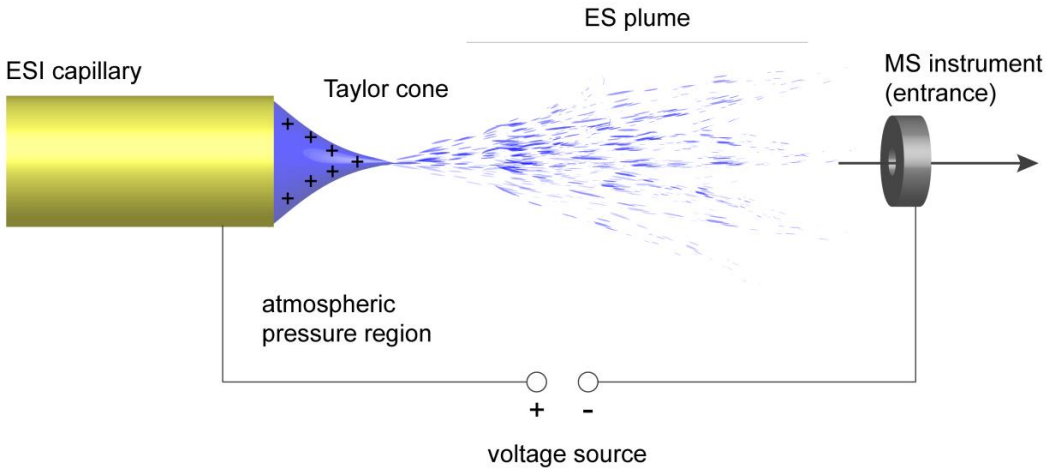

Figure 2.8: Schematic overview of an electrospray ionization (ESI) source.

Three different mechanisms are described for the formation of ions out of small and charged ES droplets (Figure 2.9). According to the ion evaporation model (IEM),[82-84] small ions are released from charged ESI droplets. For larger analytes, such as compactly folded globular proteins, it is more likely that analyte and charges of the analyte-containing droplet are desolvated together. According to the charge residue model (CRM),[82-84] it is assumed that solvent evaporates from the small ES droplets until the analyte molecule plus the charge of the droplet are left. So-obtained ionized species are also referred to as quasi-molecular ions. For unfolded proteins, the ion formation is assumed to occur according to the chain ejection model (CEM).[82-84] Unfolded proteins exhibit a large content of solvent-accessible non-polar side chains. These side chains are assumed to interact preferentially with the interface of ES droplet, which is in direct contact with the non-polar air phase. Charge-repulsive interactions may promote the stepwise ejection of the unfolded protein out of the ES droplet. For membrane proteins, the CRM and CEM are the most relevant mechanisms for the description of their ionization by ESI.

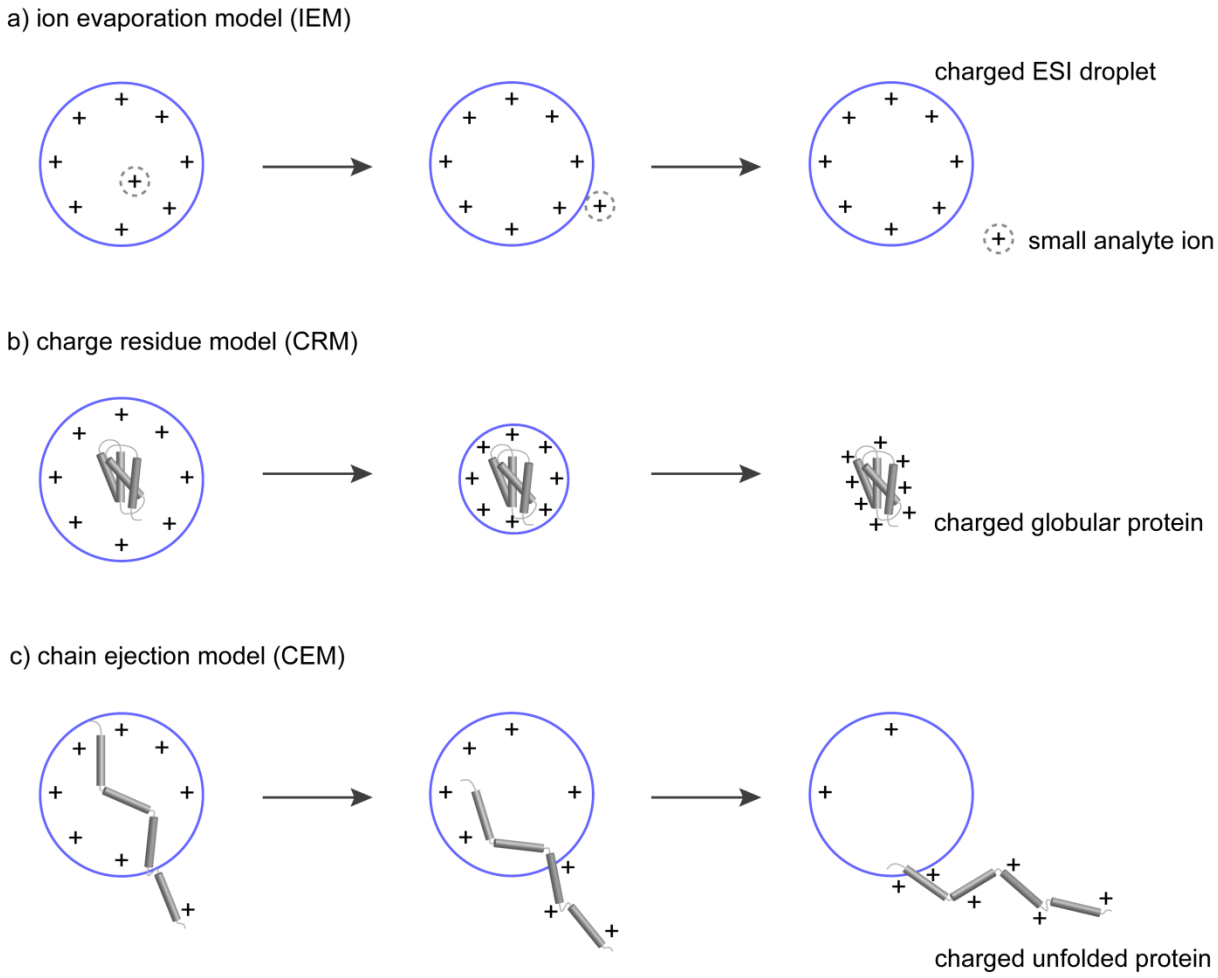

Figure 2.9: Schematic overview about different ion release mechanisms in ESI: a) ion evaporation model (IEM), b) charge residue model (CRM), and c) chain ejection model (CEM).

2.2.2 Q-ToF and Orbitrap Mass Spectrometers

Until today, most of the ESI-MS experiments on membrane proteins have been conducted with quadrupole-time-of-flight (Q-Tof) instruments. A schematic presentation of a relevant instrument setup is shown in the Figure below (Figure 2.10).[11, 13] Briefly, ions that are generated by nESI travel through the entrance of the mass spectrometer and are focused by ion guides to facilitate their transmission to the quadrupole region. Here, specific ion populations can be selected according to their *mass-to-charge ratio* (*m/z*). The ions are subsequently injected into the collision cell by means of an injection voltage (collision voltage), where they undergo collisions with neutral gas molecules, such as argon. A second ion guide to the time-of-flight (ToF) analyzer transfers the ions, which finally enables the determination of their *m/z* values. The molecular mass of membrane proteins can range from several kilo daltons up to mega daltons. In comparison to small molecules, the ions formed by large membrane protein complexes exhibit therefore an enormous kinetic energy and the ion beam is defocused upon nESI.[85] They travel among inappropriate trajectories, which can hamper their transmission to the ToF analyzer. To overcome these limitations, MS instruments that are optimized for the analysis of large membrane protein complexes are operated at elevated pressures.[85]

This includes an increase in pressure of the source region and collision cell (Figure 2.10).[85, 86] By doing so, membrane protein ions undergo not only more collisions with neutral gas molecules within the collision cell but also directly upon entering the MS instrument. The kinetic energy of the ions can dissipate into the surrounding gas, which lowers their kinetic energy and facilitates the appropriate back-focusing of their trajectories using the ion guides. This effect is also referred to as "collisional cooling" or "collisional focusing" and has been discovered for large soluble protein complexes, such as for the 20S proteasome (692 kDa) and tetrameric ADH (~ 147 kDa),[85, 86] and membrane proteins.[87]

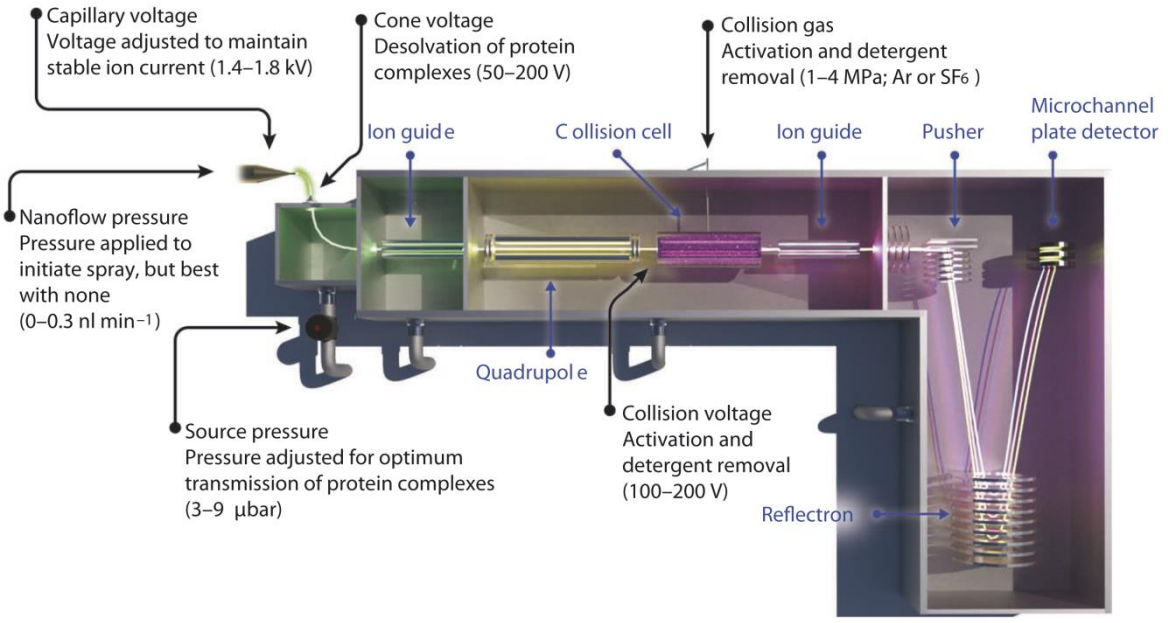

Figure 2.10: Schematic overview of a quadrupole-time-of-flight (Q-ToF) mass spectrometer used for the nESI-MS analysis of intact membrane protein complexes. The image was taken from reference[13] with the permission of Nature Springer (Copyright 2013).

Furthermore, conventional quadrupoles support the acquisition of ions with *m/z* values up to 4000. For the analysis of larger biomolecules, quadrupoles can be operated at lower radio frequencies, which helps to increase the available *m/z* range up to 32000.[88, 89] In addition, different mass analyzer setups have been explored for the MS analysis of membrane proteins, which include Orbitrap- and Fourier transform-ion cyclotron resonance (FT-ICR) mass analyzers.[90-93] The main advantage of both setups over Q-ToF systems is that they can acquire mass spectra with very high resolution by using only seconds of acquisition time. High resolution is very important for the qualitative and quantitative analysis of ligand-bound states. In the case of lipids, for example, *m/z* differences between a free protein and its protein-lipid-complex are very small. Using the Orbitrap technology it was recently demonstrated that one can resolve even multiple binding events in protein complexes formed with lipids that differ only in the length of their alkyl chains.[92] For the soluble protein complex GroEL (~ 800 kDa), for example, it was also recently shown that molecular weight differences below 1% of the total complex mass could be easily resolved, which enables one to distinguish between GroEL complexes formed with ADP and ATP.[91]

The Q Exactive hybrid quadrupole-Orbitrap mass spectrometer has been recently explored for investigating membrane protein complexes (Figure 2.11).[92, 94] Ions generated by nESI are guided by complex ion optics to a quadrupole. Analogues to Q-ToF systems, the quadrupole can be operated at low radio frequencies to support the transmission of large membrane protein complexes. The ions are then guided into the higher-energy collisional dissociation (HCD) cell, where ion activation can be achieved through collisions with neutral gas molecules. The ions are subsequently subjected into the C-trap, where the ion packages are focused prior to their injection to the Orbitrap mass analyzer. The ions traverse around a central, spindle-shaped electrode, whereby the image current of the axial motion of the ions is picked up by a detector. Similarly to FT-ICR, the detected rotational frequency of the ions can be Fourier-transformed to yield high resolution mass spectra. Elevated collision gas pressure (~ 10^{-9} mbar) can be applied within the HCD cell to optimize the transmission of large ions.[92]

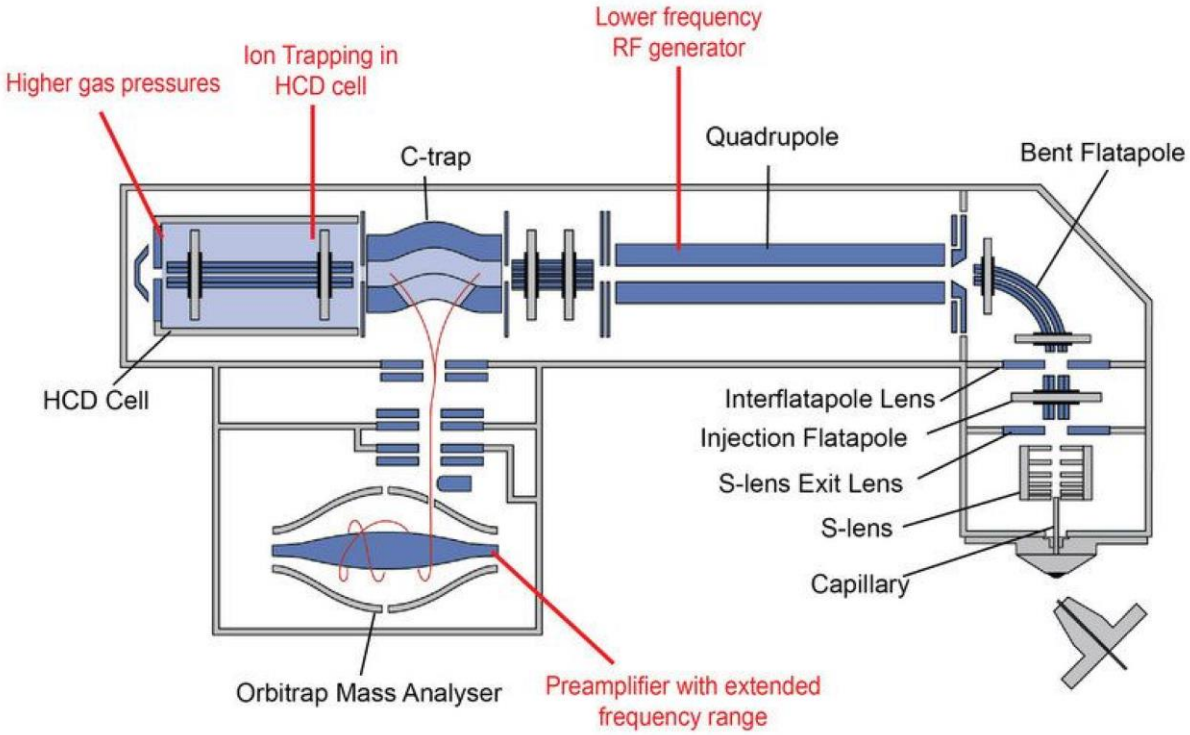

Figure 2.11. Schematic overview of a Q Exactive hybrid quadrupole-Orbitrap mass spectrometer used for the nESI-MS analysis of intact membrane protein complexes. The image was taken from reference[92] with the permission of Nature Springer (Copyright 2016).

2.2.3 The Protective Role of the Detergent

The ability to maintain and analyze non-covalent interactions of complex membrane protein assemblies by MS is not only supported by the development of new instruments, but also by the use of detergents. Several studies point to the fact that detergents can act as a key player for the preservation of native membrane protein structures during their transfer from solution into the vacuum of a MS instrument by nESI.[21] This sub-chapter discusses the general role of detergents for the structural preservation and analysis of membrane proteins by native MS. The acquisition of well-resolved membrane protein mass spectra requires the removal of the detergent environment upon nESI of protein-detergent mixtures. This can be achieved, for example, by laser-induced heating or by

raising the injection voltage that accelerates the ions into the collision cell.[13, 18, 95] At low collision voltages, weakly resolved and very broad signals appear (Figure 2.12), which indicate that the membrane protein is still trapped within the detergent environment.[18] Once the collision voltage is enhanced the loss of detergent molecules occurs, which is reflected by an increase in resolution of the protein mass spectrum (Figure 2.12). Further increase in collision voltage can lead to the disruption of the membrane protein complex. As shown in case of the ELIC pentamer, an asymmetric charge state distribution can be observed upon collision-induced dissociation (CID, Figure 2.12). This is commonly observed for large protein complexes and can be attributed to partial unfolding of monomeric subunits.[96, 97] They can take up a disproportionally large amount of charges during nESI and repulsive Coulomb interactions subsequently facilitate their dissociation from the protein complex.

In 2009, Friemann *et al.* investigated the protective role of detergent aggregates for membrane proteins during the transport into the vacuum.[98] Molecular dynamics (MD) simulations were performed with the outer membrane protein A (OmpA) from *E. coli* embedded in a dodecylphosphocholine (DPC) detergent micelle (80 DPC molecules) that was surrounded by a thin water layer. The results obtained under vacuum conditions indicated that the majority of structural changes occurred within the detergent aggregate that surrounded the membrane protein, while the structure of the protein within the detergent complex was not very sensitive to the evaporation process.

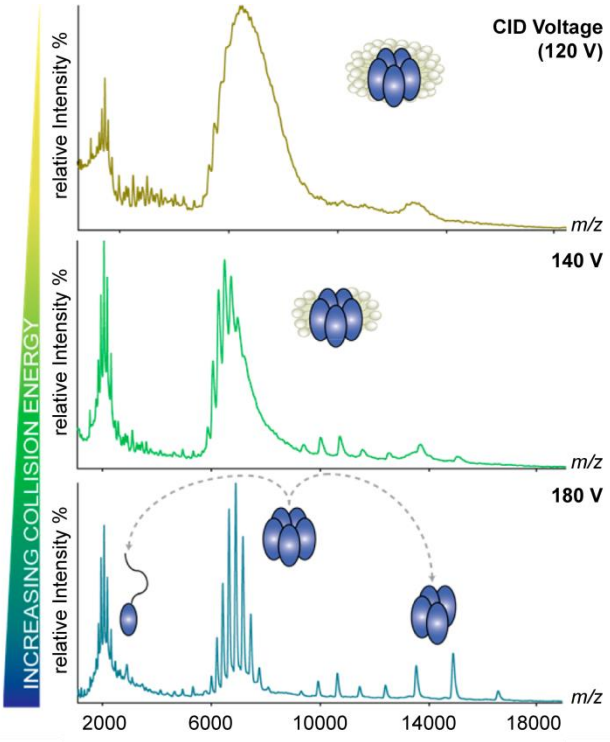

Figure 2.12: Mass spectra of the pentameric ligand-gated ion channel (ELIC) encapsulated in DDM acquired at different collision voltages upon nESI. Increasing the collision voltage (120 V – 140 V) leads to the removal of the detergent environment, as indicated by the increase in resolution of the protein signals. At higher collision voltages (180 V) the disruption of the membrane protein complex is obtained. The image was taken from reference[18] with the permission of the American Chemical Society (Copyright 2015).

This led to the conclusion that water and surfactant molecules could act as a safeguard by protecting the membrane protein from dehydration-related conformational changes,[98] which is in line with the results obtained from native MS experiments.[13, 18, 21]

The protective role of the detergents was further investigated by Borysik *et al*. who studied the effect of nESI on the structure of empty detergent aggregates and membrane protein-detergent complexes with MS techniques.[15, 16, 99] MS-based experiments on a series of *n*-trimethylammonium bromide detergents revealed that large detergent clusters were formed during nESI of detergent solutions.[99] The size of the formed clusters increased with the charge state of the cluster and decreased with the length of the detergent's alkyl spacer. Moreover, the size of the detergent cluster was independent from the detergent concentration in solution. These results are in strong contrast to the thermodynamics of micelles formed in solution and indicated that the structure of detergent aggregates underwent a pronounced structural transition during nESI. More importantly, CID experiments that were performed on individual cluster ion populations revealed that asymmetric charge separation and neutral loss of detergents occured from precursor ions.[15, 99] This implied two possible mechanisms that can explain the protective role of detergents for membrane protein MS (Figure 2.13): 1.) The energy taken up by the membrane protein-detergent complex through collisions with neutral gas molecules can dissipate through the loss of neutral detergent molecules or clusters. 2.) The dissociation of charged detergent clusters reduces the impact of repulsive Coulomb interactions, which prevents the protein structure from Coulomb-driven unfolding. A mechanistic study on the bacterial outer membrane protein (PagP) finally confirmed that that the release of bound detergents is central to the survival of native-like protein conformations in vacuum (Figure 2.13).[16] With completing the detergent removal the structural collapse or dissociation of the protein becomes the dominant pathway.[15, 16] Further results presented by Reading and Liko *et al.* suggest that membrane proteins with greater detergent-encapsulated areas are better able to tolerate collisional activation without unfolding than those in which this area is proportionally smaller.[14]

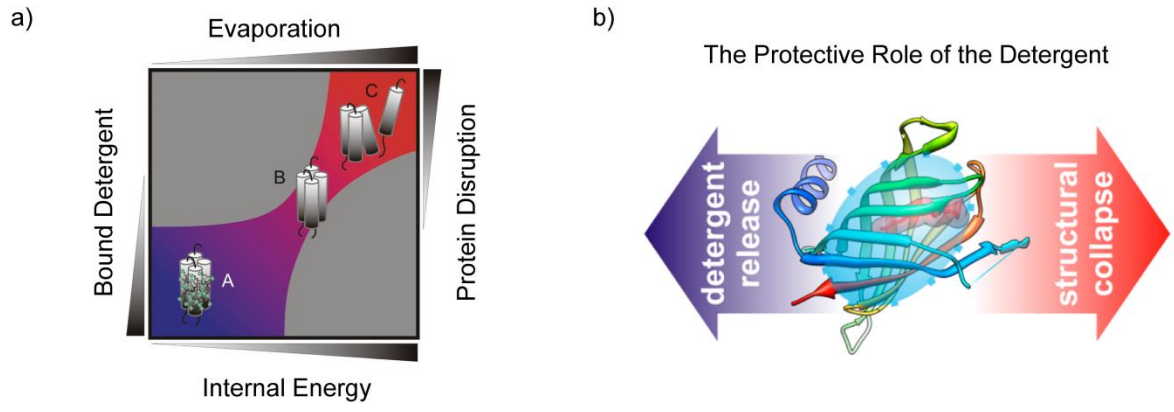

Figure 2.13: Suggested effect of internal energy rate and bound detergent amounts on protein disruption. a) Three different protein populations are suggested. In population A, the internal energy is low and the amount of bound detergent is high, which results in featureless mass spectra. In population C, the internal energy is high, bound detergents are removed, and protein disruption occurs. In-between, the detergent-free protein population B is observed, which can be characterized by MS techniques. b) Detergent release prevents the protein structure from collapsing. The images were taken from reference[15] (left) and reference[16] (right) with the permissions of the Royal Society of Chemistry (Copyright 2012) and the American Chemical Society (Copyright 2013), respectively

2.2.4 Charge Reduction

A central aspect in the vacuum chemistry of detergents is their propensity to remove charges from membrane proteins.[14] As mentioned above, charge reduction can lower the effect of Coulomb-driven protein unfolding and is therefore of general interest for the analysis of compact protein structures by mass spectrometry. Different charge-reducing strategies have been developed for proteins, which include the use of ammonium acetate buffer,[100] crown-ethers,[96] bipolar buffer gas,[101] acetonitrile vapor,[17] or basic solution additives that compete either with charging of the protein during nESI or removing the charge from the protein by CID.[17, 102, 103]

For membrane proteins, however, the charging mechanism might be more complex than for soluble proteins, because the protein is surrounded by detergents at the moment when charging occurs. To explore the relationship between detergent chemistry and membrane protein charge states, Reading and Liko *et al*. investigated a dataset of 49 combinations of membrane proteins and detergents.[14] The authors found that nESI-MS experiments with saccharide detergents consistently gave higher membrane protein charge states than C8E4 or LDAO (Figure 2.14). The charge-reducing nature of LDAO was not further declared, while the authors suggested that clusters formed by C8E4 served as low-molecular-mass charge carriers that reduced the charge in nESI droplets and therefore the charge of membrane proteins.[14] This is also in line with the strong propensity of polyethylene glycols to complex cations and can explain why C8E4 can also promote charge reduction of soluble proteins.[14, 104] The comparative analysis of DDM, C8E4, and LDAO indicated that the charge reducing properties of these detergents relied on the chemical properties of the detergent head group rather than on the properties of the hydrophobic tail.[14]

The main challenge arising from the use of charge-reducing detergents relies on the fact that they often denature membrane proteins.[17, 102] Therefore, alternative charge reduction methods have been examined, which involve the use of non-denaturing and non-charge-reducing saccharide detergents together with acetonitrile vapor and charge-reducing solution additives, such as imidazole.[17] The mass spectrum of OmpF released from OG, for example, showed a most abundant charge state of 22+ (Figure 2.14). When adding acetonitrile vapor to the ESI plume, the protein charge states shifted to lower values. Similar charge reduction was observed upon addition of imidazole. Moreover, charge reduction was most pronounced when both strategies were applied simultaneously (Figure 2.14). By doing so, compactly folded states of OmpF and a P-glycoprotein could be maintained, which was not possible before without adding charge-reducing agents or detergents. This highlights the great importance of methods that enable membrane protein charge reduction on-demand.

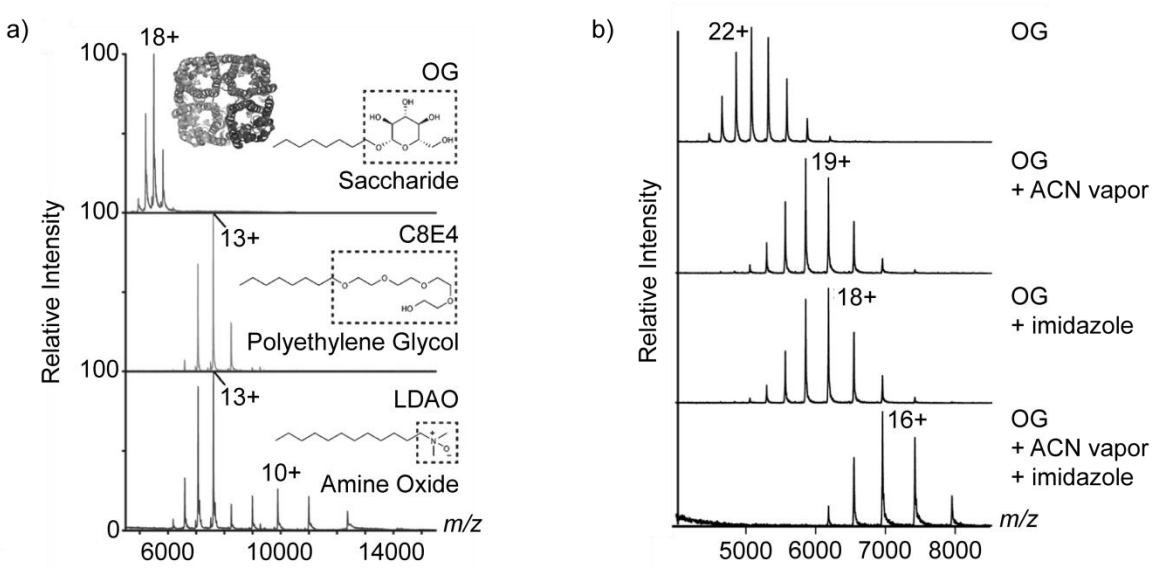

Figure 2.14: Detergent families and alternative methods that modulate charge states of membrane proteins. a) Mass spectra of aquaporin channel (AqpZ) from *E. coli* upon removal of different detergent environments. Lower charge states are obtained from polyethylene glycol and amine oxide detergents. b) Mass spectra of the outer membrane protein F (OmpF) from *E. coli* released from OG with different ESI source conditions and solution additives. Lower charge states were obtained, when the ES plume was treated with acetonitrile (ACN) vapor or when imidazole was added to solution. When both strategies were used simultaneously, the charge was reduced even further. The images were taken from reference[14] (left) and reference[17] (right) with permissions of John Wiley and Sons (Copyright 2015) and the American Chemical Society (Copyright 2014), respectively.

2.2.5 Detergent Screening for Membrane Protein Purification

Detergents that are suitable for native MS ideally transfer membrane proteins intact into the vacuum of MS instruments, are removed at low activations conditions, and promote charge reduction. Structural biologists are furthermore interested in the identification of detergents that are suitable for membrane protein purification, which is traditionally evaluated by means of gel-filtration chromatography.[10] Gel-filtration columns are packed with porous material, for example, dextran polymer beads, and aqueous buffers can be used as eluent. Larger analytes can pass the column faster than smaller analytes, because they interact less efficiently with the pores of the stationary phase. Although the data obtained from gel-filtration chromatography are of low resolution, this technique allows one to follow changes in membrane protein's monodispersity upon solubilization with different detergents.[10]

The state-of-the-art of detergent-screening methodologies was recently complemented by a protocol from Laganowsky *et al.* that summarized opportunities and limitations of native MS in terms of detergent-oriented membrane protein purification.[13] According to this protocol, membrane proteins can be routinely expressed with protease-cleavable fusions, such as a green-fluorescent protein (GFP) and a N-terminal His-tag, which allows one to validate the expression level by optical methods and, which facilitates the isolation of the targeted protein by immobilized metal ion affinity chromatography (IMAC).[105, 106] The proteins can be directly isolated with a detergent of choice and subsequently solubilized in different detergents by using gel-filtration chromatography. To evaluate how the individual detergents affect the membrane protein structure, the samples are subjected to nESI-MS analysis (Figure 2.15).

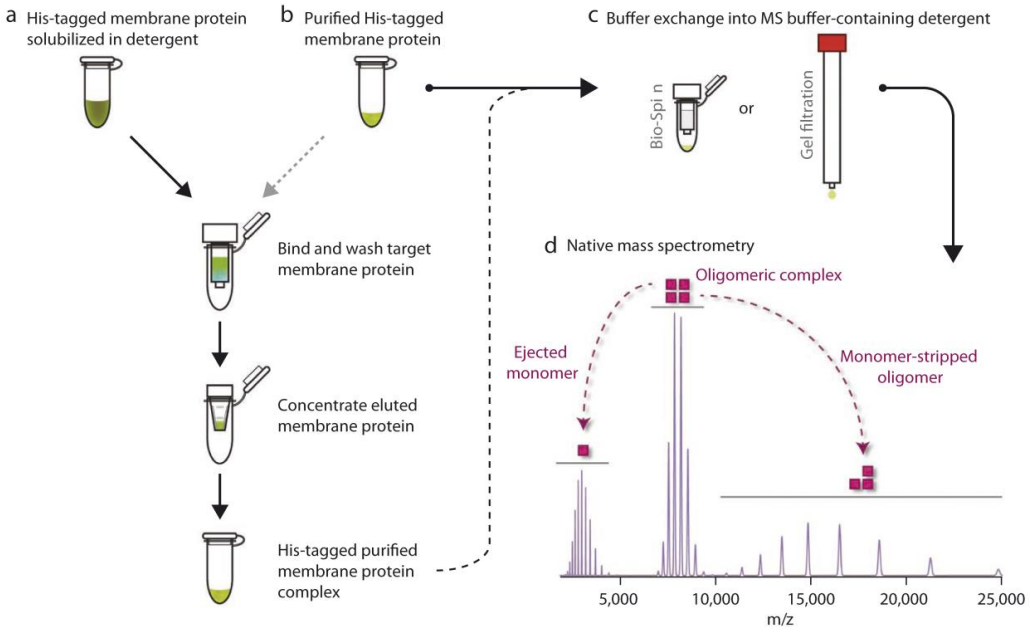

Figure 2.15: Identification of detergents that are suitable for membrane protein purification by means of native MS. (a) Membrane protein can be purified by protein extraction and immobilized metal ion chromatography (IMAC) with a detergent of interest. (b) Detergent can be screened by starting with a purified membrane protein. To do so, the detergent environment can be exchanged by gel-filtration chromatography. (c) So-obtained membrane protein samples are transferred into MS-compatible buffer. (d) nESI-MS analysis can provide directly information about sample homogeneity, oligomeric state, and molecular mass of the membrane protein. The image was taken from reference[13] with the permission of Nature Springer (Copyright 2013).

In contrast to gel-filtration chromatography, a diverse set of information can be gained from so-obtained membrane protein mass spectra (Figure 2.15).[13] The spectra give information on the molecular mass of a membrane protein complex and can also identify associated adducts (if present). Collision-induced dissociation can be used to disrupt the complex, which allows one to unravel the subunit composition of membrane protein assemblies. In addition, the impact of the detergent, temperature, and small ligands, such as drugs, nucleotides or lipids, on the oligomerization and stability of membrane protein complexes can be investigated.[13, 19, 47, 75, 94, 107-109] Complex instability is readily recognized, for example, when the membrane protein complex is not observable in the mass spectrum. Moreover, the spectral homogeneity and resolution of protein signals increase as a function of purification.[13]

More remarkably, native MS enables the identification of co-purified lipids in form of protein-lipid complexes and one can classify them into three different binding modes (Figure 2.16):[18] (1) Co-purified membrane lipids can be detected in the form of non-specific nESI adducts upon protein isolation.[75] They can either stabilize the structure of membrane proteins or act as substrate, which regulates the structure and function of a membrane protein. (2) Endogenously-bound lipids that are embedded within the membrane protein complexes can be identified upon dissociating them into individual subunits.

These lipids mediate the structure and interplay of sub-units interactions like in the cases of ATPases/synthases.[108] (3) Also interfacial lipids, which mediate the oligomerization of membrane proteins, can be distinguished.[47, 94] The ability to capture co-purified membrane depends on the chemical nature of the detergent. The use of high detergent concentrations (1w%) during the extraction of membranes may be the critical step at which significant delipidation takes place (Figure 2.16).[20] The detergent's potential to delipidate membrane proteins can thereby be evaluated by applying protein extraction and native MS analysis in combination (Figure 2.15).

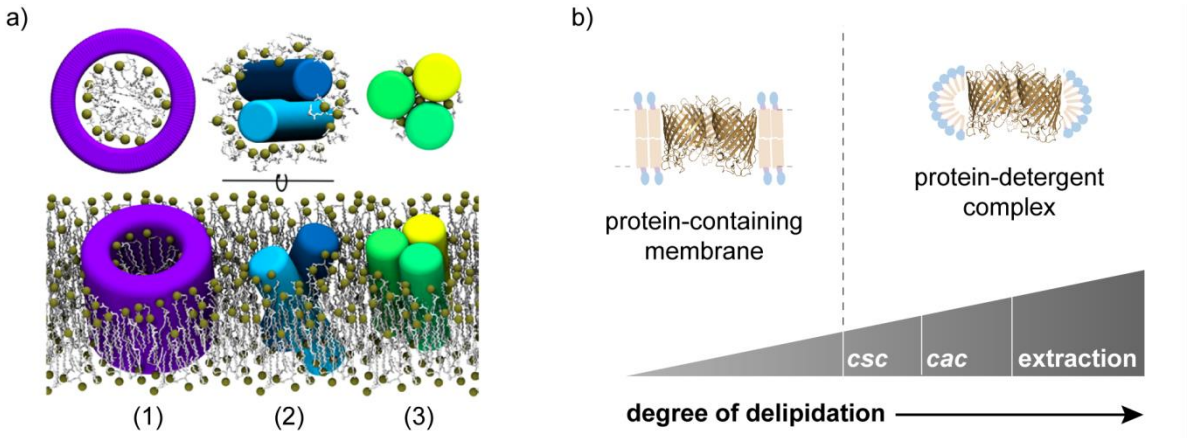

Figure 2.16: Lipid-binding modes and concentration dependency of membrane protein delipidation in the presence of detergents. a) Overview about protein-lipid interactions, such as (1) endogenously bound lipids as part of the protein structure, (2) binding of membrane lipids to the outer surface of membrane proteins, and (3) binding of interfacial lipids between protein-protein contacts. b) Protein delipidation occurs most significantly during protein extraction (detergent concentration ~ 1w%) and to a much lesser extent when lower detergent concentrations are applied, for example, the *critical solubilization concentration* (*csc*) or *critical aggregation concentration* (*cac*). The image a) was taken from reference[18] with the permission of the American Chemical Society (Copyright 2015).

Systematic native MS experiments of Reading and Liko *et al.* revealed that saccharide detergents exhibit a lower propensity to delipidate membrane proteins during protein extraction than polyethylene glycol and amino oxide detergents (Figure 2.17).[14] This is in line with the finding that saccharide detergents denature membrane proteins to a lesser extent than the other two detergent families, because lipids are essential for stabilizing membrane protein structures. When comparing the gas-phase properties of these detergent families, it becomes apparent that the delipidating properties of a detergents are inversely correlated to its charge-reducing properties (Figure 2.17).[14] Akin to condensed phase applications,[37] the choice of the detergents consequently needs be adjusted to the scope of the native MS experiment.[13] While non-charge-reducing saccharide detergents are more desirable for lipid-identification experiments, charge-reducing detergent families facilitate the nESI-MS analysis of membrane proteins under more gentle CID conditions and may reduce the impact of Coulomb-induced protein unfolding. As discussed before in Chapter 2.2.5, one can also apply saccharide detergents in combination with alternative charge-reducing methods, for example, by treating the ES plume with acetonitrile vapor or by using basic solution additions.[17, 102]

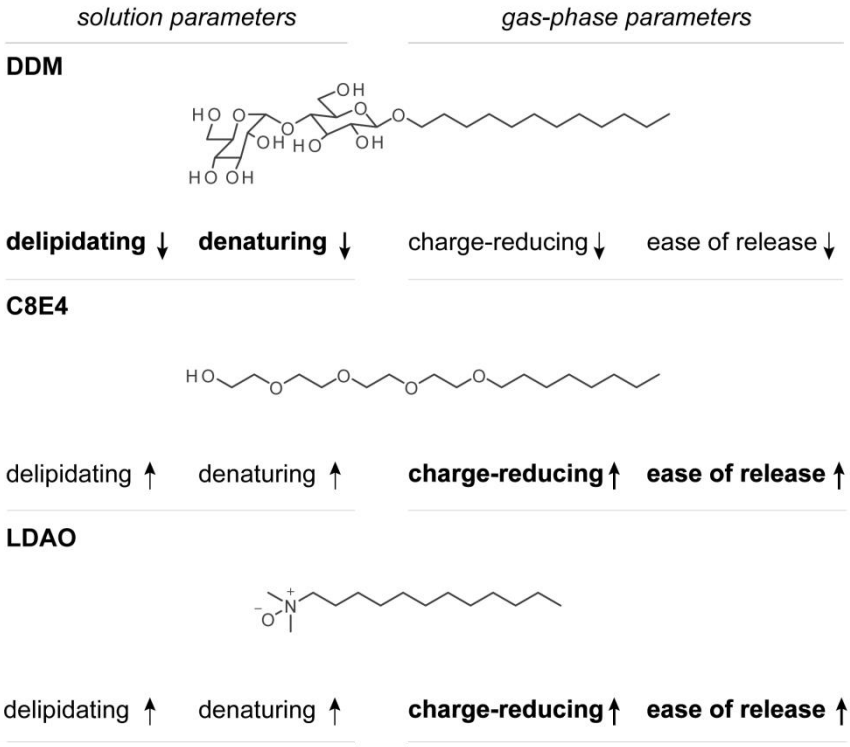

Figure 2.17: Solution and gas-phase parameters of DDM, C8E4, and LDAO which are important for the native MS analysis of membrane proteins. Charge-reducing detergents are more delipidating and denaturing to membrane proteins than non-charge-reducing detergents. Favorable features of individual detergents are highlighted in bold.

To yield general guidelines that allow one to estimate the properties of detergents for native MS applications, one would need to complement the molecular understanding of the detergent's solution properties (Gilbert G. Privé)[20] with the molecular understanding of their gas-phase properties (Reading and Liko).[14] By doing so, the following contradiction becomes apparent: Detergents that cover ideal properties for nESI-MS, for example, soft release conditions and charge-reducing properties, are more delipidating and are more denaturing to membrane proteins than detergents that are less suitable for nESI-MS (Figure 2.18). However, the estimations drawn from these guidelines may not apply to all proteins and exceptions to these estimations may be found in particular cases.

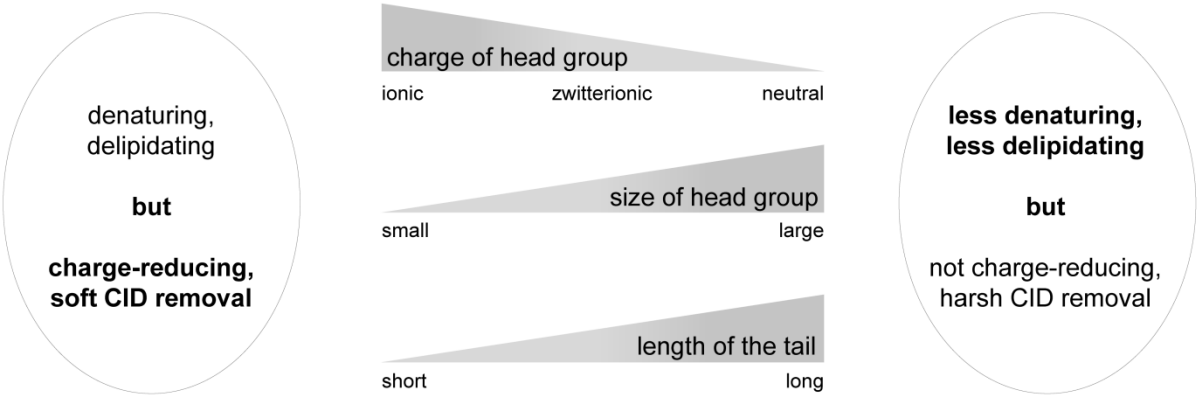

Figure 2.18: General design considerations that help to estimate the detergent's solution and gas-phase parameters in relation to the molecular structure.

2.2.6 Limitations and Further Opportunities

Despite all the above-mentioned opportunities that are provided by the investigation of membrane proteins with detergents and native MS, several general limitations related to the following features of MS were reported by Hernandez and Robinson:[110] (i) As the mass and heterogeneity of a membrane protein complex increases, the transmission, desolvation, and detection of ions becomes more challenging. Moreover, heterogeneous complex mixtures can contain multiple complexes that are close in mass and *m/z*, which can complicate the unique identification of the subunit composition. The currently on-going development of high resolution FT-ICR and Orbitrap mass analyzers can help to overcome these limitations.[90-93] However, accurate sample characterization may require not only testing of different sample conditions but also on different MS instruments, which are expensive and often only available in a few specialized labs. (ii) Membrane protein complexes and subunits cover a broad range of different *m/z* values. Due to differences in their ionization efficiency, the obtained intensity ratios or relative signal abundances are not quantitative. This aspect dictates also the ability to detect (iii) solution-phase species by MS. As the solvent environment is removed during the transfer into the vacuum of a MS instrument, the permittivity coefficient (ε) of the environment decreases dramatically, for example, ε_{water} ~ 80 and ε_{vacuum} ~ 1. Compared to hydrophobic interactions, electrostatic interactions become significantly stronger upon desolvation.[111] It can be therefore difficult to detect a complex by nESI-MS, if its subunits are primarily held together by hydrophobic interactions.[110] (iv) ESI techniques require the transfer of protein complexes into a ESI-compatible buffer, which differs from purification and storage buffers. Changes in the structure of membrane proteins that might be associated with a change of the buffer environment are often overlooked.

Further challenges are associated with the use of detergents for native MS applications. This includes the detergent's ability to denature membrane proteins in solution and unfavorable MS properties (Figure 2.18). Although detergents facilitate the analysis of protein-lipid interactions by MS, they can compete with lipids for lipid-binding sides and therefore only a reduced number of protein-lipid interactions may be observed upon protein extraction.[18, 21, 112] Laganowsky *et al.* found that protein-lipid complexes can be also detected upon nESI of protein-detergent mixtures to which lipids were exogenously added.[19] Gas-phase unfolding protocols can be used to monitor the resistance of membrane protein ions against collision-induced unfolding as a function of lipids (Figure 2.19).[19, 113] This allows one to rank lipids according to their relevance for the structure and function of a particular membrane protein.[19] The applied detergent concentrations are thereby about the detergent's *cac* and are therefore below a concentration level at which protein delipidation predominantly occurs (Figure 2.16). In addition, different alternative carrier systems have been explored, which include amphiphols and nanodiscs.[21] Amphiphols can be more effective than DDM in maintaining native membrane protein structures and interactions during nESI and therefore present a valuable alternative to detergents.[114] More recently it was shown that membrane protein-nanodisc complexes can be used to study the stoichiometry and dissociation behavior of large lipid shells that surround membrane proteins (> 60 lipids per protein ion, Figure 2.19).[115] Marty *et al.* suggested that the MS analysis of these nanodisc complexes will facilitate studies on the interface between membrane proteins and their lipid environment.[115] More information about this research area is provided elsewhere.[21]

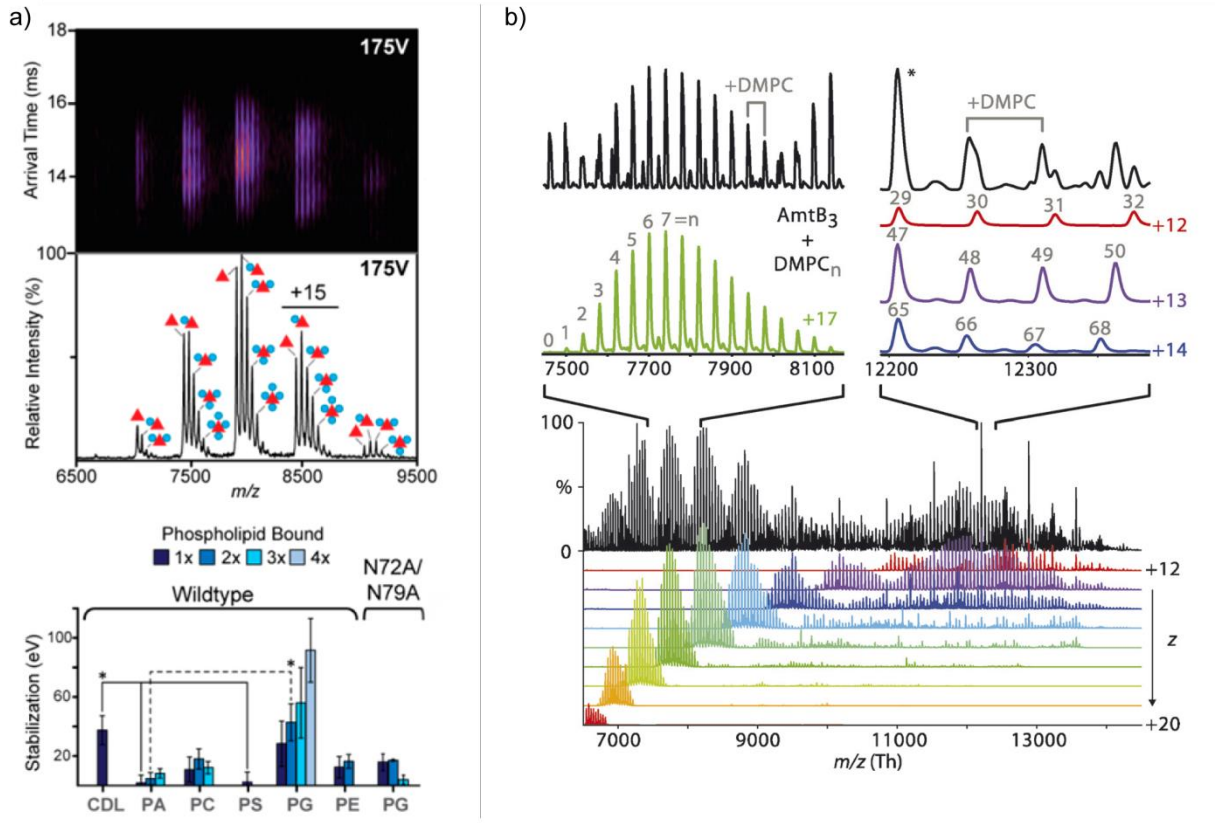

Figure 2.19: Investigating stabilizing effects of lipids (left) and probing the lipid annular belt of membrane protein complexes formed with nanodiscs (right) by MS techniques. a) Lipids that are exogenously added to protein-detergent mixtures can be detected and analyzed in the form of protein-lipid complexes by IM-MS (top). Monitoring the gas-phase unfolding of different AmtB-lipid complexes (charge state 15+) revealed stabilizing effects of lipids on AmtB. b) Spectrum of AmtB-nanodisc complexes that are composed of DMCP lipids and a scaffold protein. Zooming into the most abundant charge states revealed multiple lipid-bound states and the number of DMCPs bound to AmtB is annotated in grey. Deconvolted charge states from 12+ to 20+ are shown below. The images were taken from reference[19] (left) and reference[115] (right) with the permissions of Springer Nature (Copyright 2014) and John Wiley and Sons (Copyright 2015), respectively.

2.3 The Family of Oligoglycerol Detergents

The desire to synthesize detergents, which cover optimal properties for membrane protein research, has driven the development of new detergent scaffolds.[116-122] A detergent family which has attracted attention in recent years for biomedical applications are oligoglycerol detergents (OGDs).[22, 28, 29] Their molecular architecture consists of a non-ionic, dendritic, triglycerol head group, a hydrophobic tail, and both elements are held together by a connecting linker (Figure 2.20). Their modular architecture is very close to those of mono- or diglycerol ethers, specifically the monoalkylated ones, which have found various applications in industry, for example, as emulsifiers or additives in cosmetics, pharmaceuticals, printing inks, etc.[123-125] Although more than 80 different OGD structures have been published during the last 20 years, the family of OGDs has not yet been considered for membrane protein research.[23-27, 29, 126-143]

Apart from mono- and diglycerol, OGD head groups are made of triglycerol derivatives, which are considered to be dendritic molecules or dendrons (Figure 2.20).[144] They exhibit a single chemically addressable group at the core position (focal point) and are classified by generations, which refer to the number of repeated branching cycles that are introduced during its synthesis (Figure 2.20). Dendrons are perfect molecules, monodisperse, and highly symmetrical. The functional properties of a dendron are dominated by the number of functional groups at the periphery and the size of the backbone structure. Moreover, the focal point allows one to couple the dendron to a residue of choice. This includes not only hydrophobic residues but also biomolecules or synthetic polymers.[22]

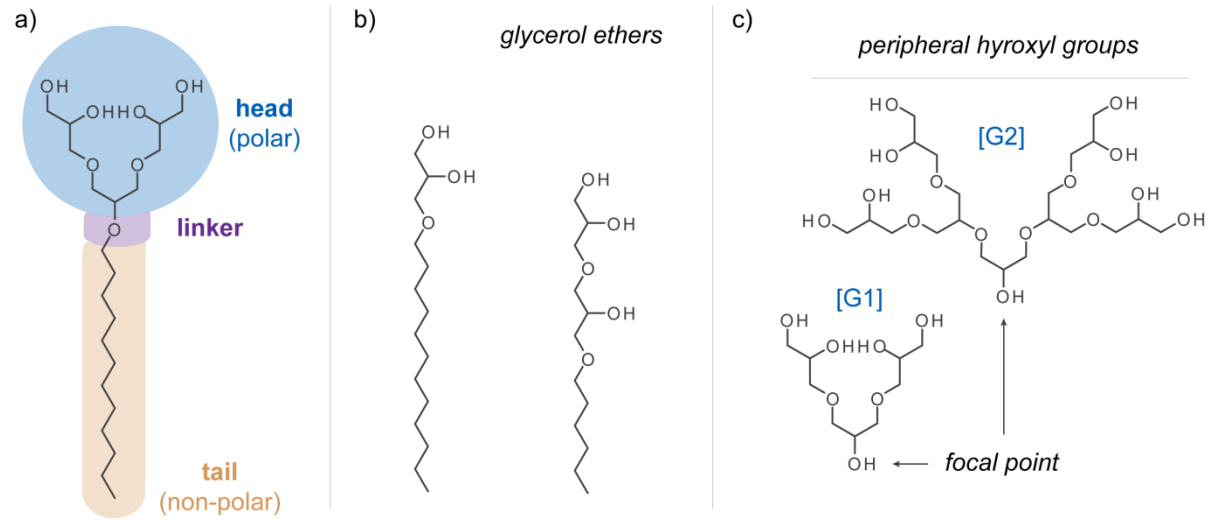

Figure 2.20: Different glycerol-based architectures: a) Principal structure of oligoglycerol detergents (OGDs), which comprise a head group, linker, and tail. a) – b) Amphiphilic mono- and diglycerol ethers, which have been developed between the early 1930s and 1980s, respectively. c) First- and second-generation triglycerol dendrons [G1] – [G2] have been developed by Wyszogrodzka *et al.* in 2008. First-generation triglycerol [G1] is used as primary material for the synthesis of dendritic OGDs.

2.3.1 Synthesis and Modification of Acetal-protected Oligoglycerol Dendrons

Dendritic OGDs are in many ways very promising for membrane protein applications. Some of the reasons are that the required oligoglycerol starting material is non-ionic, highly water soluble, and straightforward in its production.[126, 127] Buhleier *et al.* published the very first dendron structures in 1978,[145] while Haag and co-workers reported the first triglycerol dendrons 30 years later.[126, 127, 146] Today, first-generation triglycerol [G1] is used as the primary starting material for the synthesis of OGDs, which can be synthesized on laboratory scales with multiple strategies.[123, 147-149] In industry, triglycerol is obtained from the oligomerization of glycerol or epichlorohydrin (Figure 2.21).[123, 149, 150] Glycerol is a very attractive material, because it is widely available as a byproduct of the vegetable oil industry and only a small part is obtained from fossil chemistry.[123] The oligomerization of glycerol or epichlorohydrin not only produces triglycerols with 1,3-substituted core structures but also other triglycerol regioisomers (Figure 2.21). Meulenaer *et al.* and Sayoud *et al.* showed that individual regioisomer abundances can be readily followed by liquid and gas chromatographic methods.[151, 152]

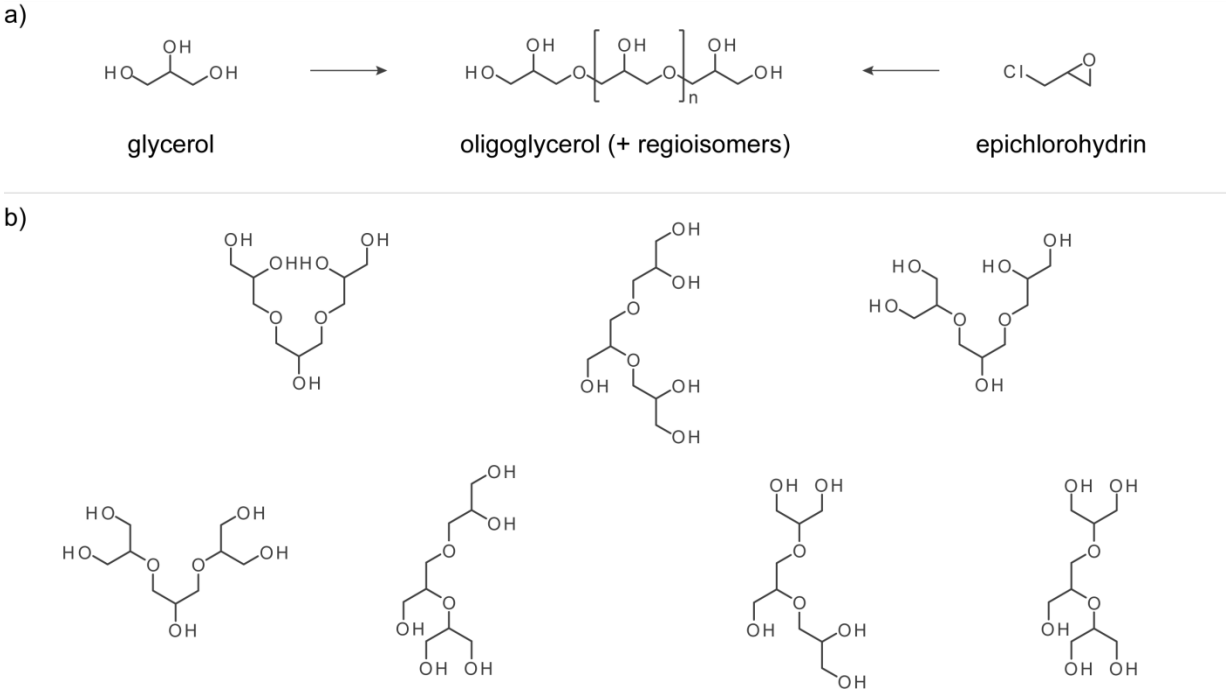

Figure 2.21: Synthesis of oligoglycerol and regioisomers of triglycerol. a) The synthesis of oligoglycerol mixtures starts from glycerol or epichlorohydrin and is accompanied by the formation of different oligoglycerol regioisomers. b) The structures of seven triglycerol regioisomers are shown. The upper left two triglycerol regioisomers abundantly form during industrial oligoglycerol synthesis.

Acetal protecting the peripheral hydroxyl groups of triglycerol allows one to independently address the hydroxyl group at the focal point.[127] The acetal-protected form of triglycerol ([pG1]-OH) was first mentioned in literature in 1974[153] but Wyszogrodzka *et al.* reported the probably most straightforward approach for its synthesis in 2008 (Figure 2.22).[127] Conveniently, triglycerol can be easily isolated upon acetal protection of oligoglycerol mixtures by normal phase column purification. By doing so, the desired product is obtained in form of acetal-protected triglycerol ([pG1]-OH, Figure 2.22). Interestingly, a co-purification of other actetal-protected triglycerol regioisomers has not been reported to date. Furthermore, two alternative routes have now been established for the preparation of [pG1]-OH, which either include a convergent or a divergent strategy.[126, 127] When using the convergent way,[127] methallyl dichloride is reacted with two equivalents of DL-1,2-isopropylidene-glycerol. The resulting [pG1]-ene is then further converted into [pG1]-OH by ozonolysis and reduction (Figure 2.22). According to the divergent way,[126] a glycerol derivative is used, whose secondary hydroxyl group is protected, for example, with a benzyl group. Allylation of the primary hydroxyl groups and dihydroxylation of the double bonds gives [pG1]-OBn. Subsequent acetal protection of the peripheral hydroxyl groups and removal of the benzyl-protecting group gives [pG1]-OH (Figure 2.22).

The methallyl chloride route is used to produce higher generations of actetal-protected triglycerol dendrons.[127] For the synthesis of [pG2]-OH, for example, one needs to react two equivalents of [pG1]-OH with methallyl dichloride under basic conditions (Figure 2.22). Ozonolysis of the resulting product followed by a reductive work up gives the desired [pG2]-OH. Multiple repetitions of this process result in higher generations of acetal-protected dendron, such as [pG3]-OH and [pG4]-OH.

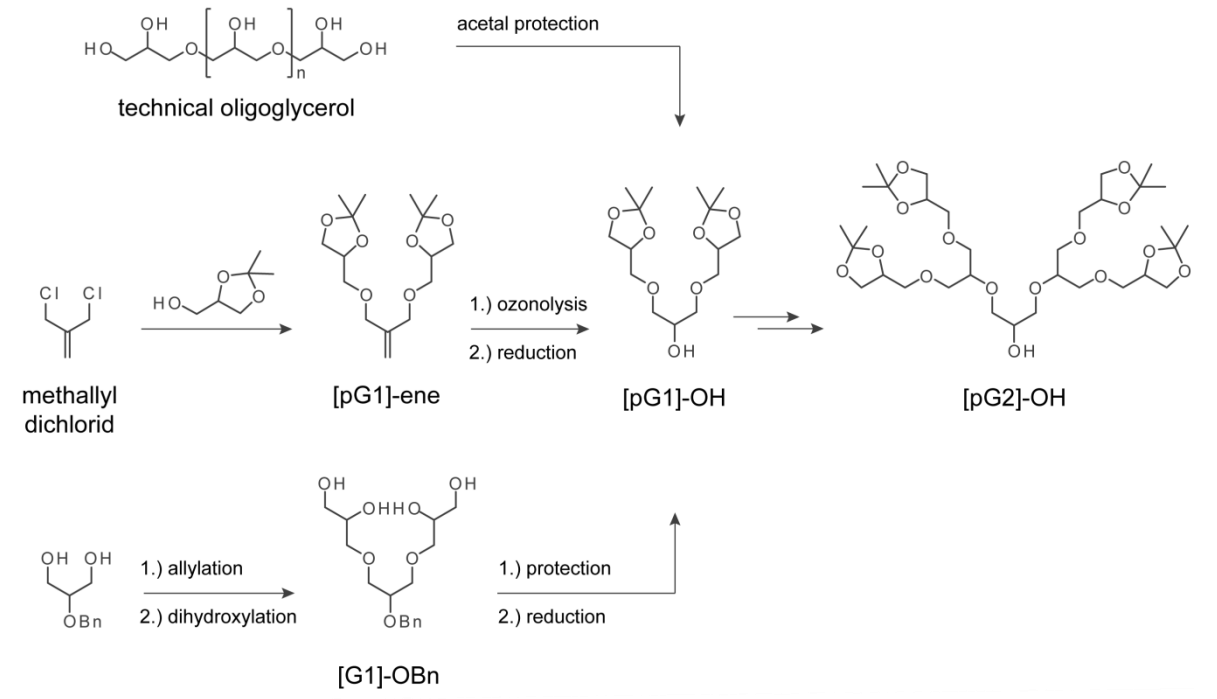

Figure 2.22: Main synthetic routes that lead to first- and second-generation, acetal-protected triglycerol dendron, [pG1]-OH and [pG2]-OH.

The hydroxyl group at the focal point of acetal-protected triglycerol dendrons can be converted to various functional groups. This process is called focal point transformation and allows one to connect the dendron with a moiety of choice *via* different coupling strategies (Figure 2.23). Hydrophobic moieties, *i.e.*, for detergents, can be readily attached to the hydroxyl group of [pG1]-OH *via* ether coupling or esterification.[143] Other functional groups that can be introduced include, for example, mesylate, allyl- or propargyl moieties, an azide or an amine group (Figure 2.23).[143] Mesylates are good leaving groups for ether coupling reactions.[132] Allylation of the hydroxyl group enables coupling of hydrophobic residues *via* thiols.[133] The attachment of azidated hydrophobic residues can be afforded *via* "click-chemistry" with proparglylated dendrons.[140] The same is true for azidated dendrons, which requires hydrophobic moieties with alkyne groups.[127] Azides can be further converted to amine groups, which gives full access to amide coupling strategies.[27]

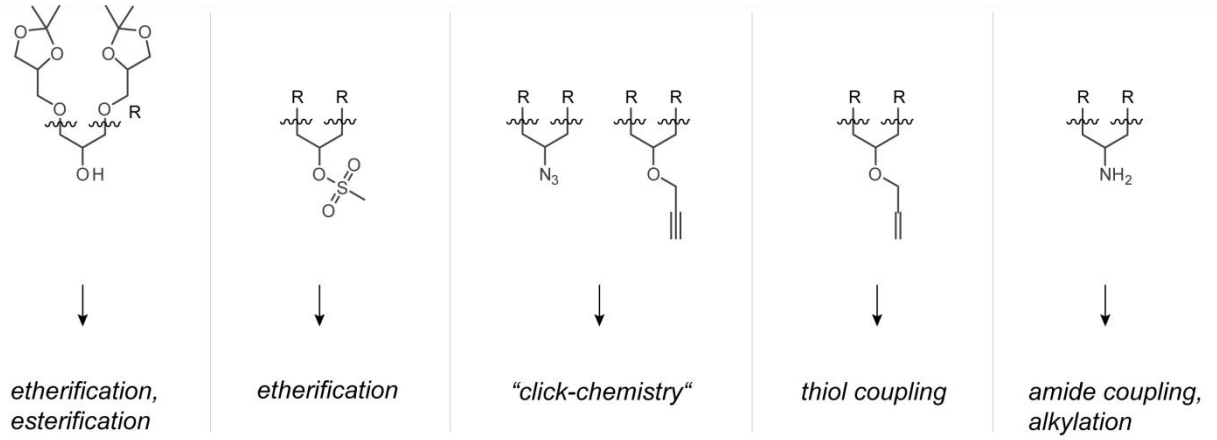

Figure 2.23: Different focal point groups of acetal-protected triglycerol and related coupling reactions.

2.3.1 Modular Detergent Design and Applications

The first detergents that can probably be referred to as OGDs were monoalkylated diglycerol ethers (Figure 2.24). These detergents were patented by B. R. Harris in 1938 in his effort to develop new emulsifiers that would improve the stability of suspensions between oil and water.[124] Driven by the same motivation, other monoalkylated and acylated oligoglycerol derivatives were developed in the following decades (Figure 2.24).[125, 154, 155]

The application of dendritic OGDs has particularly attracted much attention as the aid to increase the solubility of hydrophobic drugs.[146] Dendritic glycerols turned out to be biocompatible and could significantly increase the water solubility of hydrophobic cancer drugs, *i.e.*, paclitaxel.[156] Similar results were obtained from glycerol polymers.[157] On the other hand, the main benefit in using dendritic glycerols arises from their perfectly defined structure, which facilitates the implementation of structure-property studies.[127] The first studies that targeted the structure-based understanding of the dendritic OGD's propensity to solubilize hydrophobic drugs were conducted with triglycerol-based biphenyl structures (Figure 2.24).[126] A modular echange of the OGD head group size revealed how tuning the structure of these detergents could control the solubilization of hydrophobic Nile Red. Similar experiments were performed with core-multishell OGDs that were obtained from oligoacetylen cores.[127] Compared to the biphenyl structures, the capability of core-multishell OGDs to solubilize Nile Red increased by a factor of 200. Both papers demonstrated the great potential of the modular OGD concept for structure-property studies and paved the way for the application-oriented optimization of numerous OGD scaffolds.[23-27, 29, 126-143]

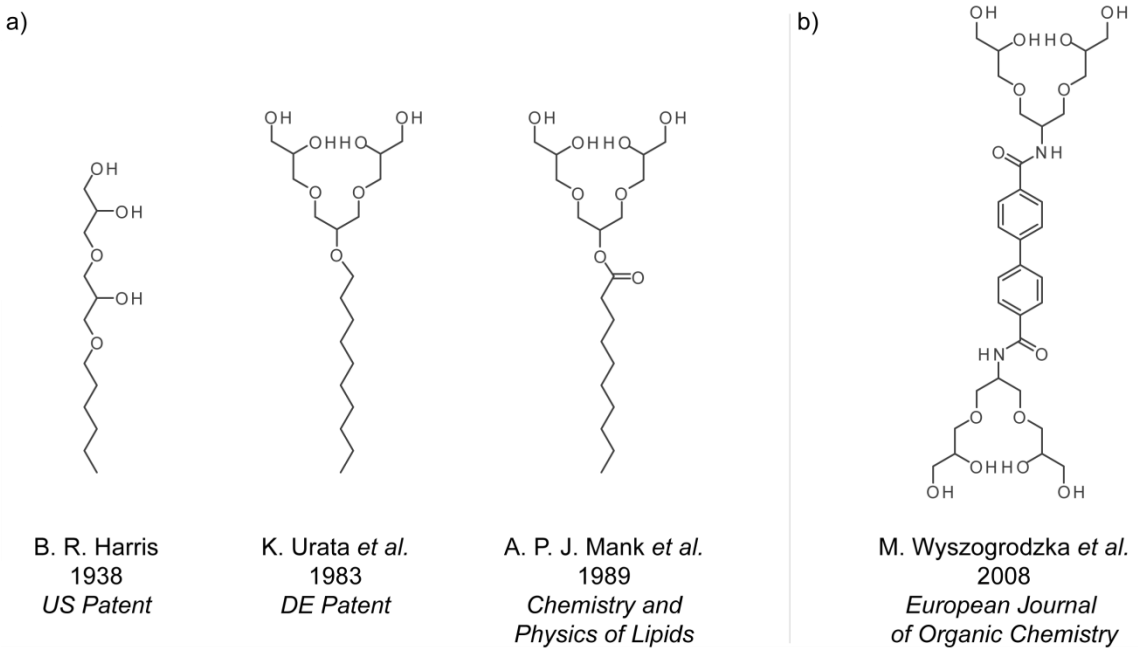

Figure 2.24: Molecular structure of OGDs that have been explored as a) emulsifiers for applications in cosmetic and food industry or b) for the solubilization of hydrophobic drugs.

After this, the aggregation behavior of monoalkylated, dendritic OGDs was studied in solution. Trappmann *et al.* published a set of seven OGDs, which were made of different dendron generations, [G1] – [G3], two sorts of alkyl spacers, C11 or C16, and a mono- or biaromatic spacers (Figure 2.25).[131] Depending on the size of the OGD head group, the self-assembly of these molecules produced worm-like micelles or micelles with *cac* values in the micromolar range (Figure 2.25). In addition, increasing the size of the OGD head group decreased the aggregation number and alkyl spacer packing density of the aggregates. Similarly to the above-mentioned core-multishell structures, the solubilization of hydrophobic Nile Red and pyrene could be controlled by tuning not only the size of the OGD head group and aromatic linker but also by tuning the length of the hydrophobic tail.[126, 127, 131] The uptake of hydrophobic guests did not affect the geometry of the aggregates, which was the first example of a shape-persistent aggregate from a non-ionic detergent.[131, 137] Subsequently, different dendritic OGD architectures were developed and their modular structures were optimized for individual drug delivery application as well as for the solubilization of carbon nanotubes.[28] More recently it was shown how the morphology of self-assembled nanostructures can be controlled by tuning the molecular structure of OGDs.[140]

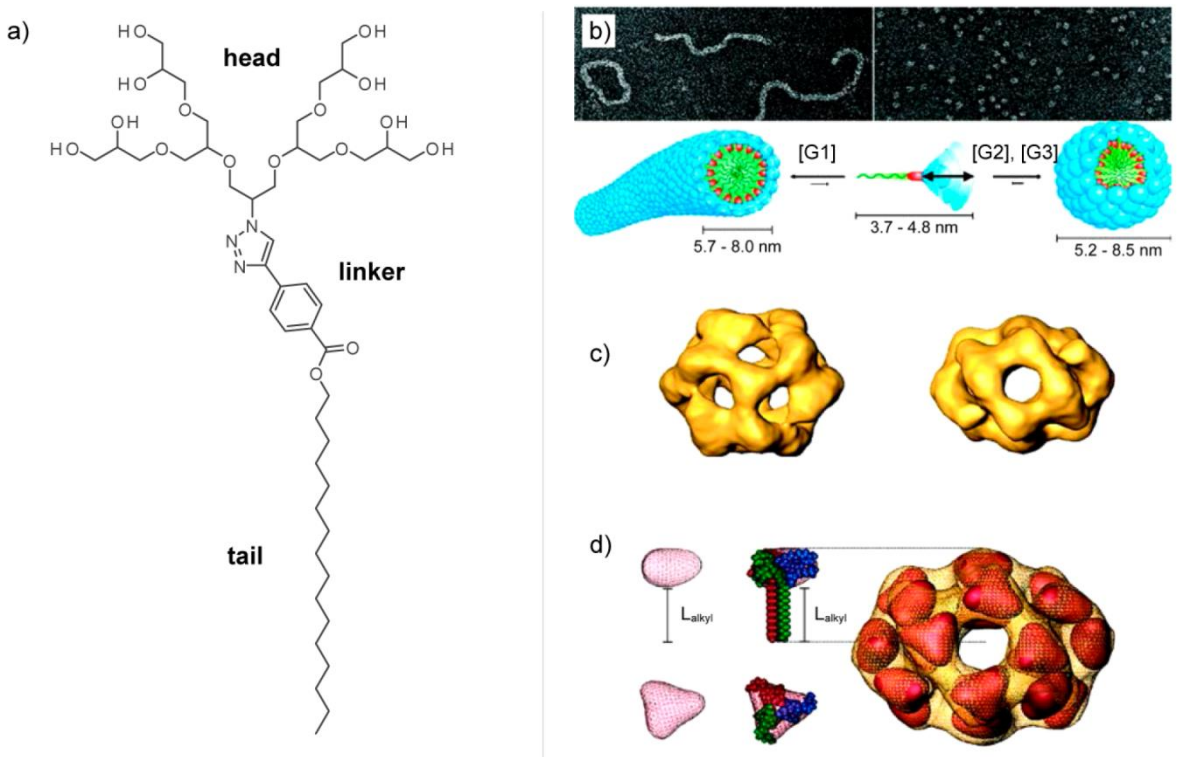

Figure 2.25: Head-tail OGDs exhibit unique self-assembly and solubilization properties for hydrophobic compounds in aqueous solution. a) Exemplary structure of a [G2] OGD published by Trappmann *et al.* b) Dendron generation-dependent change in self-assembly. c) 3D reconstruction of shape persistent micelles with different orientations. c) Structural arrangement of [G2] OGDs within the reconstructed micelle. The images b), c), and d) were redrawn from reference[131] with the permission of the American Chemical Society (Copyright 2010).

Owing to the ability of tuning the size and hydrophylicity of dendritic OGD head groups in a generation-dependent manner, these substituents have been explored for tuning the optical properties of fluorescent dyes, for example, perylenebisimides (PBIs).[27, 129, 135, 136] This particular system is very hydrophobic and its aggregation in water is accompanied by a decrease in fluorescence intensity, which can be a limiting factor for optical imaging applications.[129] Müllen and coworkers demonstrated that one can reduce the aggregation of PBI in water by functionalizing its core with bulky, water-soluble substituents.[158] With this regard, the first core-unsubstituted, triglycerol-based PBIs have been synthesized by Heek *et al.*[129] The authors showed that attaching [G4] triglycerol dendrons on each flank of a PBI was necessary for enabling the complete suppression of PBI aggregation in water (Figure 2.26). This concept could be also transferred to core-unsubstituted, dendronized PBIs with a monofunctional PEG chain, which were successfully applied as fluorescence labels upon bioconjugation to the antibody cetuximab (Figure 2.26).[27] Similar trends in aggregation suppression were confirmed in the case of hydrophobic cyanine dyes upon modification with [G1] triglycerol dendrons.[26] The concept was further refined with the modification of triglycerol dendrons by sulfate groups. Due to additional electrostatic repulsion forces, sulfated trigylcerol dendrons turned out to more efficient in suppressing the aggregation of hydrophobic substituents than non-ionic ones.[141] This enabled, for example, increasing the PBIs' fluorescence quantum yields in water to 100% by reducing the dendron generation from non-ionic [G3] to sulfated [G2] (Figure 2.26).[27]

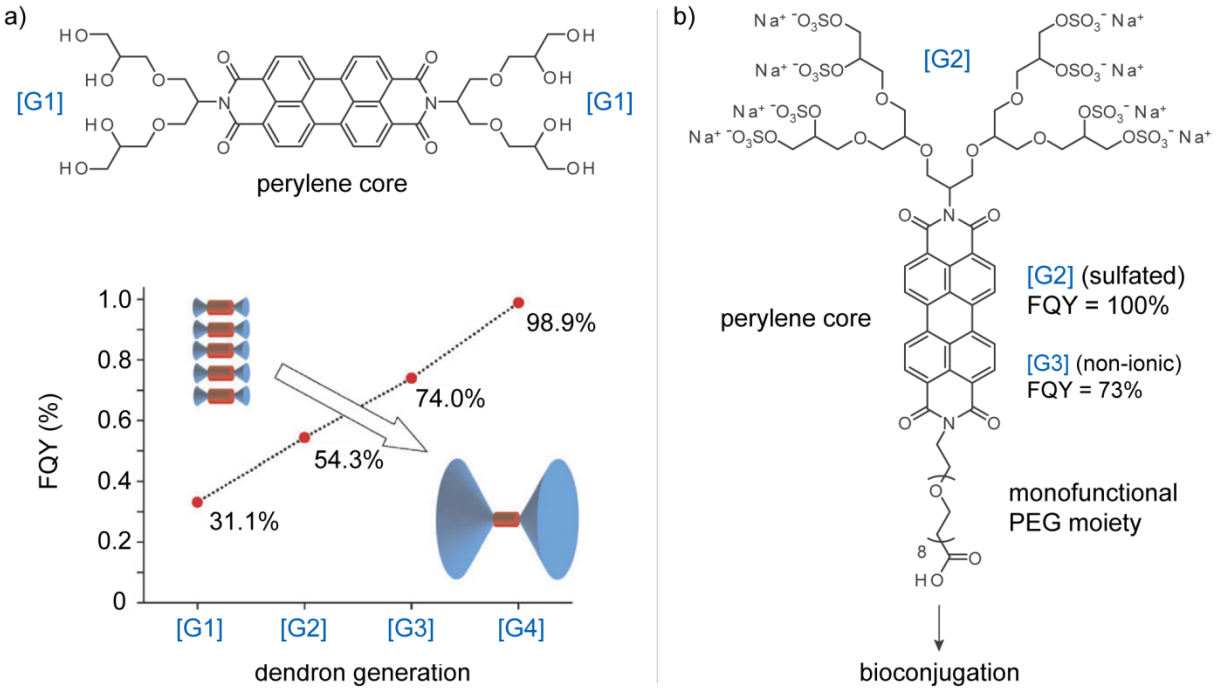

Figure 2.26: The size of the OGD head group affects the optical properties of amphiphilic, core-unsubstituted perylenebisimides (PBIs). a) Large non-ionic OGD head groups reduced the aggregation and improved the fluorescence quantum yields (FQYs) of PBIs in water. b) Structure-property study on dendronized PBIs with a monofunctional PEG chain confirmed that electrostatic repulsion forces, which arise from sulfated OGD head groups, can suppress PBI aggregation more efficiently than non-ionic ones. The image shown in a) (bottom) was redrawn from reference[129] with the permission of the Royal Society of Chemistry (Copyright 2010).

In addition, the potential of dendritic, monoalkylated OGDs to be used as antifouling agents for surfaces has been evaluated.[23-25] First, different generations of triglycerol dendron were functionalized with alkanethiols and so-obtained OGDs were immobilized on gold surfaces (Figure 2.27).[23] The best protein resistance was found for surfaces that were functionalized with [G1] OGDs. The authors suggested that decreasing the size of the OGD head group enhanced the OGD packing density on gold surfaces, which possibly resulted in a better prevention from protein adsorption. Further attempts to control bioadhesion by changing the hydrophobicity of surfaces were examined with azobenzene-based OGDs.[25] Changing the isomeric state of azobenzene between *trans* and *cis* can be triggered by light or heat and is accompanied by a change in geometry and polarity.[159] Azobenzene-based OGDs alone could not be readily switched on gold surfaces, which was most likely a result of the high molecular packing density.[160] This led to the development of a supramolecular host-guest approach with OGDs based on azobenzene and adamantane, which formed complexes with surface-immobilized ß-cyclodextrin receptors (Figure 2.27).[25] In contrast to pure azobenzene-based OGD monolayers, the new supramolecular OGDs could be readily switched in solution and on surfaces. This led to the obtainment of surfaces whose hydrophobicity could be reversibly changed by irradiation with light. Among a series of OGDs with different dendron generations, the most promising results in terms of light-induced hydrophobicity changes on surfaces were obtained from [G2] OGDs.[25]

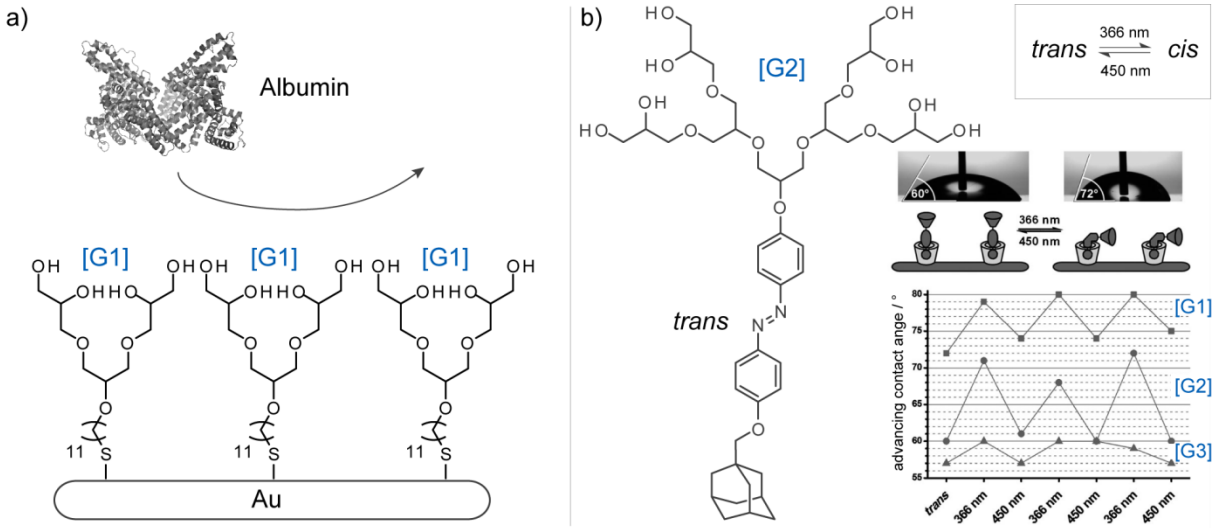

Figure 2.27: Exploring the potential of OGDs to be used as antifouling agents for gold surfaces. a) Among a series of alkanethiol OGDs, best antifouling properties were found for [G1] OGDs. b) Light-induced changes in surface hydrophobicity could be obtained with OGDs based on azobenzene and adamantate, which were immobilized on gold surfaces by complex formation with surface-immobilized ß-cyclodextrin receptors. A clear switching behavior of the contact angle and hence the hydrophobicity of the surface could be demonstrated. In particular, changes of the contact angle around 65° have been discussed as transition between fouling and non-fouling surfaces.[161] The image shown in b) was taken from reference[25] with the permission of John Wiley and Sons (Copyright 2014).

Further attempts to control the self-assembly of detergents in solution by light resulted in the development of different azobenzene-based OGDs. Studying the aggregation behavior of azobenzene-based, head-tail OGDs revealed that assembly and disassembly of micelle formation could be controlled by irradiation with light.[132] Further results showed that the light-induced changes in micelle formation dramatically influenced their potential to solubilize hydrophobic guest molecules (Figure 2.28).[132, 162] More recently, a photoresponsive dendritic bolaamphiphile was developed containing an azobenzene, which was on each flank functionalized with an alkyl chain and a dendron (Figure 2.28).[139] This new amphiphile readily self-assembled into twisted tape morphologies when azobenzene was in the *trans* state. Photoirradiation of the solution resulted in *trans* to *cis* isomerization and the complete disappearance of the tape-like aggregates was obtained. These results emphasized the application of photoswitchable OGDs for the development of responsive drug delivery systems.

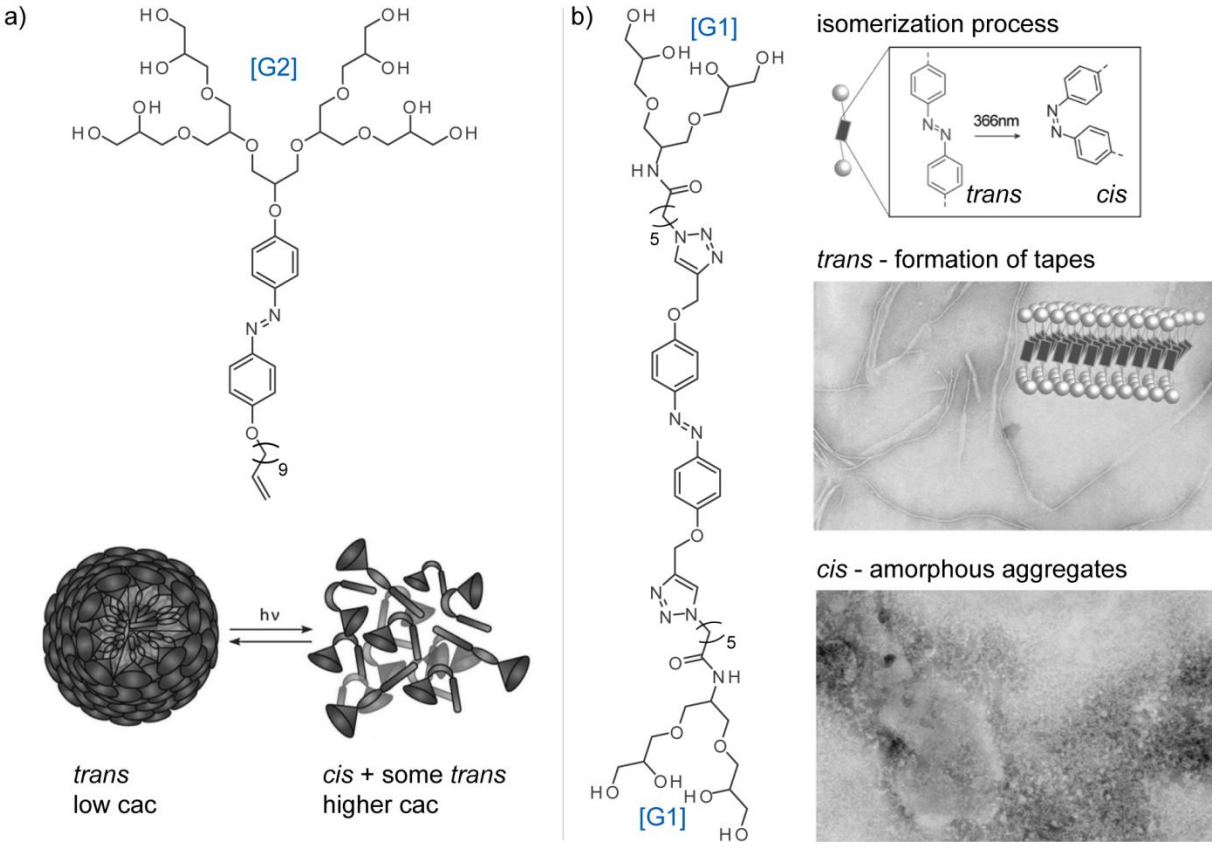

Figure 2.28: The photoresponsive self-assembly of azobenzene-based OGDs was investigated in solution. a) The micelle formation of aobenzene-based, head-tail OGDs could be controlled by changing the isomeric state from *trans* to *cis*. b) Azobenzene-based bolaamphiphile self-assembled into to tape-like aggregates, when the azobenzene moiety was in the *trans* state. Isomerization to *cis* led to the complete break-up of the tape-like structures. The images were redrawn from reference[132] (left) and reference[139] (right) with the permission of the Royal Society of Chemistry (Copyright 2011 and 2015, respectively).

In summary, the architecture of OGDs has proven to be highly modular. Today available synthetic protocols allow one to rapidly exchange individual OGD building blocks, which include the structure of the head group, linker, and tail. With more than 10 different amphiphilic OGD architectures and more than 80 individual OGD structures that have been published between 1938 and today, it has been demonstrated how the structure of OGDs can be tailored for individual applications. This includes drug-delivery applications, surface modifications, and the development of dye labels for optical imaging in biological samples. Taken together, the here-mentioned advantages of OGDs therefore emphasize the application of this detergent family in the development of new detergents with tailor-made properties for native MS applications on membrane proteins.[23-27, 29, 126-143]

3. Aims

The overall aim of this thesis is dedicated to evaluate the potential of dendritic OGDs for the purification and native MS analysis of membrane proteins. In particular, it will be investigated if the modular architecture of OGDs allows one to adjust their molecular structure to the scope of individual native MS applications, such as protein extraction, charge reduction, and the ability to detect protein complexes formed with co-purified membrane lipids.

In the first part of this thesis, therefore, the design concept and synthesis of a novel and highly modular OGD library is presented. In the next step, it will be evaluated how far the modular architecture of OGDs allows one to tailor membrane protein charge states on-demand. Because membrane proteins are very expensive and difficult to handle, it will be also discussed if inexpensive soluble proteins can be used to identify charge-reducing detergents in advance. Furthermore, the potential of OGDs for the isolation of membrane proteins from biological membranes will be tested. Subsequent native MS experiments will be conducted to unravel how protein charge reduction and the detection of protein complexes formed with co-purified membrane lipids can be optimized by tuning the molecular structure of OGDs. In this context, it will be also examined if OGDs can facilitate the structural analysis of challenging membrane proteins with pharmaceutical relevance, such as GPCRs, which would be of great interest for structural biology and medicinal chemistry.

4. Chapter I – A New Library of Oligoglycerol Detergents

4.1 Introduction

Detergent engineering is a major challenge to all aspects of membrane protein research and especially to those that involve the use of native MS. Suitable detergents not only preserve the native structure of proteins in solution, they also support the transport and release of membrane proteins from solution into the vacuum of a mass spectrometer. Gaining insights about how chemical tuning of detergents can lead to the protection membrane protein structures in both environments adds a new dimension in complexity to the development of new detergents and is of enormous interest for structural biology.

Reading and Liko *et al.* evaluated recently the utility of three detergent families that are most commonly used for the native MS analysis of membrane proteins, *e.g.*, saccharide, polyethylene glycol, and amine oxide detergents.[14] Saccharide detergents are able to protect the native structure of many different membrane proteins in solution.[20] Native MS experiments with these detergents, however, suffer from the harsh activation conditions required for detergent removal and high protein charge states that are obtained upon protein release.[14] Their low propensity to delipidate membrane proteins during isolation from biological membranes facilitates the identification and ranking of structurally relevant lipids by means of MS techniques.[13, 19] Amine oxide- or polyethylene glycol detergents, on the other hand, exhibit a greater propensity to denature membrane proteins in solution, because they are effective in delipidation.[20] However, upon nESI they can be removed under gentle activation conditions and provide low protein charge states.[14] This led to the conclusion that most available detergent families are suitable either for protein purification, promoting protein charge reduction, or for detecting lipid bound states, but rarely cover all aspects.

In this thesis the current state of the art of detergent engineering is complemented by investigating the family of OGDs. These detergents exhibit a modular architecture which comprises an oligoglycerol head group, a hydrophobic tail, and a connecting linker group (Figure 4.1). Synthetic procedures allow one to systematically exchange individual building blocks, which is a valuable perquisite for structure-property studies.[127, 128, 131] Previous investigations were focused on the molecular understanding of the OGD's aggregation behavior and the utility of their aggregates to be used as nanocarriers for the solubilization of hydrophobic drugs.[22, 28] This thesis evaluates now, if the modular architecture of OGDs can be used to optimize the purification and native MS analysis of membrane proteins on-demand. For this purpose, a new library of OGD regioisomer mixtures **1** – **8** is presented, whose design concept and synthesis are discussed in this chapter (Figure 4.1).

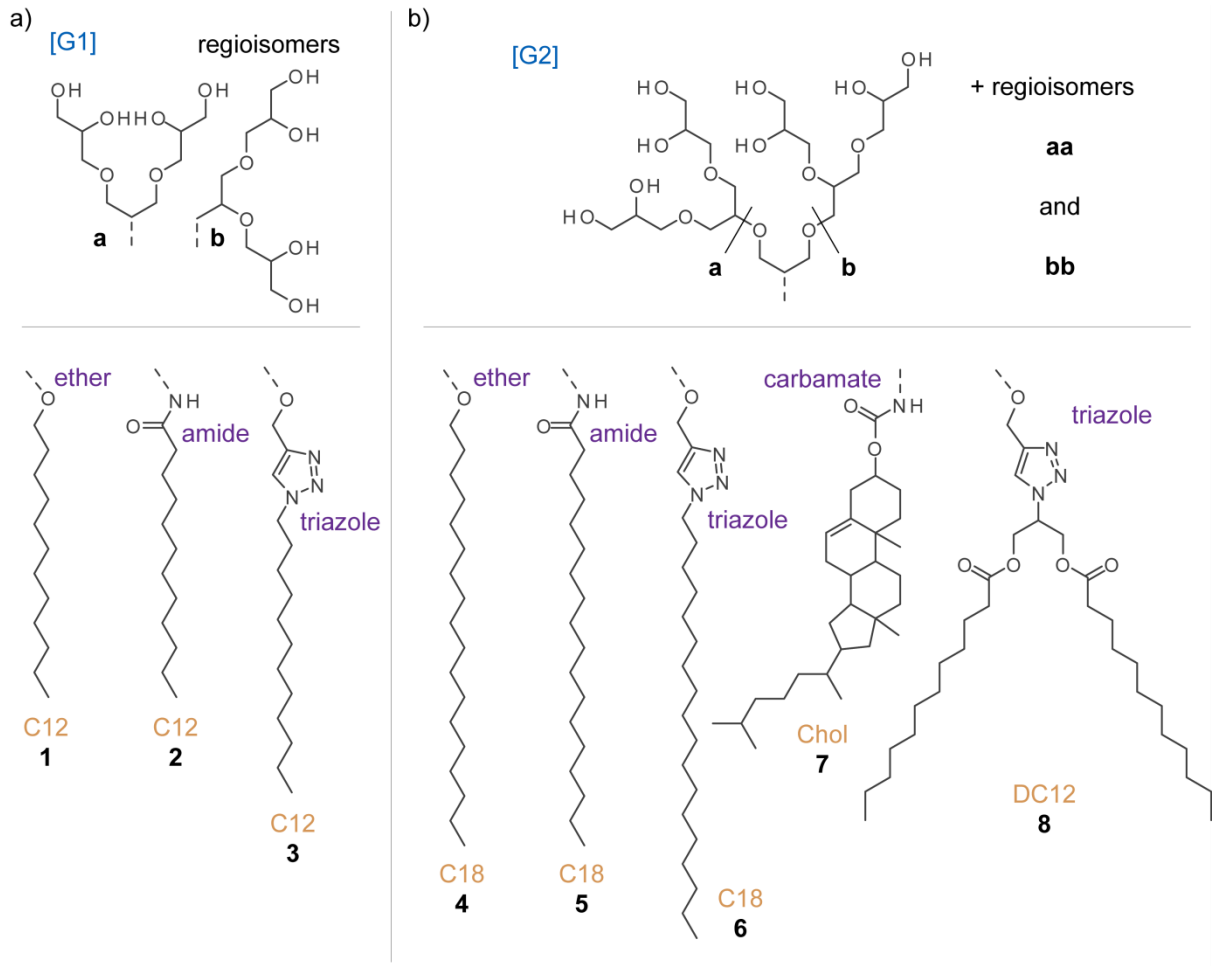

Figure 4.1: A new library of OGD regioisomer mixtures **1** – **8**, whose design and synthesis are described in this chapter. The [G1] OGD mixtures **1** – **3** consist of two detergent regioisomers, while the [G2] OGD mixtures **4** – **8** consist of three detergent regioisomers. These regioisomers differ with respect to the structure of the head group (blue) and exhibit similar linkers (violet) and tails (orange).

4.2 Experimental Details

General Information about Synthesis, Purification, and Characterization

Synthetic procedures that were used for the preparation of OGD regioisomer mixtures **1** – **8** are summarized in Chapter 8.1 (Appendix). OGD structures that are discussed throughout this thesis are abbreviated by the following formula: "D-L-H." The letter "D" represents the head group either in its acetal-protected state [pGX] or unprotected state [GX]. The letter "X" represents the generation of triglycerol dendron. The letter "L" represents the functional group at the focal point and the letter "H" represents the hydrophobic tail. Synthetic procedures that were used for the preparation of [G2]-carbamate-Chol **7** were provided by Svenja C. Ehrmann. With the exception of [G1]-ether-C12 **1a**[125] and [G2]-triazole-DC12 **8aa**,[140] the here presented OGDs and OGD mixtures have not been published before (Figure 4.1).

Chemicals were purchased from Sigma-Aldrich (Germany), Acros Organics (Germany), Alfa Aesar (Germany), Fluka (Germany), Fischer Scientific (Deutschland), Merk (Germany), TCI (Germany), and were used as supplied. Ethyl acetate (EtOAc) and (*n*-hexane) were distilled before they were used.

Other solvents were used without purification. Technical oligoglycerol was purchased from Fluka (product number: 17782) or Sigma-Aldrich (product number: 17782 Aldrich). Technical oligoglycerol from Solvay (product number: TM4516) was a gift from Dr. Monika Wyszogrodzka. Dry solvents were purchased in bottles sealed with a septum or tapped from a solvent purification system (MS-SPS-800) that was purchased from M. Braun (Germany). Deionized water (H_2O) used for synthesis was used from the tap and was provided by a deionization system installed in the Freie Universität's Institute of Chemistry and Biochemistry. Argon and oxygen were purchased from Linde (Germany) and used as supplied. Ion exchange residues, such as Amberlite® IR-120(H) and Lewatit K 6267, were washed with methanol (MeOH) and dried for 12 hours in the open air prior to their use.

For working under dry and oxygen-free reactions conditions, chemicals and solvents were handled under argon atmosphere. To support dry and oxygen-free reaction conditions the glassware was evacuated, baked out at 300 °C with a heat gun, and filled with argon. Solvents that were used in the absence of oxygen were degassed prior to their use by repeated introduction of argon gas.

For reaction monitoring and purification procedures normal phase (NP) thin-layer chromatography (TLC) analysis was applied. NP TLC plates (DC-Fertigfolien ALUGRAM® Xtra SIL G/UV_{254}) based on silica (SiO_2) were purchased from Macherey-Nagel (Germany). Silica gel (60 M) for preparative normal phase column chromatography was purchased from Macherey-Nagel. For NP TLC analysis and manual NP column purification mixtures of organic solvents (*v*:*v*) were prepared. If necessary, MeOH was added in percent per volume to the prepared mixtures (*v*:*v* + *v*%). TLC plates were either analyzed under UV irradiation (254 nm) using a lamp from CAMAG (Germany) or by staining the TLC plates either with cerium reagent (940 mL H_2O, 60 mL H_2SO_4, 25 g molybdic acid, 10 g cerium(IV) sulfate) or a potassium permanganate solution (250 mL H_2O, 2.5 g potassium permanganate). The respective staining reagents were prepared by Katharina Goltsche. For the staining process, the TLC plates were fully submerged into the staining solution, excess of staining reagent was wiped off with cellulose, and the plate was heated up to 300 °C with a heat gun until staining was completed.

The final detergent batches **1** – **8** were purified by preparative reversed phase (RP) high pressure liquid chromatography (HPLC). The samples obtained upon acetal deprotection were dissolved in mixtures of deionized H_2O and MeOH (*v*:*v*, 1:1) and passed through an syringe filter (RC, 0.2 µM) prior to purification. For preparative RP HPLC purification, a home-built HPLC system was used which was equipped with a LC-8A pump from Shimadzu (Germany), a UV variable wavelength monitor, and a differential refractometer from Knauer (Germany). As stationary phase a pre-packed Kinetex EVO C18 column was used (pore size: 100 Å, particle size: 5 µm, length: 250 mm, diameter: 21.2 mm), purchased from phenomenex (Germany). Degassed mixtures of H_2O and MeOH were used (*v*:*v*) and thermally equilibrated upon mixing for at least 16 h prior to use. Data processing and analysis was performed with an analog recorder L250E from Knauer. The RP HPLC system was designed and constructed by Dr. Carlo Fasting.

Mass spectra were acquired on an Agilent 6210 ESI-TOF (ESI-ToF) from Agilent Technologies (Santa Clara, CA, USA). The solvent flow rate was adjusted to 4 µL/min and the spray voltage was set to 4 kV. Drying gas flow rate was set to 15 psi (1 bar). All other parameters were adjusted for a maximum abundance of the relative $[M+H]^+$. The instrument was operated by the Core Facility BioSupraMol of the Freie Universität Berlin.

^{1}H NMR, ^{13}C NMR and DEPT135 spectra were acquired using the following NMR instruments: Bruker DPX400 (^{1}H NMR: 400 MHz, ^{13}C NMR: 100 MHz), Jeol ECX400 (^{1}H NMR: 400 MHz, ^{13}C NMR: 100 MHz), Jeol ECP 500 (^{1}H NMR: 500 MHz, ^{13}C NMR: 125 MHz), Bruker AVANCEIII500 (^{1}H NMR: 500 MHz, ^{13}C NMR: 125 MHz) or Bruker AVANCEIII700 (^{1}H NMR: 700 MHz, ^{13}C NMR: 175 MHz). All instruments were operated by the Core Facility BioSupraMol of the Freie Universität Berlin. Data processing was performed with MestReNova (*v*6.0.2-5475).

Analyzing Oligoglycerol Regioisomer Proportions

Relative regioisomer proportions of [pG1]-OH, *e.g.*, (**a**:**b**), were analyzed by means of analytical normal phase (NP) HPLC. For NP HPLC analysis, a Nucleosil column from Macherey Nagel was used as stationary phase (pore size: 50 Å, particle size: 5 µm, length: 250 mm, diameter: 4 mm), while mixtures of *n*-hexane and isopropanol were used (*v*:*v*) as mobile phase. The NP HPLC system was equipped with a smartline pump 1050, a smartline UV detector 2550, and a smartline RI detector 2300, which were purchased from Knauer. Data processing and analysis was performed with ChromeGate Client Viewer (*v.*3.3.2) from Knauer. The NP HPLC system was operated by Marleen Selent. Regioisomer proportions of other [pG1]-based mixtures were characterized by ^{1}H or ^{13}C NMR. To determine their relative regioisomer proportions the relative intensities of the focal point signals were extracted from the NMR spectra. For this purpose, relevant ^{13}C NMR spectra were acquired using the inverse-gated mode and the sample concentrations were about 180 mg/mL. Regioisomer mixtures of [G1] OGD mixtures **1** – **3** were analyzed by analytical RP HPLC. Experiments were performed in isocratic mode with a system from Knauer, equipped with two Smartline 1000 pumps, variable wavelength UV detector 2500, and an Autosampler 3950. As stationary phase a pre-packed Kinetex EVO C18 column was used (pore size: 100 Å, particle size: 5 µm, length: 250 mm, diameter: 4.6 mm), purchased from phenomenex. Degassed mixtures of H_2O and MeOH were used (*v*:*v*) and thermally equilibrated upon mixing for at least 12 hours prior to use. Data processing and analysis was performed with ChromeGate Client Viewer (*v.*3.3.2) from Knauer.

Relative regioisomer proportions of [pG2]-based derivatives and [G2] OGD mixtures **4** – **8**, *e.g.*, (**aa**:**ab**:**bb**), were analyzed by ^{13}C NMR as described above. The sample concentrations were about 200 – 300 mg/mL. Relevant NMR spectra of intermediates and final products as well as HPLC chromatograms are shown in the Chapters 8.2 and 8.3 (Appendix).

4.3 Results and Discussion

4.3.1 Design Concept

The suitability of a detergent to be used for the isolation and native MS analysis of membrane proteins depends on the chemical nature of the head group, linker, and tail.[14, 20, 113] To investigate the impact of all three structural OGD parameters, a bottom-up approach was pursued, which involved the systematic testing of different OGD building block combinations. For this purpose, two sets of [G1] and [G2] triglycerol regioisomer mixtures were prepared, **1** – **3** and **4** – **8** (Figure 4.1). The OGD mixtures **1** – **3** and **4** – **6** consisted of [G1] and [G2] triglycerol regioisomers, which were connected to linear alkyl spacers *via* different linker units, such as ether, amide, or triazole groups.

The lengths of the chosen alkyl spacer, *e.g.*, C12 or C18, provided sufficient amphiphilic character, but kept the detergent mixtures soluble in water. The OGD mixtures **1** – **6** allowed one to investigate the structural impact of the OGD head group, linker, and tail on the OGDs' ability to solubilize and extract membrane proteins from biological membranes. Due to the outstanding solubility of the [G2] head group, also a very hydrophobic double chain motive and cholesterol moiety could be used to obtain water-soluble detergent mixtures **7** and **8**, respectively.

Detergent parameters that are important for the native MS analysis of membrane proteins include protein charge reduction and the ability to detect protein-lipid complexes upon protein extraction from biological membranes.[14, 17] Literature data point to the fact that charge reduction can be achieved by using basic solution additives.[17, 102] To account for the utility of OGDs for tuning charge states of membrane proteins, therefore, linker groups with different basicities were introduced between head group and tail (**1** – **3**, **4** – **6**; Figure 4.1). Furthermore, the library of OGDs **1** – **8** exhibited great potential to evaluate the impact of the detergent structure on the utility to facilitate the detection of protein-lipid complexes. In addition, the here-presented OGD library **1** – **8** offered for the first time the possibility to compare the potential of OGD regioisomer mixtures over individual OGD regioisomers for protein purification and native MS applications on membrane proteins.

4.3.2 Synthesis and Characterization of [pG1]-OH Regioisomer Mixtures

The synthesis of OGD detergent mixtures **1** – **8** started from the isolation of [pG1]-OH. The required starting material for [pG1]-OH was technical oligoglycerol, which contained variable amounts of different glycerol oligomers, such as mono-, di-, tri-, and tetraglycerol. To obtain [pG1]-OH from this heterogeneous material, technical oligoglycerol was reacted with 2,2´-dimethoxypropane under acidic conditions using *para* toluenesulfonic acid monohydrate (PTSA*H_2O).[127] The desired [pG1]-OH product fraction was subsequently isolated by means of column chromatography (Figure 4.2). Analytical NP HPLC revealed two fractions which belonged to individual regioisomers of [pG1]-OH. They exhibited similar molecular masses, but differed in the connectivity between individual glycerol units (**a**, **b**, Figure 4.2). The two triglycerol regioisomers that are known to be most frequently formed during the production of technical oligoglycerol were related to the [pG1]-OH regioisomers found here (**a**, **b**, Figure 4.2).[152] This led to the conclusion that both triglycerol regioisomers were simultaneously acetal protected and co-purified under the employed experimental conditions.

Their relative proportions (**a**:**b**) as well as the overall yield of [pG1]-OH strongly depended on the commercial oligoglycerol source (Figure 4.2). This is expected since it is known that the regioisomer composition within technical oligoglycerol can vary with the manufacturing process.[151, 152] Excluding oligoglycerol mixtures from Solvay or Sigma-Aldrich, the oligoglycerol mixture from Fluka provided significant proportions of both regioisomers and was therefore used for the preparation of the OGD regioisomer mixtures **1** – **8** (Figure 4.2). In order to confirm the structural identity of both [pG1]-OH regioisomers, their $^{1}H/^{13}C$ NMR spectra were compared with NMR reference data (Figure 4.3). Because NMR reference data were only available for [pG1]-OH (**a**),[127] a short reaction sequence was explored that led to the obtainment of [pG1]-OH (**b**) within six synthetic steps.

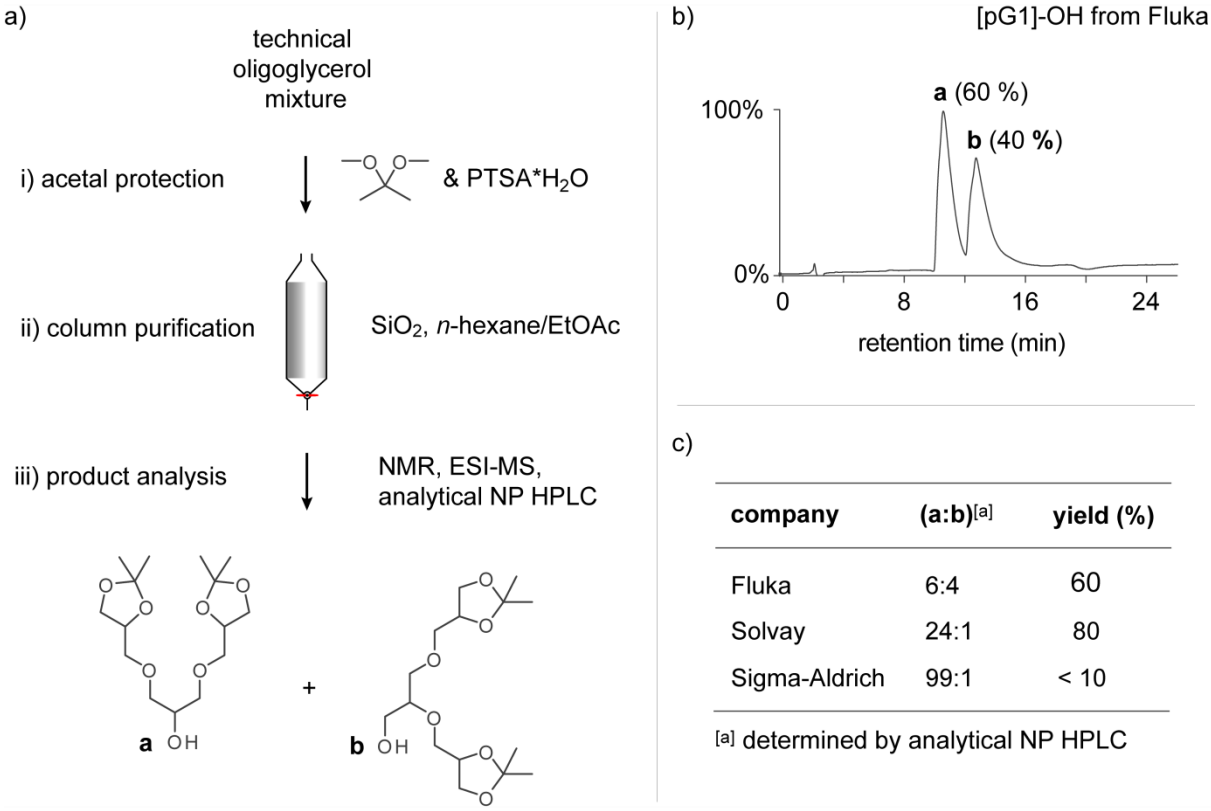

c)

company	(a:b)[a]	yield (%)
Fluka	6:4	60
Solvay	24:1	80
Sigma-Aldrich	99:1	< 10

[a] determined by analytical NP HPLC

Figure 4.2: Synthesis and NP HPLC analysis of [pG1]-OH. a) Applied procedure for the isolation of [pG1]-OH (**a**,**b**) from technical oligoglycerol. b) Chromatogram of [pG1]-OH upon isolation from Fluka oligoglycerol revealed significant proportions of two regioisomers. c) Regioisomer proportions (**a**:**b**) and overall yields (%) obtained from different oligoglycerol sources.

The synthesis of [pG1]-OH (**b**) started from DL-1,2-isopropylideneglycerol (Scheme 4.1). This material was benzylated under S_N2 conditions in DMF and the acetal protecting group of the obtained product [pG0]-OBn was removed under acidic conditions. The free hydroxyl groups of so-obtained [G0]-OBn were reacted with allyl bromide under basic conditions and the product [G0diallyl]-OBn was isolated by column chromatography.[26] The double bonds of this intermediate product were further dihydroxylated with potassium osmate dihydrat (K_2Os_4*$2H_2O$), trimethylamine N-oxide (TMANO), and citric acid using a procedure of Paulus *et al.*[163] Potassium osmate was removed upon complete dihydroxylation with an ion exchange resin (Lewatit K 6267) and the desired product [G1]-OBn was obtained upon column chromatography. The free hydroxyl groups of [G1]-OBn were subsequently acetal protected under acidic conditions using 2,2´-dimethoxypropane and PTSA*H_2O, and column purification gave [pG1]-OBn. To obtain the final product [pG1]-OH (**b**), the benzy-protecting group of [pG1]-OBn was removed under reductive conditions (Scheme 4.1). The first attempt to achieve the reductive removal of the benzyl-protecting group of [pG1]-OBn was performed by means of hydrogen gas (H_2) and palladium on carbon (Pd/C) in MeOH. TLC analysis revealed the complete consumption of the starting material upon 12 h, however, multiple by-products and only low product yields of about 20% for the desired [pG1]-OH (**b**) were observed upon column purification. This is not surprising since it is known that commercially available Pd/C catalysts can contain noticeable amounts of palladium(II) chloride.[164] This impurity can lead to the release of hydrochloric acid (HCl) when Pd/C is added to solvents, such as water or MeOH.

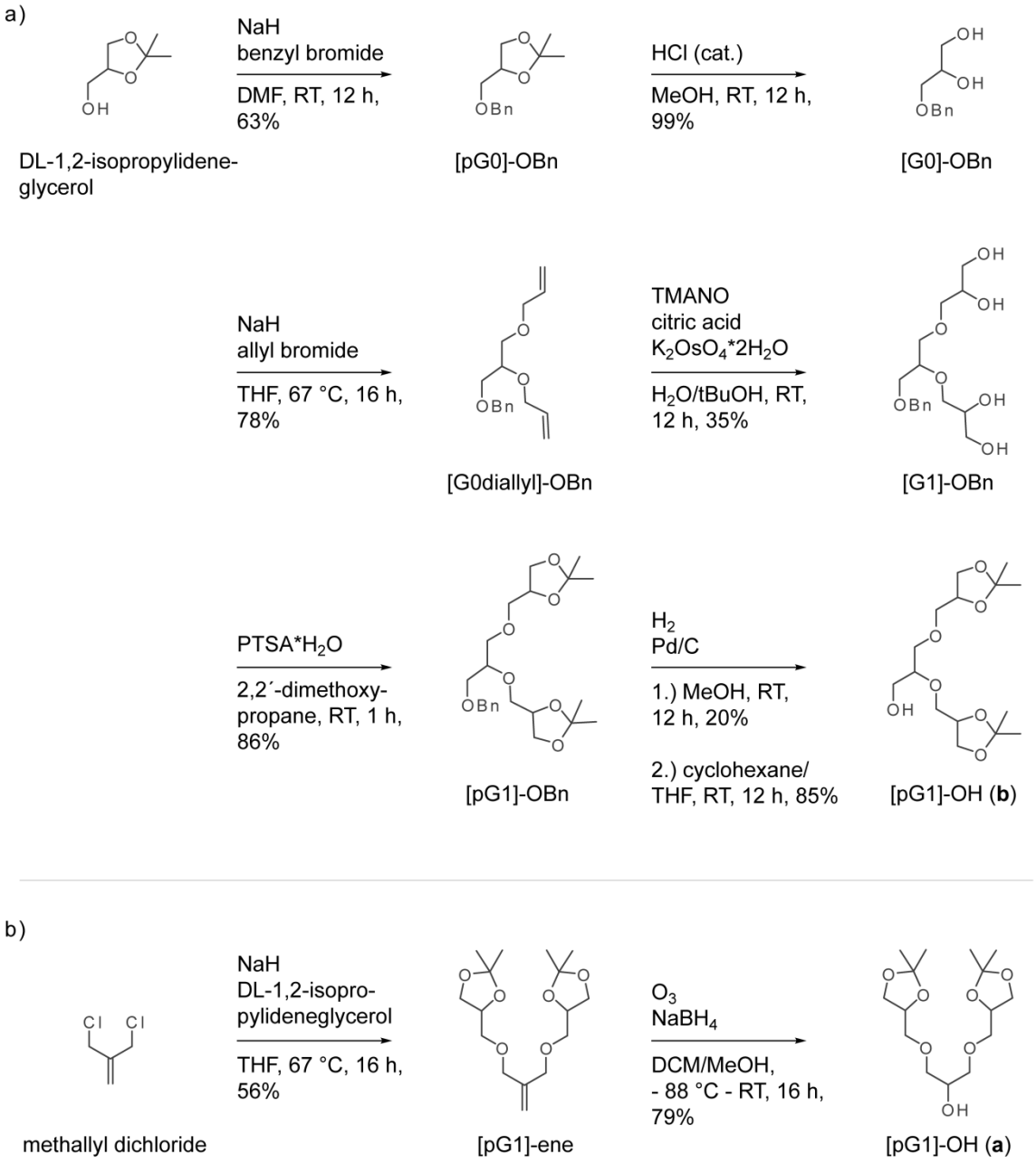

Scheme 4.1: Synthesis of individual [pG1]-OH regioisomers a) [pG1]-OH (**b**) and b) [pG1]-OH (**a**).

The release of hydrochloric acid in the presence of such protic solvents can trigger unintended side reactions, for example, the cleavage of acetal protecting groups. To circumvent this problem, the solvent conditions were changed to a mixture of THF and cyclohexane. As a consequence, the intensity of by-products noticed by TLC analysis was drastically reduced and the desired product [pG1]-OH (**b**) could be finally obtained upon column chromatography with good yields of about 85% (Scheme 4.1).

For the sake of completeness, also the individual regioisomer [pG1]-OH (**a**) was synthesized by using the so-called methallyl dichloride route (Scheme 4.1).[127] To do so, methallyl dichloride was reacted with two equivalents of DL-1,2-isopropylideneglycerol under basic conditions and the product [pG1]-ene was isolated by column chromatography.

The double bond of [pG1]-ene was then converted into an hydroxyl group *via* ozonolysis followed by a reductive work up using an excess of sodium borohydride. Purification by column chromatography gave the desired product [pG1]-OH (**a**) in good yields. Having synthesized both [pG1]-OH regioisomers (**a**, **b**), their $^{1}H/^{13}C$ NMR data were finally compared to those obtained from the regioisomers obtained upon HPLC separation.

The ^{1}H NMR spectrum of the individually synthesized derivative [pG1]-OH (**a**) showed five distinguishable signals between 4.5 – 3.2 ppm (Figure 4.3a). This was expected, because the aliphatic backbone consisted of two different methanetriyl groups (>CH-) and three methylene groups ($-CH_2-$).[127] This is also in line with the finding that five clearly separated signals were obtained in the ^{13}C NMR spectrum between 82 – 82 ppm.[127] The NMR data obtained from the reference compound [pG1]-OH (**a**) perfectly matched with those obtained from the first HPLC fraction (Figure 4.3a). Signals that arose from acetal-protecting groups are not considered in this discussion, because no pronounced differences between the two regioisomers were found.

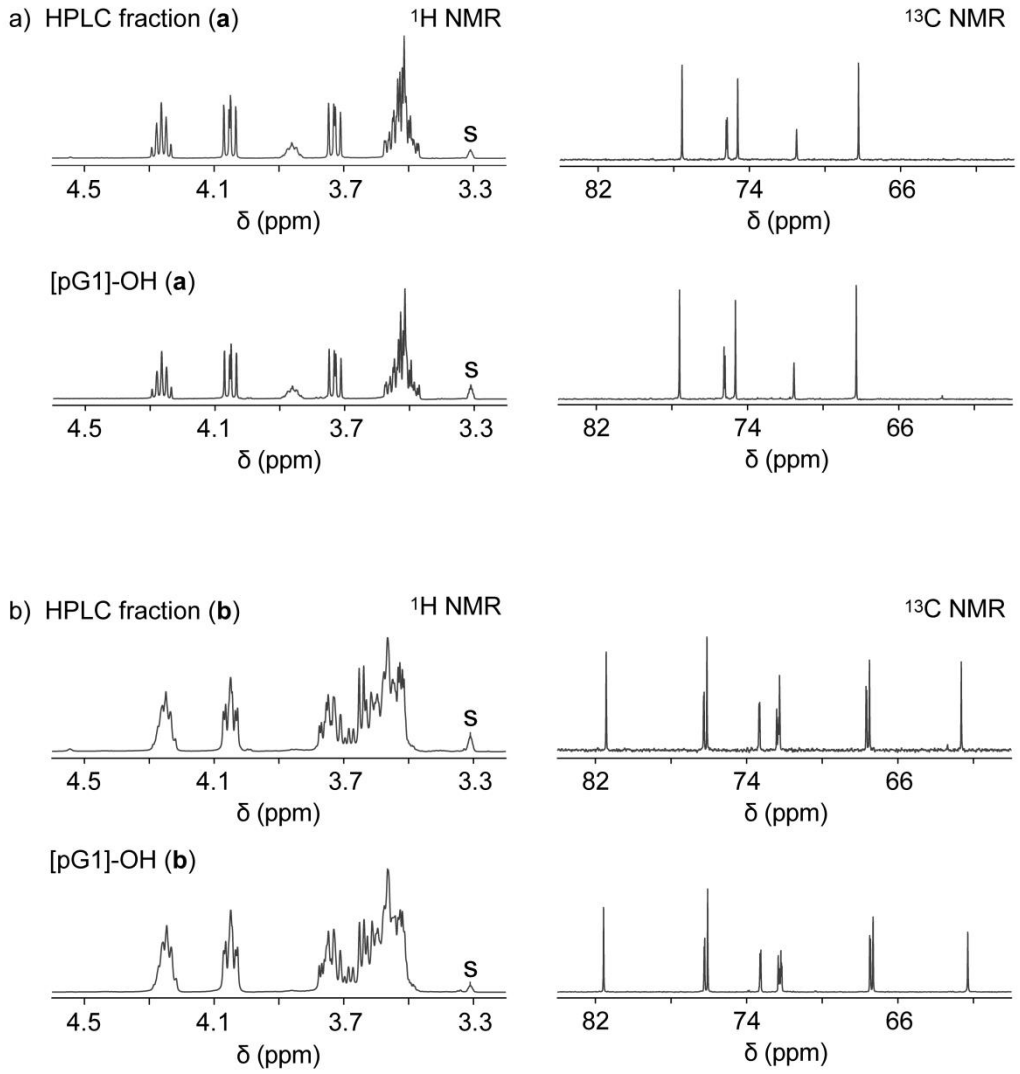

Figure 4.3: Comparison of $^{1}H/^{13}C$ NMR data between individually synthesized reference regioisomers [pG1]-OH (**a**, **b**) and the individual product fractions received from NP HPLC separation. Signals arising from [D4] MeOH are labeled with an **s**.

On the other hand, the backbone of [pG1]-OH (**b**) comprised three different methanetriyl groups (>CH-) and six different methylene groups (-CH_2-). Compared to [pG1]-OH (**a**), the ^{13}C NMR spectrum of [pG1]-OH (**b**) showed therefore a larger number of virtually distinguishable signals (Figure 4.3b). Due to strong overlapping signals, no useful conclusions concerning the structure of [pG1]-OH (**b**) could be drawn from the ^{1}H NMR spectrum (Figure 4.3b). However, the ^{1}H/^{13}C NMR data obtained from [pG1]-OH (**b**) perfectly matched with those obtained from the second HPLC fraction (Figure 4.3b). Taken together, the comparative fingerprint NMR analysis therefore confirmed the structural identity of both [pG1] OH (**a**,**b**) regioisomers, which were obtained upon acetal protection of technical oligoglycerol. Furthermore, splitting of individual ^{13}C NMR signals was observable (Figure 4.3). This indicated that the respective regioisomer batches contained different stereoisomers, which differed with respect to the orientation of the secondary hydroxyl groups. Previous studies on OGD stereoisomers showed that the orientation of hydroxyl groups within the head group could affect the aggregate morphology, which was formed by the self-assembly of OGDs.[142] For reasons of simplicity, this aspect was not further pursued during this work.

4.3.3 Synthesis of [G1] Oligoglycerol Detergents

For the preparation of the proposed [G1] OGD mixtures **1** – **3**, the free hydroxyl group at the focal points of the [pG1]-OH regioisomers (**a**, **b**) were either directly alkylated,[125] propargylated,[140] or converted into an amino group *via* three steps, which included mesylation,[127] azidation,[127] and reductive amination (Scheme 4.2).[27] For the preparation of the [G1] OGD mixture **1**, the regioisomer mixture [pG1]-OH (**a**:**b**, 6:4) was alkylated under S_N2 conditions at room temperature (RT) in dimethylformamide (DMF, Scheme 4.2a). Sodium hydride (NaH) was used as base and 1-bromododecane as alkylation reagent. The so-obtained product [pG1]-ether C12 (**a**:**b**) was purified by column chromatography. Subsequent cleavage of the acetal protecting groups using catalytic amounts of HCl and MeOH gave the final product mixture [G1]-ether-C12 (**a**:**b**, 6:4) **1**. The final regioisomer proportions were similar to those of the starting material, which indicated that they retained during synthesis and purification.

To obtain the [G1] OGD mixture **2** the focal points of the [pG1]-OH (**a**:**b**, 6:4) regioisomers were reacted with methanesulfonyl chloride (MsCl) in toluene and a slight excess of triethylamine (NEt_3) (Scheme 4.2b).[127] The product mixture obtained from this reaction was reacted with sodium azide (NaN_3) in DMF, which gave [pG1]-N_3 (**a**:**b**, 6:4). The reduction of the azide groups to amines was achieved by hydrogenation with H_2 and Pd/C in MeOH.[27] The so-obtained product [pG1]-NH_2 (**a**:**b**, 6:4) was reacted with dodecanoic acid by using a N-hydroxysuccinimide (NHS)-activated coupling strategy.[165] Dodecanoic acid and NHS were dissolved in dry DCM, the mixture was cooled down to 5 °C, and N,N'-dicyclohexylcarbodiimide (DCC) was added. [pG1]-NH_2 (**a**:**b**, 6:4) was added after one hour and the mixture was stirred overnight at RT. Column chromatography led to the obtainment of the desired [pG1]-amide-C12 (**a**:**b**) mixture. The final [G1]-amide-C12 (**a**:**b**, 6:4) **2** product mixture was obtained upon removal of the acetal protecting groups under acidic conditions. Similarly to the synthesis of [G1] ether-C12 (**a**:**b**, 6:4) **1**, the initial regioisomer proportions of [pG1]-OH (**a**:**b**, 6:4) retained over the individual synthesis and purification steps.

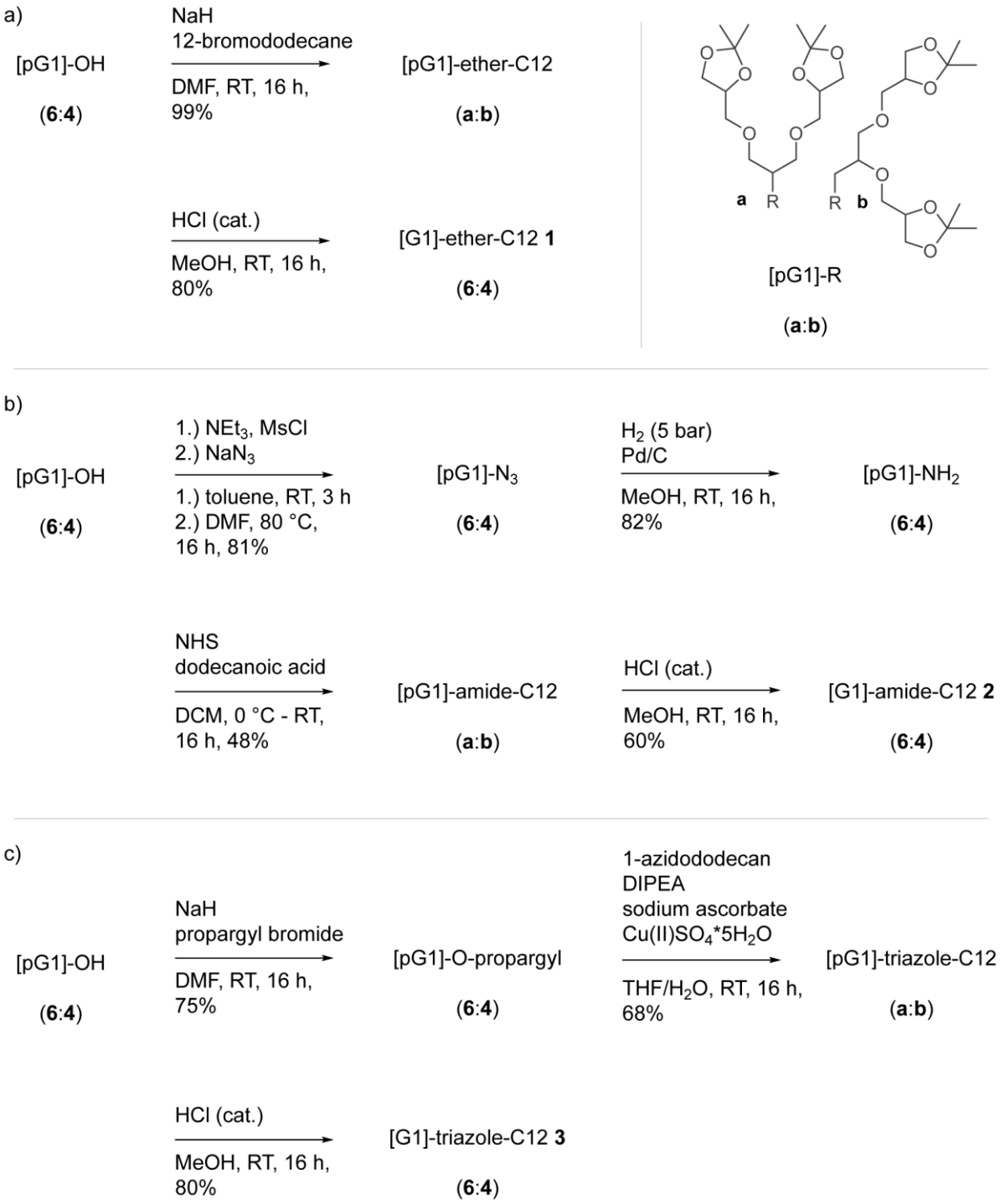

Scheme 4.2: Utilized reaction sequences that led to the obtainment of a) – c) different [G1] OGD regioisomer mixtures **1** – **3**. Regioisomer proportions that were not determined are labeled with (**a**:**b**). The general structures of the acetal-protected [pG1]-R regioisomers are shown exemplarily (top). The structures of the final products are shown in Figure 4.1.

The [G1] OGD mixture **3** was prepared by reacting [pG1]-OH (**a**:**b**, 6:4) with propargyl bromide under S_N2 conditions in DMF (Scheme 4.2c).[140] The obtained product mixture [pG1]-O-propargyl (**a**:**b**, 6:4) was purified by column chromatography and reacted subsequently with 1-azidododecane by using a modified procedure of Sharpless *et al.*[127, 140] To do so, the [pG1]-O-propargyl (**a**:**b**, 6:4) mixture and 1-azidododecane were suspended in THF and H_2O followed by the addition of N,N-diisopropyl-ethylamine (DIPEA), sodium ascorbate, and copper(II) sulfate penta-hydrate ($Cu(II)SO_4*5H_2O$). The desired [pG1]-triazole-C12 (**a**:**b**) was finally converted to [G1]-triazole-C12 (**a**:**b**, 6:4) **3** by cleaving the acetal protecting groups. The continuous HPLC or NMR analysis of almost all intermediates and final products indicated that the regioisomer proportions of [pG1]-OH (**a**:**b**, 6:4) retained during all functionalization and purification steps (Scheme 4.2). The obtained results demonstrated the great robustness of the regioisomer proportions against the applied synthesis and purifications procedures and that the here-mentioned literature procedures can be utilized for the synthesis of OGD regioisomer mixtures.

4.3.4 Synthesis and Characterization of [pG2]-OH Regioisomer Mixtures

The synthesis of the next higher generation of acetal-protected triglycerol [pG2]-OH was achieved in a convergent way (Scheme 4.3).[127] To do so, two equivalents of the [pG1]-OH (**a**:**b**, 6:4) regioisomer mixture were reacted with methallyl dichloride in THF and NaH was used as base. The resulting [pG2]-ene (**aa**:**ab**:**bb**, 4:4:1) regioisomer mixture was isolated by column chromatography and the double bond of [pG2]-ene was converted into a hydroxyl group by ozonolysis and reduction with sodium borohydride.[127] The product mixture [pG2]-OH (**aa**:**ab**:**bb**, 4:4:1) was subsequently isolated by column purification. The three suggested regioisomers of [pG2]-ene and [pG2]-OH exhibited similar focal point structures, respectively, and differed with respect to the structure of their triglycerol side chains (**aa**, **ab**, **bb**, Scheme 4.3).The individual regioisomers were first characterized for [pG2]-OH (**aa**, **ab**, **bb**). To do so, individual reference isomers [pG2]-OH (**aa** and **bb**) were prepared and the three [pG2]-OH samples were analyzed by automated NP HPLC and $^1H/^{13}C$ NMR. The chromatograms obtained from [pG2]-OH (**aa**, **ab**, **bb**) and [pG2]-OH (**aa**) looked very similar and a quantification of the regioisomer content by analytical NP HPLC was therefore hampered under the employed experimental conditions (Figure 8.22, Appendix).

The three samples [pG2]-OH (**aa**), [pG2]-OH (**bb**), and [pG2]-OH (**aa**, **ab**, **bb**) were subsequently analyzed by NMR spectroscopy. The ^1H NMR signals observed between 4.3 – 4.0 ppm exhibited similar chemical shifts and were similarly shaped (Figure 4.4a-c). Furthermore, strong overlapping signals were obtained between 3.9 – 3.5 ppm. Although each signal pattern exhibited an individual shape, it was very difficult to draw meaningful conclusions concerning the structural identity of each sample. Signals that arose from acetal protecting groups are again not considered in this discussion, because no pronounced differences between the three regioisomers could be found.

On the other hand, the ^{13}C NMR spectra looked remarkably different (Figure 4.4a-c). For example, the spectrum obtained from [pG2]-OH (**aa**) showed seven different signals, while the spectrum of [pG2]-OH (**bb**) showed eleven virtually distinguishable signals. The number of individual signals was in line with the number of different -CH- and $-CH_2-$ groups of their individual glycerol backbones.

The spectrum obtained from the proposed [pG2]-OH (**aa**, **ab**, **bb**) regioisomer mixture reflected spectral features of both isomers (Figure 4.4c). This provided first evidence that the two reference isomers [pG2]-OH (**aa**, **bb**) were part of the [pG2]-OH (**aa**, **ab**, **bb**) mixture. Interestingly, ^{13}C NMR signals that arose from their focal points appeared between 71.2 – 70.4 ppm. Comparing the ^{13}C NMR spectrum of [pG2]-OH (**aa**) with that of [pG2] OH (**bb**) revealed a small shift of the focal point signal of about one ppm (Figure 4.4a-b). This showed that both regioisomers can be differentiated by ^{13}C NMR, particularly, by analyzing the chemical shifts their focal point signals. The focal point signals of both reference isomers appeared also in the spectrum of the proposed [pG2]-OH (**aa**, **ab**, **bb**) mixture. Interestingly, a third signal appeared between those of [pG2]-OH (**aa**) and [pG2]-OH (**bb**), which could be explained by the presence of the third regioisomer [pG2]-OH (**ab**, Figure 4.4c).

The regioisomer proportions [pG2]-OH (**aa**:**ab**:**bb**, 4:4:1) calculated from the relative focal point signal intensities showed that the sample mainly contained [pG2]-OH (**aa**) and [pG2]-OH (**ab**) and only minor amounts of [pG2]-OH (**bb**). The focal point analysis of the precursor [pG2]-ene revealed a similar intensity pattern, which indicated that three regioisomers [pG2]-ene (**aa**, **ab**, **bb**) were formed during the reaction between [pG1]-OH (**a**:**b**, 6:4) and methallyl dichloride (Figure 8.10, Appendix). During the course of the reaction, mainly [pG2]-ene (**aa**) and [pG2]-ene (**ab**) and only minor amounts of [pG2]-ene (**bb**) were formed. Furthermore, the data indicated that the regioisomer proportions of [pG2]-ene fully retained during conversion to [pG2]-OH and purification.

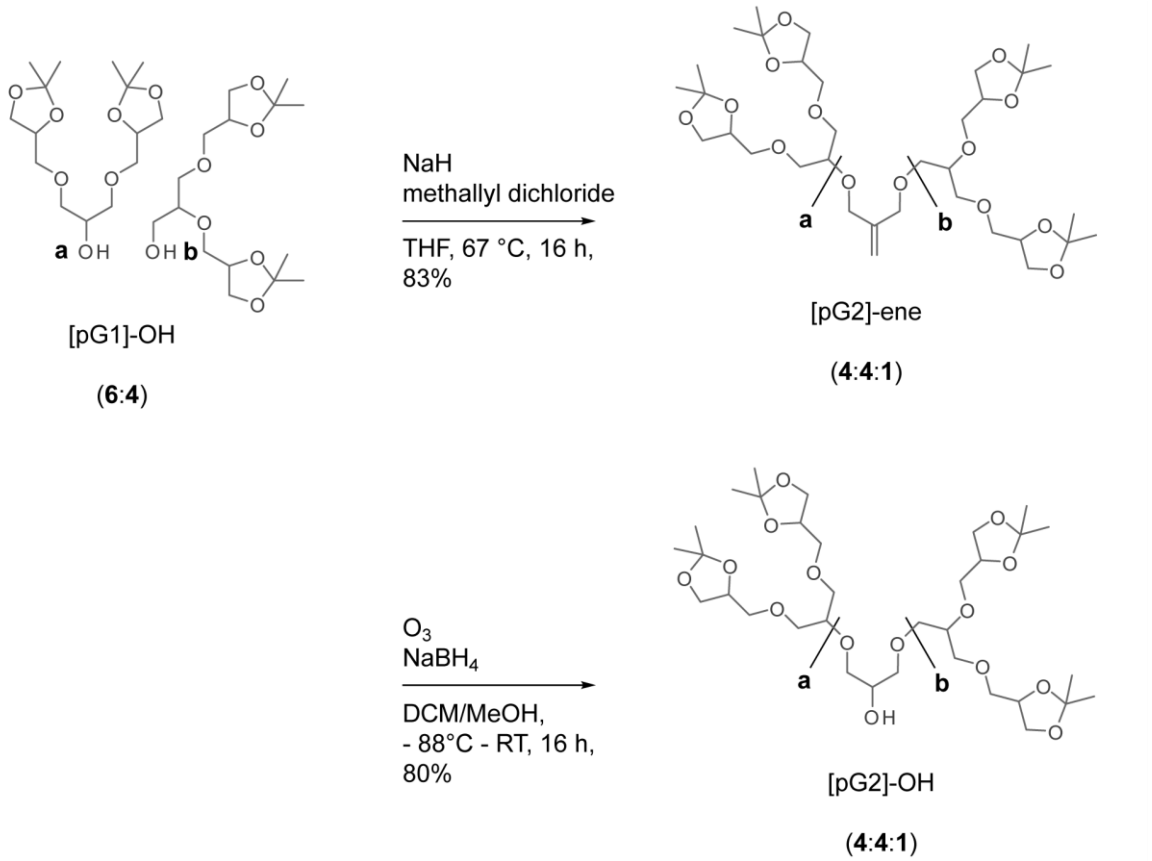

Scheme 4.3: Synthesis of a [pG2]-OH (**aa**:**ab**:**bb**) regioisomer mixture. Three regioisomers of [pG2]-ene were obtained (**aa**:**ab**:**bb**), which differ with respect to the structure of their side chains. The regioisomer proportions retained during conversion to [pG2]-OH. The mixed isomers [pG2]-ene (**ab**) and [pG2]-OH (**ab**) are shown exemplarily.

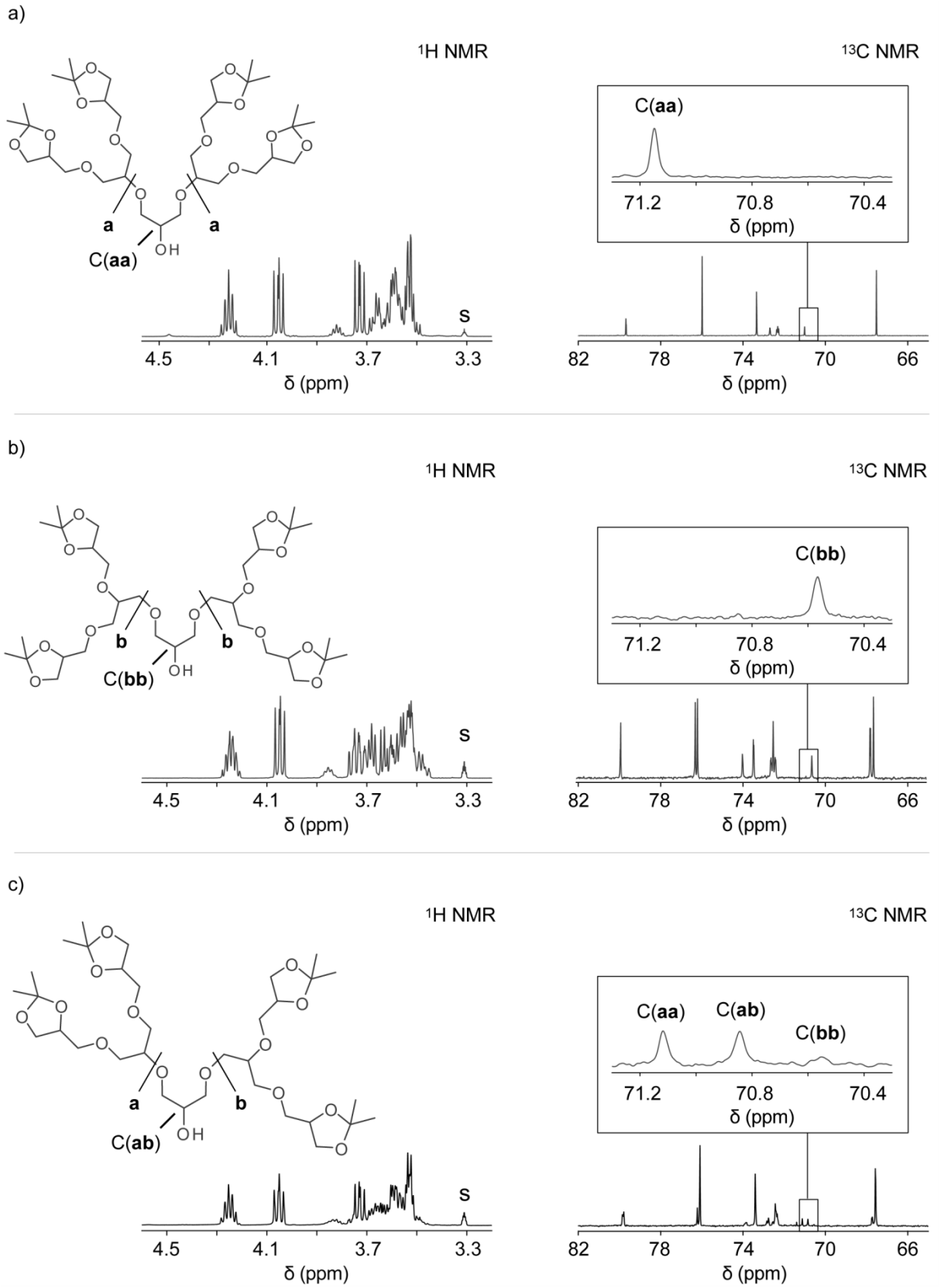

Figure 4.4: $^{1}H/^{13}C$ NMR spectra obtained from a) [pG2]-OH (**aa**), b) [pG2]-OH (**bb**), and c) the regioisomer mixture [pG2]-OH (**aa**, **ab**, **bb**). Regioisomers could be differentiated by their ^{13}C focal point signals, *e.g.*, C(**aa**), C(**ab**), or C(**bb**). Signals of [D4] MeOH are labeled with **s**.

At least two explanations are available that help to explain the asymmetric distribution among the different regioisomers of [pG2]-ene (**aa**:**ab**:**bb**, 4:4:1): First, the focal points of the two [pG1]-OH regioisomers exhibited either a secondary hydroxyl group (**a**) or a primary hydroxyl group (**b**). The secondary alkoxyde of [pG1]-OH (**a**) that was formed upon deprotonation with NaH was possibly more nucleophilic than the alkoxyde formed by [pG1]-OH (**b**). This may facilitated the formation of [pG2]-ene (**aa**, **ab**) under the chosen conditions. Second, the amount of [pG1]-OH (**a**) within the starting material was higher than that of [pG1]-OH (**b**), which possibly promoted the formation of the regioisomers [pG2]-ene (**aa**) and [pG2]-ene (**ab**), too.

4.3.5 Synthesis of [G2] Oligoglycerol Detergents

In the penultimate part of this chapter, synthetic procedures that lead to obtaining the [G2] detergent mixtures **4** – **8** are described. Having established the synthesis of [pG2]-OH (**aa**, **ab**, **bb**), the free hydroxyl groups at the focal points of the [pG2]-OH regioisomers were first connected to C18 chains *via* ether, amide or, triazole groups to obtain **4** – **6** (Scheme 4.4). For this purpose, the regioisomer mixture of [pG2]-OH (**aa**:**ab**:**bb**, 4:4:1) was either alkylated,[125] propargylated,[140] or converted into an amino group by using the before-mentioned literature procedures.[27, 127]

For the synthesis of the [G2] OGD mixture **4**, the regioisomer mixture [pG2]-OH (**aa**:**ab**:**bb**, 4:4:1) was deprotonated with NaH in DMF and subsequently reacted with 18-bromooctadecane (Scheme 4.4a). First, the reaction was run at RT for 16 hours, which led to the product [pG2]-ether-C18 only with low yields (<10%). Significantly better results were obtained when the reaction was performed at 80 °C. Here, the product [pG2]-ether-C18 (**aa**:**ab**:**bb**) could be isolated by column purification with a yield of 68%. The acetal protecting groups were subsequently removed under acidic conditions to obtain the product [G2]-ether-C18 (**aa**:**ab**:**bb**, 4:4:1) **4**. Similarly to the before-described synthesis of [G1]-ether-C12 (**a**:**b**, 6:4) **1**, the initial regioisomer proportions retained.

The synthesis of the [G2] OGD **5** was afforded within four steps (Scheme 4.4b). First, the [pG2]-OH (**aa**:**ab**:**bb**, 4:4:1) regioisomer mixture was reacted with MsCl and a slight excess of NEt_3 in toluene.[127] The obtained product was dissolved in DMF and reacted with NaN_3. The product mixture obtained from this reaction [pG2]-N_3 (**aa**:**ab**:**bb**, 3:4:1) was further converted to [pG2]-NH_2 (**aa**:**ab**:**bb**, 4:4:1) under reductive conditions using H_2 and Pd/C.[27] The latter was reacted with stearoyl chloride under basic conditions in dichloromethane (DCM). The resulting product [pG2]-amide-C18 (**aa**:**ab**:**bb**) was isolated and cleavage of the acetal protecting groups under acidic conditions gave the desired product mixture [G2]-amide-C18 (**aa**:**ab**:**bb**, 4:4:1) **5**.

After this, the [G2] OGD mixture **6** was prepared (Scheme 4.4c). First, the [pG2]-OH (**aa**:**ab**:**bb**, 4:4:1) regioisomer mixture was reacted with propargyl bromide in DMF under basic conditions. The product mixture [pG2]-O-propargyl (**aa**:**ab**:**bb**, 4:4:1) was coupled with 1-azido-octadecane using a modified procedure of Sharpless *et al.*[127, 140] [pG2]-triazole-C18 (**aa**:**ab**:**bb**) was then deprotected under acidic conditions to give the final [G2] OGD mixture [G2]-triazole-C18 (**aa**:**ab**:**bb**, 1:2:1) **6**. Here, a significant deviation from the initial regioisomer proportions was obtained. Similarly to the other OGD mixtures, the product **6** was purified by RP HPLC. The shapes of the eluted peaks were usually very broad for [G2] OGDs and differences during the manual peak fractioning procedures could have affected the regioisomer proportions.

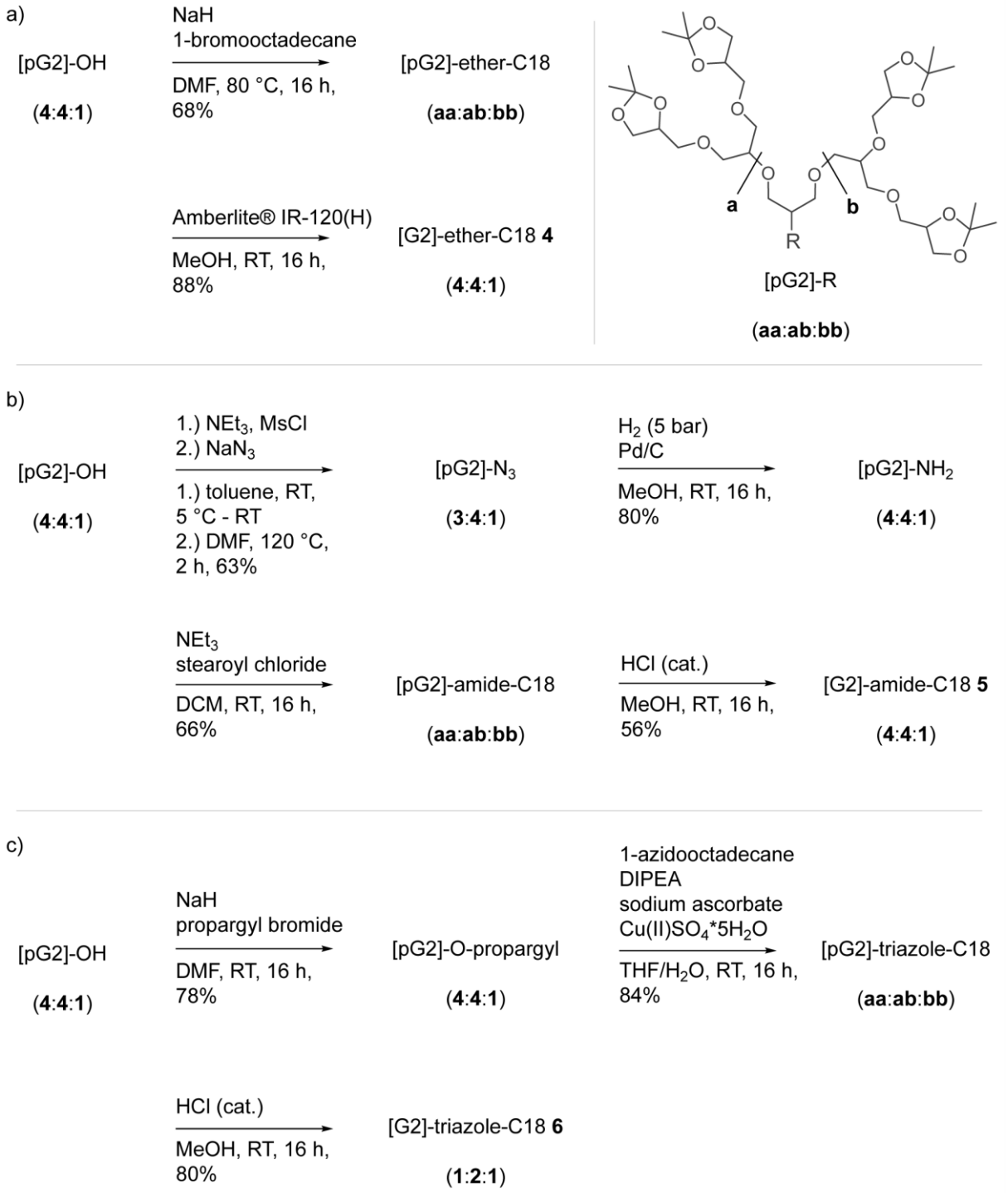

Scheme 4.4: Utilized reaction sequences that led to the obtainment of a) – c) different [G2] OGD regioisomer mixtures **4** – **6**. Regioisomer proportions that were not determined are labeled with (**aa**:**ab**:**bb**). The general structure of an acetal-protected regioisomer [pG2]-R (**ab**) is shown exemplarily. The structures of the final products are shown in Figure 4.1.

The next [G2] OGD mixture **7** was obtained from a reaction of the [pG2]-NH_2 (**aa**:**ab**:**bb**, 4:4:1) mixture with cholesterol chloroformate (Scheme 4.5). To do so, cholesterol chloroformate was dissolved in dry DCM and NEt_3 was added. The [pG2]-NH_2 (**aa**:**ab**:**bb**, 4:4:1) mixture was subsequently added and the mixture was stirred for 16 hours at RT. The reaction mixture was directly subjected to column purification, which gave the desired product [pG2]-carbamate-Chol (**aa**:**ab**:**bb**). Removal of the acetal protecting groups led to the desired product [G2]-carbamate-Chol (**aa**:**ab**:**bb**, 9:5:1) **7**.

Finally, the [G2] detergent mixture **8** was synthesized according to a procedure of Thota *el at.* (Scheme 4.5).[140] For this purpose, the [pG2]-O-propargyl (**aa**:**ab**:**bb**, 4:4:1) mixture was suspended with dodecanoic acid, 2-azido-1,3-propanediyl ester in THF and H_2O followed by the addition of DIPEA, sodium ascorbate and Cu(II)SO_4*5H_2O. The product [pG2]-triazole-DC12 (**aa**:**ab**:**bb**) was isolated by means of column chromatography. The acetal protecting groups were removed under acidic conditions with Amberlite® IR-120(H) and MeOH. The desired product [G2]-triazole-DC12 (**aa**:**ab**:**bb**, 9:5:1) was obtained upon RP HPLC purification. The regioisomer proportions of **7** and **8** were different to that of the respective starting material and were most likely affected by preparative RP HPLC purification.

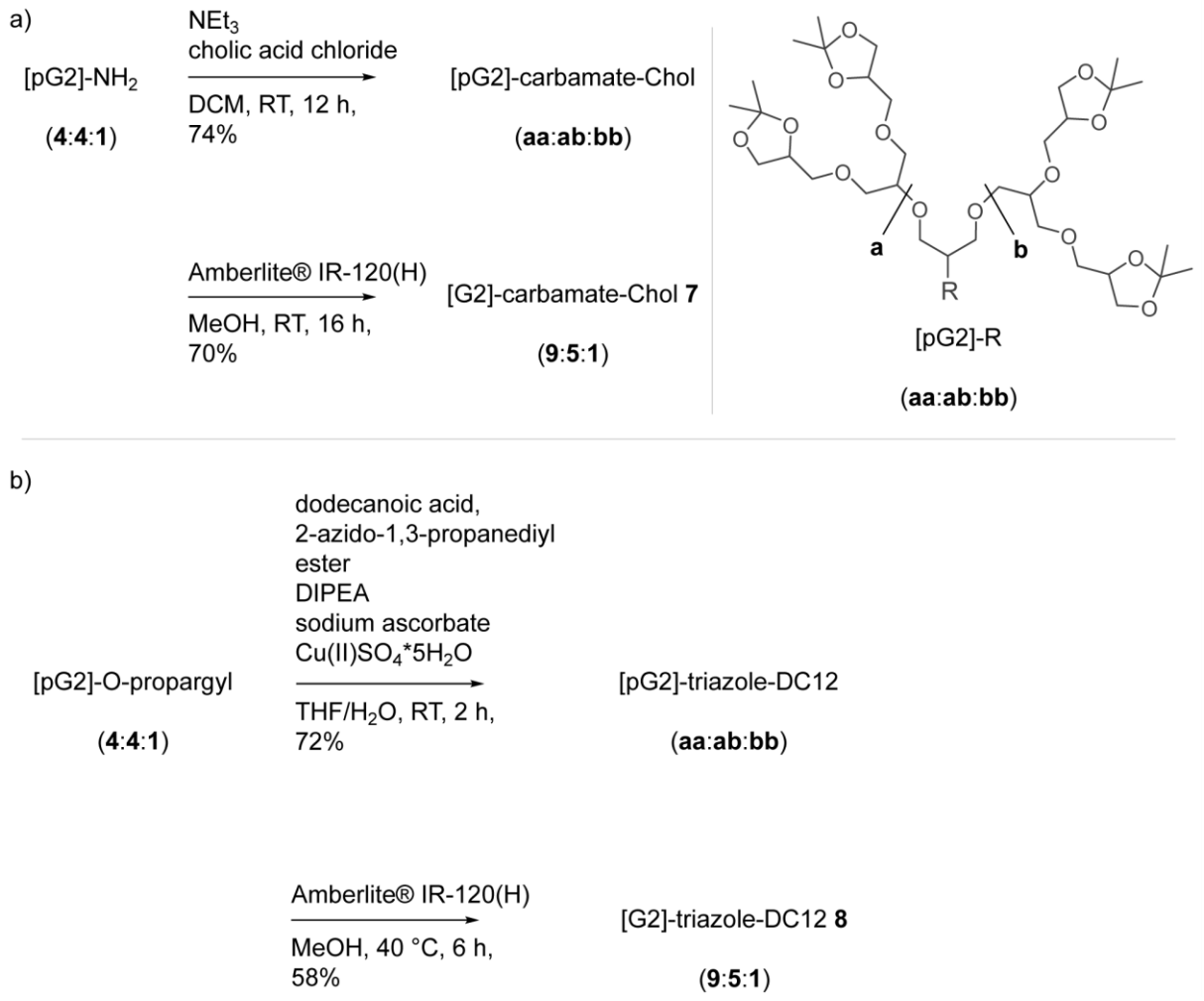

Scheme 4.5: Utilized reaction sequences that were applied for the preparation of [G2] OGD mixtures a) **7** and b) **8**. Regioisomer proportions that were not determined are labeled with (**aa**:**ab**:**bb**). The general structure of an acetal-protected regioisomer [pG2]-R (**ab**) is shown exemplarily (top). The structures of the final products are shown in Figure 4.1.

4.4 Conclusions

In summary, the synthesis of a new library of OGDs was introduced, which consisted of [G1] and [G2] OGD head group regioisomer mixtures, different linker groups, and hydrophobic tails. The data showed that literature procedures that were available for the synthesis of individual OGD regioisomers could be also utilized for the synthesis of OGD regioisomer mixtures. The required starting material for OGD synthesis, *e.g.*, regioisomer mixtures of [pG1]-OH, could be obtained in one step by acetal protection of technical oligoglycerol. The obtained regioisomer proportions depended significantly on the commercial oligoglycerol source and could fluctuate along the synthesis of [G2] OGDs. Liquid chromatography methods and NMR data that were developed in this thesis can help to validate the regioisomer proportions during all stages of synthesis. This will facilitate the quality control of OGD synthesis in future.

The enormous potential of the here-presented OGD library relies on its modular design, which will allow one to systematically investigate the impact of the molecular detergent structure on the OGDs' utility to purify membrane proteins and to facilitate their analysis by native MS. Furthermore, the here presented OGD library provides the unique ability to evaluate the benefit of OGD regioisomer mixtures over individual OGD regioisomers for protein purification and native MS applications.

5. Chapter II – The Potential of Oligoglycerol Detergents for Protein Mass Spectrometry

5.1 Introduction

Nanoelectrospray ionization-mass spectrometry (nESI-MS) is a valuable tool for the structural investigation of membrane proteins. Mixtures of membrane proteins and detergent aggregates can be transferred into the vacuum of a mass spectrometer by means of nESI, where the excess of the detergent is subsequently removed *via* thermal activation.[75] The increase in internal energy in complexes formed between membrane proteins and detergents mainly dissipates through the loss of detergent molecules, which can protect the protein structure from perturbation even under very harsh MS instrument conditions.[15, 16] The ability to gently transfer membrane protein complexes to the vacuum of a MS instrument is useful not only for the elucidation of unknown subunit stoichiometry, but also for the assessment of the structural impact of small non-covalently bound ligands, such as nucleotides, drugs, or lipids.[11, 13] The activation conditions required for detergent removal and the charge state of the released protein are important parameters for the preservation of native-like protein structures.[14] High protein charge states together with high collisional activation promote Coulomb-driven unfolding of the protein, whereas low charge states in combination with soft release conditions are more likely to yield compact structures and to maintain a native membrane protein subunit stoichiometry.[17]

Recent results showed that the chemical nature of detergents altered the charge states of membrane proteins significantly.[14] Membrane proteins that are released from saccharide detergents, for example, exhibit high charge states that are close to the Rayleigh-limit of charged nESI droplets. Detergents based on tetraethylene glycol or amine N-oxide, on the other hand, exhibit strong charge-reducing properties and are removed in vacuum under gentle activation conditions. Furthermore, literature data provide strong evidence that membrane protein charge states can be reduced by the addition of basic solution additives or organic solvents, such as imidazole and acetonitrile.[17, 102]

In this chapter, it is investigated if membrane protein charge reduction can be enabled by tuning the structure of OGDs. For this purpose, a diverse set of OGD regioisomer mixtures **1** – **6** was chosen, which comprised regioisomer mixtures derived from first [G1] and second [G2] generation oligoglycerol dendron, linker groups with different basicities (ether, amide, and triazole), and two different alkyl spacers (C12 and C18, Figure 5.1). The structural diversity of **1** – **6** relied mainly on the size of their dendritic oligoglycerol head groups and hydrophobic tail and the chemical nature of the linker that was embedded in-between.

Membrane proteins, however, present an exceptionally challenging class of biomolecules which are occasionally difficult to handle and expensive to manufacture. The size of a new detergent library can be a limiting factor for the fast and efficient flow of detergent screenings. To allow one to identify charge-reducing detergents in advance, a tandem mass spectrometry (MS/MS) approach was introduced that helps to evaluate the charge-reducing properties of OGDs without the consumption of expensive membrane protein samples.

For this purpose, three soluble proteins were assessed as model systems for the investigation of defined protein-detergent complexes (PDCs) by MS/MS: two hydrophilic proteins, ubiquitin (8.5 kDa) and myoglobin (16.9 kDa) which are known to not bind detergents in solution under native conditions, and ß-lactoglobulin (BLG, 18.4 kDa), a more amphiphilic protein that is suggested to play an important role in the transport of amphiphilic molecules.[166] In line with this suggestion, it was found that BLG exhibits a greater propensity to form PDCs upon nESI than ubiquitin or myoglobin. Systematic MS/MS experiments on singly bound PDCs formed between BLG and **1** – **6** revealed how the distinct building blocks or functional groups of OGDs mediate the removal of sodium ions and protons from protein ions during PDC dissociation. Finally, it is discussed how far the results received from the MS/MS approach are transferable to membrane proteins.

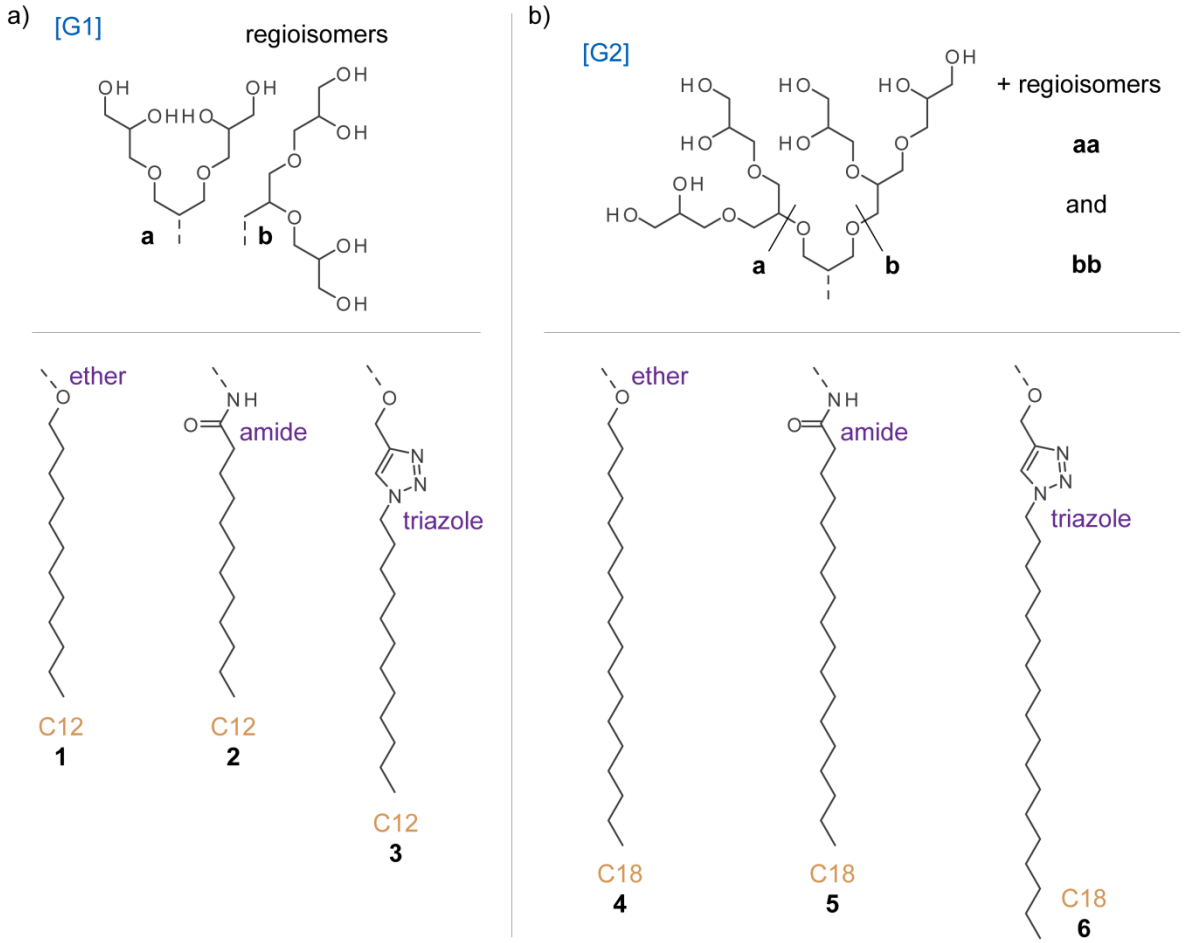

Figure 5.1: Library of a) [G1] and b) [G2] OGD regioisomer mixtures **1** – **6** to be explored for tuning of protein charge states and the solubilization of membrane proteins. The [G1] OGD mixtures **1** – **3** and [G2] OGD mixtures **4** – **6** comprise different head group regioisomers, hydrophobic tails, and different connecting linkers, such as ether-, amide, and triazole groups.

5.2 Experimental Details

Materials and Reagents

All chemicals, solvents and buffers were purchased from Merck (Germany), Sigma Aldrich (Germany), Alfa Aesar (Germany) and Fluka (Germany). The OGDs **1** – **6** were synthesized as discussed before in Chapter 4.3.

Preparation of Mixtures between Soluble Proteins and Detergents

Soluble proteins, *e.g.*, ubiquitin, myoglobin, and BLG, were dissolved in ammonium acetate (10 mM) buffer to a final concentration of 1 mg/mL. The protein samples (500 µL) were then loaded into Amicon-Ultra 0.5 mL centrifugal devices (Merck Millipore, Germany). The molecular weight cut-off (MWCOs) of the centrifugal devices was adjusted to the molecular weight of ubiquitin (MWCO = 3 kDa), myoglobin, and BLG (MWCO = 10 kDa). The samples were concentrated (14000 x g, 10 min) using a Heraeus Pico 17 centrifuge (Thermo-Scientific, USA), diluted with ammonium acetate buffer (10 mM) to a final volume of 500 µL, and concentrated again. This procedure was repeated five times. The protein concentration was determined upon the final centrifugation step by means of UV/VIS spectroscopy using the molar extinction coefficients at 280 nm of ubiquitin (1490 $M^{-1}\cdot cm^{-1}$), myoglobin (holo form) (13940 $M^{-1}\cdot cm^{-1}$), and BLG (17600 $M^{-1}\cdot cm^{-1}$).[167-169] Equimolar protein detergent mixtures (1:1, 50 µM) were prepared by appropriate dilution to generate a 1:1 complex stoichiometry and the samples were subjected to nESI-MS analysis. The sample conditions, including protein concentration, buffer concentration, and concentration of the amphiphilic molecule, were adapted from Seo *et al*.[170]

Nanoelectrospray Ionisation Mass Spectrometry

Mass spectra were measured in positive ion mode using a modified Ultima high-mass quadrupole-time of flight (Q-ToF) mass spectrometer (Waters Micromass, Manchester, UK) equipped with a Z-spray nanoflow nESI ionization source.[13] The required borosilicate capillaries were prepared according to a previously described procedure.[171] Data acquisition and analysis were performed by means of MassLynx (V4.1). Capillary voltage (1.2 kV), cone voltage (35 V), RF lens (50 V), collision gas pressure (P_{argon} ~ $5\cdot10^{-3}$ mbar), and collision voltage (2 V) were adjusted to optimize the intensity of singly bound protein-detergent complexes (PDCs) in the *m/z* range between 200 and 5000. The sample conditions and instrumental parameters are summarized in Scheme 5.1. External *m/z* calibration was performed by means of CsI solutions (20 mg/mL, H_2O:isopropanol, *v*:*v*, 1:1). The intensities obtained from the individual protein signals (apo form) were extracted from the mass spectra and plotted as a function of the protein charge state. The data were fitted to a Gaussian function and the charge state (x-value) at maximum intensity was taken as the average charge state (z_{ave}). Supplementary data are provided in Chapter 8.5 (Appendix).

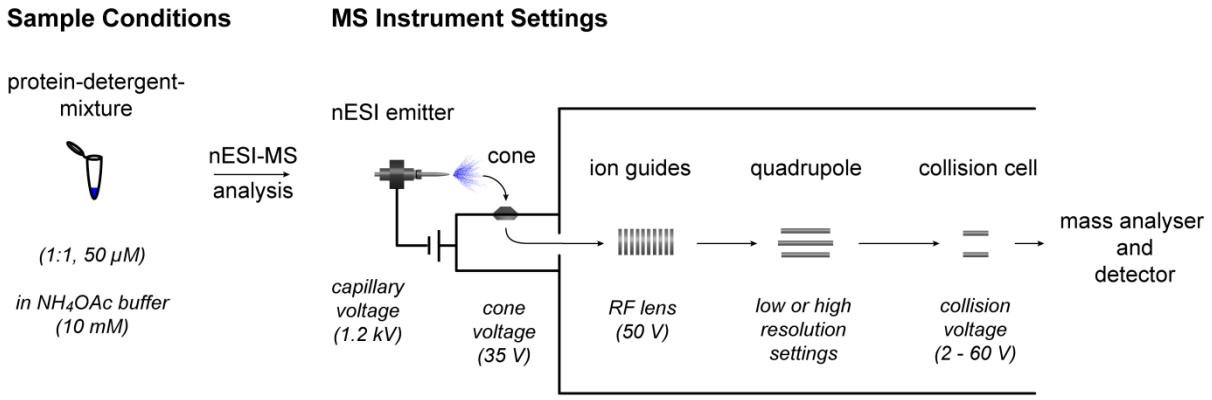

Scheme 5.1: Sample conditions and instrument settings applied for the investigation of PDCs in the vacuum of a MS instrument. Argon was used as collision gas ($5x10^{-3}$ mbar).

Detergent Exchange and nESI-MS Experiments with Membrane Proteins

Detergent exchange experiments were performed with OmpF which was purified before in the reference detergent octyl β-D-glucopyranoside (OG). The purified OmpF sample was a gift from PhD Joseph Gault. Detergent exchange from OG to **1** – **6** was performed by means of gel filtration chromatography. As stationary phase a pre-packed Superdex 200 10/300 GL column (GE Healthcare, product number: 17-5175-01) was used, which was operated with a ÄKTA setup. Detergent-containing ammonium acetate buffer (200 mM) with OGD concentrations of about one or two times of its *cac* were used as the mobile phase (Table 5.1). The eluted protein samples were concentrated using Amicon-Ultra 0.5 mL centrifugal devices (MWCO = 150 kDa) prior to their nESI-MS analysis using a modified Q Exactive nESI-MS instrument (Thermo-Scientific).[92, 172] This instrument was operated by Idlir Liko. Data analysis and processing was performed with Xcalibur (v2.2) and OriginPro (v9.1). The z_{ave} values were calculated as described above for soluble proteins.

Critical Aggregation Concentration of OGDs

The *cac* values of the OGDs **1** – **6** were determined by means of dynamic light scattering (DLS) according to a procedure of Skhiri *et al.*[173] Serial dilutions with OGD concentrations between 10^{-8} and 10^{-2} M were prepared in MilliQ water. The samples were filtered (RC, 0.2 µm) and equilibrated for 16 hours at RT prior to their analysis. The samples were transferred into a quartz cuvette (material: Quarz Suprasil, width x length: 2 mm x 10 mm) and analyzed with a Zetasizer Nano-ZS ZEN3600 (Malvern, UK). The instrument was operated with the Zetasizer Software (v7.11) and the following acquisition parameters were used:

Material: Polystyrene Latex
Dispersant: Water
Sample viscosity parameters: Use dispersant viscosity as sample viscosity
Temperature: 22.5 °C
Equilibration time: 120 seconds
Cell type: Quarz cuvettes
Measurement angle: 173° Backscatter

Measurement duration: Manual
Number of runs: 11
Run duration: 10 seconds
Number of measurements: 3
Delay between the measurements: 0 seconds
Data processing: General purpose (normal resolution).

The derived count rate values obtained from three measurements (per concentration) were averaged and the logarithm of the derived count rate average was plotted against the logarithm of the concentration (Figure 5.2).[173] The double logarithmic plots showed two characteristic regions: a) at flat regions with low count rates at lower OGD concentrations and b) a linear growth in the derived count rate at higher OGD concentrations (Figure 5.2). The individual regions were fitted to linear functions and the *cac* value was calculated from their intersection (x-value). These values are summarized in Table 5.1. Supplementary data are provided in Chapter 8.4 (Appendix).

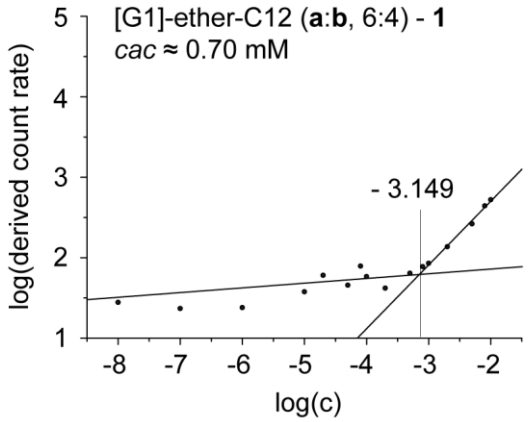

Figure 5.2: Double logarithmic plot of the derived count rate average against the concentration obtained from the OGD mixture [G1]-ether-C12 (**a**:**b**, 6:4) **1**. The derived count rate average was determined by dynamic light scattering (DLS). The intersection between the linear fit and the baseline was taken as the *cac*.

Table 5.1: Summary of *cac* values of the OGD batches **1** – **6** that were determined by DLS.

[G1] OGD mixture	***cac* (mM)**	**[G2] OGD mixture**	***cac* (mM)**
[G1]-ether-C12 (**a**:**b**, 6:4) **1**	0.70	[G2]-ether-C18 (**aa**:**ab**:**bb**, 4:4:1) **4**	0.30
[G1]-amide-C12 (**a**:**b**, 6:4) **2**	0.30	[G2]-amide-C18 (**aa**:**ab**:**bb**, 4:4:1) **5**	0.32
[G1]-triazole-C12 (**a**:**b**, 6:4) **3**	0.55	[G2]-triazole-C18 (**aa**:**ab**:**bb**, 1:2:1) **6**	0.28
[G1]-triazole-C12 (**a**) **3a**	0.47		
[G1]-triazole-C12 (**b**) **3b**	0.39		

5.3 Results and Discussion

5.3.1 Mass Spectra of Mixtures between OGDs and Soluble Proteins

In order to evaluate the charge reducing-properties of OGDs without consuming expensive membrane protein samples, the dissociation behavior of PDCs formed with soluble proteins was investigated. For this purpose, it was first necessary to identify a soluble protein that showed sufficient binding to detergent molecules upon nESI. Therefore, equimolar mixtures of the non-ionic [G1] OGD mixture **1** with ubiquitin, myoglobin, and BLG were analyzed by nESI-MS. The mixtures were transferred into the vacuum by nESI from ammonium acetate buffer (10 mM) under instrumental conditions chosen to optimize the intensity of PDC signals (Scheme 5.1, Experimental Details). First, ubiquitin and myoglobin were tested. The mass spectra revealed low average charge states (z_{ave}) for ubiquitin (5+) and myoglobin (8+, Figure 5.3a-b, respectively), which is commonly observed for both proteins under native MS conditions.[170, 171] Because only minor amounts of PDCs were observed, the mass spectra looked remarkably similar to previously reported data from detergent-free protein samples.[174, 175] In contrast to the data obtained from ubiquitin and myoglobin, the mass spectrum of BLG showed three monomeric protein species that corresponded to BLG bearing either no, one, or two covalently attached lactose moieties.[176] For all monomeric forms of BLG, the formation of PDCs was obtained (Figure 5.3c). The z_{ave} of BLG (7+) was equally low as in the cases of ubiqutin and myoglobin.[170]

For myoglobin and ubiquitin, no complex formation with non-ionic detergents in solution has been reported to date. Due to the high analyte concentration (50 µM) it is very likely that the obtained PDCs originated simply from non-specific adduct formation during the nESI process.[85] This implies that simply higher detergent concentrations are needed to maximize the PDC intensity, which is in line with previous observations.[177, 178] The outstanding propensity of BLG to show PDCs, on the other hand, is likely a result of its amphipilic properties. The barrel-like protein structure exhibits a hydrophobic core that is capable of forming inclusion complexes with amphiphilic molecules in solution,[166, 179] which can be also transferred into the gas phase by nESI.[180, 181] To test in addition the capability of BLG to form PDCs *via* non-specific nESI contacts with detergents, mass spectra at higher detergent concentrations were recorded (500 µM). The intensity pattern observed among free BLG and its PDCs at high detergent concentrations can be perfectly described by a Poisson distribution (Figure 8.26, Appendix). This clearly confirmed that the PDC formation at high detergent concentration can be triggered by enhancing the propability of randomly occuring contacts between protein and detergent molecules during nESI.[14] Considering the results for ubiquitin and myoglobin, it could therefore be concluded that at lower detergent concentrations (50 µM) also non-specific adduct formation during the nESI process contributed to the PDC intensity of BLG, but clearly only to a small extent (Figure 5.3a-c). Taken together, BLG was found to be the most suitable soluble protein for providing intense PDC signals under the employed experimental conditions.

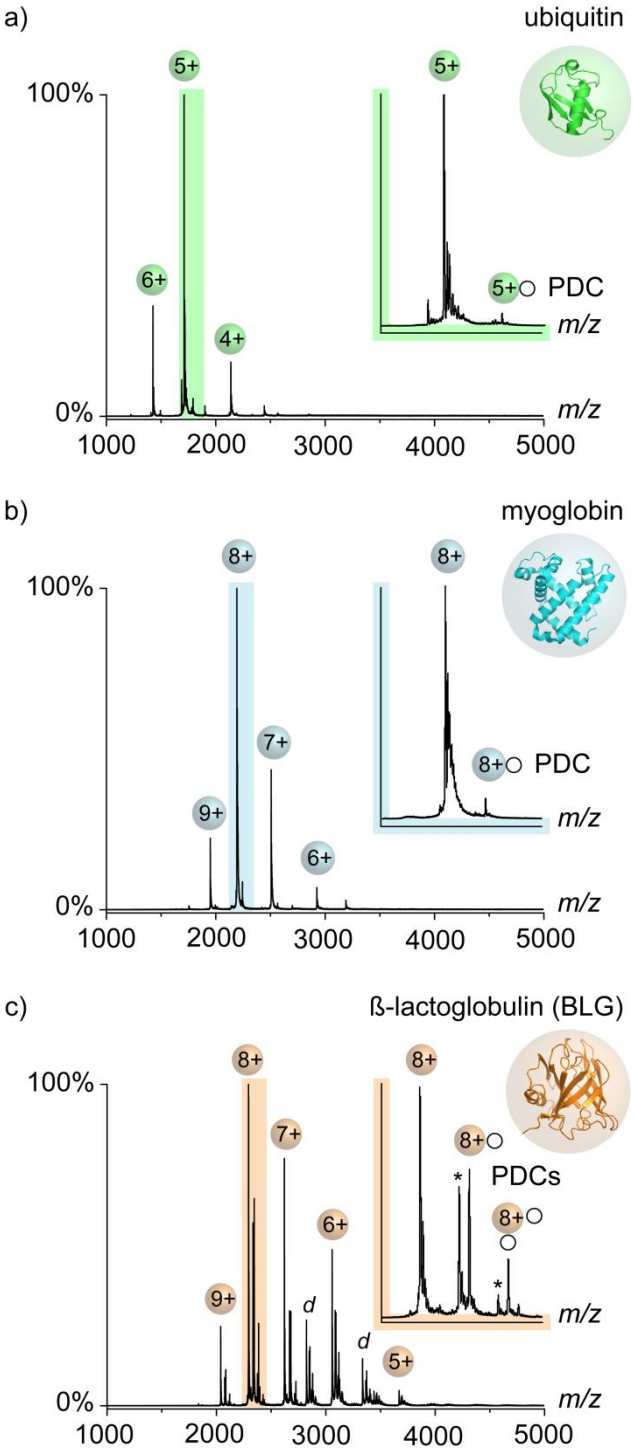

Figure 5.3: Mass spectra (nESI, positive mode) of three model proteins that were dissolved in NH_4OAc buffer (10 mM) and in the presence of equimolar amounts of the [G1] OGD mixture **1**: a) ubiquitin, b) myoglobin (holo form) and c) ß-lactoglobulin (BLG). BLG dimers are labeled with *d* and lactosylated forms of BLG are labeled with an asterisk.

5.3.2 Dissociation Behavior of PDCs - Impact of Ion Adducts and OGD Structure

Once BLG was identified as suitable model protein to obtain intense PDC signals upon nESI of equimolar protein-detergent mixtures, the dissociation behavior of the PDCs was studied by means of MS/MS experiments. In order to take into account that the gas-phase dissociation of protein complexes is dependent on the protein charge states,[96] the MS/MS experiments were focused systematically on the most abundant protein charge state 8+ (Figure 5.4).

The mass spectrum of singly-bound PDC ions obtained for BLG and **1** showed one intense peak for the fully protonated PDC and further signals of minor intensity that correspond to mixed sodiated forms (Figure 5.4a). To examine the impact of sodium and proton binding, different quadrupole settings were used to enable the isolation of i) mainly fully protonated- or ii) mixtures of protonated and mixed sodiated PDC ions (Figure 5.4b-c, respectively). To enhance the intensity of the mixed sodiated ions, sodium chloride (500 µM) was added to the samples (Figure 5.4a). The selected ion populations were then thermally activated by increasing the collision voltage (Scheme 5.1). Upon full dissociation of the PDC, the appearance of three new ion populations was observed which corresponded to BLG of two different charge states (8+ and 7+) and singly sodiated detergent ions (Figure 5.4b-c). Interestingly, the extent in BLG charge reduction was proportional to the amount of singly sodiated detergent ions that were released from the PDC. This showed that the charge reducing properties of **1** relied exclusively on the detergent's ability to remove sodium cations from the PDC. Detergent molecules of **1** that did not capture a sodium cation were consequently dissociated from the complex as neutral species. Similar results were obtained for the individual [G1] OGD regioisomers of **1**, which revealed that the ability to remove sodium cations did not change with the structure of the triglycerol head group regioisomers (Figure 8.27 and Figure 8.28, Appendix).

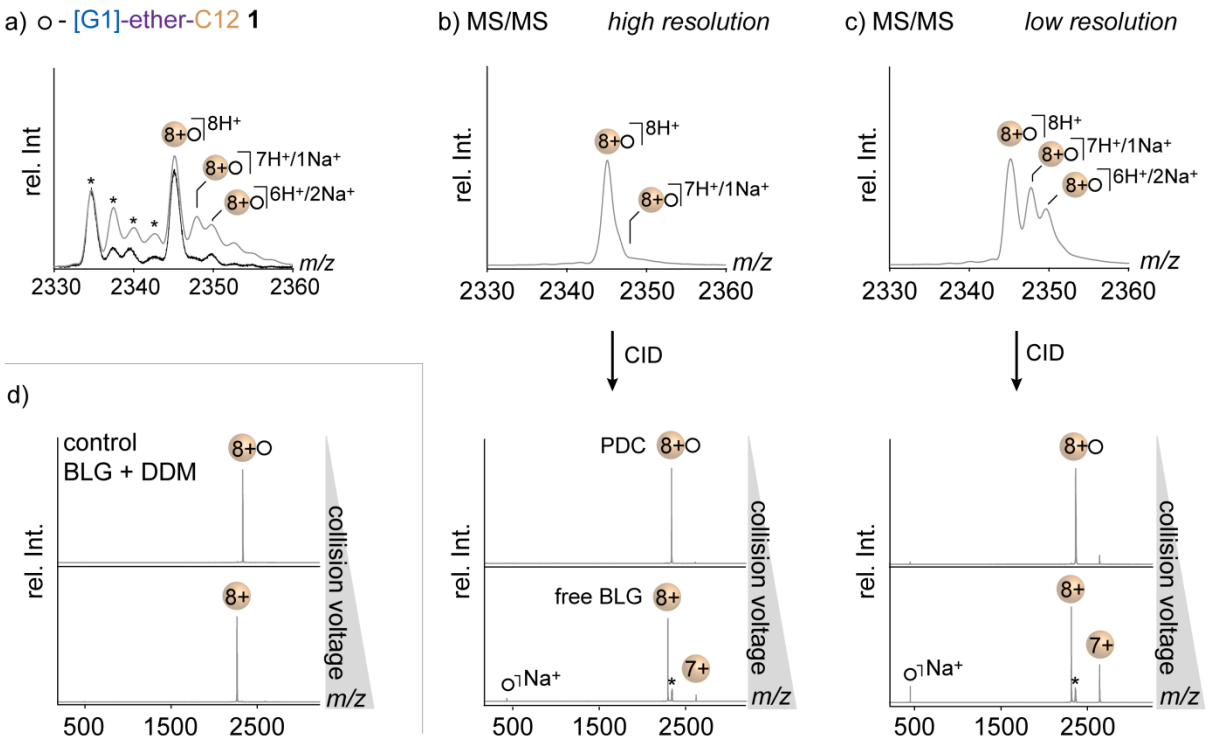

Figure 5.4: Tandem mass spectrometry (MS/MS) experiments revealed the influence of proton and sodium binding on the dissociation behavior of PDCs formed by BLG and **1**. a) Zoom into MS spectrum of the PDC at charge state (z = 8+) when analyzed in the absence (black) or presence of NaCl (500 µM, grey). b-c) MS/MS spectra obtained from different quadrupole settings (top) and MS/MS spectra before and after collision-induced dissociation (CID, collision voltage range: 2 - 30 V) of the parent ion populations. d) For comparison, the results obtained for PDCs formed by BLG and DDM at low resolution settings are shown. Lactosylated forms of BLG are labeled with an asterisk.

The origin of this behavior possibly lies in the structural similarity between trigylcerol and 18-crown-6, which is known to have a high binding affinity to smaller alkali cations.[182] For comparison, the performance of the detergent DDM was tested, which is an important standard in structural biology and one of the most widely used detergents in native MS (Figure 5.4). DDM and **1** exhibited similar alkyl spacers and linker groups but differed in the structure of their head groups. The comparatively rigid disaccharide structure of DDM, for example, was less similar to that of crown ethers and, as a consequence, no charge reduction of BLG was observed, irrespective of the sodium adduct intensity (Figure 5.4). This implied that the triglycerol head groups of **1** are indeed the major coordination sites for sodium ions.

To assess the impact of the linker between head group and tail, MS/MS experiments on fully protonated PDCs were performed (without the addition of sodium chloride) (Figure 5.5). In agreement with the results discussed above, no charge reduction of BLG was observed in the case of **1**, which indicated that the detergent molecules dissociated as neutral species in the absence of sodium adducts. Surprisingly, when exchanging the ether linkage between the detergent's head group and tail for an amide bond **2** or triazole group **3**, an increase in protein charge reduction was observed (Figure 5.5). The extent of protein charge reduction observed among **1** – **3** was thereby proportional to the loss of protonated detergent molecules.

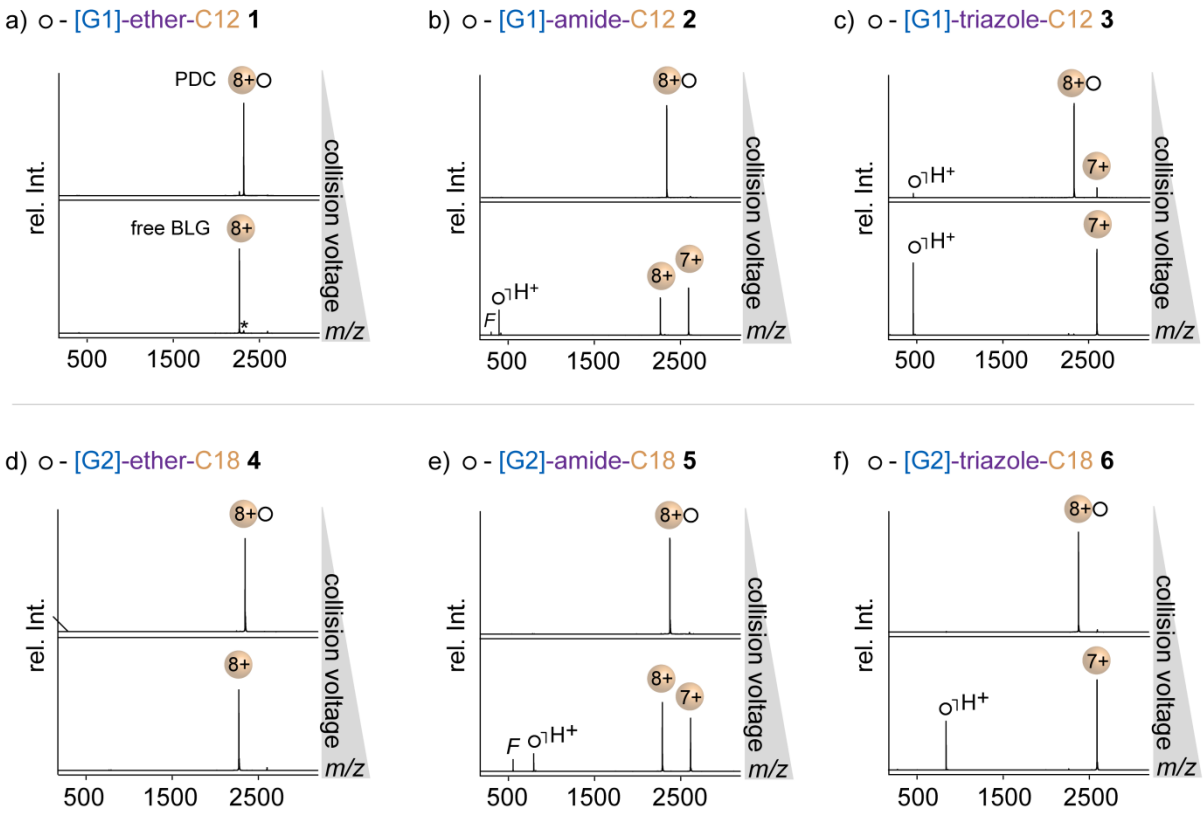

Figure 5.5: MS/MS spectra before and after full dissociation of PDCs (*z* = 8+, collision voltage range: 2 - 30 V) obtained from BLG and a) – c) [G1] OGD mixtures **1** – **3** (top) or d) – f) [G2] OGD mixtures **4** – **6** (bottom). High resolution quadrupole settings were optimized to obtain maximum intensity of fully protonated PDCs prior to CID. Lactosylated forms of BLG are labeled with an asterisk, detergent fragments are labeled with *F*.

Similar trends in charge reduction were observed for the [G2] detergent mixtures **4** – **6**, which gave clear evidence that the detergent's ability to pick up a proton from the PDC is related to the chemical properties of the linker between head group and tail (Figure 5.5). This trend is expected because the affinity of the linkages to abstract a proton is directly correlated to their gas phase basicity, *e.g.*, ether (~ 790 kJ/mol), amide (~ 820 kJ/mol) and triazole group (~ 900 kJ/mol).[183] In other words, the greater the basicity of the detergent, the more likely it is for a detergent to pick up a proton from the protein during PDC dissociation. This is also consistent with the difference in charge-reducing properties between DDM (790 kJ/mol) and LDAO (950 kJ/mol) observed during nESI-MS analysis of membrane proteins.[14] Taken together, the MS/MS data indicate that the dissociation behavior is significantly influenced by the protonation/sodiation ratio of the PDC, but also by the structural properties of the detergent, including the chemical properties of the head group and linker.

5.3.3 Impact of OGD Structure on Membrane Protein Charge States

To examine if the trends in protein charge reduction observed from the soluble protein BLG and **1** – **6** are transferable to membrane proteins, nESI-MS experiments were performed with OmpF. This membrane protein was purified before in the reference detergent OG and detergent exchange experiments from OG to **1** – **6** were performed by means of gel filtration chromatography. Stable membrane protein solutions were obtained only for [G1] OGDs **1**, **3** and for [G2] OGDs **4**, **6**, which indicated that these detergents are suitable for the solubilization of OmpF. In case of **2** and **5**, precipitation of OmpF was observed, which indicated that OGDs, which exhibit an amide linkage were less suitable for membrane protein solubilization. Various amphiphiles are available for membrane protein solubilization, which consist of amide groups.[59, 64, 114] It can therefore not be conlcuded that detergents with amide bonds are generally not suited for the fabrication of protein-compatible detergents. However, OmpF is a comparatively robust membrane protein, which is compatible to a broad spectrum of different detergent families.[184] This led to the suggestion that the OGD mixtures **2** and **5** are possibly also less suitable for the solubilization of other membrane proteins.

Upon successful exchange of the detergent environment from OG to **1**, **3**, **4**, and **6**, the samples were transferred into the vacuum of a modified Q Exactive MS instrument using nESI. The detergent environment was removed upon nESI by collisional activation, which enabled the acquisition of membrane protein mass spectra in case of **1**, **3**, and **4** (Figure 5.6). Even under harshest instrument conditions, however, no protein mass spectrum could be obtained in case of **6**, which indicated that the combination of a [G2] head group, a linear C18 alkyl spacer, and a connecting triazole group is less suitable for the nESI-MS analysis of membrane proteins. In contrast, the mass spectra obtained from the OGD mixtures **1**, **3**, and **4** revealed highly resolved and intense signals of OmpF in its native trimeric state (Figure 5.6). This showed that the three OGD mixtures **1**, **3**, and **4** are able to preserve the native oligomeric state of OmpF in solution.

The z_{ave} values of OmpF obtained from **1** (18+) and **4** (18+) were similar to that observed from OG (19+), which has been classified as a non-charge reducing detergent (Figure 5.6).[14] The data obtained from **1** and **4** showed that varying the size of the dendritic head group and hydrophobic tail did not alter their charge-reducing properties. This was in good agreement with results reported for the reference detergents OG and *n*-dodecyl ß-D-maltoside (DDM), which both differ with respect to the

size of the head group (mono- or disaccharide) and hydrophobic tail (C8 or C12) and do not exhibit charge-reducing properties.[14] In contrast, a significant reduction in charge state was found when the ether linkage of **1** (18+) was substituted for a triazole unit **3** (15+, Figure 5.6a-c). As discussed above, this trend was expected, because the ability of the OGD linker to abstract protons from the protein ion can be directly related to its gas-phase basicity. Further experiments on the individual OGD regioisomers of **3** revealed that the ability to abstract charges did not depend on the structure of the triglycerol head group (Figure 8.29, Appendix). This underlined that the triazole linker of **3** was the key element responsible for charge reduction and led to the conclusion that membrane protein charge states could simply be tuned by adjusting the detergent's basicity.

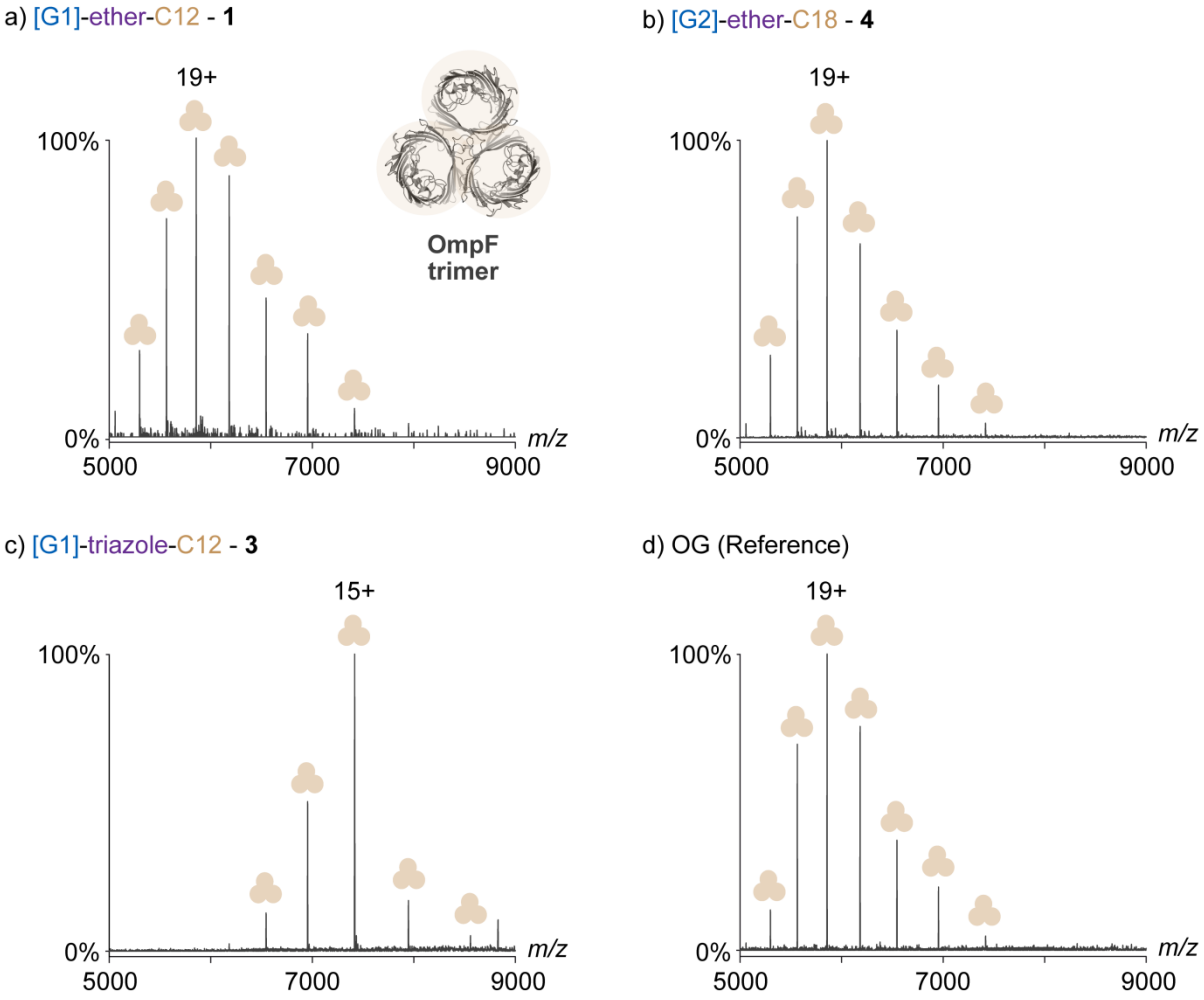

Figure 5.6: nESI-MS analysis of trimeric OmpF upon detergent exchange from detergent octyl β-D-glucopyranoside (OG) to OGD mixtures a) **1**, b) **4**, and c) **3**. d) For comparison the mass spectrum taken from the reference OG is shown. Increasing the size of the OGD head group and tail from **1** to **4** did not lead to a change in protein charge states. A substitution of the ether moiety in **1** by the more basic triazole in **3** led to a substantial charge reduction of OmpF.

5.4 Conclusions

In summary, it was shown how protein charge states could be on-demand tailored by tuning the molecular structure of OGDs. First, the applicability of ubiquitin, myoglobin, BLG and a set of six tailored OGD mixtures **1** - **6** was evaluated for the investigation of PDCs in the vacuum of a MS instrument. Due to its outstanding propensity to show intense PDC signals upon nESI of protein-detergent mixtures, the soluble protein BLG was found to be most suitable for evaluating the gas-phase properties of detergents under the employed experimental conditions. Tandem MS experiments on PDCs formed by BLG and **1** - **6** revealed how the detergent's propensity to remove charges from protein ions could be modulated by tuning the structure of OGDs. The data indicated that the structural similarity of the OGD head group to crown ethers enabled the efficient removal of sodium cations from protein ions during PDC dissociation. In addition, the detergent's propensity to remove protons from protein ions could be addressed by tuning the basicity of the OGD structure.

More remarkably, it was for the first time demonstrated that OGDs can be used for the solubilization and native MS analysis of the membrane protein OmpF. Comparing the data obtained from BLG and OmpF confirmed that the detergent's ability to promote charge reduction was not necessarily coupled to the fact, that the targeted protein is a membrane protein, which is in line with results obtained from Reading and Liko *et al.*[14] This led to the conclusion that charge-reducing properties of detergents can be examined either by studying the dissociation behavior of PDCs formed with soluble proteins or by direct nESI-MS analysis of membrane proteins.

The ability to probe charge-reducing properties of detergents with soluble proteins can help to identify detergents for native MS applications that need to exhibit charge-reducing properties on-demand. Analyzing the dissociation behavior of PDCs formed with soluble proteins can thereby solve the qualitative question whether a detergent exhibits charge-reducing properties or not. The here-presented workflow will therefore help to pre-select charge-reducing detergents from new detergent libraries without consuming expensive membrane protein samples. The data presented in this chapter also revealed that charge-reducing detergents were not necessarily suitable for the solubilization or native MS analysis of membrane proteins. Therefore, more effort will be invested on the understanding about how the compatibility of detergents to membrane proteins can be modulated by tuning the structure of detergents.

6. Chapter III – Detergent Design for Native Mass Spectrometry of Membrane Proteins

6.1 Introduction

Membrane proteins are located in cellular membranes and fulfill functions that are vital for life of all organisms. Investigating the membrane proteome is consequently of great interest for medicinal chemistry and structural biology. However, cellular membranes are very heterogeneous and highly dynamic, which represents a major challenge for application of common biophysical techniques. Biological membranes are therefore traditionally dissolved with detergents, whose aggregates allow one to stabilize native protein structures in aqueous solution apart from its native host environment.

A breakthrough came with the first demonstration that detergent aggregates can protect native membrane protein structures during transport from solution into the vacuum of a mass spectrometer.[75] Protein-detergent mixtures can be transferred into the vacuum of a MS instrument by nanoelectrospray ionization (nESI), where subsequent removal of the detergent environment ideally leads to the release of intact membrane protein complexes. The chemical properties of detergents dictate the activation energies required for detergent removal and also affect the charge states of so-obtained membrane protein ions.[14] Acquired protein mass spectra provide information on oligomeric states of membrane protein assemblies, and their gas-phase dissociation pattern allows unraveling their native subunit connectivity and stoichiometry.[11, 13] Furthermore, the purification of membrane proteins by detergents leads to co-purification of lipids.[20] The choice of the detergent alters the extent of co-purification and enables the detection of protein complexes formed with structurally relevant lipids.[18] MS techniques allow one to distinguish between endogenously bound membrane lipids and those that are embedded within the protein structure.[18] Also lipids that are exogenously added to the sample can be ranked by MS techniques according to their relevance for structure and function of membrane proteins.[19]

Detergents that are suitable for native MS applications on membrane proteins need to cover a balance of appropriate solution and gas-phase properties. Currently available detergent families, however, are either suited for isolating proteins, promoting charge reduction, or the ability to detect protein complexes formed with co-purified membrane lipids.[14, 20] The present chapter evaluates whether one can overcome these limitations by exploring the family of non-ionic OGDs. A set of five OGD regioisomer mixtures **1**, **3**, **4**, **7**, and **8** was chosen, which comprised different building block combinations, such as first- [G1] and second-generation [G2] oligoglycerol regioisomers, different linker groups and hydrophobic tails (Figure 6.1). To explore the potential of these OGDs for extracting membrane proteins from biological membranes, two membrane proteins were selected *E.coli*: a) a green fluorescent protein (GFP) construct of the aquaporine channel (AqpZ) and b) a maltose binding protein (MBP) construct of the ammonia channel (AmtB). Aquaporins are channel proteins that facilitate the diffusion of water through lipid membranes. Their role as water transport system was first directly proven by Peter C. Agre and colleagues, who received the Nobel Prize in Chemistry for their discovery in 2003.[185] On the other hand, ammonia channel proteins mediate the transport of ammoniac (NH_3) or ammonium ions (NH_4^+).[186, 187]

At the time of its publication in 2004, the crystal structure of AmtB from *E. coli* could be looked at with the highest resolution of any integral membrane protein.[188] Both membrane proteins are compatible to a broad range of detergent families, have been extensively studied by native MS, and were therefore considered as ideal model proteins.[13, 14] Furthermore, the utility of OGDs for the analysis of pharmaceutically relevant membrane proteins was discovered, such as for the multidrug and toxic compound extrusion protein (MATE)[189, 190] and the neurotensin receptor 1 (NTSR1)[172] – a member of the challenging GPCR protein family.[30, 172] Native MS experiments with these five membrane proteins revealed how the molecular architecture of OGDs can be used for optimizing protein extraction, charge reduction, and the ability to detect binding with co-purified membrane lipids on-demand.

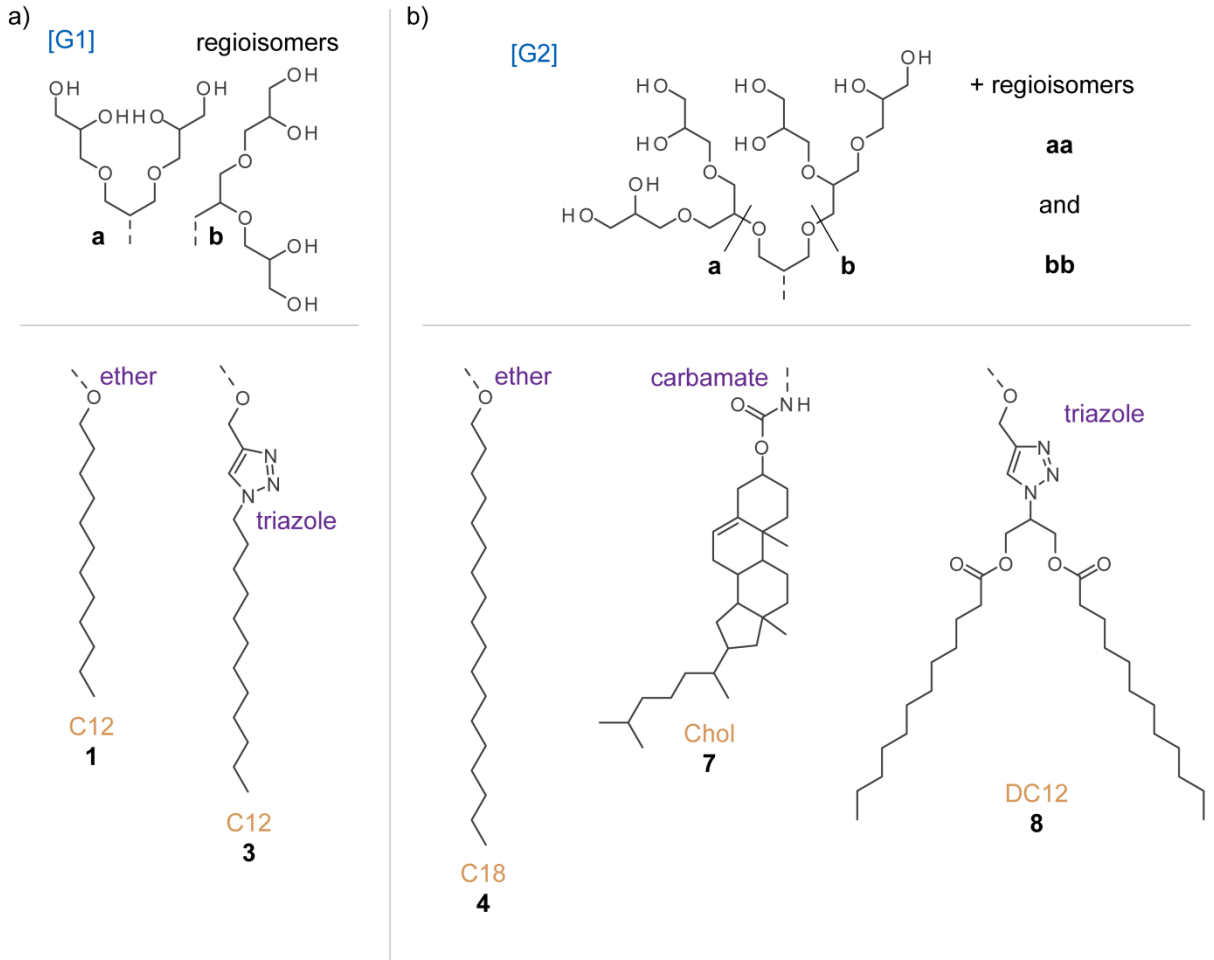

Figure 6.1: Library of a) [G1] and b) [G2] OGD mixtures **1**, **3**, **4**, **7**, and **8** to be explored for isolating membrane proteins, tuning charge states, and supporting the ability to detect protein complexes formed with co-purified membrane lipids by nESI-MS. The [G1] OGD mixtures **1** and **3**, and [G2] OGD mixtures **4**, **7** and **8** comprise different head group regioisomers, hydrophobic tails, and different connecting linkers, such as ether-, carbamate, and triazole groups.

6.2 Experimental Details

Membrane Preparation and Protein Extraction

The following steps were performed using a procedure of Laganowsky *et al*.[19] Gene vectors for overexpression of the His-tagged (6 x His) membrane protein constructs AqpZ-GFP, AmtB-MBP, and MATE-GFP were provided by Idlir Liko. The protein plasmids of AqpZ-GFP, AmtB-MBP, and MATE-GFP were transformed into *E. coli* BL21 (DE3) Gold (Agilent). Several colonies were incubated in medium (LB Broth, 50 mL of 5 g/L yeast extract, 10 g/L peptone from casein, and 10 g/L sodium chloride) and grown overnight at 37 °C. One liter of medium was subsequently incubated with overnight culture (7 mL) and grown at 37 °C until the culture reached an optical density value (OD_{600nm}) of 0.6 – 0.8. Next, isopropyl b-D-1-thiogalactopyranoside (IPTG) was added to the culture at a final concentration of 0.5 mM and the cultures were grown for another three hours at 37 °C. The cells were subsequently collected by centrifugation (5000 x g, 10 min, 4 °C).

Protein-containing membranes for membrane protein extraction were prepared upon protein expression. To do so, the harvested cell pellets were resuspended in lysis buffer (20 mM Tris, 300 mM NaCl, pH = 7.4) and supplemented with a protease inhibitor tablet (Roche). The cell suspension was homogenized by passing it several times through an M-110 PS microfluidizer (Microfluidics). Insoluble material was removed by centrifugation (20000 x g, 20 min, 4 °C) and the supernatant was again centrifuged (100000 x g, 2 h, 4 °C). The yielded membranes were resuspended in ice-cold resuspension buffer (20 mM Tris, 100 mM NaCl, 0.2 *v*/*v* glycerol) and homogenized using a Potter-Elvehjem Teflon pestle and glass tube.

Membranes were subsequently solubilized with detergents and the targeted membrane proteins were purified by IMAC. Membrane aliquots (0.5 mL) were treated with a mixture of resuspension buffer (3.5 mL) and an aqueous solution, which contained a detergent of choice (1 mL, 5w%). The mixtures were agitated gently overnight at a temperature of 4 °C and subsequently centrifuged (21000 x g, 40 min, 4 °C). The pellets were discarded and the supernatants were subjected to IMAC purification. IMAC columns were packed by loading 500 µL Ni-Agarose suspension (Quiagen) into a 1000 µL empty column (Bio-spin chromatography columns, Bio-Rad). The suspensions were settled down by a short centrifugation step (1000 x g, 1 min). The columns were opened on the bottom and washed with water (3 x 500 µL), IMAC wash buffer (1 x 500 µL, 50 mM Tris, 200 mM NaCl, 20 mM imidazole, 0.1 *v*/*v* glycerol, detergent of choice – Table 6.1), IMAC elution buffer (1x 500µL, 50 mM Tris, 100 mM NaCl, 500 mM imidazole, 0.1 *v*/*v* glycerol, detergent of choice – Table 6.1), and IMAC wash buffer (5 x 500 µL). The supernatant obtained upon centrifugation of the solubilized membranes was loaded on the IMAC columns and every column was washed with IMAC wash buffer (5 x 500 µL), and IMAC buffer mixture (2 x 500 µL of wash buffer/elution buffer mixture, *v*:*v*, 9:1). The wash solutions were discarded and the proteins were finally eluted using IMAC elution buffer (1 x 550 µL). The protein solutions of AqpZ-GFG and AmtB-MBP were analyzed by SDS Page (Figure 6.2). Pre-packed NuPage™ 4 – 12% Bis-Tris gels from Invitrogen (Thermo-Scientific) were used and SeeBlue® Plus2 Pre-Stained Standard was used as molecular weight marker.

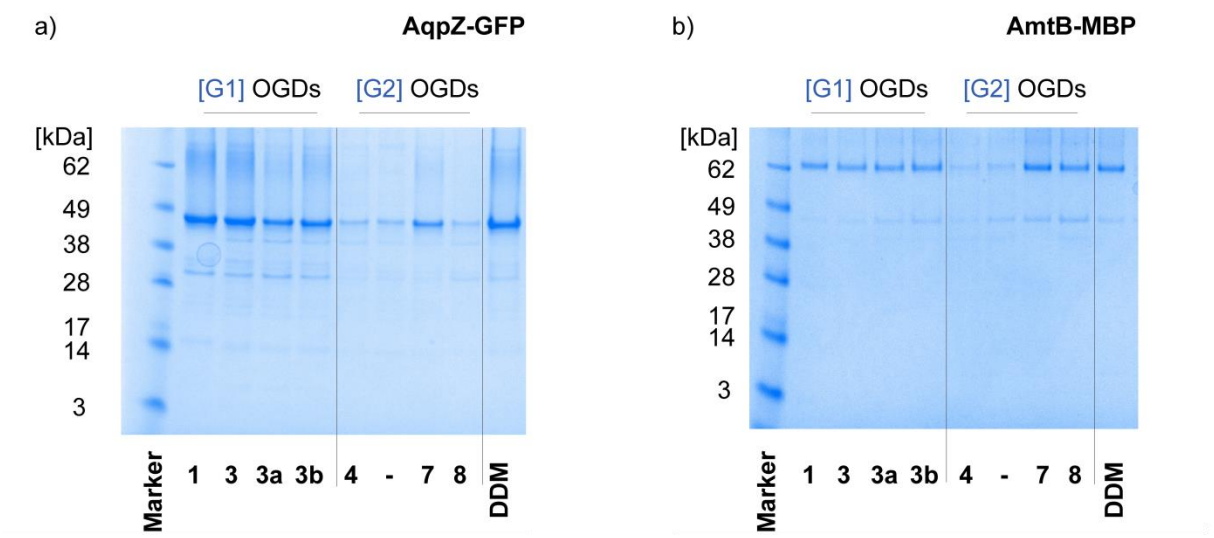

Figure 6.2: SDS Page analysis of membrane proteins samples a) AqpZ-GFP (52.7 kDa) and b) AmtB-MBP (86.3 kDa) upon extraction from biological membranes and IMAC purification. The comet-like appearance of individual bands reflected the heterogeneity of the isolated protein-detergent mixtures.[191]

Table 6.1: Detergent concentrations applied for membrane solubilization, IMAC purification, and buffer exchange into nESI-MS Buffer. Further information about *cac* values is given in Chapter 4.2.

Detergent Abbreviation	**cac (mM)**	**Membrane Solubilization (1w%)**	**IMAC Wash Buffer**	**IMAC Elution Buffer**	**nESI-MS Buffer**
[G1]-ether-C12 (**a**:**b**, 6:4) **1**	0.70	36xcac	2xcac	2xcac	1xcac
[G1]-triazole-C12 (**a**:**b**, 6:4) **3**	0.55	39xcac	2xcac	2xcac	2xcac
[G1]-triazole-C12 (**a**) **3a**	0.47	44xcac	2xcac	2xcac	2xcac
[G1]-triazole-C12 (**b**) **3b**	0.39	53xcac	2xcac	2xcac	2xcac
[G2]-ether-C18 (**aa**:**ab**:**bb**, 4:4:1) **4**	0.30	44xcac	2xcac	2xcac	2xcac
[G2]-carbamate-Chol (**aa**:**ab**:**bb**, 9:5:1) **7**	0.16	67xcac	2xcac	2xcac	2xcac
[G2]-triazole-DC12 (**aa**:**ab**:**bb**, 9:5:1) **8**	0.06	167xcac	2xcac	2xcac	2xcac
DDM	0.11	156xcac	2xcac	2xcac	2xcac

Analyzing the Membrane Protein Concentration upon Extraction

UV/VIS analysis was applied to determine the relative protein concentration upon IMAC. The freshly eluted protein solutions were concentrated in Amicon-Ultra 0.5 mL centrifugal devices (MWCO = 150 kDa), diluted with IMAC wash buffer (500 µL) and concentrated again by centrifugation. Buffer exchange into nESI-MS Buffer (200 mM NH_4OAc and detergent of choice – Table 6.1) was performed with a centrifugal buffer exchange device (Micro Bio-Spin 6. Bio-Rad). All protein samples were concentrated to equal volumes and the relative protein concentrations were determined by UV/VIS spectroscopy using a NanoDrop photospectrometer (DeNovix). The obtained absorbance values (A_{485} for AqpZ-GFP and A_{280} for AmtB-MBP) were normalized to the values obtained from DDM and plotted against the respective detergent abbreviation (Figure 6.3, Results and Discussion).

nESI-MS analysis of Extracted Membrane Protein Samples

The membrane protein samples in nESI-MS buffer were delivered to a modified Q extractive MS instrument that was operated in positive ion mode with a nESI source. Typical instrument parameters were as follows: injection flatapole (7.9 V), inter-flatapole (6.9 V), bent flatapole (5.9 V), transfer multipole (4 V), and voltage applied to the higher-energy collisional dissociation (HCD) cell for detergent (200 V). Spectra were acquired with ten microscans and averaged with a noise level parameter of three. The nESI-MS instrument was operated by PhD Idlir Liko. Data were analyzed with Xcalibur (v2.2) and data processing was performed with OriginPro (v9.1). The z_{ave} values of membrane proteins were calculated as described before in Chapter 4.2. The lipid masses (ligand bound states) were calculated by subtracting the *mass-to-charge ratios* "*m/z*" of two neighboring protein signals of the same charge state "*z*," for example, apo form "*n*" and protein plus one ligand attached to it "*n+1*." The calculated difference "Δ*(m/z)*" was multiplied with the charge state value "***z****"* to obtain the respective ligand mass:

$$ligand\ mass = \Delta(m/z) \cdot z = |(m/z)_n - (m/z)_{n+1}| \cdot z$$

The mass of every ligand was determined between five and six times from different signals. The obtained values were averaged and the standard deviation (SD) was calculated. The ligands were assigned by comparing their masses (±SD) with those of relevant membrane lipids. The molecular masses of the membrane lipids were taken from literature.[19] The z_{ave} values and lipid data are summarized in Table 6.2. Supplementary data are provided in Chapter 8.5 (Appendix).

Detergent Exchange and nESI-MS Analysis of NTSR1

The membrane protein neurotensin receptor 1 (NTSR1) was provided by Hsin-Yung Yen and was solubilized in a mixed detergent system, that contained *n*-dodecyl ß-D-maltoside (DDM), cholesterol, and foscholine.[172] The mixed detergent environment was exchanged to OGD mixtures **1** and **7**, as described before in Chapter 4.2. The protein-detergent mixtures were analyzed by nESI-MS using the above-described procedure. PhD Hsin-Yung Yen operated the nESI-MS instrument and designed the experiments that were used to estimate proportions of functional NTSR1 upon detergent exchange.

Table 6.2: Summary of native MS data obtained for AqpZ-GFP, AmtB-MBP, MATE-GFP, and NTSR1. The data include protein abbreviations, OGD abbreviations, average charge states (z_{ave}), calculated lipid masses, abbreviations of assigned lipids, molecular masses of the assigned lipids,[19] and molecular masses of OGDs.

Protein	OGD	z_{ave}	(Ligand Mass ± SD) [Da]	Assigned Lipid	Lipid Mass [Da]	OGD Mass [Da]
AqpZ-GFP	**1**	30+	-	-	-	-
	3	25+	-	-	-	-
	3a	-	-	-	-	-
	3b	-	-	-	-	-
	4	29+	-	-	-	-
	7	30+	(901 ± 2), (1414 ± 3)	DEPC, CDL	898.3, 1430.0	947.6
	8	28+	(1372 ± 4)	CDL	1430.0	1055.6
	DDM	-	-	-	-	-
AmtB-MBP	**1**	43+/32+	-	-	-	-
	3	38+/29+	-	-	-	-
	3a	38+/27+	-	-	-	-
	3b	38+/27+	-	-	-	-
	4	-	-	-	-	-
	7	48+	(983 ± 3), (1400 ± 1)	PI, CDL	977.1, 1430.0	947.6
	8	40+/30+	(1394 ± 1)	CDL	1430.0	1055.6
	DDM	-	-	-	-	-
MATE-GFP	**1**	16+	(1407 ± 1)	CDL	1430.0	408.3
	7	16+	(1407 ± 1)	CDL	1430.0	947.6
NTSR1	**1**	10+	-	-	-	-
	7	10+	-	-	-	-

6.3 Results and Discussion

6.3.1 Expression and Purification of Membrane Proteins

The two proteins AqpZ-GFP and AmtB-MBP were overexpressed in *E. coli* and isolated with different OGD mixtures **1**, **3**, **4**, **7**, and **8** by membrane solubilization and IMAC. The relative protein quantities were subsequently determined by UV/VIS spectroscopy and plotted against the detergent abbreviations (Figure 6.3). To discuss the results obtained from the OGD mixtures in a more general context, the relative protein quantities were compared to those obtained from the reference detergent *n*-dodecyl ß-D-maltoside (DDM), which is a current standard in structural biology.[192]

The amounts of AqpZ-GFP obtained from the [G1] OGD mixtures **1** and **3** were about two times higher than DDM, which indicated their great potential for the isolation of large protein quantities from biological membranes (Figure 6.3a). Interestingly, the protein amounts received from **3** were higher than that of the individual regioisomers **3a** and **3b**. Mixtures of different amphiphilic molecules, such as detergent/lipid or detergent/polymer formulations, are known alternatives to classic detergents and can help to improve the isolation of membrane proteins.[41] However, such a pronounced synergistic increase in protein quantity arising from a mixture of detergent regioisomers has remarkably not been reported before. The protein amounts obtained from the [G2] OGDs **4**, **7**, and **8**, on the other hand, were up to ten times lower than for DDM, which indicated that synergistic effects that may have arisen from regioisomer mixtures were of minor relevance for the larger [G2] detergents (Figure 6.3). This is expected since it is known that detergents with bulky head groups are less effective in membrane solubilization, which consequently can limit the isolation of large protein quantities.[40] Taken together, the data show that the protein quantities received from protein extraction can be significantly controlled by changing the structure of the OGD head group and tail. Similar trends in protein concentration obtained upon IMAC were obtained for AmtB-MBP, which showed that the utility of the chosen OGD mixtures to extract membrane proteins from biological membranes could be transferred to other membrane proteins (Figure 6.3b).

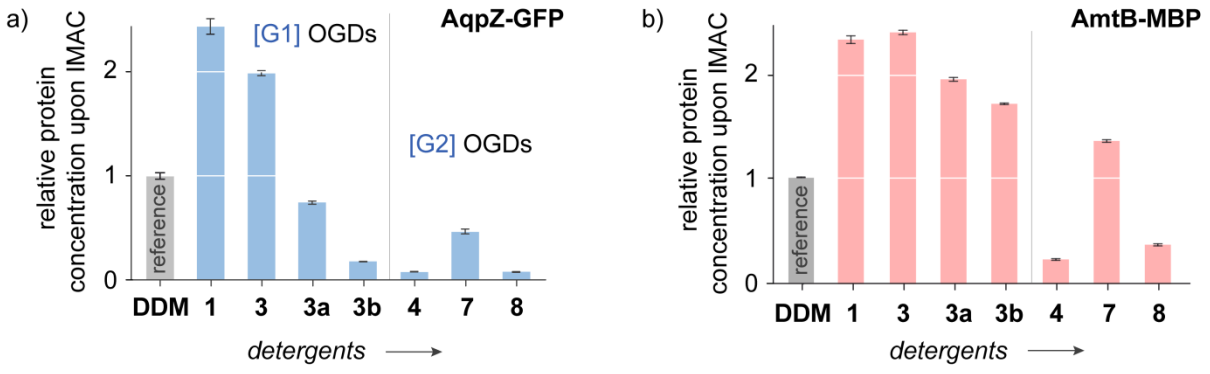

Figure 6.3: Relative protein quantities obtained for the membrane protein a) AqpZ-GFP and b) AmtB-MBP upon membrane solubilization and IMAC purification with the reference detergent DDM, [G1] OGDs and [G2] OGDs. Higher protein quantities were obtained, when [G1] OGD mixtures were used. The [G1] OGD regioisomer mixture **3** led to higher protein quantities than the individual regioisomers **3a** and **3b**.

6.3.2 Structural Analysis of Isolated Membrane Proteins

To probe the structural integrity of the protein-detergent mixtures obtained upon extraction from biological membranes, nESI-MS experiments were performed. The membrane protein AqpZ-GFP forms native tetramers in biological membranes with a molecular mass of about 210 kDa.[14] The mass spectra obtained from **1** and **3** revealed well-resolved signals of the tetrameric apo form of AqpZ-GFP, which showed that both OGD mixtures could preserve the native oligomeric state of AqpZ-GFP during membrane solubilization, IMAC purification, and nESI-MS (Figure 6.4a). The pronounced shift in z_{ave} of AqpZ-GFP between **1** (30+) and **3** (25+) is in line with the results observed for OmpF before in Chapter 4.3. The data confirmed that membrane protein charge states could be tuned by changing the basicity of the linker between the OGD head group and tail. Furthermore, the mass spectra showed predominantly the apo form of AqpZ-GFP, which indicated that the protein-detergent mixtures carried only minor amounts of co-purified membrane lipids (Figure 6.4a).[18, 19] From the individual [G1] OGD regioisomers **3a** and **3b**, however, weakly resolved and broad charge state distributions were obtained, which indicated that the protein structure became heavily perturbed during the isolation process (Figure 8.30, Appendix). A possible explanation is that the [G1] OGD mixture **3** caused less protein denaturation during the employed isolation procedure than the individual OGD regioisomers **3a** and **3b**, which would be in line with the different protein quantities obtained upon isolation (Figure 6.4).

For the [G2] OGD mixture **4**, similarly poor spectra were obtained, which indicated that the combination of a linear C18 alkyl chain and a [G2] head group was less suitable for protein isolation (Figure 8.31, Appendix). In strong contrast, much better results were found for the combination of the [G2] head group and more lipid-like hydrophobic tails. The mass spectra obtained using the [G2] OGDs **7** and **8** revealed not only signals for tetrameric apo form of AqpZ-GFP, but also those of ligand-bound states (Figure 6.4b). The ligand masses agreed very well with those of cardiolipid (CDL) and 1,2-dierucoyl-*sn*-glycero-3-phosphocholine (DEPC), which are highly relevant for the structure and function of AqpZ (Table 6.2).[19] The appearance of intense lipid-bound states upon extraction and purification of AqpZ-GFP with **7** and **8** indicated that the respective [G2] OGD mixtures carried larger amounts of co-purified membrane lipids than those of the [G1] OGDs **1** and **3**. The data therefore provided indirect evidence for the extent of membrane lipid co-purification from biological membranes. Furthermore, the ability to detect protein complexes formed with membrane lipids could be tuned by the structure of the detergent's head group and tail (Figure 6.4a-b). The differences in z_{ave} between the OGD mixtures **1** (30+), **3** (25+), **7** (30+), and **8** (28+) provided first evidence that protein charge reduction and lipid binding could be individually addressed, by tuning either the basicity of the linker or the structure of the OGD head group and tail, respectively (Figure 6.4a-b).

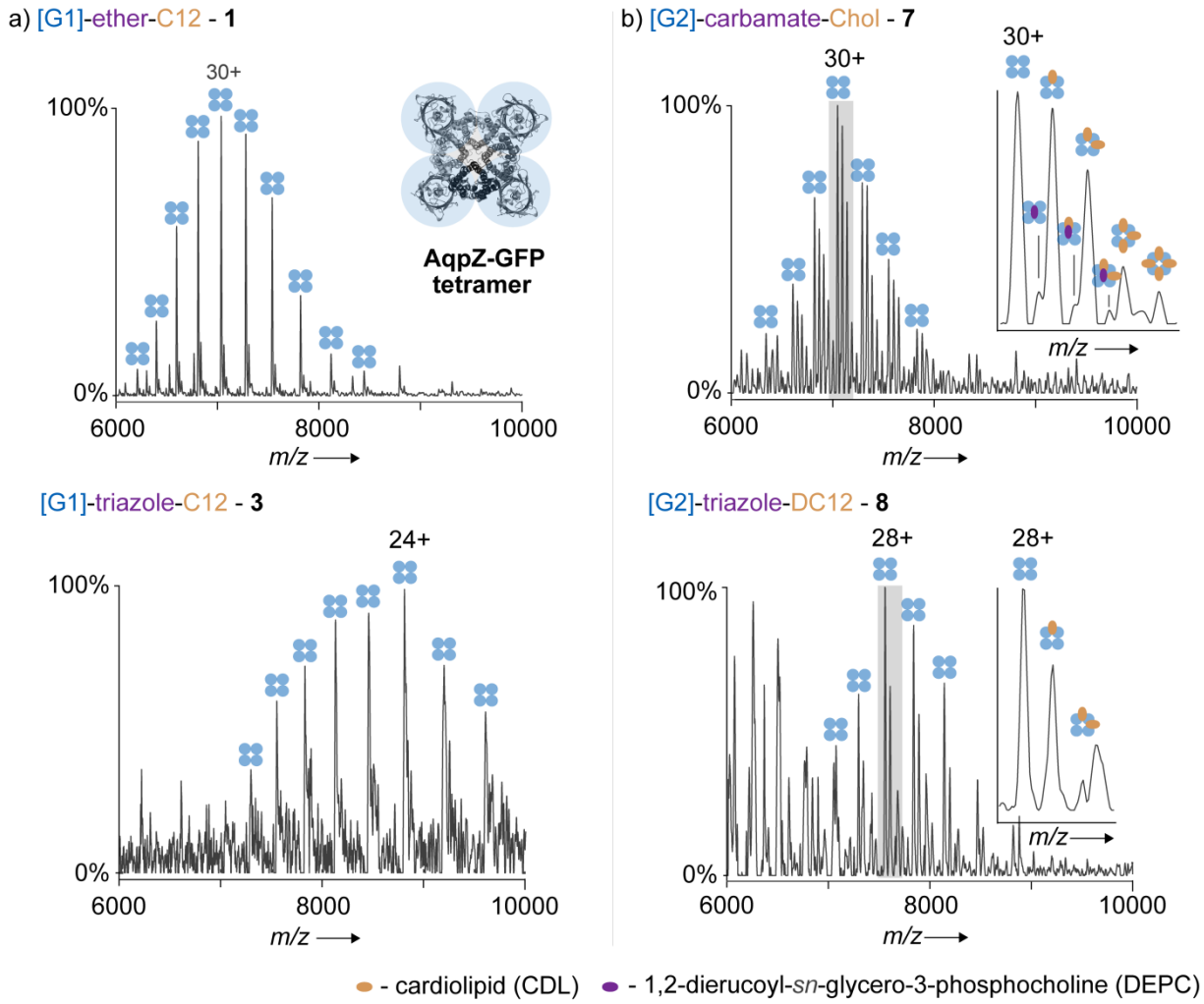

Figure 6.4: Mass spectra obtained upon isolation of tetrameric AqpZ-GFP from biological membranes (CID voltage = 200 V). a) [G1] OGDs facilitated the extraction of large protein amounts and protein charge reduction (bottom), but no protein-lipid complexes were detected, which pointed to a low concentration of co-purified membrane lipids. b) Using a [G2] head group and a lipid-like hydrophobic tail enabled the detection of protein-lipid complexes with structurally relevant membrane lipids. Increasing the basicity of the linker led to charge reduction, irrespective of head group and tail.

Similar trends in protein charge reduction and lipid binding were observed for AmtB-MBP (Figure 6.5). The mass spectra obtained from [G1] OGDs revealed bimodal charge state distributions and a systematic down-shift in both z_{ave} values was obtained between **1** (43+/32+) and **3** (38+/29+). From the individual [G1] OGD regioisomers **3a** and **3b**, well-resolved protein mass spectra were obtained (Figure 8.31, Appendix). Contrary to the results obtained from AqpZ-GFP, this indicated that the protein structure of AmtB-MBP became less denatured during isolation with the individual regioisomers. This was in line with the high amounts of AmtB-MBP obtained upon isolation with the regioisomers **3a** and **3b**. The mass spectra obtained from AmtB-MBP upon isolation with the [G2] OGDs **7** and **8** revealed not only signals for tetrameric apo form of AmtB-MBP but also for those of ligand-bound states (Figure 6.5b). Here, the ligand masses matched to the ones from cardiolipid (CDL) and 1,2-dioleoyl-*sn*-glycero-3-phospho-(1´-myo-inositol-3´-phosphate) (PI, Table 6.2).

Moreover, the differences in z_{ave} between the OGD mixtures **1** (43+/32+), **3** (38+/29+), **7** (48+), and **8** (40+/30+) confirmed that the ability to tune protein charge reduction and the ability to detect lipid-bound states could be addressed individually, either by tuning the basicity of the linker or the structure of the OGD head group and tail, respectively. The ability to gain free control over protein purification, charge reduction, and lipid co-purification has not been reported so far for other detergent families. This highlights the great potential of the modular OGD architecture to be tuned for individual native MS applications. Furthermore, the appearance of the bimodal charge state distributions of AmtB-MBP was investigated. To do so, membrane protein mass spectra with **1** and **3** were acquired at different activation conditions (Figure 6.6). The spectra revealed that the relative intensity of the individual charge state distributions changed with the applied collision voltage (Figure 6.6). Intense signals of highly charged protein ions (low *m/z*) were obtained at low collision voltages (100 V), whereby at elevated collision voltages (≥ 150 V) a significant increase in intensity for charge-reduced protein ions was observed (high *m/z*).

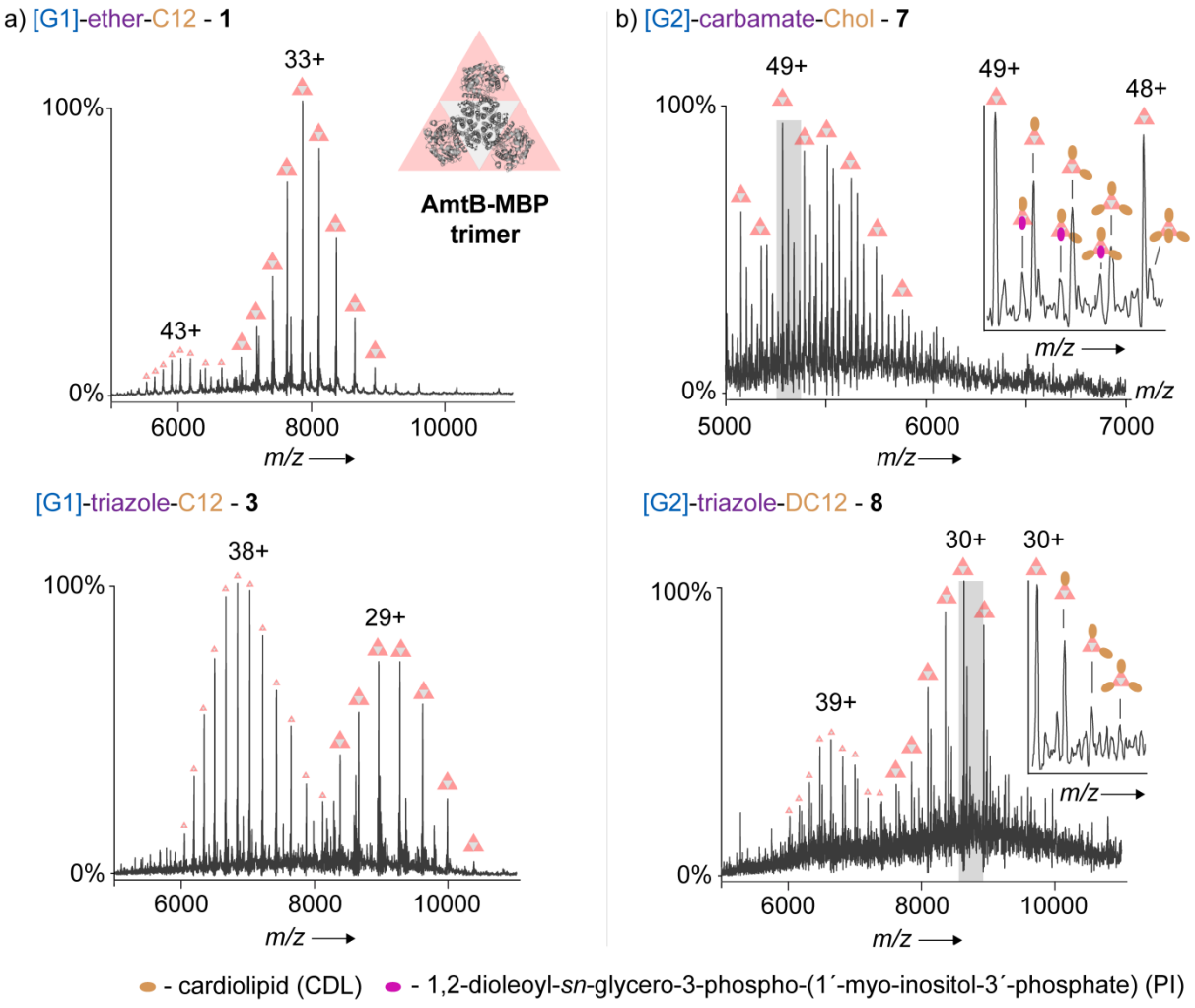

Figure 6.5: Mass spectra obtained upon isolation of trimeric AmtB-MBP from biological membranes (CID voltage = 200 V). a) [G1] OGDs facilitated again the extraction of large protein amounts, but no protein-lipid complexes were detected, which pointed to a low concentration of co-purified membrane lipids. b) Using a [G2] head group and a lipid-like hydrophobic tail enabled the detection of protein-lipid complexes with structurally relevant membrane lipids. Increasing the basicity of the linker promoted protein charge reduction, irrespective of head group and tail.

At least two explanations were available for the appearance of bimodal charge state distributions: First, the protein-detergent mixtures carried additional basic impurities, such as imidazole. According to Reading and Liko *et al.*, the removal of basic impurities may occurred subsequently to the detergent removal, which would be in agreement with the formation of a charge-reduced ion population, when elevated collision energies were applied (Figure 6.6).[14] Second, charge state distributions could be affected by the compactness of the protein structure.[193] Unfolded protein structures can exhibit larger solvent-assessable surface areas than compact protein conformations and can therefore pick up larger amount of charges during the nESI process.[193-195] Different folding states of AmtB-MBP in solution could therefore explain the appearance of multimodal charge state distributions.[195] Furthermore, the amount of energy that is transferred to the protein ions during CID commonly increases with the protein charge state. At comparable CID and sample conditions, the detergent removal for a highly charged membrane protein could occur more readily than for a more charge-reduced membrane protein, which would be in line with the here-obtained results (Figure 6.6).

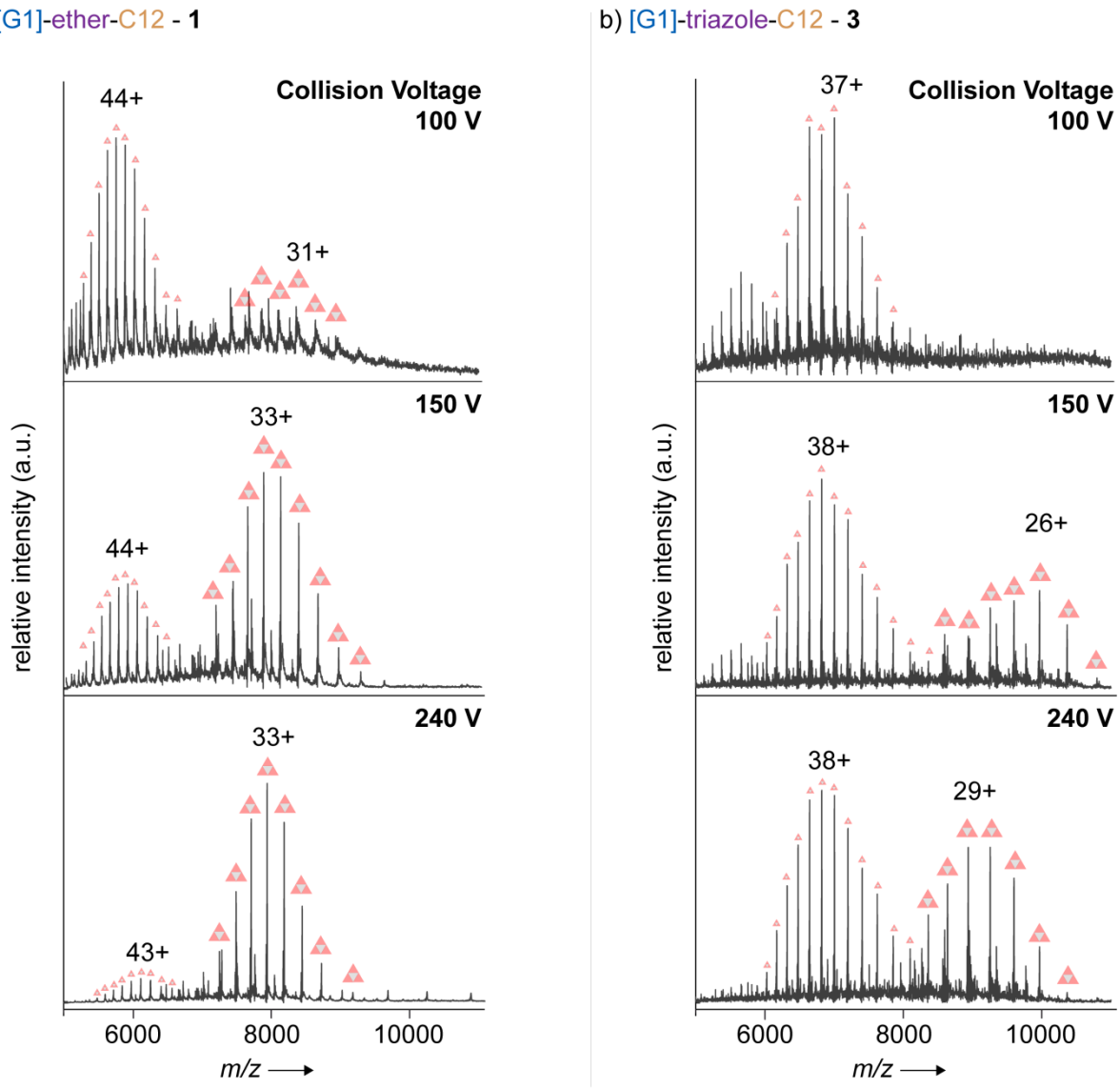

Figure 6.6: Mass spectra of AmtB-MBP released from the OGD mixtures **1** and **3** at different collision voltages. The intensity of charge-reduced protein signals increased at elevated collision voltages.

In strong contrast to the results obtained from the OGD mixtures **1**, **3**, **4**, **7**, and **8**, the reference detergent DDM did not lead to interpretable mass spectra for AqpZ-GFP and AmtB-MBP (Figure 6.7). Even when employing highest collision voltages (240 V), only insufficient detergent removal and poorly resolved spectra were obtained. The here-mentioned challenge to acquire membrane protein mass spectra by means of DDM is commonly reported in literature.[14] Due to its capability to preserve the native structure of many membrane proteins upon isolation, however, DDM is still indispensable for membrane protein research.[20, 40, 41] In comparison, membrane proteins are easily released from the OGD environment by CID, which highlights the great potential of the OGD family to be used for the direct native MS analysis of membrane proteins upon extraction from biological membranes.

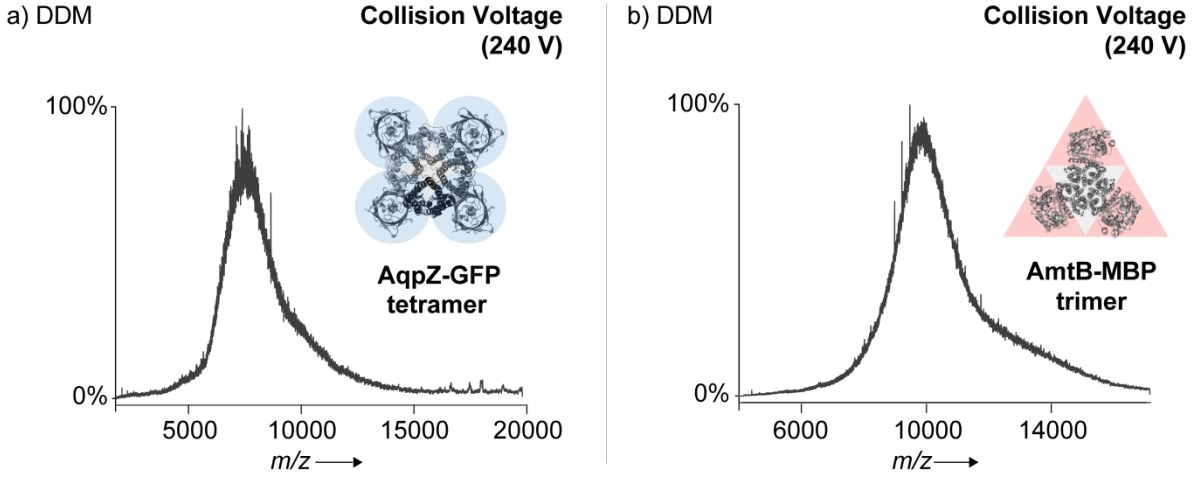

Figure 6.7: Mass spectra of AqpZ-GFP and AmtB-MBP released from the reference detergent DDM. Even at highest collision voltages (240 V) only insufficient detergent removal and poorly resolved spectra were obtained.

6.3.3 Towards Membrane Proteins with Pharmaceutical Relevance

Once it was confirmed that OGD mixtures can facilitate the purification and native MS analysis of AqpZ-GFP and AmtB-MBP, their utility for the nESI-MS analysis of pharmaceutically relevant membrane proteins was tested, such as MATE and NTSR1. Akin to AqpZ and AmtB, MATE is compatible to a broad range of detergents and has been intensively investigated by native MS before.[14] On the other hand, only one detergent mixture has yet been reported for the membrane protein NTSR1 that comprises ideal properties for its purification and native MS analysis, which consists of DDM, cholesterol, and foscholine.[172] Despite their pharmaceutical relevance, MATE-GFP and NTSR1 are present as monomers in biological membranes with molecular masses of 78.2 kDa and 37.3 kDa, respectively.[14, 172]

MATE-GFP was overexpressed in *E. coli* and the protein was purified as described above using the OGD mixtures **1** and **7**. Subsequent nESI-MS analysis of the isolated samples revealed highly resolved mass spectra of monomeric MATE-GFP (Figure 6.8a). No significant shifts in z_{ave} were obtained between **1** (16+) and **7** (16+), which confirmed that both OGD mixtures comprised no charge reducing properties. In case of **1**, lipid-bound states of minor intensity between MATE-GFP and CDL were obtained (Figure 6.8a).

In contrast, the intensity of lipid-bound states was significantly enhanced in case of **7**, which was similar to the results obtained for AqpZ-GFP and AmtB-MBP before. The results obtained from MATE-GFP therefore reconfirmed that the ability to detect protein complexes with membrane lipids upon extraction could be tuned by changing the structure of the OGD head group and tail.

More remarkably, detergent exchange experiments revealed that the respective OGD mixtures can be also utilized for the solubilization of NTSR1. No protein precipitation occurred visibly upon transferring NTSR1 from the trimeric detergent mixture (DDM, cholesterol, foscholine) to the OGD mixtures **1** and **7**. The nESI-MS analysis of both samples revealed highly resolved mass spectra of NTSR1 with similar z_{ave} values for **1** (10+) and **7** (10+, Figure 6.8). The narrow and unimodal charge state distributions obtained were similar to data that have been reported in literature from the nESI-MS analysis of functional NTSR1s.[172] The data shown here therefore indicated that native folding of NTSR1 could be possibly preserved upon detergent exchange to OGDs **1** and **7** in solution.

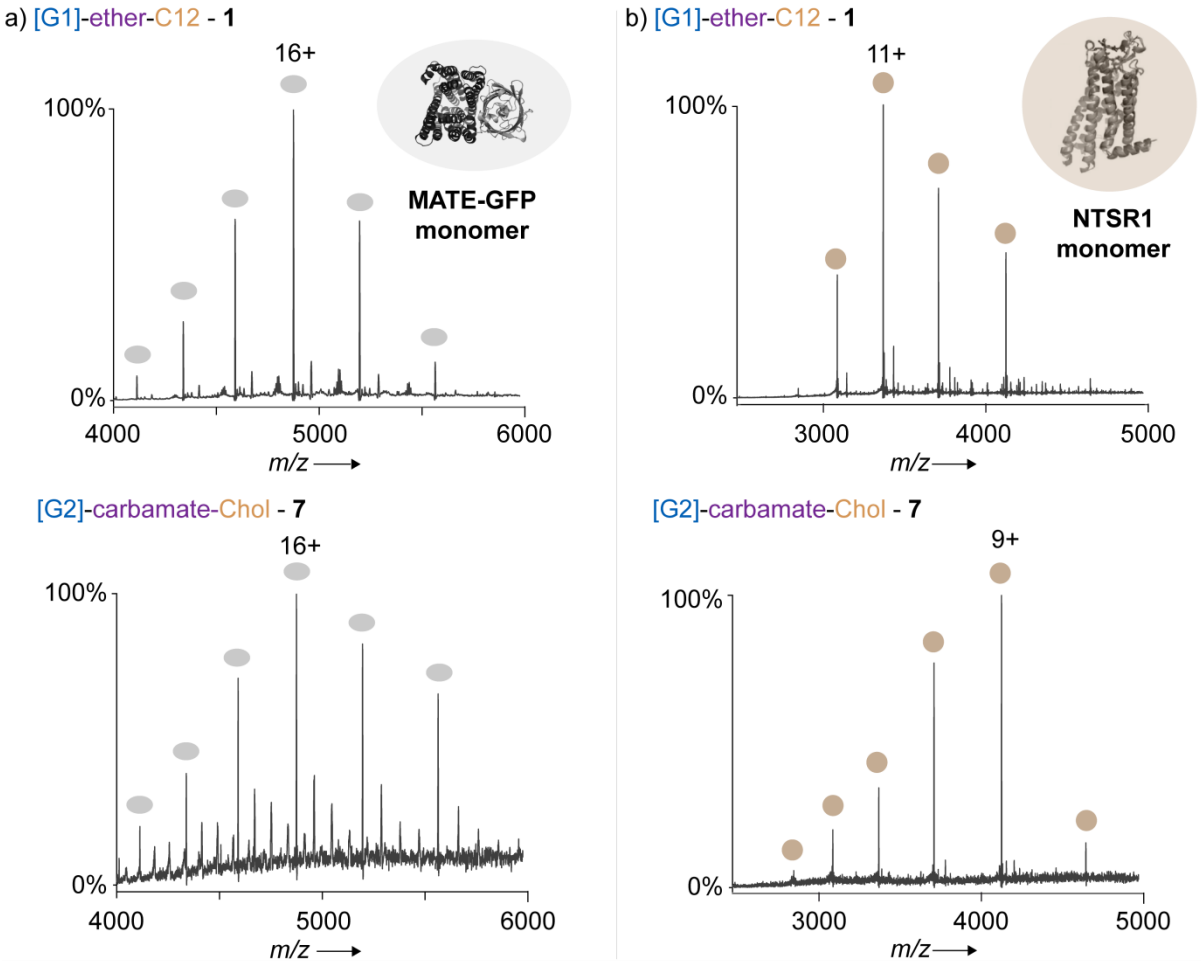

Figure 6.8: Mass spectra of a) MATE-GFP upon isolation from biological membranes and b) NTSR1 upon detergent exchange from a mixture of DDM, cholesterol, and foscholine to the OGD mixtures **1** and **7** (CID voltage = 200 V).

To evaluate the utility of OGDs to preserve functional states of NTSR1, a previously established fluorescence assay was applied.[172, 196] To do so, NTSR1 was solubilized in the reference detergent lauryl maltose neopentyl glycol (LMNG). This detergent does not facilitate the native MS analysis of this protein; however, it is known to properly preserve functional states of NTSR1.[172, 196] Next, NTSR1 was solubilized in the OGD mixtures **1** and **7**. To all three samples, a tenfold excess of a dye-labeled ligand was added – called BODIPY-NT(8-13), which is suggested to exhibit a high binding affinity exclusively to native NTSR1.[196] Upon incubation for 60 minutes, the excess of ligand was removed by gel-filtration chromatography and the remaining fluorescence of the sample was measured. The detected fluorescence intensity was then divided by the protein concentration and the data were normalized to the intensity obtained from the LMNG sample (Figure 6.9). As a control, NTSR1 solubilized in LMNG without BODIPY-NT(8-13) was analyzed, too.

Compared to LMNG, a slight reduction in fluorescence intensity was obtained for **1** and **7** (Figure 6.9). The intensity was found to be reduced to 80% for **1** and to 60% for **7**. The control sample showed no fluorescence intensity, which confirmed that the obtained fluorescence intensity from the other samples originated from the added BODIPY-NT(8-13). By assuming that the remaining fluorescence intensity originated only from the NTSR1 complex formed with BODIPY-NT(8-13), it could be concluded that significant proportions of functional NTSR1 retained upon detergent exchange from LMNG to the OGD mixtures **1** and **7**.

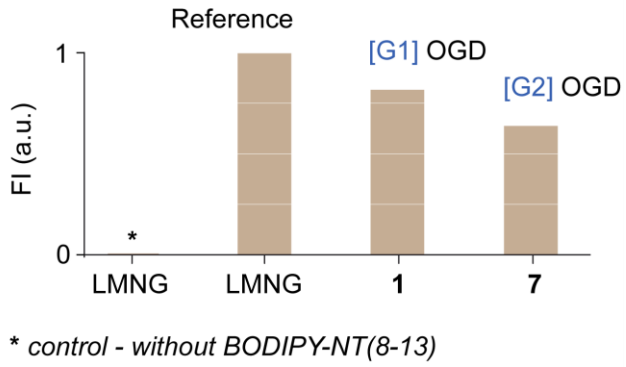

Figure 6.9: Normalized fluorescence intensity (FI) obtained from mixtures between NTSR1 and the fluorescent dye-labeled ligand BODIPY-NT(8-13) in different detergent environments. By assuming that the detected FI mainly originated from complexes formed by BODIPY-NT(8-13) and functional NTSR1, the data indicated that significant proportions of functional NTSR1 were retained upon detergent exchange from lauryl maltose neopentyl glycol (LMNG) to the OGD mixtures **1** and **7**.

6.4 Conclusions

In summary it was demonstrated that the family of OGDs offered new opportunities for optimizing the purification and native MS analysis of membrane proteins. It was shown in detail how the modular architecture of OGDs could be used to independently optimize protein purification, charge reduction, and the ability to detect protein complexes formed with co-purified membrane lipids by native MS. Extraction experiments revealed that the membrane protein amounts that could be isolated from biological membranes were very sensitive to the structure of the OGD head group and tail. OGDs that comprised a smaller [G1] head group and a linear tail extracted membrane proteins more efficiently than OGDs that had a bigger [G2] head group and a linear tail. The obtained difference between [G1] and [G2] OGDs confirmed that the detergent's capability to extract membrane proteins was inversely correlated to the size of its head group. The extraction efficiency of [G2] OGDs, however, could be significantly improved by changing linear alkyl spacers with more lipid-like tails.

Further native MS experiments revealed that both structural parameters, *e.g.*, head group and tail, altered the extent of membrane lipid co-purification. For [G1] OGDs, no complexes formed with membrane lipids were detected by nESI-MS. In strong contrast, mass spectra acquired by means of [G2] OGDs consistently showed intense signals of membrane proteins in complexes with structurally relevant membrane lipids. More remarkably, exchanging the basicity of the linker between the OGD head group and tail also enabled tuning of membrane protein charge states.

Taken all together, the obtained data confirmed that protein purification could be optimized by tuning the structure of the OGD head group and tail. Subsequent nESI-MS analysis of the so-obtained protein-detergent mixtures revealed that protein charge reduction and the ability to detect binding to structurally relevant membrane lipids could be independently addressed by tuning either the basicity of the linker or the structure of the head group and hydrophobic tail, respectively. Moreover, OGDs were found to be suitable for the native MS analysis of membrane proteins that were of pharmaceutical relevance, such as MATE or NTSR1 – a member of the challenging GPCR family. Although none of the here-investigated OGDs covered all desired properties at once, their modular architecture allowed one to tailor their properties for individual native MS applications on-demand. The ability to facilitate the structural analysis of pharmaceutically relevant membrane proteins by OGDs makes this detergent family even more valuable for native MS applications.

7. Overall Summary and Future Perspective

Taken together, the non-ionic family of OGDs turned out to be a promising tool-box for the structural investigation of membrane proteins. The modular exchange of individual detergent building blocks enabled for the first time the directed support of fundamental aspects in membrane protein research, such as membrane protein purification and native MS applications. With a set of eight different OGD regioisomer mixtures and five membrane proteins it was shown how protein extraction from biological membranes, tuning of charge states, and the ability to detect protein complexes formed with co-purified membrane lipids could be improved on-demand by controlling the molecular structure of OGDs.

7.1 Summary

In the first part of this thesis, the synthesis of a new OGD library was presented. The obtained detergent batches consisted of OGD regioisomer mixtures, including first- [G1] or second-generation [G2] triglycerol head group regioisomers, different hydrophobic tails, and variable connecting linker groups. The starting materials that were used for the preparation of OGDs were regioisomer mixtrues of [pG1]-OH and [pG2]-OH. Two different [pG1]-OH regioisomers were obtained from acetal protection of technical oligoglycerol mixtures. Their molar ratio depended significantly on the commercial oligoglycerol source and using these mixtures for preparing the next higher dendron generation led to the obtainment of three [pG2]-OH regioisomers. With this regard, liquid chromatography methods and spectroscopic reference data were developed, which enabled validating the regioisomer content during almost all stages of OGD synthesis. The here-provided NMR data and liquid chromatography methods will help to control the regioisomer content during OGD synthesis in future.

In the second part, the potential of the modular OGD library to be used for the directed manipulation of membrane protein charge states was explored. The charge-reducing properties of OGDs were first evaluated by tandem MS experiments on protein complexes formed with the soluble model protein BLG. The dissociation pattern of these complexes revealed that the crown ether-like structure of the OGD head group enabled the removal of sodium cations from PDCs, while the basicity of the linker group was important for the removal of protons. Moreover, it was for the first time proven that OGDs could enable the solubilization and native MS analysis of membrane proteins by means of the membrane protein OmpF. A comparative study with BLG and the trimeric membrane protein OmpF confirmed not only that membrane protein charge states could be adjusted by tuning the detergent's basicity, but also that charge-reducing properties of detergents could be evaluated without consuming expensive membrane protein samples.

The last part of this thesis evaluated how protein purification and their analysis by native MS could be optimized by tuning the molecular structure of OGDs. The protein extraction capability of OGDs was found to be very sensitive to the size of the OGD head group and the structure of the hydrophobic tail. The best performance was obtained from [G1] OGD mixtures, while the performance of [G2] OGDs could be improved by using lipid-like hydrophobic tails instead of long linear alkyl spacers.

More surprisingly, [G1] OGD regioisomer mixtures could extract higher protein amounts than individual ones. Certain OGD mixtures thereby outperformed the detergent DDM, which is a current standard in structural biology. The obtained results therefore demonstrated the enormous potential of OGDs for isolating large protein quantities. Subsequent analysis of so-obtained protein-detergent mixtures by native MS revealed that protein charge reduction and the ability to detect protein complexes formed with co-purified membrane lipids could be independently optimized by tuning either the basicity of the linker or the structure of OGD head group and tail, respectively. Highly resolved membrane protein mass spectra could be obtained directly upon protein extraction. In strong contrast, only insufficient detergent removal and poorly resolved protein spectra were obtained in case of DDM. In comparison, membrane proteins were easily released from OGDs, which enabled the easy native MS analysis of a challenging GPCR. Further results indicated that functional states of this GPCR partially retained upon solubilization with OGDs. The results obtained from the last part of this thesis underlined the enormous potential of OGDs to be used for the purification and native MS analysis of membrane proteins. None of the here-investigated OGDs covered all optimal properties at once. Unless to other detergent families, the molecular structure of OGDs can be tailored on-demand for membrane protein isolation and individual applications in native MS.

7.1 Future Perspectives

Finding the right detergent for an application in membrane protein research is currently a major challenge. This process can be very time and sample consuming, because the detergent's utility is often difficult to predict. The ability to tailor the structure of OGDs for protein isolation and native MS applications is therefore a breakthrough and will facilitate the structural investigation of the membrane proteome. The compatibility of OGDs to the five membrane proteins investigated here indicated that OGDs may be widely applicable to other membrane proteins. Further experiments will be conducted to prove the validity of this assumption. Moreover, it would be very interesting to see if OGDs can also facilitate the application of other biophysical tools, such as NMR spectroscopy, X-ray crystallography, EM, or SANS. Similarly to the bottom-up strategy presented in this thesis, one could easily evaluate how changes in the OGD structure and regioisomer composition are affecting their utility for these biophysical tools. In subsequent stages, one could test if the design guidelines deduced from the here-presented OGDs are transferable to other detergent families. This would open new opportunities for the development of designer detergents with tailor-made properties for individual applications.

However, the structural properties of biological membranes are generally poorly duplicated in a detergent environment. The removal of the membrane environment by means of detergents is therefore often accompanied by a perturbation of the membrane protein's structure and function. Having demonstrated now that heterogeneous OGD regioisomer mixtures can outperform classic detergents in terms of protein extraction efficiency, it would be interesting to evaluate how far they can improve the preservation of functional membrane protein states. With this regard, only one experiment was performed during this thesis, which surprisingly indicated that OGD mixtures can preserve functional states of a GPCR. In this context, more experiments will be conducted to underline the consistency of this remarkable result.

Furthermore, it will be investigated if the benefits that arose from [G1] OGDs regioisomer mixtures can be also obtained from other sorts of isomer mixtures, such as diastereoisomers. The alpha- and beta-form of DDM, for example, can show similar membrane protein extraction efficiencies but the mixture of both has not been systematically evaluated yet.[197] Using heterogeneous detergent mixtures as alternatives may help to overcome the general limitations that are associated with the usage of detergents as membrane mimic.

Seen from a broader perspective, the obtained results finally demonstrated the great potential of bottom-up strategies for gaining a structure-based understanding about the detergent's utility for membrane protein research. The implementation of this empirical approach requires simply the screening of diversified detergent libraries. From a synthetic point of view, however, the provision of large detergent libraries is very costly and also membrane proteins are expensive to manufacture. Native MS can help to decrease the required sample amounts and new synthetic concepts need to be examined that can dramatically reduce the synthetic effort, which is required for detergent synthesis. Pharmaceutical companies have already shown a possible solution: They demonstrated the great potential of combinatorial chemistry for the hit-to-lead optimization of medicinal drugs. With this regard, the potential of combinatorial chemistry concepts for facilitating the structure-based optimization of detergents in membrane protein research will be evaluated in future.

7. References

[1] Vinothkumar, K. R.; Henderson, R., Structures of membrane proteins. *Q Rev. Biophys.* **2010**, *43*, 65-158.

[2] Almén, M. S.; Nordström, K. J. V.; Fredriksson, R.; Schiöth, H.B., Mapping the human membrane proteome: a majority of the human membrane proteins can be classified according to function and evolutionary origin. *BMC Biology* **2009**, *7*, 1-14.

[3] Overington, J. P.; Al-Lazikani, B.; Hopkins, A. L., How many drug targets are there? *Nat. Rev. Drug Discov.* **2006**, *5*, 993-996.

[4] Fagerberg, L.; Jonasson, K.; von Heijne, G.; Uhlén, M.; Berglund, L., Prediction of the human membrane proteome. *Proteomics* **2010**, *10*, 1141-1149.

[5] Shimizu, K.; Cao, W.; Saad, G.; Shoji, M.; Terada, T., Comparative analysis of membrane protein structure databases. *BBA - Biomembranes* **2018**, *1860*, 1077-1091.

[6] Arora, A.; Tamm, L. K., Biophysical approaches to membrane protein structure determination. *Curr. Opin. Struct. Biol.* **2001**, *11*, 540-547.

[7] Moraes, I.; Evans, G.; Sanchez-Weatherby, J.; Newstead, S.; Stewart, P.D.S., Membrane protein structure determination - The next generation. *Biochim. Biophys. Acta*. **2014**, *1838*, 78-87.

[8] Breyton, C.; Gabel, F.; Lethier, M.; Flayhan, A.; Durand, G.; Jault, J. M.; Juillan-Binard, C.; Imbert, L.; Moulin, M.; Ravaud, S.; Härtlein, M.; Ebel, C., Small-angle neutron scattering for the study of solubilised membrane proteins. *Eur. Phys. J. E*. **2013**, *36*, 1-16.

[9] Rawson, S.; Davies, S.; Lippiat, J. D.; Muench, S. P., The changing landscape of membrane protein structural biology through developments in electron microscopy. *Mol. Membr. Biol.* **2016**, *33*, 12-22.

[10] Löw, C.; Moberg, P.; Quistgaard, E.M.; Hedrén, M.; Guettou, F.; Frauenfeld, J.; Haneskog, L.; Nordlund, P., High-throughput analytical gel filtration screening of integral membrane proteins for structural studies. *Biochim. Biophys. Acta*. **2013**, *1830*, 3497-3508.

[11] Marcoux, J.; Robinson, C. V., Twenty Years of Gas Phase Structural Biology. *Structure* **2013**, *21*, 1541-1550.

[12] Erba, E. B.; Petosa, C., The emerging role of native mass spectrometry in characterizing the structure and dynamics of macromolecular complexes. *Protein Sci.* **2015**, *24*, 1176-1192.

[13] Laganowsky, A.; Reading, E.; Hopper, J. T. S.; Robinson, C. V., Mass Spectrometry of Intact Membrane Protein Complexes. *Nat. Protoc.* **2013**, *8*, 639-651.

[14] Reading, E.; Liko, I.; Allison, T. M.; Benesch, J. L. P.; Laganowsky, A.; Robinson, C. V., The Role of the Detergent Micelle in Preserving the Structure of Membrane Proteins in the Gas Phase. *Angew. Chem. Int. Ed.* **2015**, *54*, 4577-4581.

[15] Borysik, A. J.; Robinson, C. V., The 'sticky business' of cleaning gas-phase membrane proteins: a detergent oriented perspective. *Phys. Chem. Chem. Phys*. **2012**, *14*, 14439-14449.

[16] Borysik, A. J.; Hewitt, D. J.; Robinson, C. V., Detergent Release Prolongs the Lifetime of Native-like Membrane Protein Conformations in the Gas-Phase. *J. Am. Chem. Soc.* **2013**, *135*, 6078-6083.

[17] Mehmood, S.; Marcoux, J.; Hopper, J. T. S.; Allison, T. M.; Liko, I.; Borysik, A. J.; Robinson, C. V., Charge Reduction Stabilizes Intact Membrane Protein Complexes for Mass Spectrometry. *J. Am. Chem. Soc.* **2014**, *136*, 17010-17012.

[18] Bechara, C.; Robinson, C. V., Different Modes of Lipid Binding to Membrane Proteins Probed by Mass Spectrometry. *J. Am. Chem. Soc.* **2015**, *137*, 5240-5247.

[19] Laganowsky, A.; Reading, E.; Allison, T. M.; Ulmschneider, M. B.; Degiacomi, M. T.; Baldwin, A.J.; Robinson, C.V., Membrane proteins bind lipids selectively to modulate their structure and function. *Nature* **2014**, *510*, 172-175.

[20] Prive´, G. G., Detergents for the stabilization and crystallization of membrane proteins. *Methods* **2007**, *41*, 388-397.

[21] Marty, M. T.; Hoi, K. K.; Robinson, C. V., Interfacing membrane mimetics with mass spectrometry. *Acc. Chem. Res.* **2016**, *15*, 2459-2467.

[22] Thota, B. N. S.; Urner, L. H.; Haag, R., Supramolecular Architectures of Dendritic Amphiphiles in Water. *Chem. Rev.* **2015**, *116*, 2079 - 2102.

[23] Wyszogrodzka, M.; Haag, R., Synthesis and Characterization of Glycerol Dendrons, Self-Assembled Monolayers on Gold: A Detailed Study of Their Protein Resistance. *Biomacromolecules* **2009**, *10*, 1043-1054.

[24] Wyszogrodzka, M.; Haag, R., Study of Single Protein Adsorption onto Monoamino Oligoglycerol Derivatives: A Structure-Activity Relationship. *Langmuir* **2009**, *25*, 5703-5712.

[25] Nachtigall, O.; Kördel, C.; Urner, L. H.; Haag, R., Photoresponsive Switches at Surfaces Based on Supramolecular Functionalization with Azobenzene-Oligoglycerol Conjugates. *Angew. Chem. Int. Ed.* **2014**, *53*, 9669-9673.

[26] Wycisk, V.; Pauli, J.; Welker, P.; Justies, A.; Resch-Genger, U.; Haag, R.; Licha, K., Glycerol-Based Contrast Agents: A Novel Series of Dendronized Pentamethine Dyes. *Bioconjugate Chem.* **2015**, *26*, 773-781.

[27] Huth, K.; Heek, T.; Achazi, K.; Kühne, C.; Urner, L. H.; Pagel, K.; Dernedde, J.; Haag, R., Noncharged and Charged Monodendronised Perylene Bisimides as Highly Fluorescent Labels and their Bioconjugates. *Chem. Eur. J.* **2017**, *23*, 4849-4862.

[28] Gupta, S.; Tyagi, R.; Parmar, V. S.; Sharma, S. K.; Haag, R., Polyether based amphiphiles for delivery of active components. *Polymer* **2012**, *53*, 3053-3078.

[29] Malhotra, S.; Bauer, H.; Tschiche, A.; Staedtler, A. M.; Mohr, A.; Calderón, M.; Parmar, V. S.; Hoeke, L.; Sharbati, S.; Einspanier, R.; Haag, R., Glycine-Terminated Dendritic Amphiphiles for Nonviral Gene Delivery. *Biomacromolecules* **2012**, *13*, 3087-3098.

[30] Ma, P.; Zemmel, R., Value of novelty? *Nat. Rev. Drug Discov.* **2002**, *1*, 571-572.

[31] Whitesides, G. M.; Grzybowski, B., Self-Assembly at All Scales. *Science* **2002**, *295*, 2418-2421.

[32] Meyer, E. E.; Rosenberg, K. J.; Israelachvili, J., Recent progress in understanding hydrophobic interactions. *PNAS* **2006**, *103*, 15739-15746.

[33] Jain, N.; Trabelsi, S.; Guillot, S.; Mc Loughlin, D.; Langevin, D.; Letellier, P.; Turmine, M., Critical Aggregation Concentration in Mixed Solutions of Anionic Polyelectrolytes and Cationic Surfactants. *Langmuir* **2004**, *20*, 8496-8503.

[34] Lombardo, D.; Kiselev, M. A.; Magazù, S.; Calandra, P., Amphiphiles Self-Assembly: Basic Concepts and Future Perspectives of Supramolecular Approaches. *Adv. Cond. Matter. Phys.* **2015**, *2015*, 1-22.

[35] Israelachvili, J. N.; Mitchell, D. J.; Ninham, B. W., Theory of Self-Assembly of Hydrocarbon Amphiphiles into Micelles and Bilayers. *J. Chem. Soc., Faraday Trans. 2*. **1976**, *72*, 1525-1568.

[36] Garavito, R. M.; Ferguson-Miller, S., Detergents as Tools in Membrane Biochemistry. *J. Biol. Chem.* **2001**, *276*, 32403-32406.

[37] Kalipatnapu , S.; Chattopadhyay, A., Membrane Protein Solubilization: Recent Advances and Challenges in Solubilization of Serotonin1A Receptors. *IUBMB Life* **2005**, *57*, 505-512.

[38] Pagano, R. E.; Cherry, R. J.; Chapman, D., Phase Transitions and Heterogeneity in Lipid Bilayers. *Science* **1973**, *181*, 557-559.

[39] Simons, K.; Vaz, W. L. C., Model Systems, Lipid Rafts, and Cell Membranes. *Annu. Rev. Biophys. Biomol. Struct.* **2004**, *33*, 269-295.

[40] le Maire, M.; Champeil, P.; Möller, J. V., Interaction of membrane proteins and lipids with solubilizing detergents. *Biochim. Biophys. Acta*. **2000**, *1508*, 86-111.

[41] Seddon, A. M.; Curnow, P.; Booth, P. J., Membrane proteins, lipids and detergents: not just a soap opera. *Biochim. Biophys. Acta*. **2004**, *1666*, 105-117.

[42] Helenius, A.; Simons, K., Solubilization of Membranes by Detergents. *Biochim. Biophys. Acta*. **1975**, *415*, 29-79.

[43] Jackson, M. L.; Schmidt, C. F.; Lichtenberg, D.; Litman, B. J.; Albert, A. D., Solubilization of Phosphatidylcholine Bilayers by Octyl Glucoside. *Biochemistry* **1982**, *21*, 4576-4582.

[44] Lichtenberg, D.; Robson, R.; Dennis, E. A., Solubilization of Phospholipids by Detergents - Structural and Kinetic Aspects. *Biochim. Biophys. Acta*. **1983**, *737*, 285-304.

[45] Paternostre, M.-T.; Roux, M.; Rigaud, J.-L., Mechanisms of Membrane Protein Insertion into Liposomes during Reconstitution Procedures Involving the Use of Detergents. *Biochemistry* **1988**, *27*, 2668-2677.

[46] Kragh-Hansen, U.; le Maire, M.; Noel, J.-P.; Gulik-Krzywicki, T.; Moller, J. V., Transitional Steps in the Solubilization of Protein-Containing Membranes and Liposomes by Nonionic Detergents. *Biochemistry* **1993**, *32*, 1648-1656.

[47] Gupta, K.; Donlan, J. A. C.; Hopper, J. T. S.; Uzdavinys, P.; Landreh, M.; Struwe, W. B.; Drew, D.; Baldwin, A. J.; Stansfeld, P. J.; Robinson, C. V., The role of interfacial lipids in stabilizing membrane protein oligomers. *Nature* **2017**, *541*, 421-424.

[48] Montserret, R.; Mc Leish, M.J.; Böckmann, A.; Geourjon, C.; Penin, F., Involvement of electrostatic interactions in the mechanism of peptide folding induced by sodium dodecyl sulfate binding. *Biochemistry* **2000**, *25*, 8362-8373.

[49] Iverson, T. M.; Luna-Chavez, C.; Cecchini, G.; Rees, D. C., Structure of the Escherichia coli Fumarate Reductase Respiratory Complex. *Science* **1999**, *284*, 1961-1966.

[50] Bertero, M. G.; Rothery, R. A.; Palak, M.; Hou, C.; Lim, D.; Blasco, F.; Weiner, J. H.; Strynadka, N. C., Insights into the respiratory electron transfer pathway from the structure of nitrate reductase A. *Nat. Struct. Biol.* **2003**, *10*, 681-687.

[51] Thrash, S. L.; Otto Jr., J. C.; Deits, T. L., Effect of Divalent Ions on Protein Precipitation with Polyethylene Glycol: Mechanism of Action and Applications. *Protein Expr. Purif.* **1991**, *2*, 83-89.

[52] Michel, H. *M. Rossmann, E. Arnold (Eds.), International Tables for Crystallgraphy Volume F*. **2001**, Kluwer Academic Publishers, Dordrecht, Netherlands, 94-100.

[53] Aiyar, N.; Bennett, C. F.; Nambe, P.; Valinski, W.; Angioli, M.; Minnich, M.; Crooke, S. T., Solubilization of rat liver vasopressin receptors as a complex with a guanine-nucleotide-binding protein and phosphoinositide-specific phospholipase C. *Biochem. J.* **1989**, *261*, 63-70.

[54] Klammt, C.; Schwarz, D.; Fendler, K.; Haase, W.; Dötsch, V.; Bernhard, F., Evaluation of detergents for the soluble expression of a-helical and b-barrel-type integral membrane proteins by a preparative scale individual cell-free expression system. *FEBS J.* **2005**, *23*, 6024-6038.

[55] Klammt, C.; Schwarz, D.; Löhr, F.; Schneider, B.; Dötsch, V.; Bernhard, F., Cell-free expression as an emerging technique for the large scale production of integral membrane protein. *FEBS J.* **2006**, *18*, 4141-4153.

[56] Pucci, C. B. B.; Popot, J.-L. *Amphipols and Fluorinated Surfactants: Two Alternatives to Detergents for Studying Membrane Proteins In vitro. In: Mus-Veteau I. (eds) Heterologous Expression of Membrane Proteins. Methods in Molecular Biology (Methods and Protocols)*. **2009**, Humana Press, 219-245.

[57] Chabaud, E.; Barthélémy, P.; Mora, N.; Popot, J.-L.; Pucci, B., Stabilization of integral membrane proteins in aqueous solution using fluorinated surfactants. *Biochimie*. **1998**, *80*, 515-530.

[58] Breyton, C.; Chabaud, E.; Chaudier, Y.; Pucci, B.; Popot, J.-L., Hemifluorinated surfactants: a non-dissociating environment for handling membrane proteins in aqueous solutions? *FEBS Lett.* **2004**, *564*, 312-318.

[59] Abla, M.; Durand, G.; Breyton, C.; Raynal, S.; Ebel, C.; Pucci, B., A diglucosylated fluorinated surfactant to handle integral membrane proteins in aqueous solution. *J. Fluor. Chem.* **2012**, *134*, 63-71.

[60] Popot, J.-L., Amphipols, Nanodiscs, and Fluorinated Surfactants: Three Nonconventional Approaches to Studying Membrane Proteins in Aqueous Solutions. *Annu. Rev. Biochem.* **2010**, *79*, 737-775.

[61] Tribet, C.; Audebert, R.; Popot, J.-L., Amphipols: Polymers that keep membrane proteins soluble in aqueous solutions. *PNAS* **1996**, *93*, 15047-15050.

[62] Popot, J.-L.; Berry, E. A.; Charvolina, D.; Creuzenet, C.; Ebel, C.; Engelman, D. M.; Flötenmeyer, M.; Giusti, F.; Gohon, Y.; Hervé, P.; Hong, Q.; Lakey, J. H.; Leonard, K.; Shuman, H. A.; Timmins, P.; Warschawski, D. E.; Zito, F.; Zoonens, M.; Pucci, B.; Tribet, C., Amphipols: polymeric surfactants for membrane biology research. *Cell. Mol. Life Sci.* **2003**, *60*, 1559-1574.

[63] Ladaviére, C.; Toustou, M.; Gulik-Krzywicki, T.; Tribet, C., Slow Reorganization of Small Phosphatidylcholine Vesicles upon Adsorption of Amphiphilic Polymers. *J. Colloid Interface Sci.* **2001**, *241*, 178-187.

[64] Mc Gregor, C.-L.; Chen, L.; Pomroy, N. C.; Hwang, P.; Go, S.; Chakrabartty, A.; Privé, G. G., Lipopeptide detergents designed for the structural study of membrane proteins. *Nat. Biotechnol.* **2003**, *21*, 171-176.

[65] Prive, G. G., Lipopeptide detergents for membrane protein studies. *Curr. Opin. Struct. Biol.* **2009**, *19*, 379-385.

[66] Dürr, U. H. N.; Gildenberg, M.; Ramamoorthy, A., The Magic of Bicelles Lights Up Membrane Protein Structure. *Chem. Rev.* **2012**, *112*, 6054-6074.

[67] Bayburt, T. H.; Grinkova, Y. V.; Sligar, S. G., Self-Assembly of Discoidal Phospholipid Bilayer Nanoparticles with Membrane Scaffold Proteins. *Nano Lett.* **2002**, *2*, 853-856.

[68] Bayburt, T. H.; Sligar, S. G., Self-assembly of single integral membrane proteins into soluble nanoscale phospholipid bilayers. *Protein Sci.* **2003**, *12*, 2476-2481.

[69] Shenkarev, Z. O.; Lyukmanova, E. N.; Solozhenkin, O. I.; Gagnidze, I. E.; Nekrasova, O. V.; Chupin, V. V.; Tagaev, A. A.; Yakimenko, Z. A.; Ovchinnikova, T. V.; Kirpichnikov, M. P.; Arseniev, A. S., Lipid-Protein Nanodiscs: Possible Application in High Resolution NMR Investigations of Membrane Proteins and Membrane Active Peptides. *Biochem. (Mosc.)*. **2009**, *74*, 756-765.

[70] Milic, D.; Veprintsev, D. B., Large-scale production and protein engineering of G protein-coupled receptors for structural studies. *Front. Pharmacol.* **2015**, *6*, 1 -24.

[71] Inagaki, S.; Ghirlando, R.; Grisshammer, R., Biophysical characterization of membrane proteins in nanodiscs. *Methods* **2013**, *59*, 287-300.

[72] Wolynes, P. G., Biomolecular folding in vacuo!!!(?). *PNAS*. **1995**, *92*, 2426-2427.

[73] Ilag, L.L.; Ubarretxena-Belandia, I.; Tate, C. G.; Robinson, C. V., Drug Binding Revealed by Tandem Mass Spectrometry of a Protein-Micelle Complex. *J. Am. Chem. Soc.* **2004**, *126*, 14362-14363.

[74] Lengqvist, J.; Svensson, R.; Evergren, E.; Morgenstern, R.; Griffiths, W. J., Observation of an Intact Noncovalent Homotrimer of Detergent-solubilized Rat Microsomal Glutathione Transferase-1 by Electrospray Mass Spectrometry. *J. Biol. Chem.* **2004**, *279*, 13311-13316.

[75] Barrera, N. P.; Bartolo, N. D.; Booth, P. J.; Robinson, C. V., Micelles Protect Membrane Complexes from Solution to Vacuum. *Science* **2008**, *321*, 243 - 246.

[76] Banerjee, S.; Mazumdar, S., Electrospray Ionization Mass Spectrometry: A Technique to Access the Information beyond the Molecular Weight of the Analyte. *Int. J. Anal. Chem.* **2012**, *2012*, 1-40.

[77] Morgner, N.; Kleinschroth, T.; Barth, H.-D.; Ludwig, B.; Brutschya, B., A Novel Approach to Analyze Membrane Proteins by Laser Mass Spectrometry: From Protein Subunits to the Integral Complex. *J. Am. Soc. Mass Spectrom.* **2007**, *18*, 1429-1438.

[78] Ambrose, S.; Housden, N. G.; Gupta, K.; Fan, J.; White, P.; Yen, H.-Y.; Marcoux, J.; Kleanthous, C.; Hopper, J. T. S.; Robinson, C. V., Native Desorption Electrospray Ionization Liberates Soluble and Membrane Protein Complexes from Surfaces. *Angew. Chem. Int. Ed.* **2017**, *56*, 1-7.

[79] Wilm, M., Principles of Electrospray Ionization. *Mol. Cell. Proteomics* **2012**, *10*, 1-8.

[80] Sir Geoffrey Taylor, F. R. S., Disintegration of water drops in an electric field. *Proc. Royal Soc. Lond. A*. **1964**, *280*, 383-397.

[81] Wilm, M.; Mann, M., Analytical Properties of the Nanoelectrospray Ion Source. *Anal. Chem.* **1996**, *68*, 1-8.

[82] Iribarne, J. V.; Thomson, B.A., On the evaporation of small ions from charged droplets. *J. Chem. Phys.* **1976**, *64*, 2287-2294.

[83] Daub, C. D.; Cann, N. M., How Are Completely Desolvated Ions Produced in Electrospray Ionization: Insights from Molecular Dynamics Simulations. *Anal. Chem.* **2011**, *83*, 8372-8376.

[84] Konermann, L.; Ahadi, E.; Rodriguez, A. D.; Vahidi, S., Unraveling the Mechanism of Electrospray Ionization. *Anal. Chem.* **2012**, *85*, 2-9.

[85] Benesch, J. L. P.; Ruotolo, B. T.; Simmons, D. A.; Robinson, C. V., Protein Complexes in the Gas Phase: Technology for Structural Genomics and Proteomics. *Chem. Rev.* **2007**, *107*, 3544 - 3567.

[86] Chernushevich, I. V.; Thomson, B. A., Collisional Cooling of Large Ions in Electrospray Mass Spectrometry. *Anal. Chem.* **2004**, *76*, 1754-1760.

[87] Landreh, M.; Liko, I.; Uzdavinys, P.; Coincon, M.; Hopper, J. T.; Drew, D.; Robinson, C. V., Controlling release, unfolding and dissociation of membrane protein complexes in the gas phase through collisional cooling. *Chem. Commun.* **2015**, *51*, 15582-15584.

[88] Collings, B. A.; Douglas, D. J., An extended mass range quadrupole for electrospray mass spectrometry. *Int. J. Mass Spectrom. Ion Process*. **1997**, *162*, 121-127.

[89] Tahallah, N.; Pinkse, M.; Maier, C. S.; Heck, A. J. R., The effect of the source pressure on the abundance of ions of noncovalent protein assemblies in an electrospray ionization orthogonal time-of-flight instrument. *Rapid Commun. Mass Spectrom.* **2001**, *15*, 596-601.

[90] Hardman, M.; Makarov, A. A., Interfacing the Orbitrap Mass Analyzer to an Electrospray Ion Source. *Anal. Chem.* **2003**, *75*, 1699-1705.

[91] Rose, R. J.; Damoc, E.; Denisov, E.; Makarov, A. A.; Heck, A. J. R., High-sensitivity Orbitrap mass analysis of intact macromolecular assemblies. *Nat. Methods*. **2012**, *9*, 1084-1086.

[92] Gault, J.; Donlan, J. A. C.; Liko, I.; Hopper, J. T.; Kallol, G.; Housden, N. G.; Struwe, W. B.; Marty, M. T.; Mize, T.; Bechara, C.; Zhu, Y.; Wu, B.; Kleanthous, C.; Belov, M.; Damoc, E.; Makarov, A. A.; Robinson, C. V., High-resolution mass spectrometry of small molecules bound to membrane proteins. *Nat. Methods*. **2016**, *13*, 333-336.

[93] Lippens, J. L.; Nshanian, M.; Spahr, C.; Egea, P. F.; Loo, J.A.; Campuzano, I. D. G., Fourier Transform-Ion Cyclotron Resonance Mass Spectrometry as a Platform for Characterizing Multimeric Membrane Protein Complexes. *J. Am. Soc. Mass Spectrom.* **2018**, *29*, 183-193.

[94] Gupta, K.; Li, J.; Liko, I.; Gault, J.; Bechara, C.; Wu, D.; Hopper, J. T.; Giles, K.; Benesch, J. L. P.; Robinson, C. V., Identifying key membrane protein lipid interactions using mass spectrometry. *Nat. Protoc.* **2018**, *13*, 1106-1120.

[95] Mikhailov, V. A.; Liko, I.; Mize, T. H.; Bush, M. F.; Benesch, J. L. P.; Robinson, C.V., Infrared Laser Activation of Soluble and Membrane Protein Assemblies in the Gas Phase. *Anal. Chem.* **2016**, *88*, 7060 - 7067.

[96] Pagel, K.; Hyung, S.-J.; Ruotolo, B. T.; Robinson, C. V., Alternate Dissociation Pathways Identified in Charge-Reduced Protein Complex Ions. *Anal. Chem.* **2010**, *82*, 5363 - 5372.

[97] Zhou, M.; Wysocki, V. H., Surface Induced Dissociation: Dissecting Noncovalent Protein Complexes in the Gas phase. *Acc. Chem. Res.* **2014**, *47*, 1010-1018.

[98] Friemann, R.; Larsson, D. S. D.; Wang, Y.; van der Spoel, D., Molecular Dynamics Simulations of a Membrane Protein-Micelle Complex in Vacuo. *J. Am. Chem. Soc.* **2009**, *131*, 16606-16607.

[99] Borysik, A. J.; Robinson, C. V., Formation and Dissociation Processes of Gas-Phase Detergent Micelles. *Langmuir* **2012**, *28*, 7160-7167.

[100] Susa, A. C.; Xia, Z.; Tang, H. Y. H.; Tainer, J. A.; Williams, E. R., Charging of Proteins in Native Mass Spectrometry. *J. Am. Soc. Mass Spectrom.* **2017**, *28*, 332-340.

[101] Scalf, M.; Westphall, M. S.; Krause, J.; Kaufman, S. L.; Smith, L. M., Controlling Charge States of Large Ions. *Science* **1999**, *283*, 194-197.

[102] Liko, I.; Hopper, J. T. S.; Allison, T. M.; Benesch, J. L. P.; Robinson, C. V., Negative Ions Enhance Survival of Membrane Protein Complexes. *J. Am. Soc. Mass Spectrom.* **2016**, *27*, 1099-1104.

[103] Pacholarz, K. J.; Barran, P. E., Use of a charge reducing agent to enable intact mass analysis of cysteine-linked antibody-drug-conjugates by native mass spectrometry. *EuPA Open Proteom.* **2016**, *11*, 23-27.

[104] von Helden, G.; Wyttenbach, T.; Bowers, M. T., Conformation of Macromolecules in the Gas Phase: Use of Matrix-Assisted Laser Desorption Methods in Ion Chromatography. *Science* **1995**, *267*, 1483-1485.

[105] Drew, D.; Newstead, S.; Sonoda, Y.; Kim, H.; von Heijne, G.; Iwata, S., GFP-based optimization scheme for the overexpression and purification of eukaryotic membrane proteins in Saccharomyces cerevisiae. *Nat. Protoc.* **2008**, *3*, 784-798.

[106] Bornhorst, J. A.; Falke, J. J., Purification of Proteins Using Polyhistidine Affinity Tags. *Methods Enzymol.* **2010**, *326*, 245-254.

[107] Reading, E.; Walton, T. A.; Liko, I.; Marty, M. T.; Laganowsky, A.; Rees, D. C.; Robinson, C. V., The Effect of Detergent, Temperature, and Lipid on the Oligomeric State of MscL Constructs: Insights from Mass Spectrometry. *Chem. Biol.* **2015**, *22*,

[108] Zhou, M.; Morgner, N.; Barrera, N. P.; Politis, A.; Isaacson, S. C.; Matak-Vinković, D.; Murata, T.; Bernal, R. A.; Stock, D.; Robinson, C. V., Mass Spectrometry of Intact V-Type ATPases Reveals Bound Lipids and the Effects of Nucleotide Binding. *Science* **2011**, *334*, 380 - 385.

[109] Marcoux, J.; Wang, S. C.; Politis, A.; Reading, E.; Ma, J.; Biggin, P. C.; Zhou, M.; Tao, H.; Zhang, Q.; Chang, G.; Morgner, N.; Robinson, C. V., Mass spectrometry reveals synergistic effects of nucleotides, lipids, and drugs binding to a multidrug resistance efflux pump. *PNAS* **2013**, *110*, 9704 - 9709.

[110] Hernández, H.; Robinson, C. V., Determining the stoichiometry and interactions of macromolecular assemblies from mass spectrometry. *Nat. Protoc.* **2007**, *2*, 715-726.

[111] Daniel, J. M.; D. Friess, S.; Rajagopalan, S.; Wendt, S.; Zenobi, R., Quantitative determination of noncovalent binding interactions using soft ionization mass spectrometry. *Int. J. Mass Spectrom.* **2002**, *216*, 1 - 27.

[112] Landreh, M.; Marty, M. T.; Gault, J.; Robinson, C. V., A sliding selectivity scale for lipid binding to membrane proteins. *Curr. Opin. Struct. Biol.* **2016**, *39*, 54-60.

[113] Allison, T. M.; Reading, E.; Liko, I.; Baldwin, A. J.; Laganowsky, A.; Robinson, C. V., Quantifying the stabilizing effects of protein-ligand interactions in the gas phase. *Nat. Commun.* **2015**, *6*, 1-10.

[114] Calabrese, A. N.; Watkinson, T. G.; Henderson, P. J. F.; Radford, S. E.; Ashcroft, A. E., Amphipols Outperform Dodecylmaltoside Micelles in Stabilizing Membrane Protein Structure in the Gas Phase. *Anal. Chem.* **2015**, *87*, 1118-1126.

[115] Marty, M. T.; Hoi, K. K.; Gault, J.; Robinson, C. V., Probing the Lipid Annular Belt by Gas-Phase Dissociation of Membrane Proteins in Nanodiscs. *Angew. Chem. Int. Ed.* **2015**, *55*, 550-554.

[116] Matar-Merheb, R.; Rhimi, M.; Leydier, A.; Huché, F.; Galián, C.; Desuzinges-Mandon, E.; Ficheux, D.; Flot, D.; Aghajari, N.; Kahn, R.; Di Pietro, A.; Jault, J. M.; Coleman, A. W.; Falson, P., Structuring Detergents for Extracting and Stabilizing Functional Membrane Proteins. *PLoS One* **2011**, *6*, 1-10.

[117] Chae, P. S.; Cho, K. H.; Wander, M. J.; Bae, H. E.; Gellman, S.H.; Laible, P. D., Hydrophobic variants of ganglio-tripod amphiphiles for membrane protein manipulation. *Biochim. Biophys. Acta*. **2014**, *1838*, 278-286.

[118] Cho, K. H.; Du, Y.; Scull, N. J.; Hariharan, P.; Gotfryd, K.; Loland, C. J.; Guan, L.; Byrne, B.; Kobilka, B. K.; Chae, P. S., Novel Xylene-Linked Maltoside Amphiphiles (XMAs) for Membrane Protein Stabilisation. *ACS Chem. Biol.* **2015**, *21*,

[119] Frotscher, E.; Danielczak, B.; Vargas, C.; Meister, A.; Durand, G.; Keller, S., A Fluorinated Detergent for Membrane-Protein Applications. *Angew. Chem. Int. Ed.* **2015**, *54*, 5069-5073.

[120] Ehsan, M.; Du, Y.; Scull, N. J.; Tikhonova, E.; Tarrasch, J.; Mortensen, J. S.; Loland, C. J.; Skiniotis, G.; Guan, L.; Byrne, B.; Kobilka, B. K.; Chae, P. S., Highly Branched Pentasaccharide-Bearing Amphiphiles for Membrane Protein Studies. *J. Am. Chem. Soc.* **2016**, *138*, 3789-3796.

[121] Das, M.; Du, Y.; Ribeiro, O.; Hariharan, P.; Mortensen, J. S.; Patra, D.; Skiniotis, G.; Loland, C. J.; Guan, L.; Kobilka, B. K.; Byrne, B.; Chae, P. S., Conformationally Preorganized Diastereomeric Norbornane-Based Maltosides for Membrane Protein Study: Implications of Detergent Kink for Micellar Properties. *J. Am. Chem. Soc.* **2017**, *139*, 3072-3081.

[122] Nguyen, K.-A.; Peuchmaur, M.; Magnard, S.; Haudecoeur, R.; Boyère, C.; Mounien, S.; Benammar, I.; Zampieri, V.; Igonet, S.; Chaptal, V.; Jawhari, A.; Boumendjel, A.; Falson, P., Glycosyl-Substituted Dicarboxylates as Detergents for the Extraction, Overstabilization, and Crystallization of Membrane Proteins. *Angew. Chem. Int. Ed.* **2018**, *57*, 2948-2952.

[123] Sutter, M.; Silva, E. D.; Duguet, N.; Raoul, Y.; Métay, E.; Lemaire, M., Glycerol Ether Synthesis: A Bench Test for Green Chemistry Concepts and Technologies. *Chem. Rev.* **2015**, *115*, 8609-8651.

[124] Harris, B. R., Ethers of polyglycerols. **1938**, US 2258892A.

[125] Urata, K.; Takaishi, N.; Suzuki, Y., Neue Polyolether-Verbindungen, Verfahren zur Herstellung derselben und Kosmetika mit einem Gehalt derselben. **1983**, DE 3427093A3427091.

[126] Wyszogrodzka, M.; Möws, K.; Kamlage, S.; Wodzinska, J.; Plietker, N.; Haag, R., New Approaches Towards Monoamino Polyglycerol Dendrons and Dendritic Triblock Amphiphiles. *Eur. J. Org. Chem.* **2008**, 53-63.

[127] Wyszogrodzka, M.; Haag, R., A Convergent Approach to Biocompatible Polyglycerol "Click" Dendrons for the Synthesis of Modular Core–Shell Architectures and Their Transport Behavior. *Chem. Eur. J.* **2008**, *14*, 9202 - 9214.

[128] Setaro, A.; Popeney, C. S.; Trappmann, B.; Datsyuk, V.; Haag, R.; Reich, S., Polyglycerol-derived amphiphiles for single walled carbon nanotube suspension. *Chem. Phys. Lett.* **2010**, *493*, 147-150.

[129] Heek, T.; Fasting, C.; Rest, C.; Zhang, X.; Würthner, F.; Haag, R., Highly fluorescent water-soluble polyglycerol-dendronized perylene bisimide dyes. *Chem. Commun.* **2010**, *46*, 1884-1886.

[130] Richter, A.; Wiedekind, A.; Krause, M.; Kissel, T.; Haag, R.; Olbrich, C., Non-ionic dendritic glycerol-based amphiphiles: Novel excipients for the solubilization of poorly water-soluble anticancer drug Sagopilone. *Eur. J. Pharm. Sci.* **2010**, *40*, 48-55.

[131] Trappmann, B.; Ludwig, K.; Radowski, M. R.; Shukla, A.; Mohr, A.; Rehage, H.; Böttcher, C.; Haag, R., A New Family of Nonionic Dendritic Amphiphiles Displaying Unexpected Packing Parameters in Micellar Assemblies. *J. Am. Chem. Soc.* **2010**, *132*, 11119-11124.

[132] Kördel, C.; Popeney, C. S.; Haag, R., Photoresponsive amphiphiles based on azobenzene-dendritic glycerol conjugates show switchable transport behavior. *Chem. Commun.* **2011**, *47*, 6584-6586.

[133] Zieringer, M.; Wyszogrodzka, M.; Biskup, K.; Haag, R., Supramolecular behavior of fluorous polyglycerol dendrons and polyglycerol dendrimers with perfluorinated shells in water. *New. J. Chem.* **2012**, *36*, 402-406.

[134] Popeney, C. S.; Setaro, A.; Mutihac, R.-C.; Blümmel, P.; Trappmann, B.; Vonneman, J.; Reich, S.; Haag, R., Polyglycerol-Derived Amphiphiles for the Solubilization of Single-Walled Carbon Nanotubes in Water: A Structure-Property Study. *ChemPhysChem*. **2012**, *13*, 203-211.

[135] Heek, T.; Nikolaus, J.; Schwarzer, R.; Fasting, C.; Welker, P.; Licha, K.; Herrmann, A.; Haag, R., An Amphiphilic Perylene Imido Diester for Selective Cellular Imaging. *Bioconjugate Chem.* **2013**, *24*, 153-158.

[136] Heek, T.; Würthner, F.; Haag, R., Synthesis and Optical Properties of Water-Soluble Polyglycerol-Dendronized Rylene Bisimide Dyes. *Chem. Eur. J.* **2013**, *19*, 10911-10921.

[137] Tyagi, R.; Malhotra, S.; Thünemann, A.F.; Sedighi, A.; Weber, M.; Schäfer, A.; Haag, R., Investigations of Host-Guest Interactions with Shape-Persistent Nonionic Dendritic Micelles. *J. Phys. Chem. C*. **2013**, *117*, 12307-12317.

[138] Rodrigo, A. C.; Malhotra, S.; Böttcher, C.; Adeli, M.; Haag, R., Dendritic polyglycerol cyclodextrin amphiphiles and their self-assembled architectures to transport hydrophobic guest molecules. *RSC Adv.* **2014**, *4*, 61656-61659.

[139] Urner, L. H.; Thota, B. N. S.; Nachtigall, O.; Warnke, S.; von Helden, G.; Haag, R.; Pagel, K., Online monitoring the isomerization of an azobenzene-based dendritic bolaamphiphile using ion mobility-mass spectrometry. *Chem. Commun.* **2015**, *51*, 8801-8804.

[140] Thota, B. N. S.; v. Berlepsch, H.; Böttcher, C.; Haag, R., Towards engineering of self-assembled nanostructures using non-ionic dendritic amphiphiles. *Chem. Commun.* **2015**, *51*, 8648 - 8651.

[141] Heek, T.; Kühne, C.; Depner, H.; Achazi, K.; Dernedde, J.; Haag, R., Synthesis, Photophysical, and Biological Evaluation of Sulfated Polyglycerol Dendronized Perylenebisimides (PBIs) - A Promising Platform for Anti-Inflammatory Theranostic Agents? *Bioconjugate Chem.* **2016**, *27*, 727-736.

[142] Kumar, S.; Ludwig, K.; Schade, B.; von Berlepsch, H.; Papp, I.; Tyagi, R.; Gulia, M.; Haag, R.; Böttcher, C., Introducing Chirality into Nonionic Dendritic Amphiphiles and Studying Their Supramolecular Assembly. *Chem. Eur. J.* **2016**, *22*, 5629-5636.

[143] Haag, R.; Wyszogrodzka, M.; Wiedekind, A.; Mohr, A.; Rehage, H.; Trappmann, B., Linear-dendritische Polyglycerol-verbindungen, Verfahren zu ihrer Herstellung und ihre Verwendung. **2008**, DE 102008030992A030991.

[144] Frèchet, J. M.; Tomalia, D.A. *Dendrimers and Other Dendritic Polymers*. **2001**, John Wiley & Sons.

[145] Buhleier, E.; Wehner, W.; Vögtle, F., "Cascade" - and "Nonskid-Chain-like" Syntheses of Molecular Cavity Topologies. *Synthesis* **1978**, *2*, 155-158.

[146] Haag, R.; Wyszogrodzka, M.; Wiedekind, A.; Mohr, A.; Rehage, H.; Trappmann, B., Linear-dendritische Polyglycerol-verbindungen, Verfahren zu ihrer Herstellung und ihre Verwendung. **2008**, WO 2010000713A1.

[147] Iaych, K.; Dumarcay, S.; Fredon, E.; Gérardin, C.; Lemor, A.; Gérardin, P., Microwave-Assisted Synthesis of Polyglycerol from Glycerol Carbonate. *J. Appl. Polym. Sci.* **2010**, *120*, 2354-2360.

[148] Cassel, S.; Debaig, C.; Benvegnu, T.; Chaimbault, P.; Lafosse, M.; Plusquellec, D.; Rollin, P., Original Synthesis of Linear, Branched and Cyclic Oligoglycerol Standards. *Eur. J. Org. Chem.* **2001**, 875-896.

[149] Martin, A.; Richter, M., Oligomerization of glycerol - a critical review. *Eur. J. Lipid Sci. Technol.* **2011**, *113*, 100-117.

[150] Charles, G.; Clacens, J.-M.; Pouilloux, Y.; Barrault, J., Préparation de Diglycérol et Triglycérol par Polymérisation Directe du Glycérol en Présence de Catalyseurs Mésoporeux Basiques. *Ol., Corps Gras, Lipide*. **2003**, *10*, 74-82.

[151] De Meulenaer, B.; Vanhoutte, B.; Huyghebärt, A., Development of Chromatographic Method for the Determination of Degree of Polymerisation of Polyglycerols and Polyglycerol Fatty Acid Esters. *Chromatographia* **2000**, *51*, 44-52.

[152] Sayoud, N.; De Oliveira Vigier, K.; Cucu, T.; De Meulenaer, B.; Fan, Z.; Lai, J.; Clacens, J.-M.; Liebens, A.; Jérôme, F., Homogeneously-acid catalyzed oligomerization of glycerol. *Green Chem.* **2015**, *17*, 4307-4314.

[153] Entler, G.; Ulsperger, E., Alkylphenyl polyglycerol ethers. *J. prakt. Chem. (Leipzig)*. **1974**, *316*, 325-336.

[154] Neissner, R., Polyglycerine und Fettsäure-Polyglycerinpartialester. *Fette, Seifen, Anstrichm.* **1980**, *82*,

[155] Mank, A. P. J.; Lok, C. M.; Ward, J. P., Synthesis of acyl di- and triglycerols. *Chem. Phys. Lipids*. **1989**, *50*, 63-70.

[156] Ooya, T.; Lee, J.; Kinam, P., Effects of ethylene glycol-based graft, star-shaped, and dendritic polymers on solubilization and controlled release of paclitaxel. *J. Control. Release*. **2003**, *93*, 121-127.

[157] Türk, H.; Shukla, A.; Rodrigues, P. C. A.; Rehage, H.; Haag, R., Water-Soluble Dendritic Core–Shell-Type Architectures Based on Polyglycerol for Solubilization of Hydrophobic Drugs. *Chem. Eur. J.* **2007**, *13*, 4187-4196.

[158] Kohl, C.; Weil, T.; Qu, J.; Müllen, K., Towards Highly Fluorescent and Water-Soluble Perylene Dyes. *Chem. Eur. J.* **2004**, *10*, 5297-5310.

[159] Dhammika, H. M. B.; Burdette, S.C., Photoisomerization in different classes of azobenzene. *Chem. Soc. Rev.* **2012**, *41*, 1809-1825.

[160] Gahl, C.; Schmidt, R.; Brete, D.; Mc Nellis, E. R.; Freyer, W.; Carley, R.; Reuter, K.; Weinelt, M., Structure and Excitonic Coupling in Self-Assembled Monolayers of Azobenzene-Functionalized Alkanethiols. *J. Am. Chem. Soc.* **2010**, *132*, 1831-1838.

[161] Schwierz, N.; Horinek, D.; Liese, S.; Pirzer, T.; Balzer, B. N.; Hugel, T.; Netz, R. R., On the Relationship between Peptide Adsorption Resistance and Surface Contact Angle: A Combined Experimental and Simulation Single-Molecule Study. *J. Am. Chem. Soc.* **2012**, *134*, 19628-19638.

[162] Kördel, C.; Setaro, A.; Blümmel, P.; Popeney, C. S.; Reich, S.; Haag, R., Controlled reversible debundling of single-walled carbon nanotubes by photo-switchable dendritic surfactants. *Nanoscale* **2012**, *4*, 3029-3031.

[163] Paulus, F.; Schulze, R.; Steinhilber, D.; Zieringer, M.; Steinke, I.; Welker, P.; Licha, K.; Wedepohl, S.; Dernedde, J.; Haag, R., The Effect of Polyglycerol Sulfate Branching On Inflammatory Processe. *Macromol. Biosci.* **2014**, *14*, 643-654.

[164] Kaisalo, L.; Hase, T. A., Cleavage of the THP protecting groups under Pd/C-catalyzed hydrogenation conditions. *Tetrahedron Lett.* **2001**, *42*, 7699-7701.

[165] Liu, W.; Howarth, M.; Greytak, A. B.; Zheng, Y.; Nocera, D. G.; Ting, A. Y.; Bawendi, M. G., Compact Biocompatible Quantum Dots Functionalized for Cellular Imaging. *J. Am. Chem. Soc.* **2008**, *130*, 1274-1284.

[166] Branden, C.; Tooze, J., Beta Structures. Introduction into Protein Structure. *2nd Edition; Garland Publishing, Inc.: New York, 2003; pp 67 - 88.*,

[167] Dong, K. C.; Helgason, E.; Yu, C.; Phu, L.; Arnott, D. P.; Bosanac, I.; Compaan, D. M.; Huang, O. W.; Fedorova, A. V.; Kirkpatrick, D. S.; Hymowitz, S. G.; Dueber, E. C., Preparation of Distinct Ubiquitin Chain Reagents of High Purity and Yield. *Structure* **2011**, *19*, 1053 - 1063.

[168] Fändrich, M.; Forge, V.; Buder, K.; Kittler, M.; Dobson, C. M.; Diekmann, S., Myoglobin forms amyloid fibrils by association of unfolded polypeptide segments. *PNAS* **2003**, *100*, 15463 - 15468.

[169] Viseu, M. I.; Carvalho, T. I.; Costa, S. M. B., Conformational Transitions in ß-Lactoglobulin Induced by Cationic Amphiphiles: Equilibrium Studies. *Biophys. J.* **2004**, *86*, 2392 - 2402.

[170] Seo, J.; Hoffmann, W.; Warnke, S.; Bowers, M. T.; Pagel, K.; von Helden, G., Retention of Native Protein Structures in the Absence of Solvent: A Coupled Ion Mobility and Spectroscopic Study. *Angew. Chem. Int. Ed.* **2016**, *55*, 14173 - 14176.

[171] Göth, M.; Lermyte, F.; Schmitt, X. J.; Warnke, S.; von Helden, G.; Sobott, F.; Pagel, K., Gas-phase microsolvation of ubiquitin: investigation of crown ether complexation sites using ion mobility-mass spectrometry. *Analyst* **2016**, *141*, 5502 - 5510.

[172] Yen, H.-Y.; Hopper, J. T.; Liko, I.; Allison, T. M.; Zhu, Y.; Wang, D.; Stegmann, M.; Mohammed, S.; Wu, B.; Robinson, C. V., Ligand binding to a G protein-coupled receptor captured in a mass spectrometer. *Sci. Adv.* **2017**, *3*, 1-6.

[173] Skhiri, Y.; Gruner, P.; Semin, B.; Brosseau, Q.; Pekin, D.; Mazutis, L.; Goust, v.; Kleinschmidt, F.; El Harrak, A.; Hutchison, J. B.; Mayot, E.; Bartolo, J.-F.; Griffiths, A. D.; Taly, V.; Baret, J.-C., Dynamics of molecular transport by surfactants in emulsions. *Soft Matter* **2012**, *8*, 10618-10627.

[174] Feng, R.; Konishi, Y., Stepwise Refolding of Acid-Denatured Myoglobin: Evidence from Electrospray Mass Spectrometry. *J. Am. Soc. Mass Spectrom.* **1993**, *4*, 638 - 645.

[175] Flick, T. G.; Cassou, C. A.; Chang, T. M.; Williams, E. R., Solution Additives that Desalt Protein Ions in Native Mass Spectrometry. *Anal. Chem.* **2012**, *84*, 7511 - 7517.

[176] Leonil, J.; Molle, D.; Fauquant, J.; Maubois, J. L.; Pearce, R. J.; Bouhallab, S., Characterization by Ionization Mass Spectrometry of Lactosyl ß-Lactoglobulin Conjugates Formed During Heat Treatment of Milk and Whey and Identification of One Lactose-Binding Site. *J. Dairy Sci.* **1997**, *80*, 2270 - 2281.

[177] Loo, R. R. O.; Dales, N.; Andrews, P. C., Surfactant effects on protein structure examined by electrospray ionization mass spectrometry. *Protein Sci.* **1994**, *3*, 1975 - 1983.

[178] Landreh, M.; Costeira-Paulo, J.; Gault, J.; Marklund, E. G.; Robinson, C. V., Effects of Detergent Micelles on Lipid Binding to Proteins in Electrospray Ionization Mass Spectrometry. *Anal. Chem.* **2017**, *89*, 7425 - 7430.

[179] Le Maux, S.; Bouhallab, S.; Giblin, L.; Brodkorb, A.; Croguennec, T., Bovine β-lactoglobulin/fatty acid complexes: binding, structural, and biological properties. *Dairy Sci. & Technol.* **2014**, *94*, 409 - 426.

[180] Imre, T.; Zsila, F.; Szabó, P. T., Electrospray mass spectrometric investigation of the binding of cis-parinaric acid to bovine beta-lactoglobulin and study of the ligand-binding site of the protein using limited proteolysis. *Rapid Commun. Mass Spectrom.* **2003**, *17*, 2464 - 2470.

[181] Liu, L.; Kitova, E. N.; Klassen, J. S., Quantifying Protein-Fatty Acid Interactions Using Electrospray Ionization Mass Spectrometry. *J. Am. Soc. Mass Spectrom.* **2011**, *22*, 310 - 318.

[182] Maleknia, S.; Brodbelt, J., Gas-Phase Selectivities of Crown Ethers for Alkali Metal Ion Complexation. *J. Am. Chem. Soc.* **1992**, *114*, 4295 - 4298.

[183] Hunter, E.P.; Lias, S.G., Evaluated Gas Phase Basicities and Proton Affinities of Molecules: An Update. *J. Phys. Chem. Ref. Data*. **1998**, *27*, 413 - 656.

[184] Baeales, P. A.; Khan, S.; Münch, S. P.; Jeuken, L. J. C., Durable vesicles for reconstitution of membrane proteins in biotechnology. *Biochem. Soc. Trans.* **2017**, *45*, 15-26.

[185] Knepper, M. A.; Nielsen, S., Peter Agre, 2003 Nobel Prize Winner in Chemistry. *J. Am. Soc. Nephrol.* **2004**, *15*, 1093-1095.

[186] Zheng, L.; Kostrewa, D.; Bernèche, S.; Winkler, F. K.; Li, X.-D., The mechanism of ammonia transport based on the crystal structure of AmtB of Escherichia coli. *PNAS* **2004**, *101*, 17090-17095.

[187] Fong, R. N.; Koim, K.-S.; Yoshihara, C.; Inwood, W. B.; Kustu, S., The W148L substitution in the Escherichia coli ammonium channel AmtB increases flux and indicates that the substrate is an ion. *PNAS* **2007**, *104*, 18706-18711.

[188] Khademi, S.; O'Connell III, J.; Remis, J.; Robles-Colmenares, Y.; Miercke, L. J. W.; Stroud, R. M., Mechanism of Ammonia Transport by Amt/MEP/Rh: Structure of AmtB at 1.35 Å. *Science* **2004**, *305*, 1587-1594.

[189] Omote, H.; Hiasa, M.; Matsumoto, T.; Otsuka, M.; Moriyama, Y., The MATE proteins as fundamental transporters of metabolic and xenobiotic organic cations. *Trends Pharmacol. Sci.* **2006**, *27*, 588-593.

[190] Kuroda, T.; Tsuchiya, T., Multidrug efflux transporters in the MATE family. *Biochim. Biophys. Acta*. **2009**, *1794*, 763-768.

[191] Rath, A.; Glibowicka, M.; Nadeau, V. G.; Chen, G.; Deber, C. M., Detergent binding explains anomalous SDS-PAGE migration of membrane proteins. *PNAS* **2009**, *106*, 1760-1765.

[192] Mancia, F.; Love, J., High-throughput expression and purification of membrane proteins. *J. Struct. Biol.* **2010**, *172*, 85-93.

[193] Testa, L.; Brocca, S.; Grandori, R., Charge-Surface Correlation in Electrospray Ionization of Folded and Unfolded Proteins. *Anal. Chem.* **2011**, *83*, 6459-6463.

[194] Hall, Z.; Robinson, C. V., Do Charge State Signatures Guarantee Protein Conformations? *J. Am. Soc. Mass Spectrom.* **2012**, *23*, 1161-1168.

[195] Li, J.; Santambrogio, C.; Brocca, S.; Rosetti, G.; Carloni, P.; Grandori, R., Conformational effects in protein electrospray-ionization mass sepctrometry. *Mass Spectrom. Rev.* **2016**, *35*, 111-122.

[196] Sarkar, C. A.; Dodevski, I.; Kenig, M.; Diudli, S.; Mohr, A.; Hermans, E.; Plückthun, A., Directed evolution of a G protein-coupled receptor for expression, stability, and binding selectivity. *PNAS* **2008**, *105*, 14808-14813.

[197] Pagliano, C.; Barera, S.; Chimirri, F.; Saracco, G.; Barber, J., Vergleich der α- und β-isomeren Formen des Detergens n-Dodecyl-D-Maltosid zur Solubilisierung photosynthetischer Komplexe aus Erbsen-Thylakoid-Membranen. *Biochim. Biophys. Acta*. **2012**, *1817*, 1506-1515.

8. Appendix

8.1 Synthetic Procedures

8.1.01 [pG1]-OH Regioisomer Mixture (a, b)

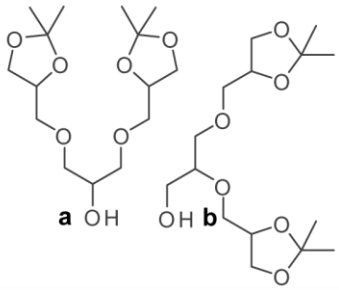

Technical triglycerol (Fluka, product number: 17782) was dissolved in 2,2´-dimethoxypropane (3 eq.) and PTSA*H_2O (0.1 eq.) was added. The reaction mixture was stirred at 40 °C for 16 h. NEt_3 (0.1 eq.) was added and the solvent was removed under reduced pressure. The raw material was purified by column chromatography (SiO_2, *n*-hexane/EtOAc, 2:1 → 1:6) and the product [pG1]-OH was obtained as pale yellow oil (**a**:**b**, 6:4, ~ 60%). ^{1}H NMR (400 MHz, [D_4] MeOH) δ = 4.28 - 4.20 (m, 1.9 H), 4.06 - 3.99 (m, 1.9 H), 3.87 - 3.80 (m, 0.8 H), 3.75 - 3.44 (m, 11 H). ^{13}C NMR (101 MHz, [D_4] MeOH) δ = 110.4, 81.4, 76.3 - 76.1, 73.9, 73.4, 72.4 - 72.3, 70.6, 67.5, 62.6, 27.0, 25.6. MS (ESI): *m/z* = 343.1739 $C_{15}H_{28}O_7Na_1^+$ (calc. 343.1727).

8.1.02 [pG0]-OBn

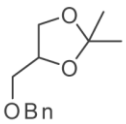

DL-1,2-Isopropylideneglycerol (2.00 g, 15.1 mmol) was dissolved in DMF (50 mL) and NaH (60w%, 2.42 g, 60.5 mmol) was added. Benzyl bromide (2.15 mL, 18.2 mmol) was added and the mixture was stirred for 12 h. The reaction was quenched with H_2O (10 mL) and the solvent was removed under reduced pressure. The residue was suspended in H_2O (100 mL) and Brine (200 mL). The aqueous layer was extracted with EtOAc (3 x 150 mL). The organic layer was dried over sodium sulfate (Na_2SO_4) and the solvent was removed under reduced pressure. Column chromatography (SiO_2, pentane/EtOAc, 10:1 → 8:1) gave the desired product [pG0]-OBn (2.10 g, 9.45 mmol, 63%). ^{1}H NMR (400 MHz, [D_4] MeOH) δ = 7.36 - 7.25 (m, 5H), 4.56 - 4.55 (s, 2H), 4.30 - 4.22 (m, 1H), 4.07 - 4.00 (m, 1H), 3.75 - 3.68 (m, 1H), 3.55 - 3.46 (m, 2H), 1.40 - 1.29 (m, 6H). ^{13}C NMR (101 MHz, [D_4] MeOH) δ = 139.5, 129.4, 128.8, 128.7, 110.5, 76.1, 74.4, 72.1, 67.6, 27.0, 25.7. MS (ESI): *m/z* = 245.1139 $C_{13}H_{18}O_3Na_1^+$ (calc. 245.1148).

8.1.03 [G0]-OBn

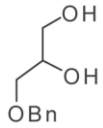

[pG0]-OBn (2.10 g, 9.45 mmol) was dissolved in MeOH (300 mL) and HCl (37%, 100 µL) was added. The mixture was stirred for 2 h at RT and the solvent was removed under reduced pressure. The residue was dissolved in MeOH (300 mL) and again HCl (37%, 100 µL) was added. The solvent was removed under reduced pressure to obtain the desired product [G0]-OBn (1.72 g, 9.43 mmol, 99%). ^{1}H NMR (400 MHz, [D_4] MeOH) δ = 7.36 - 7.22 (m, 5H), 4.53 (s, 2H), 3.84 - 3.77 (m, 1H), 3.64 - 3.45 (m, 4H). ^{13}C NMR (101 MHz, [D_4] MeOH) δ = 139.6, 129.3, 128.8, 128.6, 74.3, 72.7, 72.2, 64.5. MS (ESI): *m/z* = 205.0832 $C_{10}H_{14}O_3Na_1^+$ (calc. 205.0835).

8.1.04 [G0diallyl]-OBn

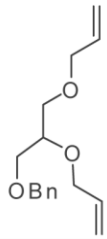

[G0]-OBn (0.50 g, 2.74 mmol) was dissolved in THF (50 mL). NaH (60w%, 0.55 g, 13.7 mmol) and catalytic amounts of 15-crown-5 were added. The mixture was stirred at 50 °C for 1 h. Allyl bromide (712 µL, 8.32 mmol), catalytic amounts of 18-crown-6, and potassium iodide were added. The mixture was stirred at 80 °C for 12 h and H_2O (10 mL) was added. The solvent was removed under reduced pressure and the residue was suspended in H_2O (50 mL) and Brine (50 mL). The aqueous layer was extracted with DCM (5 x 50 mL), the organic layer was dried over Na_2SO_4, and the solvent was removed under reduced pressure. Column chromatography (SiO_2, pentane/DCM, 1:1 → 0:1) gave [G0diallyl]-OBn (0.56 g, 2.13 mmol, 78%). ^{1}H NMR (400 MHz, [D_4] MeOH) δ = 7.36 - 7.23 (m, 5H), 5.98 - 5.80 (m, 2H), 5.33 - 5.21 (m, 2H), 5.19 - 5.09 (m, 2H), 4.52 (s, 2H), 4.16 - 4.08 (m, 2H), 4.02 - 3.92 (m, 2H), 3.73 - 3.66 (m, 1H), 3.61 - 3.48 (m, 4H). ^{13}C NMR (101 MHz, [D_4] MeOH) δ = 139.6, 136.4, 136.0, 129.4, 128.8, 128.7, 117.1, 78.5, 74.3, 73.2, 72.2, 71.1. MS (ESI): *m/z* = 285.1473 $C_{16}H_{22}O_3Na_1^+$ (calc. 285.1461).

8.1.05 [G1]-OBn

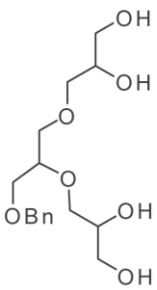

[G0diallyl]-OBn (7.29 g, 29.4 mmol) was dissolved in degassed H_2O (400 mL) and tBuOH (400 mL). TMANO (9.80 g, 130 mmol), citric acid (28.2 g, 146 mmol), and $K_2OsO_4*2H_2O$ (1.35 g, 3.67 mmol) were added. The mixture was stirred for 12 h at RT, the ion exchange resin Lewatit K 6267 (92.0 g) was added, and the mixture was stirred again for 1 h. The resin was filtered off, washed with H_2O (400 mL) and the solvent was removed under reduced pressure. Column chromatography (SiO_2, DCM/MeOH, 9:1 → 2:1) led to the desired product [G1]-OBn (3.37 g, 10.2 mmol, 35%). ^{1}H NMR (400 MHz, [D_4] MeOH) δ = 7.42 - 7.23 (m, 5H), 5.20 (s, 4H), 4.53 (s, 2H), 3.84 - 3.66 (m, 4H), 3.64 - 3.41 (m, 11H). ^{13}C NMR (101 MHz, [D_4] MeOH) δ = 139.5, 129.2, 128.8, 128.5, 79.5, 74.2, 73.9, 73.6, 72.6, 72.2 - 72.1, 71.9, 70.9, 64.2. MS (ESI): *m/z* = 353.1573 $C_{16}H_{26}O_7Na_1^+$ (calc. 353.1571).

8.1.06 [pG1]-OBn

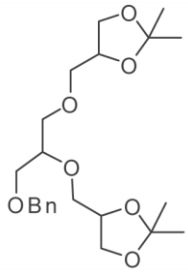

[G1]-OBn (2.82 g, 8.54 mmol) was dissolved in 2,2´-dimethoxypropane (200 mL) and PTSA*H_2O (0.30 g, 1.55 mmol) was added. The mixture was stirred for 1 h at RT and NEt_3 (110 µL, 1.55 mmol) was added. Column chromatography (SiO_2, DCM/EtOAc, 1:0 → 4:1) gave the desired product [pG1]-OBn (3.00 g, 7.31 mmol, 86%). ^{1}H NMR (400 MHz, [D_4] MeOH) δ = 7.36 - 7.24 (m, 5H), 4.53 (s, 2H), 4.26 - 4.18 (m, 2H), 4.05 - 3.99 (m, 2H), 3.77 - 3.47 (m, 11H), 1.41 - 1.28 (m, 12H). ^{13}C NMR (101 MHz, [D_4] MeOH) δ = 139.6, 129.3, 128.8, 128.6, 110.4, 79.8, 76.2 - 76.1, 74.3, 73.3, 72.5 - 72.3, 71.0, 67.7, 67.5, 27.1, 25.6. MS (ESI): *m/z* = 433.2210 $C_{22}H_{34}O_7Na_1^+$ (calc.433.2197).

8.1.07 [pG1]-OH Regioisomer (b)

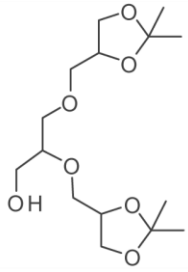

[pG1]-OBn (0.98 g, 2.39 mmol) was dissolved in a mixture of cyclohexane (5 mL) and THF (5 mL). Pd/C (10w%, 50 mg) was added and the mixture was stirred under hydrogen atmosphere (5 bar) for 12 h. The mixture was passed through a syringe filter (0.20 µm, RC) and the solvent was removed under reduced pressure. Column chromatography (SiO_2, pentane/EtOAc, 1:0 → 1:4) gave the desired product (0.66 g, 2.03 mmol, 85%). ^{1}H NMR (400 MHz, [D_4] MeOH) δ = 4.29 - 4.21 (m, 2H), 4.08 - 4.02 (m, 2H), 3.79 - 3.48 (m, 11H), 1.42 - 1.28 (m, 12H). ^{13}C NMR (101 MHz, [D_4] MeOH) δ = 110.2, 81.3, 76.1, 75.9, 73.2, 72.3 - 72.1, 67.6, 67.4, 62.5, 27.1, 25.7. MS (ESI): *m/z* = 343.1739 $C_{15}H_{28}O_7Na_1^+$ (calc. 343.1727).

8.1.08 [pG1]-ene

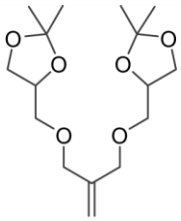

DL-1,2-Isopropylidenglycerol (5.62 g, 42.5 mmol) was dissolved in THF (125 mL) and NaH (60w%, 5.10 g, 128 mmol) was added. Catalytic amounts of 15-crown-5 were added and the mixture was stirred at 50 °C for 1 h. Methallyl dichloride (2.65 g, 21.2 mmol), catalytic amounts of 18-crown-6, and potassium iodide were added and the mixture was stirred at 80 °C for 12 h. The reaction mixture was then allowed to cool down to RT and H_2O (10 mL) was added. The solvent was removed under reduced pressure and the residue was suspended in H_2O (200 mL) and Brine (100 mL). The aqueous layer was extracted with EtOAc (3 x 150 mL). The organic layer was dried over Na_2SO_4 and the solvent was removed under reduced pressure. Column chromatography (SiO_2, pentane/EtOAc, 8:1 → 2:1) led to the obtainment of [pG1]-ene (3.75 g, 11.9 mmol, 56%). ^{1}H NMR (400 MHz, [D_4] MeOH) δ = 5.20 - 5.18 (m, 2H), 4.30 - 4.21 (m, 2H), 4.06 - 3.99 (m 6H), 3.75 - 3.69 (m, 2H), 3.52 - 3.43 (m, 4H), 1.42 - 1.31 (m, 12H). ^{13}C NMR (101 MHz, [D_4] MeOH) δ = 144.1, 114.7, 110.5, 76.1, 72.9, 72.1, 67.6, 27.1, 25.7. MS (ESI): *m/z* = 339.1802 $C_{16}H_{28}O_6Na_1^+$ (calc. 339.1778).

8.1.09 [pG1]-OH Regioisomer (a)

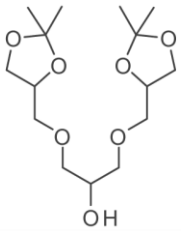

The compound [pG1]-ene (2.75 g, 8.69 mmol) was dissolved in MeOH (20 mL) and DCM (20 mL). The reaction mixture was cooled down to - 78 °C and ozone was guided through the mixture until its color changed to deep blue. Oxygen was then guided through the mixture for another 30 min and sodium borohydride was added (3.28 g, 86.9 mmol). The mixture was allowed to warm up to RT overnight (16 h) and saturated solution of NH_4Cl (35 mL) was added. The aqueous layer was extracted with DCM (6 x 50 mL). The organic layer was dried over Na_2SO_4 and the solvent was removed under reduced pressure. Column chromatography (SiO_2, DCM/EtOAc, 97:3 + 3% MeOH) gave the desired product (2.20 g, 6.86 g, 79%). ^{1}H NMR (400 MHz, [D_4] MeOH) δ = 4.30 - 4.22 (m, 2H), 4.09 - 4.02 (m, 2H), 3.90 - 3.82 (m, 1H), 3.76 - 3.70 (m, 2H), 3.59 - 3.46 (m, 8H), 1.42 - 1.30 (m, 12H). ^{13}C NMR (101 MHz, [D_4] MeOH) δ = 110.4, 76.1, 73.9, 73.4, 70.5, 67.5, 27.0, 25.6. MS (ESI): *m/z* = 343.1726 $C_{15}H_{28}O_7Na_1^+$ (calc. 343.1727).

8.1.10 [pG1]-ether-C12 (a, b)

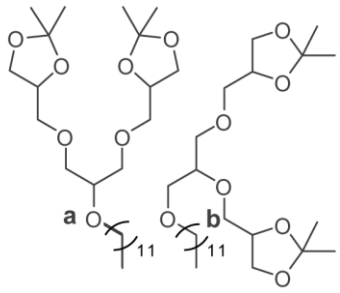

[pG1]-OH (8.00 g, 24.9 mmol, **a**:**b**, 6:4) was dried under reduced pressure (~ 10^{-2} mbar) and DMF (200 mL) was added. The flask was cooled with an ice bath and NaH (60w%, 6.24 g, 156 mmol) was added in small portions. The ice bath was removed and the mixture was allowed to warm up to RT. 12-Bromododecane (31.1 g, 124 mmol) was added slowly and the mixture was stirred for 16 h. The mixture was again cooled with an ice bath and a saturated solution of NH_4Cl (100 mL) was added slowly. The solvent was removed under reduced pressure. The residue was suspended with H_2O (200 mL), Brine (200 mL), and EtOAc (200 mL). The aqueous layer was extracted with EtOAc (4 x 200 mL). The organic layer was dried over Na_2SO_4. The solvent was removed under reduced pressure and subsequent column chromatography (SiO_2, Pentane/EtOAc, 3:1 → 1:1) gave the desired product [pG1]-ether-C12 (12.1 g, 24.8 mmol, **a**:**b**, 99%). ^{1}H NMR (400 MHz, [D_4] MeOH): δ = 4.28 - 4.19 (m, 2H), 4.08 - 4.01 (m, 2H), 3.79 - 3.40 (m, 13H), 1.60 - 1.49 (m, 2H), 1.42 - 1.23 (m, 30H), 0.94 - 0.87 (m, 3H). ^{13}C NMR (101 MHz, [D_4] MeOH): δ = 110.4, 79.1, 76.1, 73.3, 72.4 - 72.3, 71.4, 67.6, 31.6, 30.8 - 30.5, 27.1, 25.7, 23.7, 14.5. MS (ESI): *m/*z = 511.3609 $C_{27}H_{52}O_7Na_1^+$ (calc. = 511.3605).

8.1.11 [G1]-ether-C12 (a, b) - 1

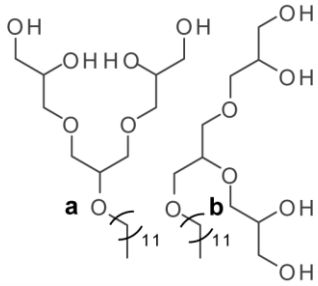

[pG1]-ether-C12 (12.0 g, 24.8 mmol, **a**:**b**) was dissolved in MeOH (1 L) and HCl (37%, 100 µL) was added. The mixture was stirred for 12 h at RT and the solvent was removed under reduced pressure. The residue was again dissolved and in MeOH (1 L) and HCl (37%, 100 µL) was added. The solvent was removed under reduced pressure. The crude material was dissolved in a mixture of H_2O and MeOH (1:1, 70 mL) and passed through a syringe filter (RC, 0.2 µm). Purification by RP HPLC (H_2O/MeOH, 3:7) gave the desired product (8.00 g, 19.6 mmol, **a**:**b** , 6:4, 80%). ^{1}H NMR (500 MHz, [D_4] MeOH): δ = 3.80 - 3.71 (m, 2H), 3.64 - 3.44 (m, 15H), 1.60 - 1.53 (m, 2H), 1.41 - 1.25 (m, 18H), 0.93 - 0.86 (m, 3H). ^{13}C NMR (126 MHz, [D_4] MeOH): δ = 77.8, 72.6 - 72.5, 71.3 - 70.7, 70.2 - 70.0, 63.1 - 63.0, 31.7, 29.7 - 29.1, 25.8, 22.4, 13.3 - 13.1. MS (ESI): *m/*z = 431.2996 $C_{21}H_{44}O_7Na_1^+$ (calc. = 431.2979).

8.1.12 [pG1]-N_3 (a,b)

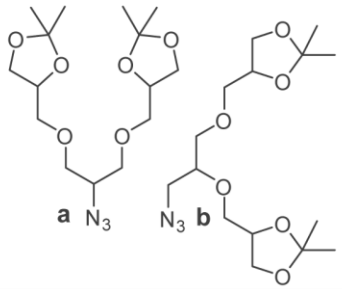

[pG1]-OH (5.50 g, 17.1 mmol, **a**:**b**, 6:4) was dissolved in toluene (150 mL), NEt_3 (2.66 mL, 20.6 mmol) was added, and MsCl (1.59 mL, 20.6 mmol) was added. The mixture was stirred for 16 h at RT, the precipitate was filtered off, and the solvent was removed under reduced pressure. The obtained raw material (7.23 g) was dissolved in DMF (100 mL), NaN_3 (5.89 g, 90.7 mmol) was added, and the mixture was stirred for 16 h at 80 °C. The excess of NaN_3 was filtered off, the solvent was removed under reduced pressure, and column purification (SiO_2, *n*-hexane/isopropanol, 15:1) gave [pG1]-N_3 (4.76 g, 13.8 mmol, **a**:**b**, 6:4, 81%). ^{1}H NMR (700 MHz, [D_4] MeOH): δ = 4.27 - 4.22 (m, 2H), 4.08 - 4.02 (m, 2H), 3.80 - 3.49 (m, 10.3H), 3.43 - 3.31 (m, 0.7H), 1.44 - 1.27 (m, 12H). ^{13}C NMR (175 MHz, [D_4] MeOH): δ = 110.4, 79.9, 76.0, 73.4 - 73.1, 72.3 - 72.0, 67.0 - 67.4, 61.9, 52.8, 27.1, 25.6.

8.1.13 [pG1]-NH_2 (a, b)

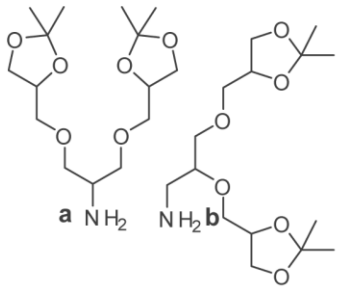

[pG1]-N_3 (2.06 g, 5.96 mmol, **a**:**b**, 6:4) was dissolved in MeOH (20 mL), Pd/C () was added, and the mixture was stirred under hydrogen atmosphere (5 bar) for 12 h at RT. The mixture was passed through a syringe filter (0.2 µm, RC). Removing the solvent under reduced pressure gave the desired product [pG1]-NH_2 (1.56 g, 4.88 mmol, **a**:**b**, 6:4, 82%). ^{1}H NMR (700 MHz, [D_4] MeOH): δ = 4.97 (s, 2H), 4.52 - 4.47 (m, 2H), 4.33 - 4.25 (m, 2H), 4.02 - 3.64 (m, 10H), 3.02 - 2.88 (m, 0.8H), 1.69 - 1.50 (m, 12H). ^{13}C NMR (175 MHz, [D_4] MeOH): δ = 110.4, 81.5 - 81.4, 76.4 - 76.1, 74.0, 73.3 - 73.0, 72.6, 72.0, 67.5, 51.7, 43.6, 27.0, 25.6. MS (ESI): *m*/z = 432.1881 $C_{15}H_{29}N_1O_6Na_1^+$ (calc. = 342.1887).

8.1.14 [pG1]-amide-C12 (a, b)

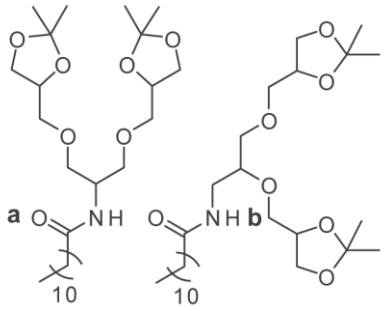

NHS (0.86 g, 7.52 mmol) and dodecanoic acid (1.25 g, 6.26 mmol) were dissolved in dry DCM (30 mL). The mixture was cooled with an ice bath, DCC was added (1.55 g, 7.52 mmol), and the mixture was stirred for 1 h at RT. [pG1]-NH_2 (2.00 g, 6.26 mmol, **a**:**b**, 6:4) was added and the mixture was stirred for another 16 h at RT. The precipitate was filtered off, the solvent was removed under reduced pressure, and column chromatography (SiO_2, DCM/EtOAc, 4:1 → 4:1 + 3% MeOH) gave the desired product (1.52 g, 3.00 mmol, **a**:**b**, 48%). ^{1}H NMR (400 MHz, [D_4] MeOH): δ = 4.86 (s, 1H), 4.30 - 4.21 (m, 2.3H), 4.20 - 4.13 (0.7H), 4.08 - 4.01 (m, 2H), 3.77 - 3.46 (m, 10H), 2.24 - 2.16 (m, 2H), 1.67 - 1.54 (m, 2H), 1.45 - 1.22 (m, 28H), 0.95 - 0.87 (m, 3H). ^{13}C NMR (101 MHz, [D_4] MeOH) δ = 176.0, 174.7, 110.9 - 110.4, 79.2 - 79.0, 76.3 - 76.0, 73.4 - 72.9, 72.4, 72.1 - 72.0, 71.2 - 71.4, 67.5 - 67.4, 50.0, 41.3, 37.0, 33.0, 30.7 - 30.2, 27.1 - 27.0, 26.2, 25.6, 23.7, 14.4. MS (ESI): *m/*z = 524.3561 $C_{27}H_{51}N_1O_7Na_1^+$ (calc. = 524.3558).

8.1.15 [G1]-amide-C12 (a, b) - 2

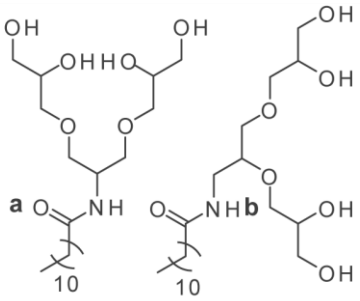

[pG1]-amide-C12 (1.52 g, 3.00 mmol, **a**:**b**) was dissolved in MeOH and HCl (37%, 100 µL) was added. The mixture was stirred for 12 h at RT and the solvent was removed under reduced pressure. The raw product was dissolved in in a mixture of H_2O and MeOH (1:1, 20 mL) and passed through a syringe filter (RC, 0.2 µm). Subsequent purification by RP HPLC (H_2O/MeOH, 3:7) gave the desired product [G1]-amide-C12 (758 mg, 1.80 mmol, **a**:**b**, 6:4, 60%). ^{1}H NMR (400 MHz, [D_4] MeOH): δ = 4.21 - 4.12 (m, 0.7H), 3.80 - 3.70 (m, 2.3H), 3.66 - 3.40 (m, 12H), 2.24 - 2.17 (m, 2H), 1.66 - 1.55 (m, 2H), 1.40 - 1.20 (m, 16H), 0.95 - 0.85 (m, 3H). ^{13}C NMR (101 MHz, [D_4] MeOH) δ = 176.3 - 176.0, 79.0, 73.7 - 73.3, 72.5 - 71.9, 71.0 - 70.9, 64.1, 50.0, 41.1 - 41.0, 36.9, 32.9, 30.6 - 30.2, 26.9, 23.6, 14.5. MS (ESI): *m/*z = 444.2944 $C_{21}H_{43}N_1O_7Na_1^+$ (calc. = 444.2932).

8.1.16 [pG1]-O-propargyl (a, b)

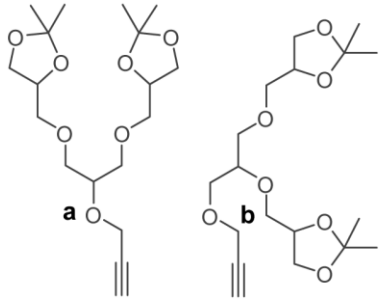

[pG1]-OH (2.50 g, 7.80 mmol, **a**:**b**, 6:4) was first dried under reduced pressure (~ 10^{-2} mbar) and then dissolved in DMF (70 mL). The mixture was cooled with an ice bath and NaH (60w%, 936 mg, 39.0 mmol) was added in small portions. The ice bath was removed and the mixture was allowed to warm up to RT. Catalytic amounts of 15-crown-5 and propargyl bromide (80w%, 4.35 mL, 39.0 mmol) were added. The mixture was stirred for 12 h and a saturated solution of NH_4Cl (50 mL) was added. The solvent was removed under reduced pressure and the residue was treated with H_2O (200 mL), EtOAc (150 mL), and Brine (100 mL). The aqueous layer was extracted with EtOAc (3 x 150 mL), the organic layer was dried over Na_2SO_4, and the solvent was removed under reduced pressure. Column chromatography (SiO_2, pentane/EtOAc, 9:1 → 1:1) gave the desired product (2.10 g, 5.85 mmol, 75%, **a**:**b**, 6:4). ^{1}H NMR (400 MHz, [D_4] MeOH): δ = 4.33 - 4.30 (m, 1.2H), 4.29 - 4.20 (m, 2H), 4.19 - 4.17 (m, 0.8H), 4.07 - 4.02 (m, 2H), 3.88 - 3.48 (m, 11H), 2.89 - 2.85 (m, 1H), 1.41 - 1.31 (m, 12H). ^{13}C NMR (101 MHz, [D_4] MeOH): δ = 110.4 - 110.3, 81.1, 80.6, 79.6, 77.7, 76.1 - 76.0, 75.7, 73.3 - 73.2, 72.4 - 72.2, 70.5, 67.7, 67.5, 59.2, 58.3 - 58.2, 27.1 - 27.0, 25.7 - 25.6. MS (ESI): *m/*z = 381.1890 $C_{18}H_{30}O_7Na_1^+$ (calc. = 381.1884).

8.1.17 [pG1]-triazole-C12 (a, b)

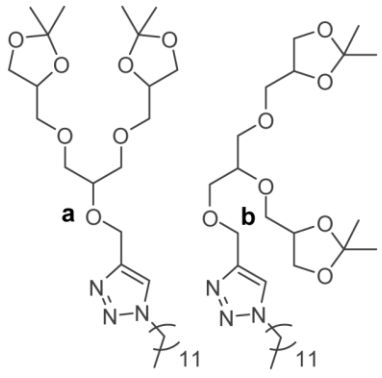

[pG1]-O-propargyl (2.00 g, 5.58 mmol, **a**:**b**, 6:4) and 1-azidododecane (1.29 g, 6.14 mmol) were dissolved in THF (5 mL) and H_2O (2 mL) was added. DIPEA (94.9 µL, 0.56 mmol), sodium ascorbate (552 mg, 2.79 mmol, dissolved in 2 mL H_2O), and Cu(II)SO_4*5H_2O (139 mg, 0.56 mmol, dissolved in 1 mL H_2O) were added. The mixture was stirred at RT for 12 h and then diluted with H_2O (40 mL). A saturated solution of EDTA (1 mL) and Brine (10 mL) were added. The aqueous layer was extracted with EtOAc (3 x 40 mL) and the solvent was removed under reduced pressure.

Column chromatography (SiO_2, DCM/EtOAc, 4:1 → 4:1 + 3% MeOH) gave the desired product (2.22 g, 3.80 mmol, **a**:**b**, 68%). ^{1}H NMR (400 MHz, [D_4] MeOH): δ = 8.03 (s, 1H), 4.80 - 4.58 (m, 2H), 4.44 - 4.36 (m, 2H), 4.27 - 4.17 (m, 2H), 4.07 - 3.98 (m, 2H), 3.75 - 3.45 (m, 11H), 1.95 - 1.86 (m, 2H), 1.39 - 1.24 (m, 30H), 0.93 - 0.86 (m, 3H).^{13}C NMR (101 MHz, [D_4] MeOH): δ = 110.5 - 110.2, 79.8 - 79.7, 78.6 - 78.5, 76.1 - 76.0, 73.6 - 73.3, 72.5 - 72.3, 71.1, 51.3, 33.0, 31.3, 30.7 - 30.1, 27.4, 27.1, 25.7 - 25.6, 23.7, 14.5. MS (ESI): *m/z*: 592.3982 $C_{30}H_{55}N_3O_7Na_1^+$ (calc. = 592.3932).

8.1.18 [G1]-triazole-C12 (a, b) - 3

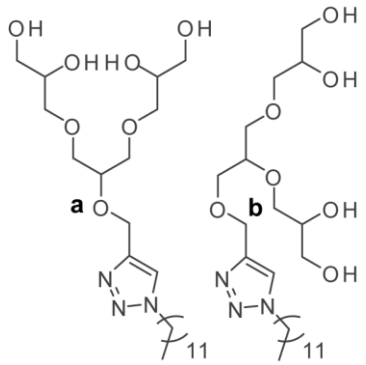

[pG1]-triazole-C12 (2.22 g, 3.80 mmol, **a**:**b**) was dissolved in MeOH (500 mL) and HCl (37%, 100 µL) was added. The mixture was stirred at RT for 12 h and solvent was removed under reduced pressure. The material was again dissolved in MeOH (500 mL) and HCl (37%, 100 µL) was added. Upon stirring for 12 h at RT the solvent was removed under reduced pressure. The crude material was dissolved in a mixture of H_2O and MeOH (1:1, 20 mL), passed through a syringe filter (RC, 0.2 µm) and purified by means of RP HPLC (H_2O/MeOH, 3:7) to give the desired product (1.48 g, 3.04 mmol, **a**:**b**, 6:4, 80%).^{1}H NMR (400 MHz, [D_4] MeOH): δ = 8.06 - 7.99 (m, 1H), 4.81 - 4.61 (m, 2H), 4.43 - 4.35 (m, 2H), 3.87 - 3.43 (m, 15H) 1.96 - 1.83 (m, 2H), 1.41 - 1.20 (m, 18H), 0.93 - 0.85 (m, 3H). ^{13}C NMR (101 MHz, [D_4] MeOH): δ = 146.1 - 145.6, 125.0 - 124.9, 73.8, 72.7, 72.3 - 72.2, 72.0, 71.1, 65.1, 64.2, 64.1, 51.2, 32.9, 31.2, 30.6 - 30.4, 30.0, 27.4, 23.6, 14.5. MS (ESI): *m/z* = 512.3357 $C_{24}H_{47}N_3O_7Na_1^+$ (calc. = 512.3306).

8.1.19 [pG2]-ene (aa, ab, bb)

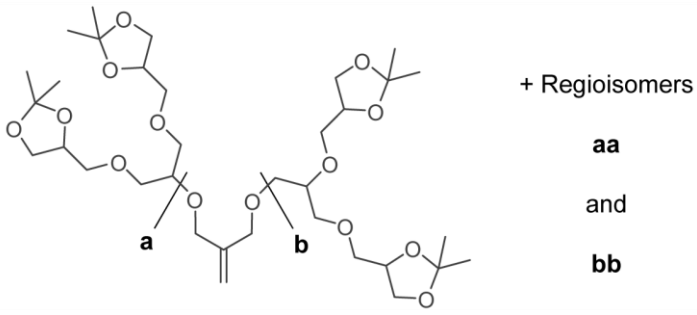

[pG1]-OH (13.6 g, 42.5 mmol, **a**:**b**, 6:4) was dried under reduced pressure (~ 10^{-2} mbar), dissolved in dry THF (125 mL), and NaH (60w%, 5.10 g, 128 mmol) was added in small portions. Catalytic amounts of 15-crown-5 were added and the mixture was stirred for 45 min at 50 °C. Methallyl dichloride (2.46 mL, 21.2 mmol), catalytic amounts of potassium iodide, and catalytic amounts of

18-crown-6 were added. The reaction was stirred at 70 °C for 24 h. The mixture was then cooled with an ice bath and H_2O (80 mL) was added slowly. The solvent was removed under reduced pressure and the crude product was mixed with Brine (200 mL) and DCM (150 mL). The aqueous layer was extracted with DCM (3 x 150 mL). The organic layer was dried over Na_2SO_4 and the solvent was removed under reduced pressure. Column chromatography (SiO_2, Pentane/EtOAc, 1:2 → 0:1) gave the desired product (12.2 g, 17.6 mmol, **aa**:**ab**:**bb**, 4:4:1, 83%).^{1}H NMR (400 MHz, [D_4] MeOH): δ = 5.22 - 2.21 (m, 2H), 4.29 - 4.22 (m, 4H), 4.19 - 4.13 (m, 2H), 4.08 - 4.01 (m, 4H), 3.79 - 3.46 (m, 24 H), 1.40 - 1.30 (m, 24H). ^{13}C NMR (101 MHz, [D_4] MeOH): δ = 145.2, 144.8, 114.5, 110.4, 79.9, 78.4, 76.1, 73.4, 72.9, 72.4 - 72.3, 71.6, 71.1, 67.7 - 67.6, 27.1, 25.7. MS (ESI): *m/*z = 715.3982 $C_{34}H_{60}O_{14}Na_1^+$ (calc. = 715.3875).

8.1.20 [pG2]-OH (aa, ab, bb)

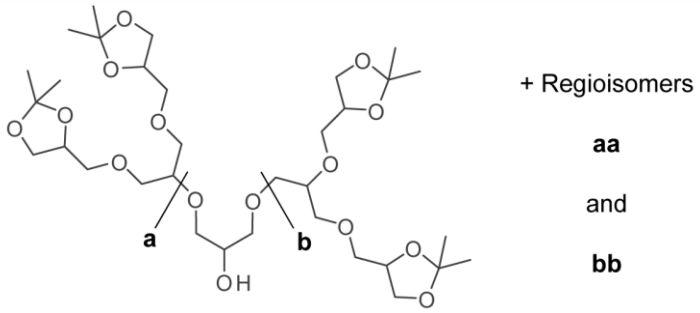

[pG2]-ene (8.00 g, 11.5 mmol, **aa**:**ab**:**bb**, 4:4:1) was dried was dried under reduced pressure (~ 10^{-2} mbar) and dissolved in a mixture of dry DCM (35 mL) and dry MeOH (35 mL). The mixture was cooled down to - 78 °C and ozone was passed through the reaction mixture until its color changed to deep blue. Oxygen was then passed through the solution until it became colorless. Sodium borohydride (4.36 g, 115 mmol) was added slowly and the mixture was allowed to heat up to RT overnight. A saturated solution of NH_4Cl (100 mL) was added and the mixture was extracted with DCM (5 x 50 mL). The organic layer was dried over Na_2SO_4 and the solvent was removed under reduced pressure. Column chromatography (SiO_2, DCM/EtOAc, 97:3 + 3% MeOH) gave the desired product (6.40 g, 9.18 mmol, **aa**:**ab**:**bb**, 4:4:1, 80%). ^{1}H NMR (400 MHz, [D_4] MeOH): δ = 4.29 - 4.21 (m, 4H), 4.08 - 4.02 (m, 4H), 3.80 - 3.47 (m, 27H), 1.42 - 1.31 (m, 24H). ^{13}C NMR (101 MHz, [D_4] MeOH): δ = 109.1, 78.5, 74.8, 72.5 - 72.1, 71.4 - 71.1, 69.8 - 69.5, 66.2, 25.8, 24.3. MS (ESI): *m/*z = 719.3920 $C_{33}H_{60}O_{15}Na_1^+$ (calc. = 719.3824).

8.1.21 [pG2]-ene (aa)

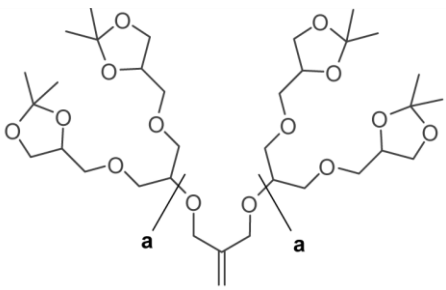

[pG1]-OH (1.00 g, 3.12 mmol, **a**) was dried under reduced pressure (~ 10^{-2} mbar), dissolved in dry THF (60 mL), and NaH (60w%, 0.18 g, 4.68 mmol) was added. Catalytic amounts of 15-crown-5 were added and the mixture was stirred for 1 h at 50 °C. Methallyl dichloride (0.17 mL, 1.48 mmol), catalytic amounts of potassium iodide, and catalytic amounts of 18-crown-6 were added. The reaction was stirred at 80 °C for 12 h. The reaction mixture was allowed to cool down to RT and H_2O (6 mL) was added. The solvent was removed under reduced pressure and the crude product was mixed with H_2O (60 mL), Brine (60 mL), and DCM (60 mL). The aqueous layer was extracted with EtOAc (6 x 50 mL). The organic layer was dried over Na_2SO_4 and the solvent was removed under reduced pressure. Column chromatography (SiO_2, pentane/EtOAc, 8:1 → 4:1 + 3% MeOH) gave the desired product (0.81 g, 1.17 mmol, **aa**, 37%). ^{1}H NMR (400 MHz, [D_4] MeOH): δ = 5.20 (s, 2H), 4.27 - 4.21 (m, 4H), 4.17 (s, 4H), 4.07 - 4.02 (m, 4H) 3.76 - 3.71 (m, 4H), 3.67 - 3.47 (m, 18H), 1.58 - 1.16 (m, 24H). ^{13}C NMR (101 MHz, [D_4] MeOH): δ = 144.9, 114.2, 110.0, 98.9, 78.2, 75.7, 73.2, 72.2, 71.4, 67.4, 63.1, 27.2, 25.9. MS (ESI): *m/z* = 715.3889 $C_{34}H_{60}O_{14}Na1^+$ (calc 715.3875).

8.1.22 [pG2]-OH (aa)

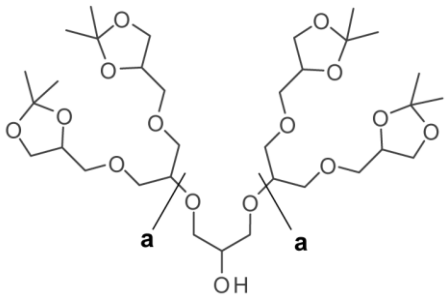

[pG2]-ene (0.81 g, 1.22 mmol, **aa**) was dried was dried under reduced pressure (~ 10^{-2} mbar) and dissolved in a mixture of dry DCM (40 mL) and dry MeOH (20 mL). The mixture was cooled down to -78 °C and ozone was passed through it until its color changed to deep blue. Ozone was then passed through it for another 30 min. Sodium borohydride (0.46 g, 12.2 mmol) was added slowly and the mixture was allowed to warm up to RT overnight. A saturated solution of NH_4Cl (30 mL) was added and the mixture was extracted with EtOAc (6 x 30 mL). The organic layer was dried over Na_2SO_4 and the solvent was removed under reduced pressure. Column chromatography (SiO_2, pentane/EtOAc, 1:1 + 3% MeOH) gave the desired product (140 mg, 190 µmol, **bb**, 15%). ^{1}H NMR (400 MHz, [D_4] MeOH): δ = 4.28 - 4.21 (m, 4H), 4.08 - 4.03 (m, 4H), 3.88 - 3.79 (m, 1H), 3.75 - 3.51 (m, 26H), 1.49 - 1.22 (m, 24H). ^{13}C NMR (101 MHz, [D_4] MeOH): δ = 110.3, 79.6, 75.9, 73.3, 72.6, 72.3 - 72.2, 71.0, 67.5, 27.1, 25.7. MS (ESI): *m/z* = 719.3813 $C_{33}H_{60}O_{15}Na_1^+$ (calc. 719.3824).

8.1.23 [pG2]-ene (bb)

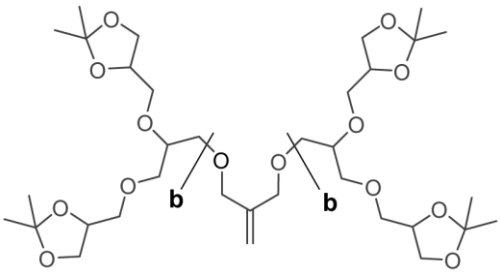

[pG1]-OH (0.65 g, 2.14 mmol, **b**) was dried under reduced pressure (~ 10^{-2} mbar), dissolved in dry THF (60 mL), and NaH (60w%, 0.13 g, 3.21 mmol) was added. Catalytic amounts of 15-crown-5 were added and the mixture was stirred for 1 h at 50 °C. Methallyl dichloride (0.11 mL, 1.02 mmol), catalytic amounts of potassium iodide, and catalytic amounts of 18-crown-6 were added. The reaction was stirred at 80 °C for 12 h. The reaction mixture was allowed to cool down to RT and H_2O (10 mL) was added. The solvent was removed under reduced pressure and the crude product was mixed with H_2O (60 mL), Brine (60 mL), and DCM (60 mL). The aqueous layer was extracted with EtOAc (6 x 50 mL). The organic layer was dried over Na_2SO_4 and the solvent was removed under reduced pressure. Column chromatography (SiO_2, pentane/EtOAc, 8:1 → 4:1 + 3% MeOH) gave the desired product (0.20 g, 0.30 mmol, **bb**, 14%). ^{1}H NMR (400 MHz, [D_4] MeOH): δ = 5.15 (s, 2H), 4.24 - 4.16 (m, 4H), 4.04 - 3.95 (m, 8H), 3.75 - 3.41 (m, 22H), 1.38 - 1.16 (m, 24H). ^{13}C NMR (101 MHz, [D_4] MeOH): δ = 144.3, 114.6, 110.4, 79.9, 76.1, 73.4, 72.9, 72.4, 71.2, 67.8, 67.6, 49.0, 27.2, 25.7. MS (ESI): *m/z* = 715.3857 $C_{34}H_{60}O_{14}Na_1^+$ (calc. 715.3875).

8.1.24 [pG2]-OH (bb)

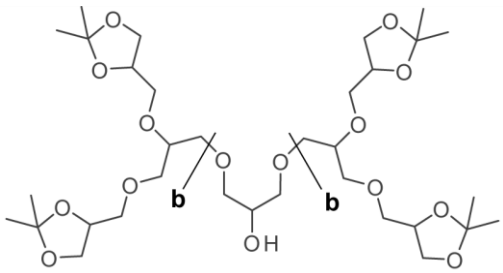

[pG2]-ene (220 mg, 0.32 mmol, **bb**) was dried was dried under reduced pressure (~ 10^{-2} mbar) and dissolved in a mixture of dry DCM (35 mL) and dry MeOH (20 mL). The mixture was cooled down to -78 °C and ozone was passed through it until its color changed to deep blue. Oxygen was then passed through it until the mixture became colorless. Sodium borohydride (0.37 g, 9.78 mmol) was added slowly and the mixture was allowed to warm up to RT overnight. A saturated solution of NH_4Cl (17 mL) was added and the mixture was extracted with EtOAc (5 x 30 mL). The solvent was removed under reduced pressure and column chromatography (SiO_2, pentane/EtOAc, 1:1 → 1:1 + 3% MeOH) gave the desired product (150 mg, 0.22 mmol, **bb**, 67%). ^{1}H NMR (400 MHz, [D_4] MeOH): δ = 4.28 - 4.21 (m, 4H), 4.07 - 4.02 (m, 4H), 3.88 - 3.83 (m, 1H), 3.78 - 3.45 (m, 27H), 1.62 - 1.11 (m, 24 H). ^{13}C NMR (101 MHz, [D_4] MeOH): δ = 110.4, 79.8, 76.1, 73.9, 73.4, 72.4, 70.6, 67.7, 67.6, 27.2, 25.7. MS (ESI): *m/z* = 719.3830 $C_{33}H_{60}O_{15}Na_1^+$ (calc. 719.3824).

8.1.25 [pG2]-ether-C18 (aa, ab, bb)

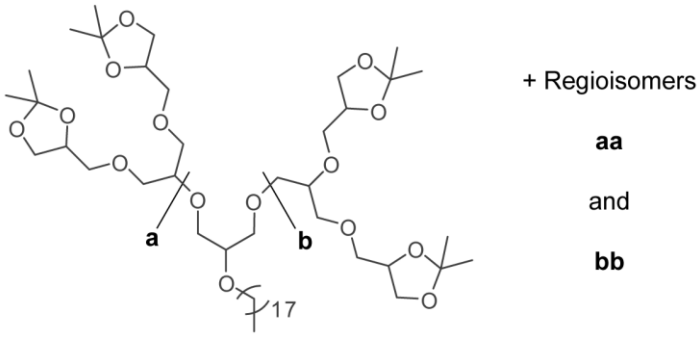

[pG2]-OH (4.80 g, 6.88 mmol, **aa**:**ab**:**bb**, 4:4:1) was dried under reduced pressure (~ 10^{-2} mbar) and dissolved in DMF (120 mL). NaH (60w%, 1.38 g, 34.4 mmol) was added in small portions and 1-bromooctadecane (11.5 g, 34.4 mmol) was added subsequently. The mixture was stirred at 80 °C for 16 h. The mixture was cooled with an ice bath and a saturated solution of NH_4Cl (50 mL) was added slowly. The solvent was removed under reduced pressure, H_2O (200 mL) was added, the aqueous layer was extracted with EtOAc (3 x 200 mL). Column chromatography (SiO_2, pentane/EtOAc, 1:1 → 1:1 + 2% MeOH) gave the desired product (4.45 g, 4.69 mmol, **aa**:**ab**:**bb**, 68%). ^{1}H NMR (400MHz, [D_4] MeOH): δ = 4.28 - 4.20 (m, 4H), 4.08 - 4.02 (m, 4H), 3.79 - 3.47 (m, 29H), 1.61 - 1.52 (m, 2H), 1.44 - 1.23 (m, 54H), 0.95 - 0.88 (m, 3H). ^{13}C NMR (101 MHz, [D_4] MeOH): δ = 110.4, 79.9 - 79.8, 76.2 - 76.0, 73.4, 72.4, 71.3 - 71.1, 67.8 - 67.6, 33.1, 31.2 - 30.5, 27.3 - 27.2,. 25.7, 23.7, 14.5. MS (ESI): *m/*z = 971.6591 $C_{51}H_{96}O_{15}Na_1^+$ (calc. = 971.6641).

8.1.26 [G2]-ether-C18 (aa, ab, bb) - 4

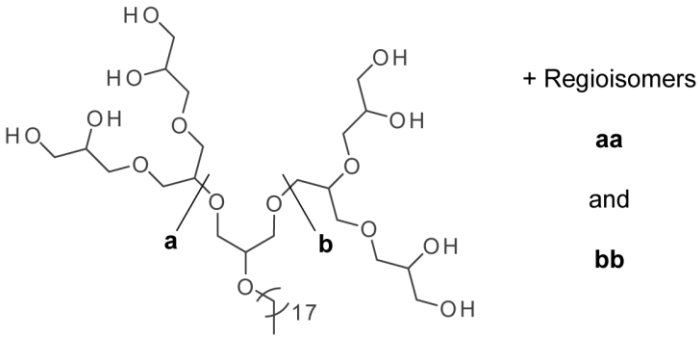

[pG2]-ether-C18 (4.40 g, 4.63 mmol, **aa**:**ab**:**bb**) was dissolved in MeOH (500 mL) and three tablespoons full with Amberlite® IR-120(H) were added. The mixture was stirred vigorously for 16 h, Amberlite® IR-120(H) was filtered off, the solvent was removed under reduced pressure, and the procedure was repeated. The crude product was dissolved in a mixture of H_2O and MeOH (1:1, 38 mL), passed through a syringe filter (RC, 0.2 µm) and purification by means of RP HPLC (H_2O/MeOH, 1:9) gave the desired product (3.20 g, 4.06 mmol, **aa**:**ab**:**bb**, 4:4:1, 88%). ^{1}H NMR (400 MHz, [D_4] MeOH): δ = 3.79 - 3.46 (m, 37H), 1.61 - 1.51 (m, 2H), 1.38 - 1.26 (m, 30H), 0.94 - 0.88 (m, 3H). ^{13}C NMR (101 MHz, [D_4] MeOH): δ = 79.8 - 79.3, 73.9, 72.9, 72.4 - 72.1, 71.4, 70.9, 64.4 - 64.3, 33.0, 31.1, 30.8 - 30.6, 30.4, 27.2, 23.7, 14.4. MS (ESI): *m/*z = 811.5476 $C_{39}H_{80}O_{15}Na_1^+$ (calc. = 811.5389).

8.1.27 [pG2]-N_3 (aa, ab, bb)

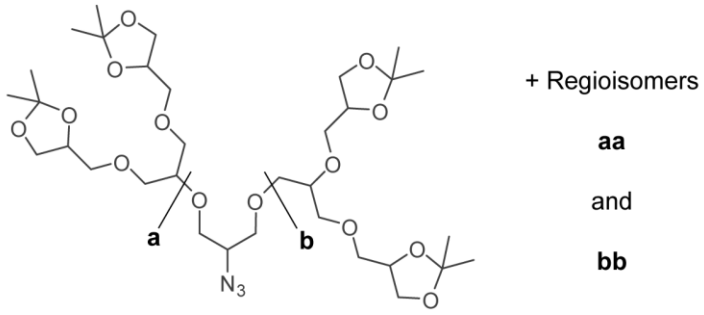

[pG2]-OH (1.50 g, 2.15 mmol, **aa**:**ab**:**bb**, 4:4:1) was dissolved in toluene (100 mL), NEt_3 (0.41 mL, 3.22 mmol) was added, and MsCl (0.22 mL, 2.78 mmol) was added. The mixture was stirred for 16 h at RT, the precipitate was filtered off, and the solvent was removed under reduced pressure. The obtained raw material was dissolved in DMF (100 mL), NaN_3 (0.70 g, 10.7 mmol) was added, and the mixture was stirred for 2 h at 120 °C. The excess of NaN_3 was filtered off, the solvent was removed under reduced pressure, and column purification (SiO_2, DCM/EtOAc, 4:1 → 3:1) gave the desired product (0.98 g, 1.35 mmol, **aa**:**ab**:**bb**, 3:4:1, 63%). ^{1}H NMR (700 MHz, [D_4] MeOH): δ = 4.27 - 4.22 (m, 4H), 4.08 - 4.02 (m, 4H), 3.80 - 3.31 (m, 27H), 1.47 - 1.28 (m, 24H). ^{13}C NMR (175 MHz, [D_4] MeOH): δ = 110.4, 82.3 - 82.0, 79.9 - 79.8, 76.1 - 76.0, 73.4, 72.5 - 72.1, 71.7, 71.1, 70.6, 67.4 - 67.5, 62.4 - 61.9, 38.1, 27.1, 25.7.

8.1.28 [pG2]-NH_2 (aa, ab, bb)

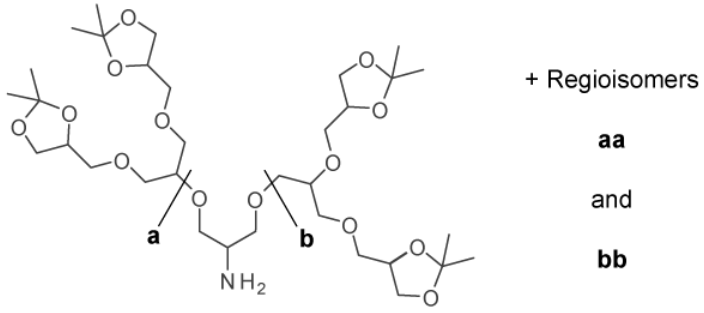

[pG2]-N_3 (1.30 g, 1.80 mmol, **aa**:**ab**:**bb**, 3:4:1) was dissolved in MeOH (10 mL) and Pd/C (100 mg) was added, and the mixture was stirred under hydrogen atmosphere (5 bar) for 16 h. The mixture was passed subsequently through a syringe filter (0.2 µm, RC) and the solvent was removed under reduced pressure to obtain the desired product (1.00 g, 1.43 mmol, **aa**:**ab**:**bb**, 4:4:1, 80%). ^{1}H NMR (700 MHz, [D_4] MeOH): δ = 4.65 (s, 2H), 4.27 - 4.21 (m, 4H), 4.06 - 4.04 (m, 4H), 3.89 - 3.77 (m, 27H), 1.46 - 1.25 (m, 24H). ^{13}C NMR (175 MHz, [D_4] MeOH): δ = 110.3, 82.2, 81.9, 79.9 - 79.6, 76.1 - 76.0, 73.8 - 73.7, 73.3, 72.7 - 72.1, 71.6 - 71.5, 70.5, 67.6 - 67.5, 52.2 - 51.6, 27.1, 25.7.

8.1.29 [pG2]-amide-C18 (aa, ab, bb)

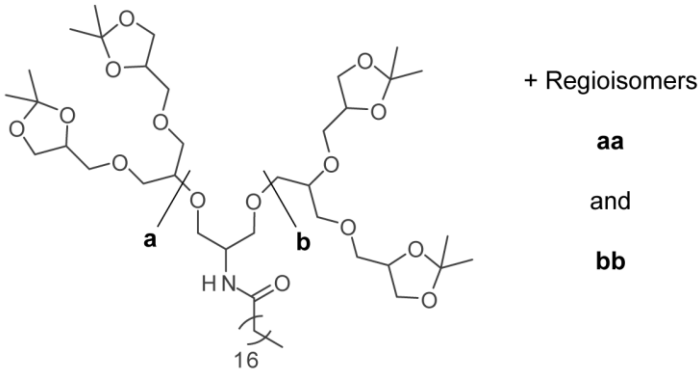

[pG2]-NH_2 (1.90 g, 2.87 mmol, **aa**:**ab**:**bb**, 4:4:1) and NEt_3 (1.48 mL, 11.5 mmol) were dissolved in DCM (10 mL). The mixture was cooled with an ice bath, stearoyl chloride (1.07 g, 3.55 mmol) was added, and the mixture was allowed to stir at RT for 16 h. The mixture was directly purified by column chromatography (SiO_2, DCM/EtOAc, 4:1 → 4:1 + 4% MeOH), which led to the obtainment of the desired product (1.82 g, 1.90 mmol, **aa**:**ab**:**bb**, 66%). ^{1}H NMR (400 MHz, [D_4] MeOH): δ = 4.29 - 4.20 (m, 4H), 4.08 - 4.01 (m, 4H), 3.79 - 3.46 (m, 27H), 2.26 - 2.16 (m, 2H), 1.65 - 1.55 (m, 2H), 1.42 - 1.24 (m, 52H), 0.95 - 0.87 (m, 3H). ^{13}C NMR (101 MHz, [D_4] MeOH): δ = 175.7, 110.4 - 110.2, 79.8 - 79.6, 76.1 - 76.0, 73.4 - 73.3, 72.5 - 72.0, 71.2 - 71.0, 70.0 - 69.8, 67.7 - 67.5, 37.1, 33.0, 30.8 - 30.3, 27.2 - 27.0, 25.7, 23.7. MS (ESI): *m/*z = 984.6684 $C_{51}H_{95}N_1O_{15}Na_1^+$ (calc. = 984.6594).

8.1.30 [G2]-amide-C18 (aa, ab, bb) - 5

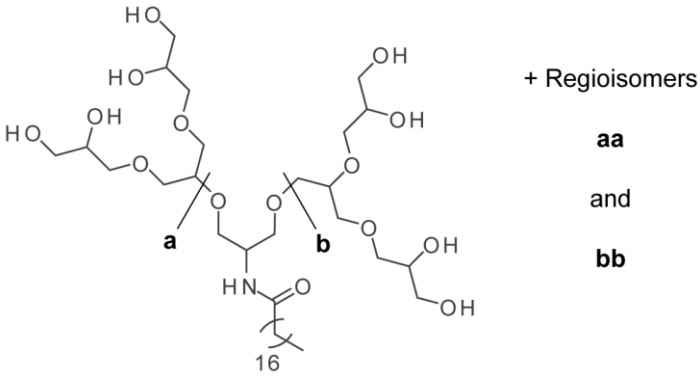

[pG2]-amide-C18 (1.90 g, 2.87 mmol, **aa**:**ab**:**bb**) was dissolved in MeOH (500 mL) and HCl (37%, 100 µL) was added. The mixture was stirred for 16 h at RT, the solvent was removed under reduced pressure and the procedure was repeated. The raw material was then dissolved in a mixture of H_2O and MeOH (1:1, 25 mL) and passed through a syringe filter (RC, 0.2 µm). Subsequent purification by means of RP HPLC (H_2O/MeOH, 1:4) gave the desired product (1.28 g, 1.60 mmol, **aa**:**ab**:**bb**, 4:4:1, 56%). ^{1}H NMR (700 MHz, [D_4] MeOH): δ = 4.19 - 4.08 (m, 1H), 3.79 - 3.74 (m, 4H), 3.71 - 3.65 (m, 5H), 3.63 - 3.44 (m, 25H), 2.25 - 2.17 (m, 2H), 1.66 - 1.55 (m, 2H), 1.41 - 1.21 (m, 28H), 0.94 - 0.86 (m, 3H). ^{13}C NMR (175 MHz, [D_4] MeOH): δ = 176.0, 79.6 - 79.5, 73.8, 72.8, 72.2 - 72.0, 71.0, 69.8, 64.3, 50.8 - 50.0, 37.0, 32.9, 30.7 - 30.0, 27.0, 23.6, 14.5. MS (ESI): *m/*z = 824.5364 $C_{39}H_{79}N_1O_{15}Na_1^+$ (calc. = 824.5342).

8.1.31 [pG2]-O-propargyl (aa, ab, bb)

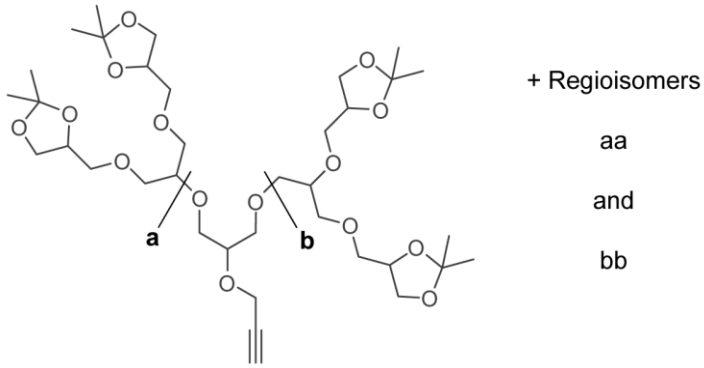

[pG2]-OH (2.00 g, 2.80 mmol, **aa**:**ab**:**bb**, 4:4:1) was dried under reduced pressure (~ 10^{-2} mbar) and dissolved in DMF (70 mL). The flask was cooled with an ice bath and NaH (60w%, 0.35 g, 14.4 mmol) was added in small portions. The ice bath was removed and the mixture was heated up to 60 °C for 30 min. The temperature was reduced to 40 °C, catalytic amounts of 15-crown-5, and propargylbromide (80w%, 1.56 mL, 14.0 mmol) were added. The mixture was stirred at 40 °C for 12 h before a saturated solution of NH_4Cl (50 mL) was slowly added. The solvent was removed under reduced pressure and the residue was mixed with H_2O (200 mL), EtOAc (150 mL), and Brine (100 mL). The aqueous layer was extracted with EtOAc (3 x 150 mL), the organic layer was dried over Na_2SO_4, and the solvent was removed under reduced pressure. Column chromatography (SiO_2, pentane/EtOAc, 3:1 → 3:1 + 2% MeOH) gave the desired product (1.60 g, 2.17 mmol, **aa**:**ab**:**bb**, 4:4:1, 78%). ^{1}H NMR (400 MHz, [D_4] MeOH): δ = 4.35 - 4.31 (m, 2H), 4.28 - 4.21 (m, 4H), 4.08 - 4.02 (m, 4H), 3.79 - 3.50 (m, 27H), 2.89 - 2.85 (m, 1H), 1.41 - 1.29 (m, 24H). ^{13}C NMR (101 MHz, [D_4] MeOH): δ = 110.3, 81.3 - 81.2, 79.8 - 79.7, 78.4 - 77.7, 76.7 - 75.7, 73.3, 72.4 - 72.3, 71.1, 67.7 - 67.5, 58.2, 27.2 - 27.1, 25.7. MS (ESI): *m/z* = 757.4073 $C_{36}H_{62}O_{15}Na_1^+$ (calc. = 757.3981).

8.1.32 [pG2]-triazole-C18 (aa, ab, bb)

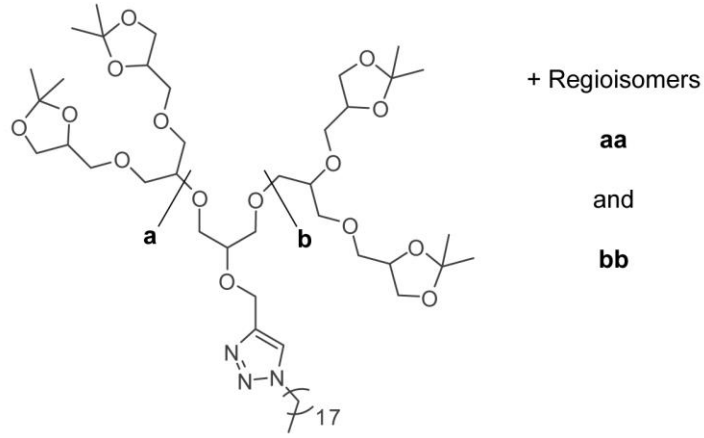

[pG2]-O-propargyl (1.60 g, 2.17 mmol, **aa**:**ab**:**bb**, 4:4:1) and 1-azidooctadecane (0.70 g, 2.30 mmol) were dissolved in a mixture of THF (5 mL) and H_2O (3 mL). DIPEA (37.0 µL, 0.21 mmol), sodium ascorbate (171 mg, 0.86 mmol, dissolved in 1 mL H_2O), and Cu(II)SO_4*5H_2O (54.1 mg, 0.21 mmol, dissolved in 1 mL H_2O) were added. The mixture was stirred at RT for 16 h and was then diluted with

H_2O (60 mL). A saturated solution of EDTA (1 mL) and Brine (20 mL) were added. The aqueous layer was extracted with EtOAc (3 x 50 mL). The organic layer was dried over Na_2SO_4 and the solvent was removed under reduced pressure. Column chromatography (SiO_2, DCM/EtOAc, 4:1 + 2% MeOH) gave the desired product (1.88 g, 1.82 mmol, **aa**:**ab**:**bb**, 84%).^{1}H NMR (400 MHz, [D_4] MeOH): δ = 7.98 (m, 1H), 4.80 - 4.76 (m, 2H), 4.43 - 4.36 (m, 2H), 4.28 - 4.19 (m, 2H), 4.06 - 4.00 (m, 4H), 3.77 - 3.47 (m, 29H), 1.96 - 1.86 (m, 2H), 1.41 - 1.26 (m, 54H), 0.93 - 0.87 (m, 3H). ^{13}C NMR (101 MHz, [D_4] MeOH): δ = 146.4, 124.8, 110.3, 79.8, 79.2, 78.9, 76.1 - 76.0, 73.4, 72.5 - 72.3, 71.2, 67.7 - 67.5, 64.3, 61.4, 51.3, 33.0, 31.3, 30.8 - 30.4, 30.1, 27.5, 27.2 - 27.1, 25.7, 23.7, 14.5. MS (ESI): *m*/z = 1052.6990 $C_{54}H_{99}N_3O_{15}Na_1^+$ (calc. = 1052.6968).

8.1.33 [G2]-triazole-C18 (aa, ab, bb) - 6

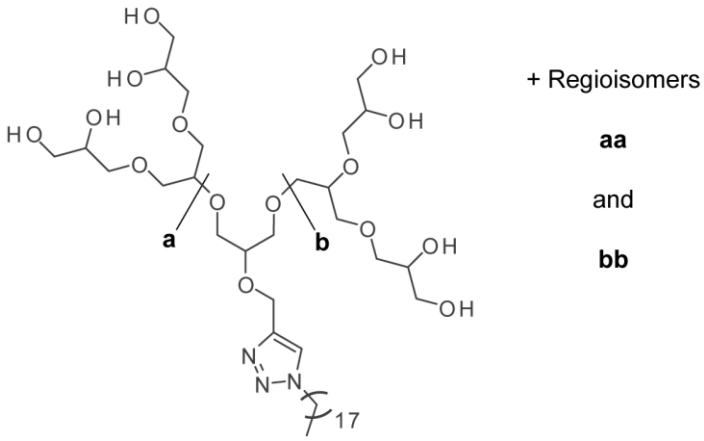

[pG2]-triazole-C18 (1.88 g, 1.82 mmol, **aa**:**ab**:**bb**) was dissolved in MeOH (500 mL) and treated with HCl (37%, 100 µL). The mixture was stirred for 16 h at RT, the solvent was removed under reduced pressure, and the procedure was repeated. The crude product was then dissolved in a mixture of H_2O and MeOH (1:1, 40 mL), passed through a syringe filter (RC, 0.2 µm), and purified by means of RP HPLC (H_2O/MeOH, 1:9) to obtain the desired product (1.26 g, 1.44 mmol, **aa**:**ab**:**bb**, 1:2:1, 80%). ^{1}H NMR (400MHz, [D_4] MeOH): δ = 8.03 (m, 1H), 4.82 - 4.75 (m, 2H), 4.44 - 4.36 (m, 2H), 3.83 - 3.44 (m, 35H), 1.95 - 1.86 (m, 2H), 1.39 - 1.21 (m, 30H), 0.93 - 0.86 (m, 3H). ^{13}C NMR (101 MHz, [D_4] MeOH): δ = 146.1, 125.0, 79.7, 79.1, 78.8, 73.8, 72.8, 72.3 - 72.0, 71.0, 64.3 - 64.1, 51.3, 33.0, 31.3, 30.7 - 30.4, 30.0, 27.4, 23.6, 14.5. MS (ESI): *m*/z = 892.5715 $C_{42}H_{83}N_3O_{15}Na_1^+$ (calc. = 892.5716).

8.1.34 [pG2]-carbamate-Chol (aa, ab, bb)

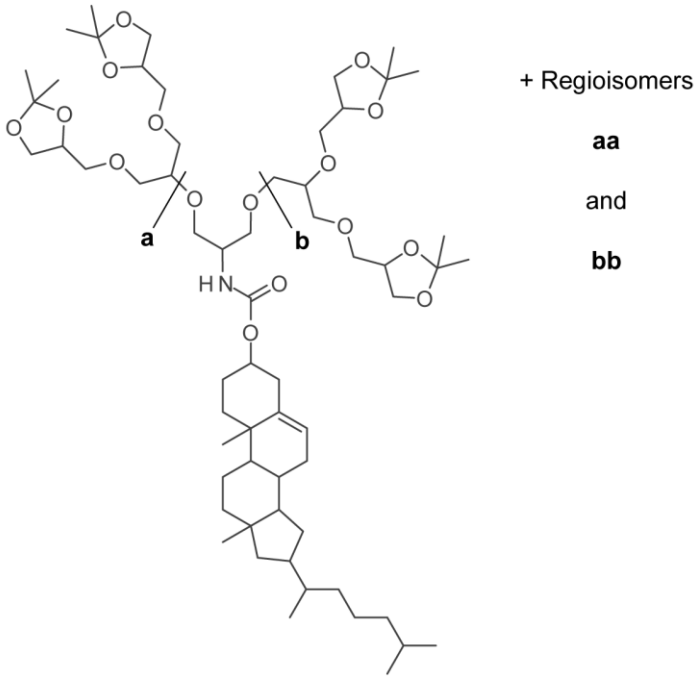

[pG2]-NH_2 (1.00 g, 1.44 mmol, **aa**:**ab**:**bb**, 4:4:1) was dried under reduced pressure (~ 10^{-2} mbar). Dry DCM (40 mL), NEt_3 (1.00 mL, 7.18 mmol), and cholic acid chloride (2.60 g, 5.78 mmol) were added. The mixture was stirred at RT for 12 h. Column chromatography (SiO_2, DCM/EtOAc, 4:1 → 1:1) led to the obtainment of the desired product (1.19 g, 1.06 mmol, **aa**:**ab**:**bb**, 74%). ^{1}H NMR (700 MHz, [D_2] DCM): δ = 5.42 - 5.41 (m, 1H), 4.48 - 4.45 (m, 1H), 4.29 - 4.92 (m, 4H), 4.07 - 4.04 (m, 4H), 3.75 - 3.47 (m, 27 H), 2.38 - 0.98 (m, 29H), 1.41 (s, 12H), 1.36 (s, 12H), 1.05 (s, 3H), 0.96 (m, 3H), 0.90 (m, 6H), 0.72 (m, 3H). ^{13}C NMR (176 MHz, [D_2] DCM): δ = 156.0, 140.4, 122.7, 109.6, 79.3, 79.1, 78.9, 75.3, 75.1, 75.0, 74.6, 72.9, 71.9, 71.8, 71.7, 71.5, 70.6, 70.5, 69.6, 69.4, 67.2, 67.1, 57.1, 56.5, 50.5, 42.7, 40.2, 39.9, 39.0, 37.4, 36.9, 36.6, 36.2, 32.3, 28.6, 28.4, 26.9, 25.6, 24.6, 24.2, 22.9, 22.7, 21.4, 19.5, 18.9, 12.0. MS (ESI): *m/*z = 1130.7350 $C_{61}H_{105}N_1O_{16}Na_1^+$ (calc. = 1130.7326).

8.1.35 [G2]-carbamate-Chol (aa, ab, bb) - 7

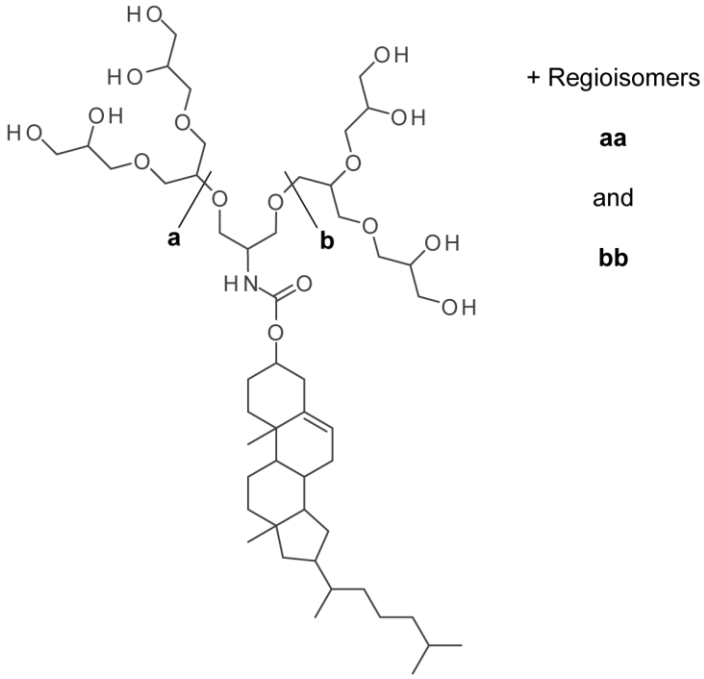

[pG2]-carbamate-Chol (1.18 g, 1.06 mmol, **aa**:**ab**:**bb**) was dissolved in MeOH (50 mL) and two tablespoons full with Amberlite® IR-120(H) were added. The mixture was stirred at RT for 16 h and Amberlite® IR-120(H) was filtered off. The solvent was removed under reduced pressure, the residue was dissolved in a mixture of H_2O and MeOH (1:1, 20 mL), and the solution was passed through a syringe filter (RC, 0.2 µm). Purification by RP HPLC (H_2O/MeOH, 5:95) gave the desired product (0.70 g, 0.74 mmol, **aa**:**ab**:**bb**, 9:5:1, 70%). ^{1}H NMR (700 MHz, [D_1] $CHCl_3$): δ = 5.38 - 5.37 (m, 1H), 4.43 - 4.35 (m, 1H), 3.79 - 3.74 (m, 4H), 3.71 - 3.66 (m, 5H), 3.62 - 3.46 (m, 26H), 2.33 - 1.07 (m, 29H), 1.02 (s, 3H), 0.93 (m, 3H), 0.87 (m, 6H), 0.71 (s, 3H). ^{13}C NMR (126 MHz, [D_1] $CHCl_3$): δ = 158.2, 141.2, 123.4, 101.7, 79.8, 73.9, 72.3, 72.1, 64.4, 58.1, 57.5, 51.6, 43.5, 42.3, 41.1, 40.6, 39.6, 38.2, 37.7, 37.3, 37.1, 36.9, 33.2, 33.0, 29.3, 29.1, 27.4, 25.3, 24.9, 23.2, 22.9, 22.1, 19.8, 19.2, 12.3. MS (ESI): *m*/z = 970.6047 $C_{49}H_{89}N_1O_{16}Na_1^+$ (calc. = 970.6074).

8.1.36 [pG2]-triazole-DC12 (aa, ab, bb)

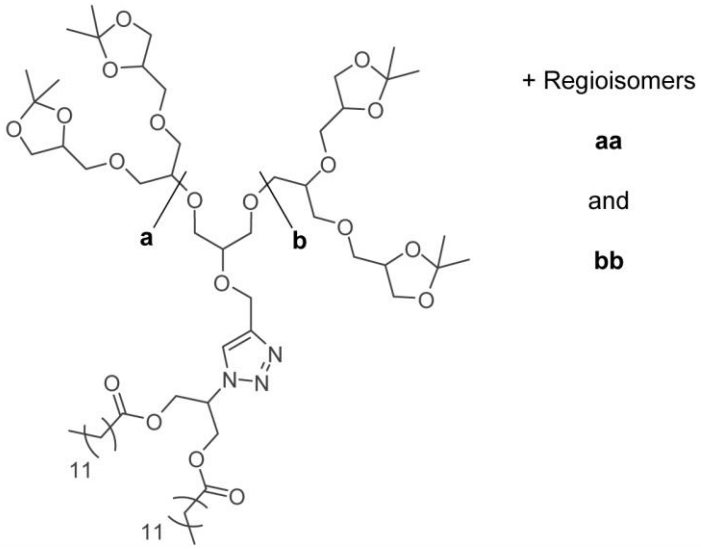

+ Regioisomers

aa

and

bb

[pG2]-O-propargyl (0.73 g, 1.00 mmol, **aa**:**ab**:**bb**, 4:4:1) and dodecanoic acid, 2-azido-1,3-propanediyl ester (0.76 g, 1.50 mmol) were dissolved in THF (3 mL) and H_2O (3 mL). DIPEA (17.5 µL, 0.10 mmol), sodium ascorbate (99.5 mg, 0.50 mmol, dissolved in 1 mL H_2O), and Cu(II)SO_4*5H_2O (24.9 mg, 0.10 mmol, dissolved in 1 mL H_2O) were added and the mixture was stirred at RT for 2 h. A saturated solution of EDTA (1 mL) and Brine (20 mL) were added. The aqueous layer was extracted with EtOAc (3 x 50 mL), the organic layer was dried over Na_2SO_4, and the solvent was removed under reduced pressure. Column chromatography (SiO_2, pentane/isopropanol, 9:1) gave the desired product (0.88 g, 0.72 mmol, **aa**:**ab**:**bb**, 72%). ^{1}H NMR (400 MHz, [D_4] MeOH): δ = 8.11 (m, 1H), 5.23 - 5.17 (m, 1H), 4.82 - 4.79 (m, 2H), 4.62 - 4.53 (m, 4H), 4.27 - 4.21 (m, 4H), 4.07 - 4.00 (m, 4H), 3.79 - 3.46 (m, 27H), 2.33 - 2.27 (m, 4H), 1.60 - 1.50 (m, 4H), 1.44 - 1.18 (m, 56H), 0.94 - 0.87 (m, 6H). ^{13}C NMR (101 MHz, [D_4] MeOH): δ = 174.3, 110.4, 79.8, 76.1, 73.4, 72.4, 67.6, 63.4, 34.6, 33.0, 30.7 - 30.4, 30.1, 27.1, 25.8, 25.7, 23.7, 14.5.

8.1.37 [G2]-triazole-DC12 (aa, ab, bb) - 8

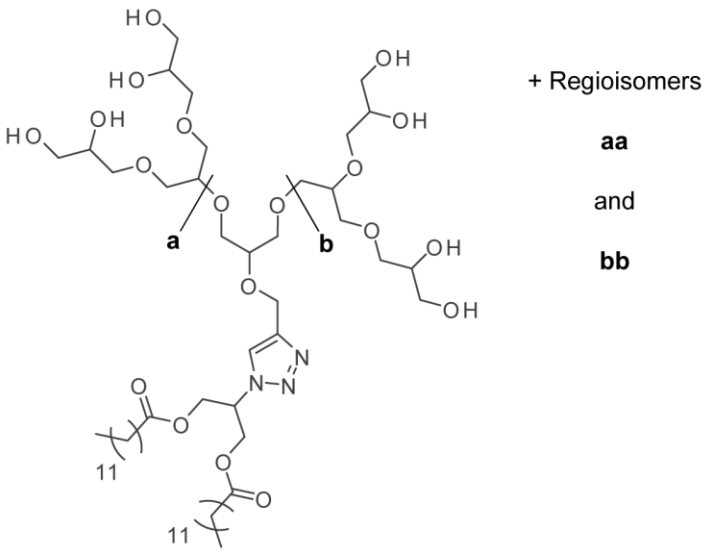

+ Regioisomers

aa

and

bb

[pG2]-triazole-DC12 (0.88 g, 0.72 mmol, **aa**:**ab**:**bb**) was dissolved in MeOH (30 mL), two tablespoons full with Amberlite® IR-120(H) were added, and the mixture was heated up to 40 °C for 6 h. Amberlite® IR-120(H) was filtered off and the solvent was removed under reduced pressure. The crude product was dissolved in a mixture of H_2O and MeOH (1:1, 15 mL) and the solution was passed through a syringe filter (RC, 0.2 µm). Purification by RP HPLC (H_2O/MeOH, 1:9) gave the desired product (0.45 g, 0.42 mmol, **aa**:**ab**:**bb**, 9:5:1, 58%). ^{1}H NMR (400 MHz, [D_4] MeOH): 8.16 (m, 1H), 5.23 - 5.18 (m, 1H), 4.81 - 4.77 (m, 2H), 4.61 - 4.54 (m, 4H), 3.81 - 3.45 (m, 35H), 2.32 - 2.29 (m, 4H), 1.59 - 1.48 (m, 4H), 1.34 - 1.22 (m, 32H), 0.93 - 0.87 (m, 6H). δ = ^{13}C NMR (101 MHz, [D_4] MeOH): δ = 174.5, 146.3, 124.9, 79.9 - 79.2, 74.0 - 73.9, 72.9, 72.4 - 72.1, 71.2, 64.4, 64.2, 63.4, 60.3, 34.6, 33.0, 30.7 - 30.4, 30.1, 25.8, 23.7, 14.4. MS (ESI): *m/z* = 1078.6623 $C_{51}H_{97}N_3O_{19}Na_1^+$ (calc. = 1078.6608).

8.2 NMR Spectra

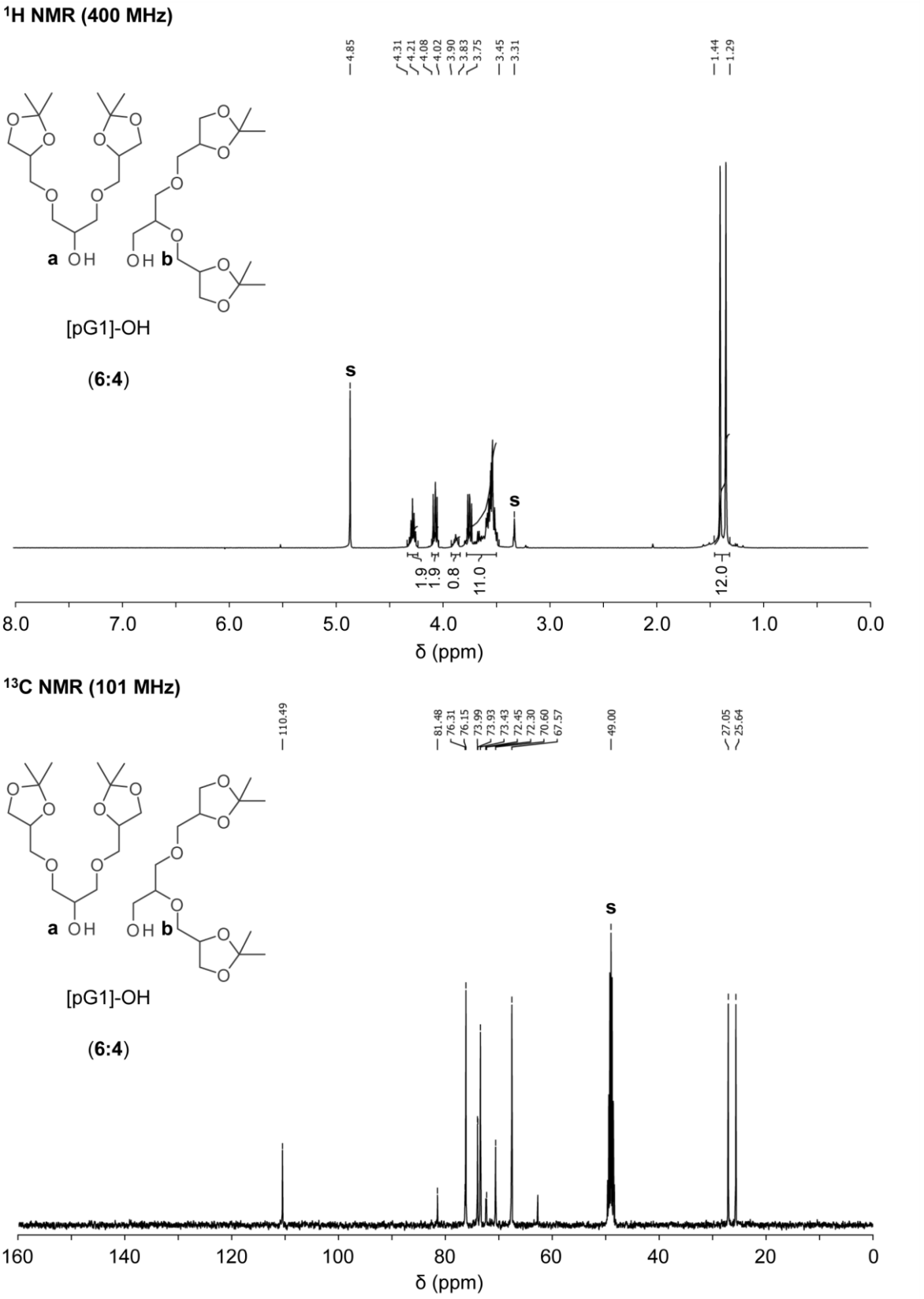

Figure 8.1: NMR Spectra of [pG1]-OH (**a**:**b**, 6:4). Solvent signals ([D_4] MeOH) are labeled with **s**.

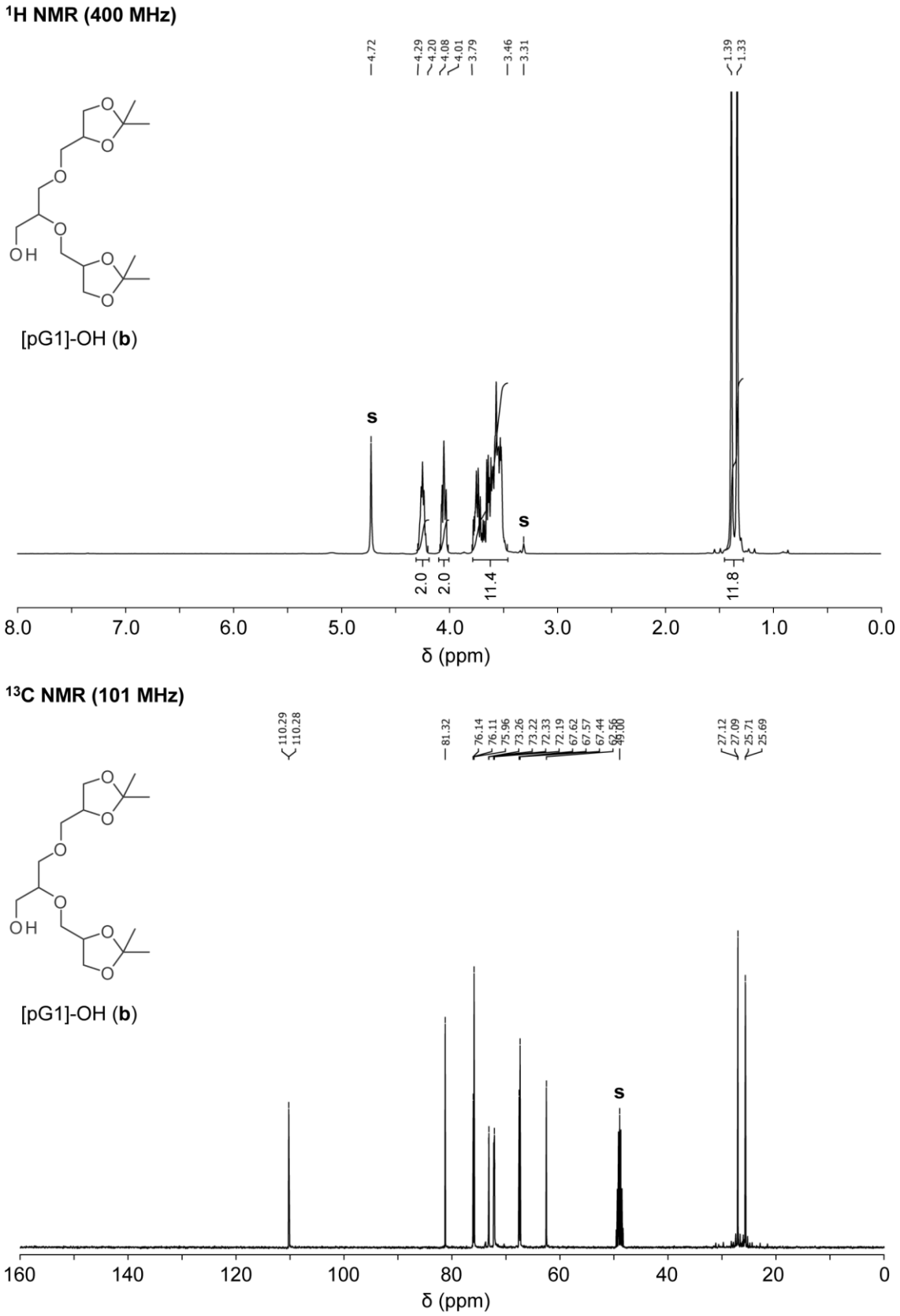

Figure 8.2: NMR Spectra of [pG1]-OH (**b**). Solvent signals ([D_4] MeOH) are labeled with **s**.

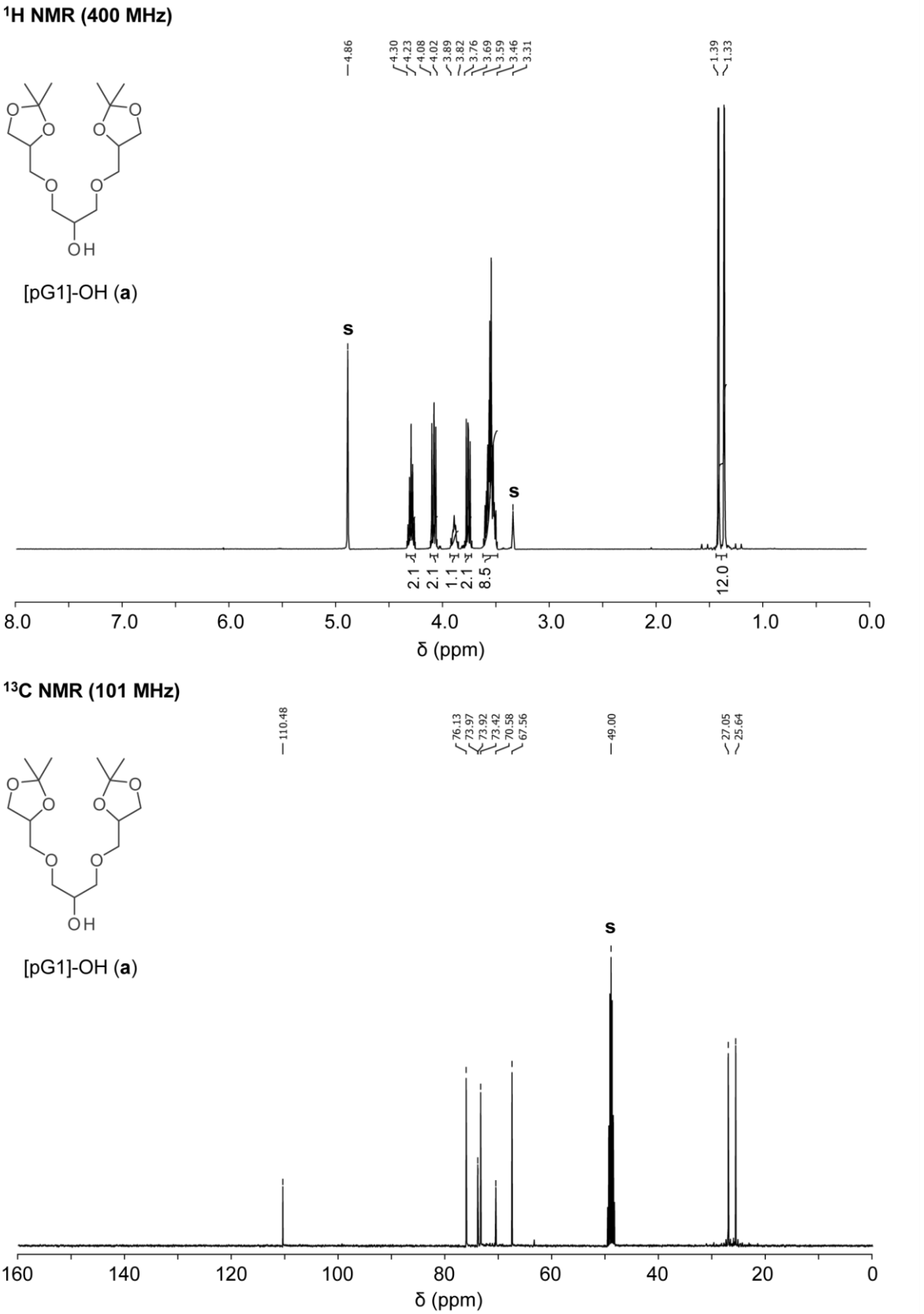

Figure 8.3: NMR Spectra of [pG1]-OH (**a**). Solvent signals ([D_4] MeOH) are labeled with **s**.

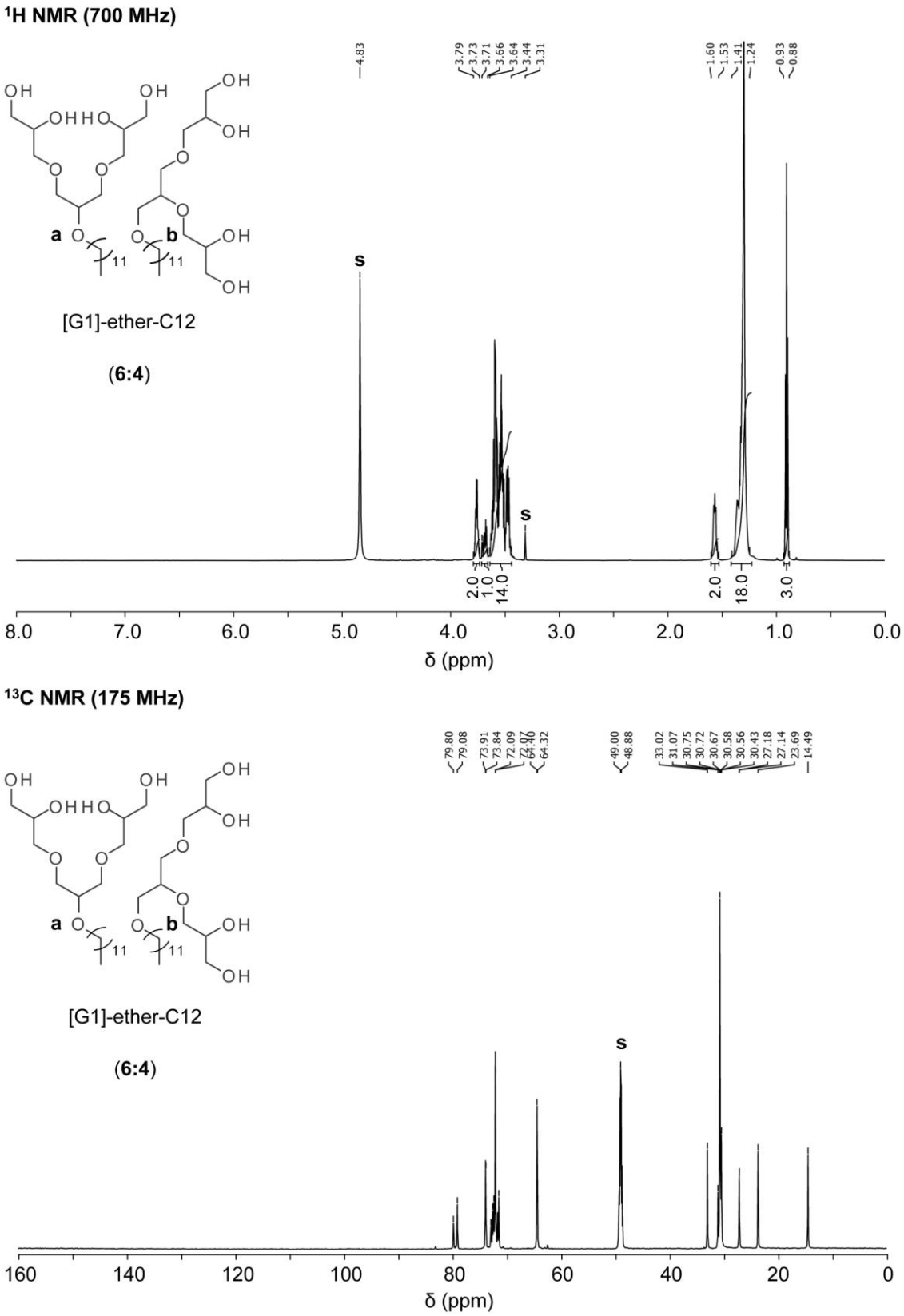

Figure 8.4: NMR Spectra of [G1]-ether-C12 (**a**:**b**, 6:4). Solvent signals ([D_4] MeOH) are labeled with **s**.

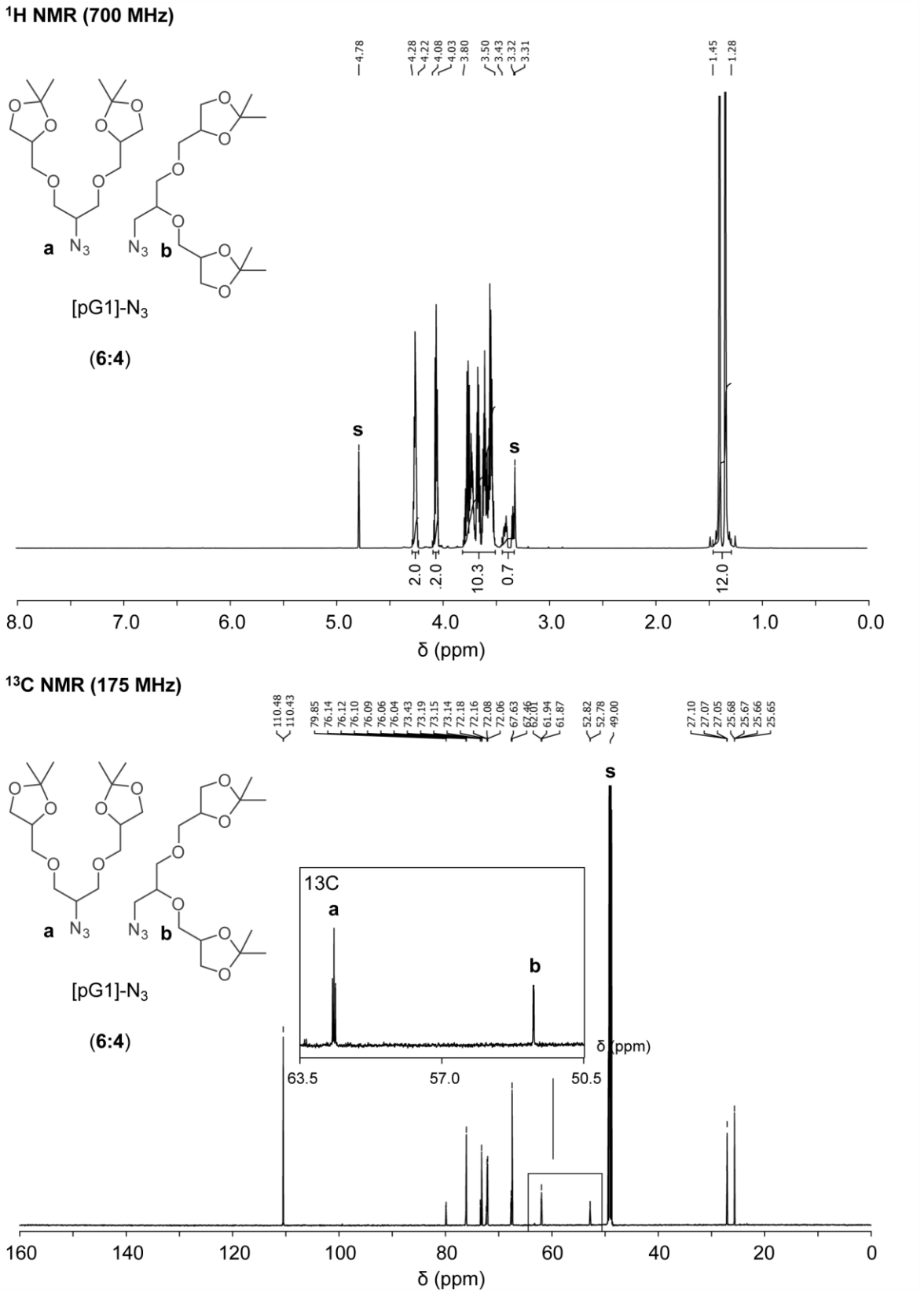

Figure 8.5: NMR Spectra of [pG1]-N_3 (**a**:**b**, 6:4). The inset within the ^{13}C NMR Spectrum (bottom) shows the signals of the focal points, which are labeled with **a** and **b**, respectively. Solvent signals ([D_4] MeOH) are labeled with **s**.

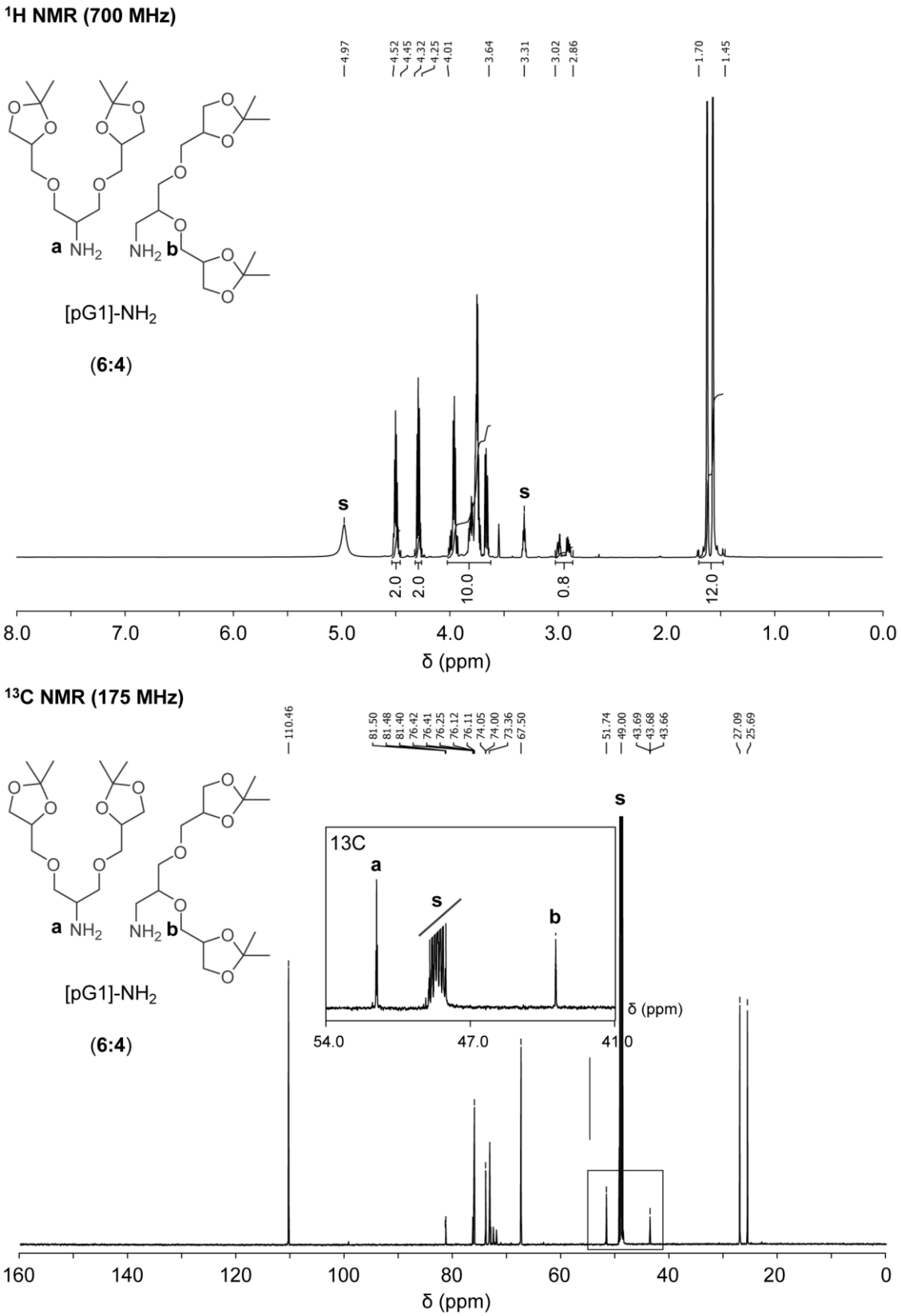

Figure 8.6: NMR Spectra of [pG1]-NH_2 (**a**:**b**, 6:4). The inset within the ^{13}C NMR Spectrum (bottom) shows the signals of the focal points, which are labeled with **a** and **b**, respectively. Solvent signals ([D_4] MeOH) are labeled with **s**.

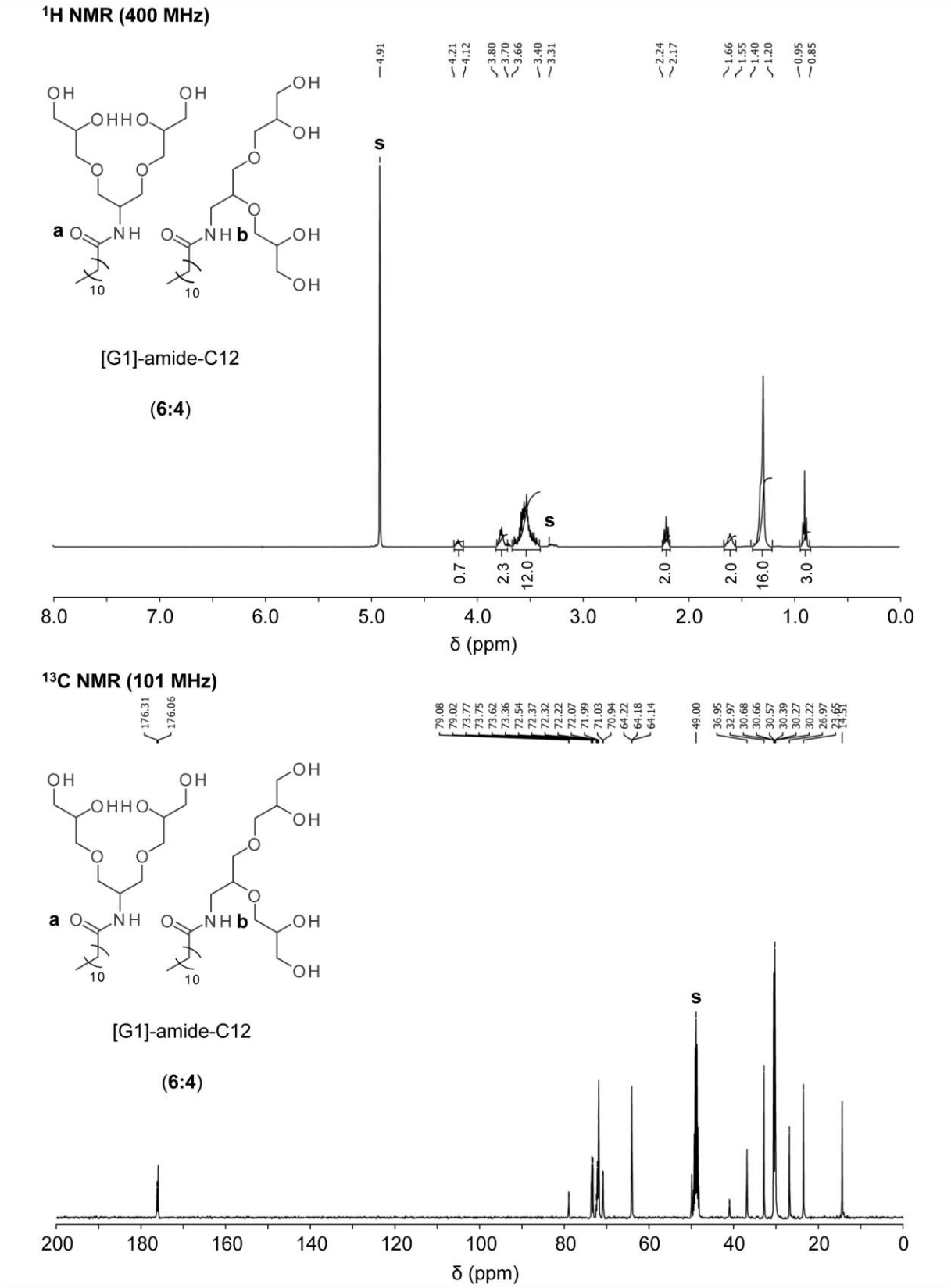

Figure 8.7: NMR Spectra of [G1]-amide-C12 (**a**:**b**, 6:4). Solvent signals ([D_4] MeOH) are labeled with **s**.

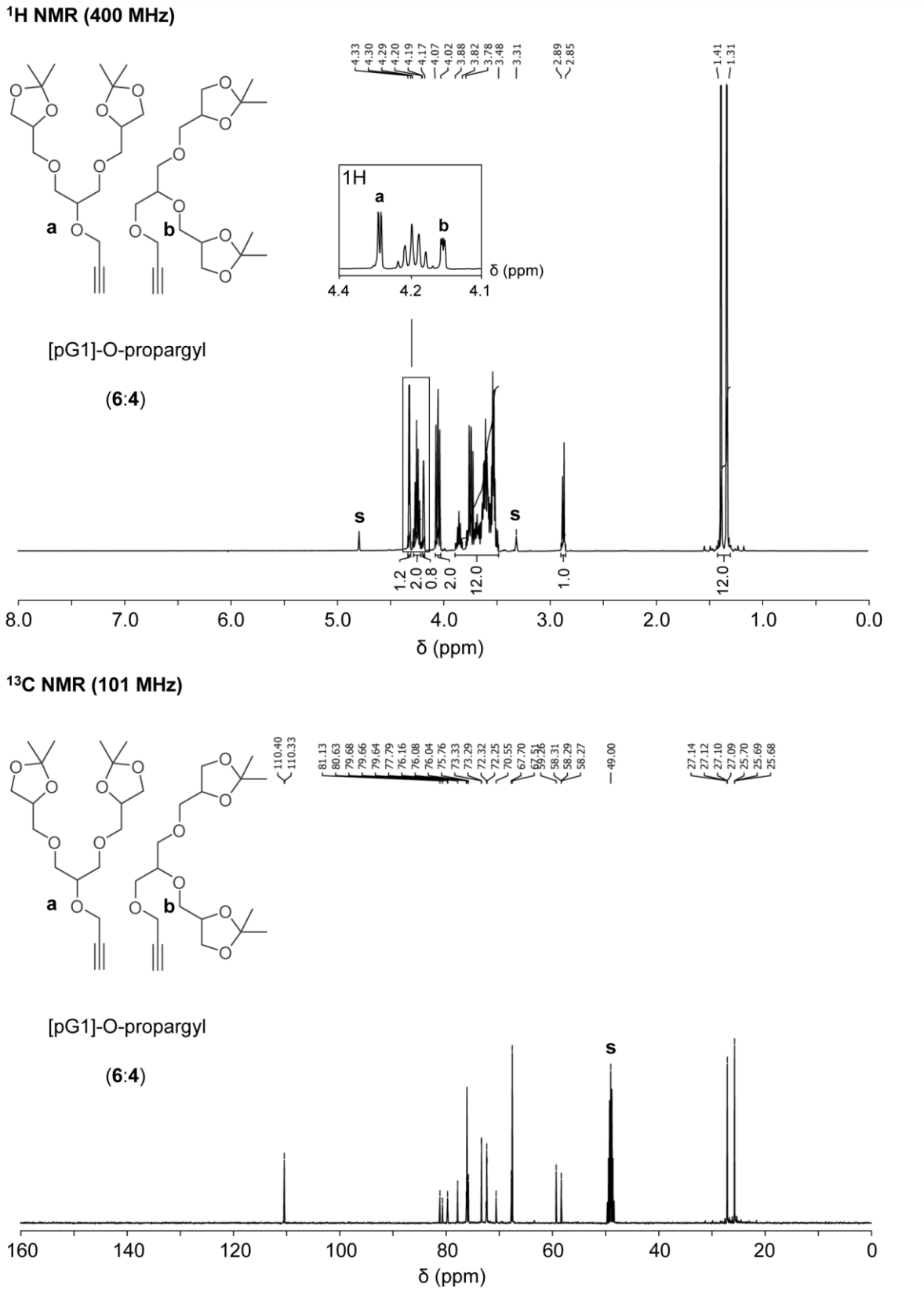

Figure 8.8: NMR Spectra of [pG1]-O-propargyl (**a**:**b**, 6:4). The inset within the ^{1}H NMR Spectrum (top) shows the signals of the focal points, which are labeled with **a** and **b**, respectively. Solvent signals ([D_4] MeOH) are labeled with **s**.

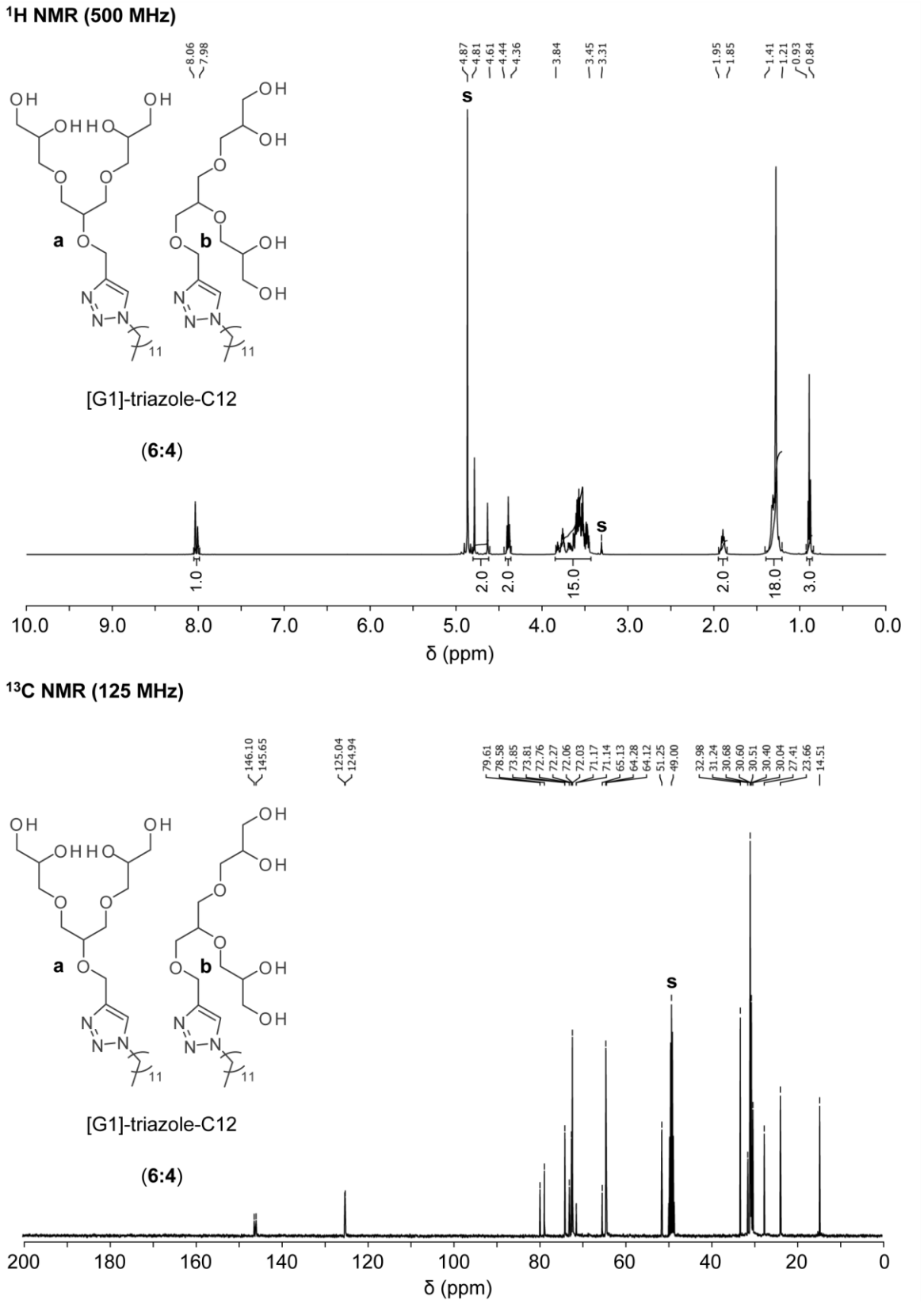

Figure 8.9: NMR Spectra of [G1]-triazole-C12 (**a**:**b**, 6:4). Solvent signals ([D_4] MeOH) are labeled with **s**.

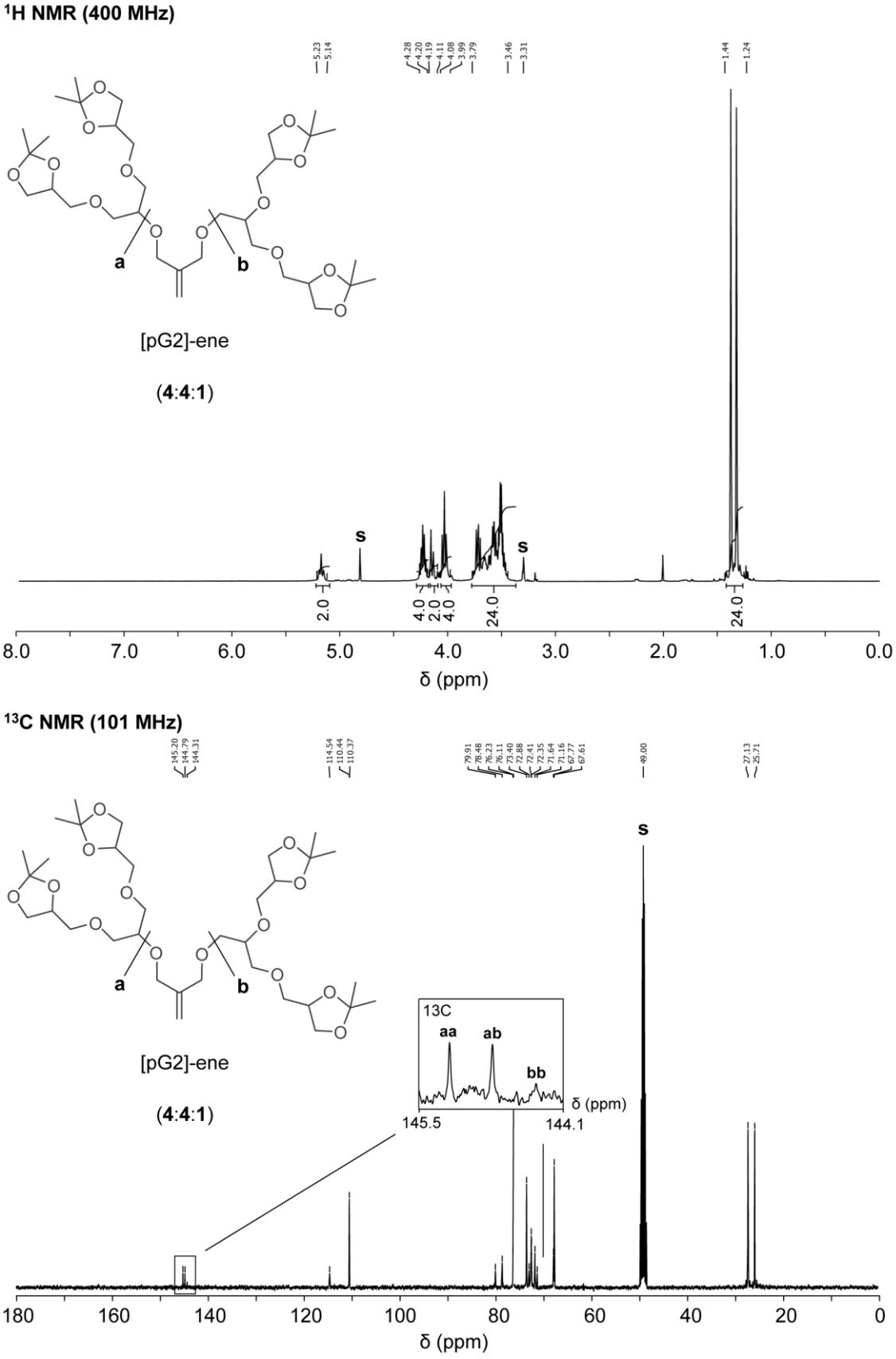

Figure 8.10: NMR Spectra of [pG2]-ene (**aa**:**ab**:**bb**, 4:4:1). The inset within the ^{13}C NMR Spectrum (bottom) shows ^{13}C signals of the focal points, which are labeled with **aa**, **ab**, and **bb**, respectively. Solvent signals ([D_4] MeOH) are labeled with **s**.

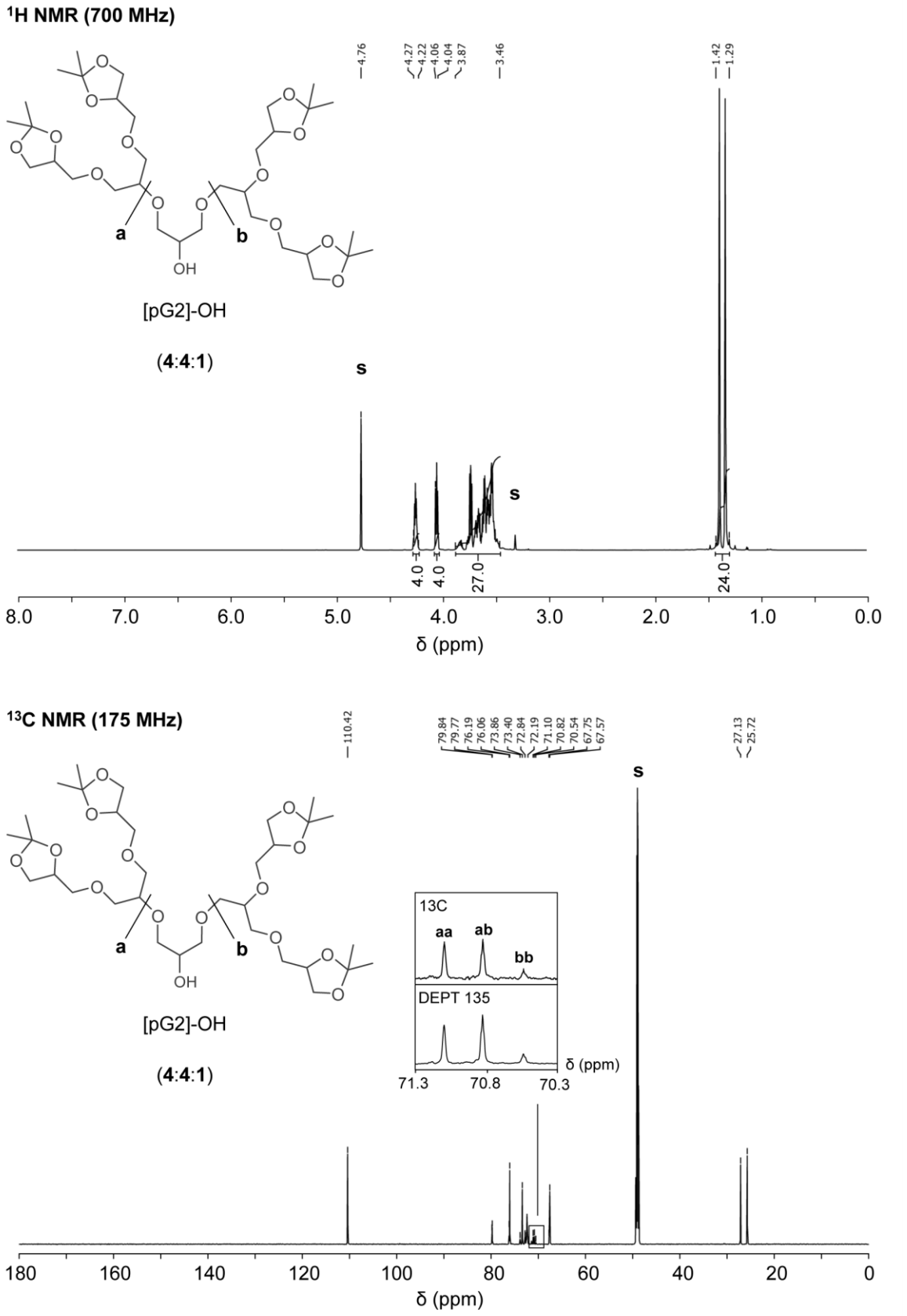

Figure 8.11: NMR Spectra of [pG2]-OH (**aa**:**ab**:**bb**, 4:4:1). The inset within the ^{13}C NMR Spectrum (bottom) shows ^{13}C and DEPT135 signals of the focal points, which are labeled with **aa**, **ab**, and **bb**, respectively. Solvent signals ([D_4] MeOH) are labeled with **s**.

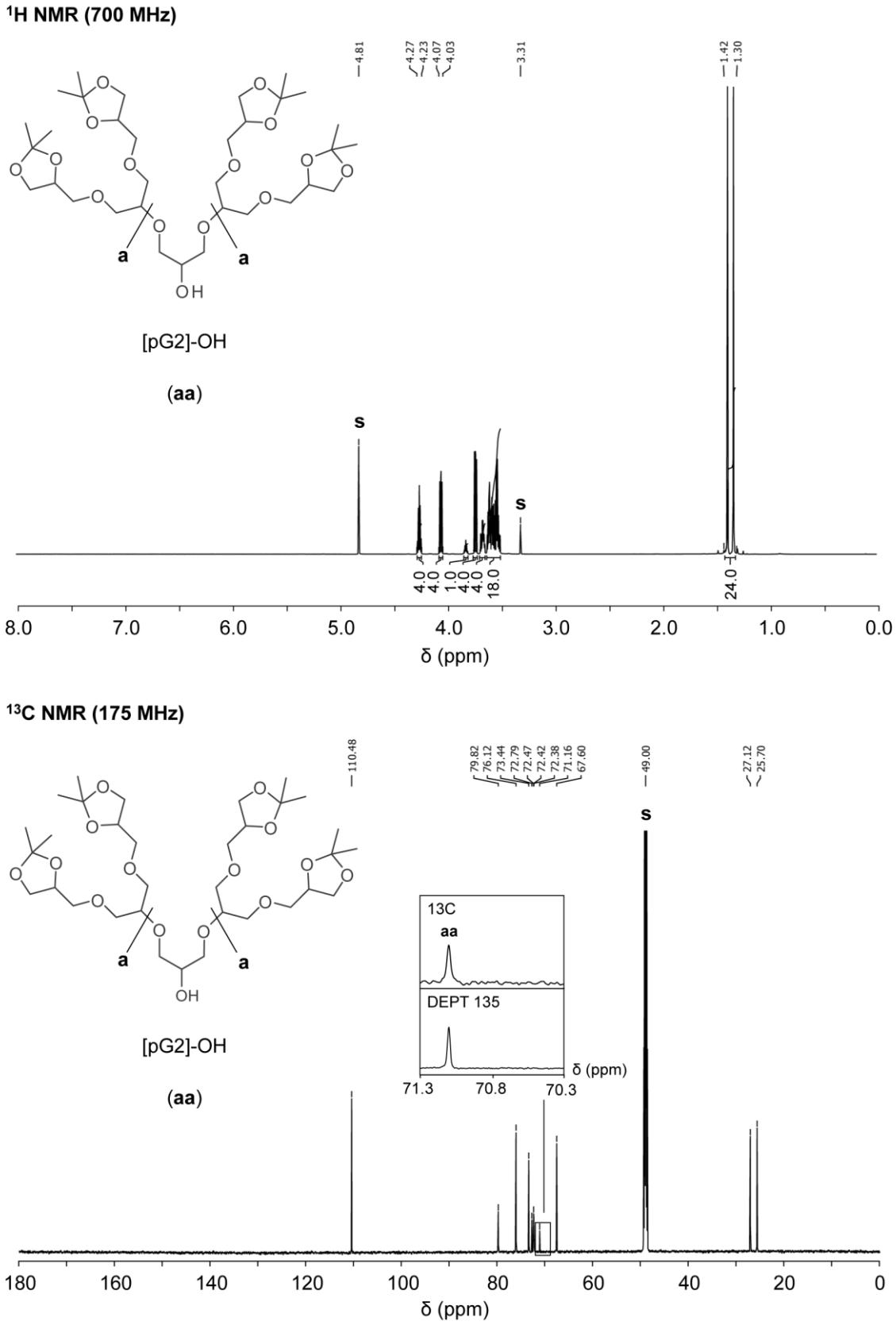

Figure 8.12: NMR Spectra of [pG2]-OH (**aa**). The inset within the ^{13}C NMR Spectrum (bottom) shows ^{13}C and DEPT135 signals of the focal point, which is labeled with **aa**. Solvent signals ([D_4] MeOH) are labeled with **s**.

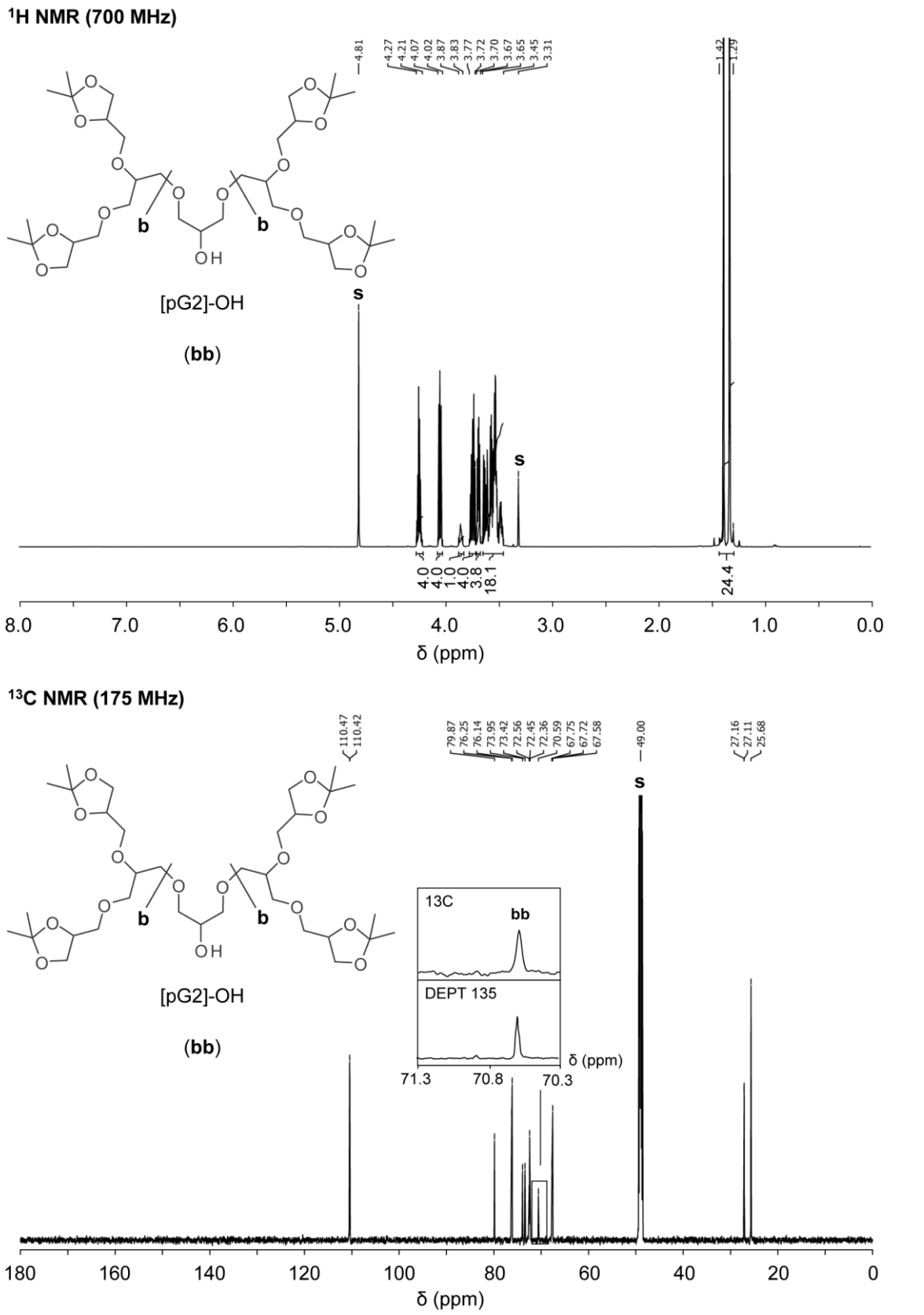

Figure 8.13: NMR Spectra of [pG2]-OH (**bb**). The inset within the ^{13}C NMR Spectrum (bottom) shows ^{13}C and DEPT135 signals of the focal point, which is labeled with **bb**. Solvent signals ([D_4] MeOH) are labeled with **s**.

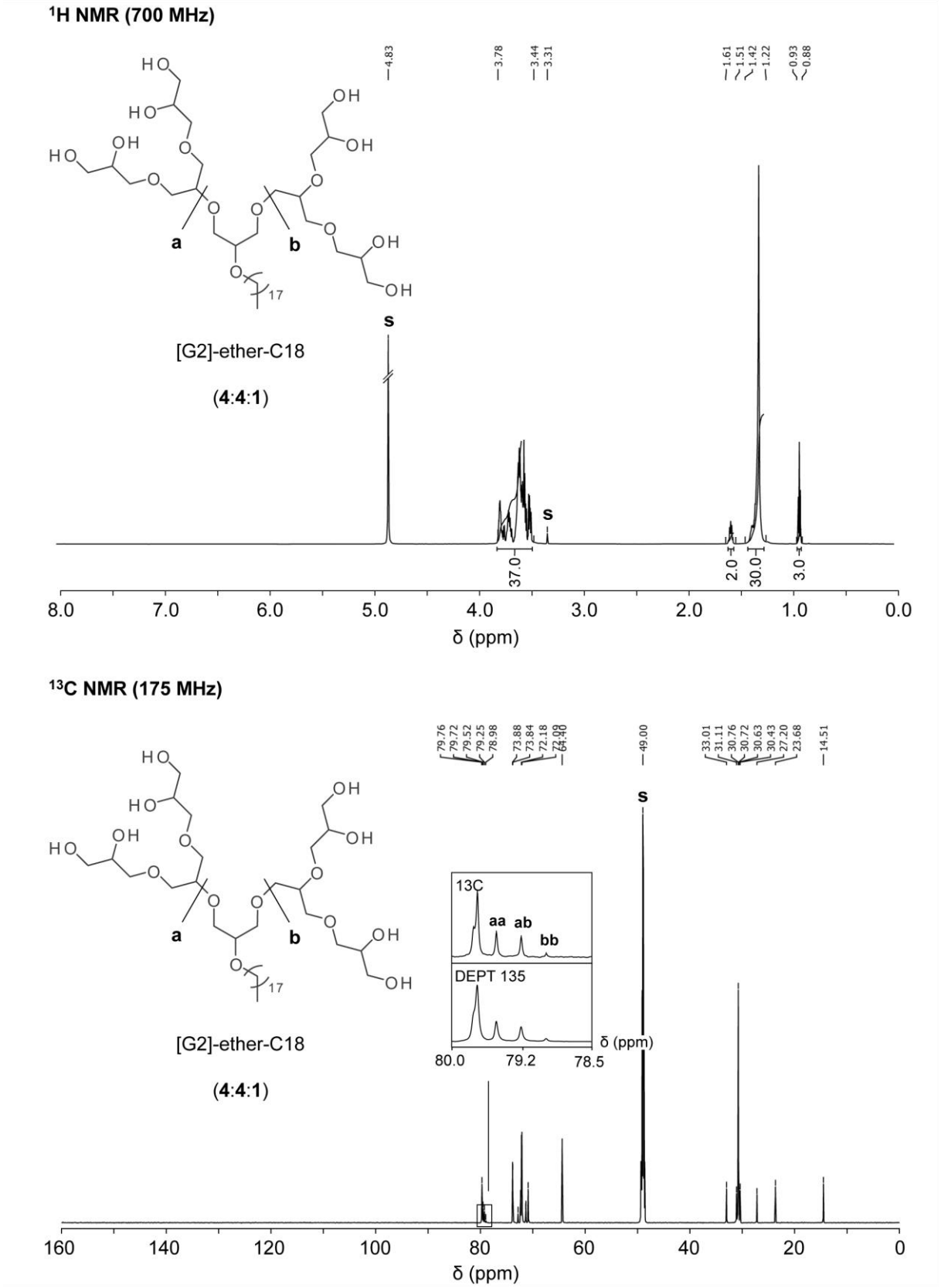

Figure 8.14: NMR Spectra of [G2]-ether-C18 (**aa**:**ab**:**bb**, 4:4:1). The inset within the ^{13}C NMR Spectrum (bottom) shows ^{13}C and DEPT135 signals of the focal points, which are labeled with **aa**, **ab**, and **bb**, respectively. Solvent signals ([D_4] MeOH) are labeled with **s**.

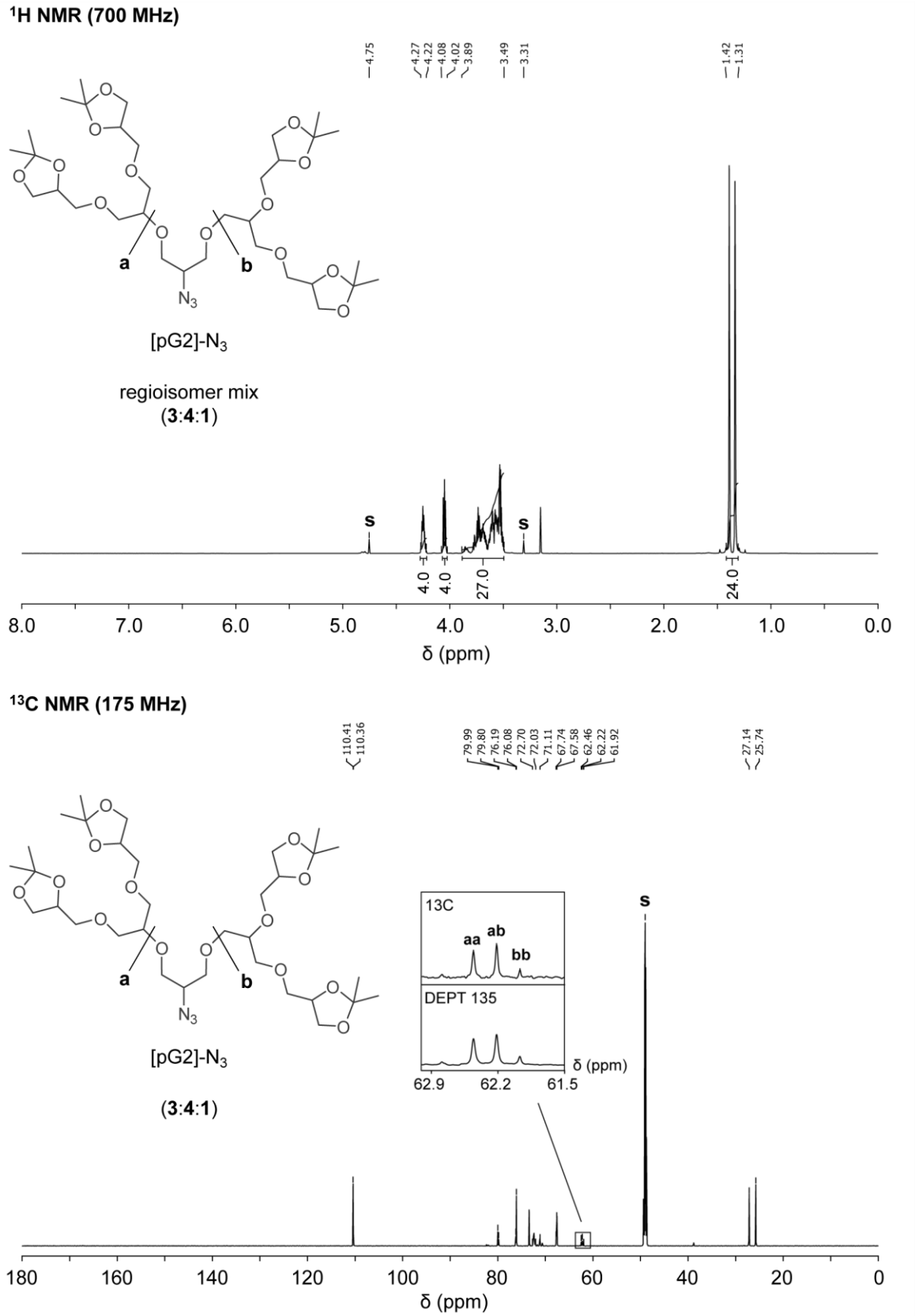

Figure 8.15: NMR Spectra of [pG2]-N_3 (**aa**:**ab**:**bb**, 3:4:1). The inset within the ^{13}C NMR Spectrum (bottom) shows ^{13}C and DEPT135 signals of the focal points, which are labeled with **aa**, **ab**, and **bb**, respectively. Solvent signals ([D_4] MeOH) are labeled with **s**.

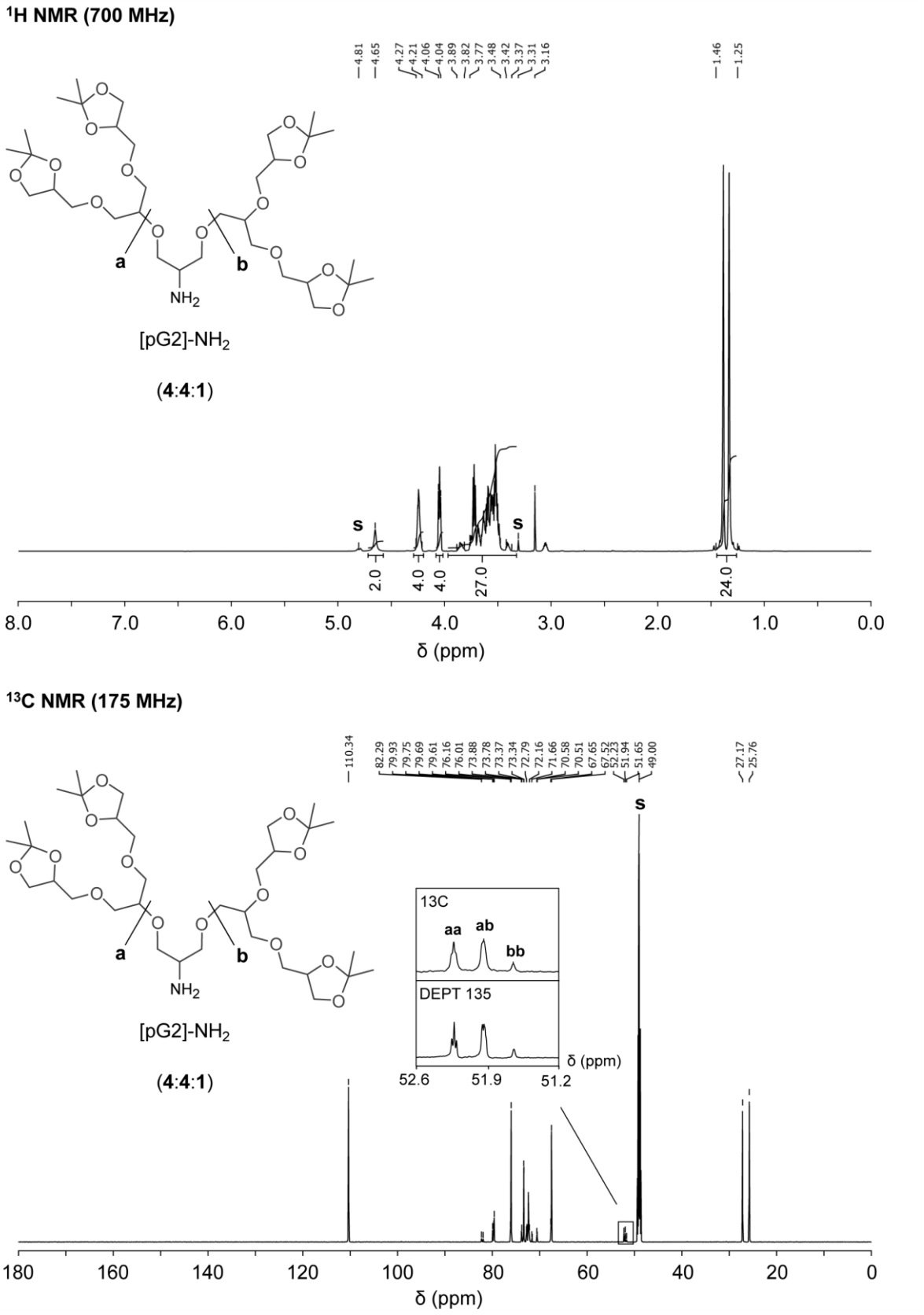

Figure 8.16: NMR Spectra of [pG2]-NH_2 (**aa**:**ab**:**bb**, 4:4:1). The inset within the ^{13}C NMR Spectrum (bottom) shows ^{13}C and DEPT135 signals of the focal points, which are labeled with **aa**, **ab**, and **bb**, respectively. Solvent signals ([D_4] MeOH) are labeled with **s**.

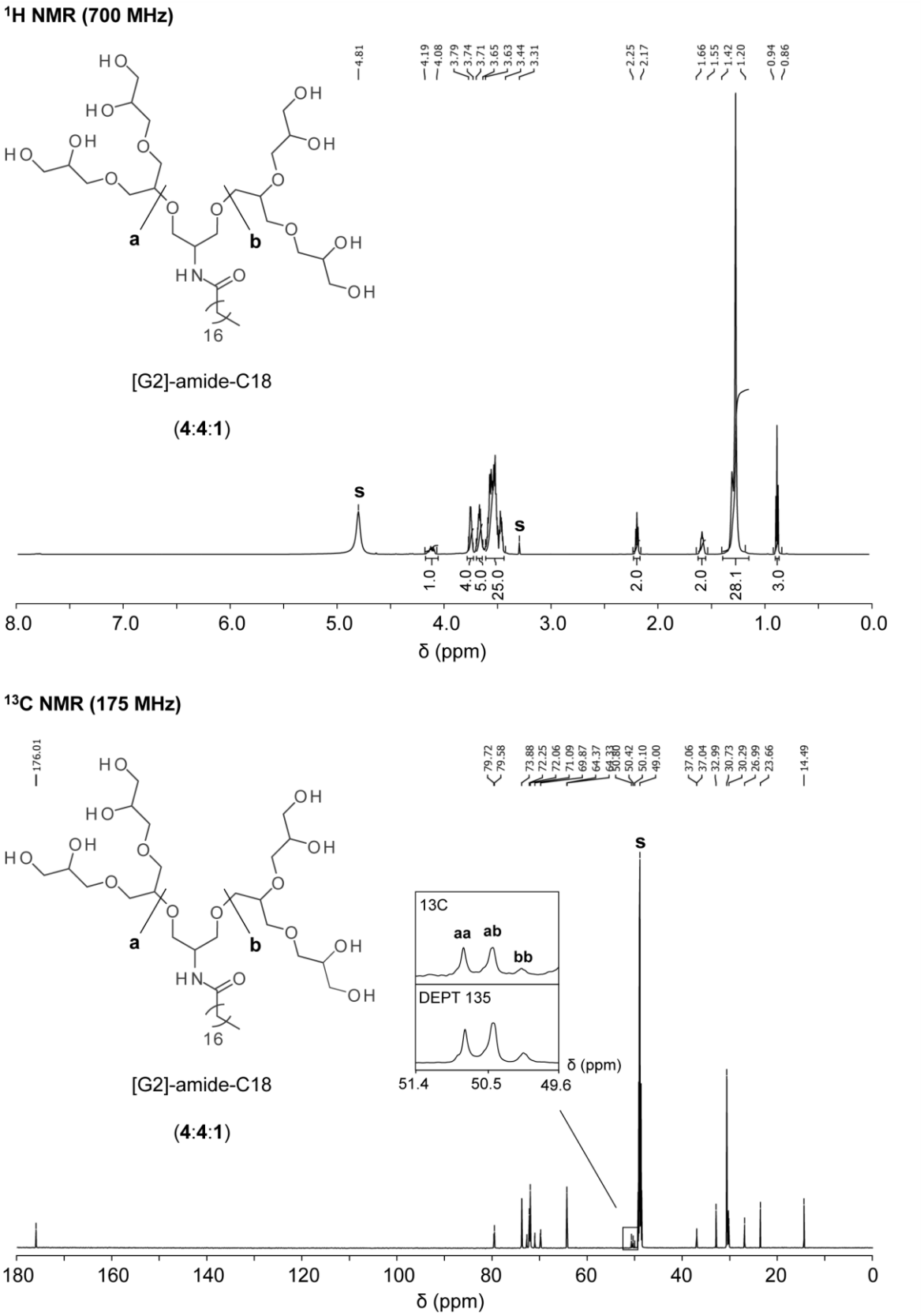

Figure 8.17: NMR Spectra of [G2]-amide-C18 (**aa**:**ab**:**bb**, 4:4:1). The inset within the ^{13}C NMR Spectrum (bottom) shows ^{13}C and DEPT135 signals of the focal points, which are labeled with **aa**, **ab**, and **bb**, respectively. Solvent signals ([D_4] MeOH) are labeled with **s**.

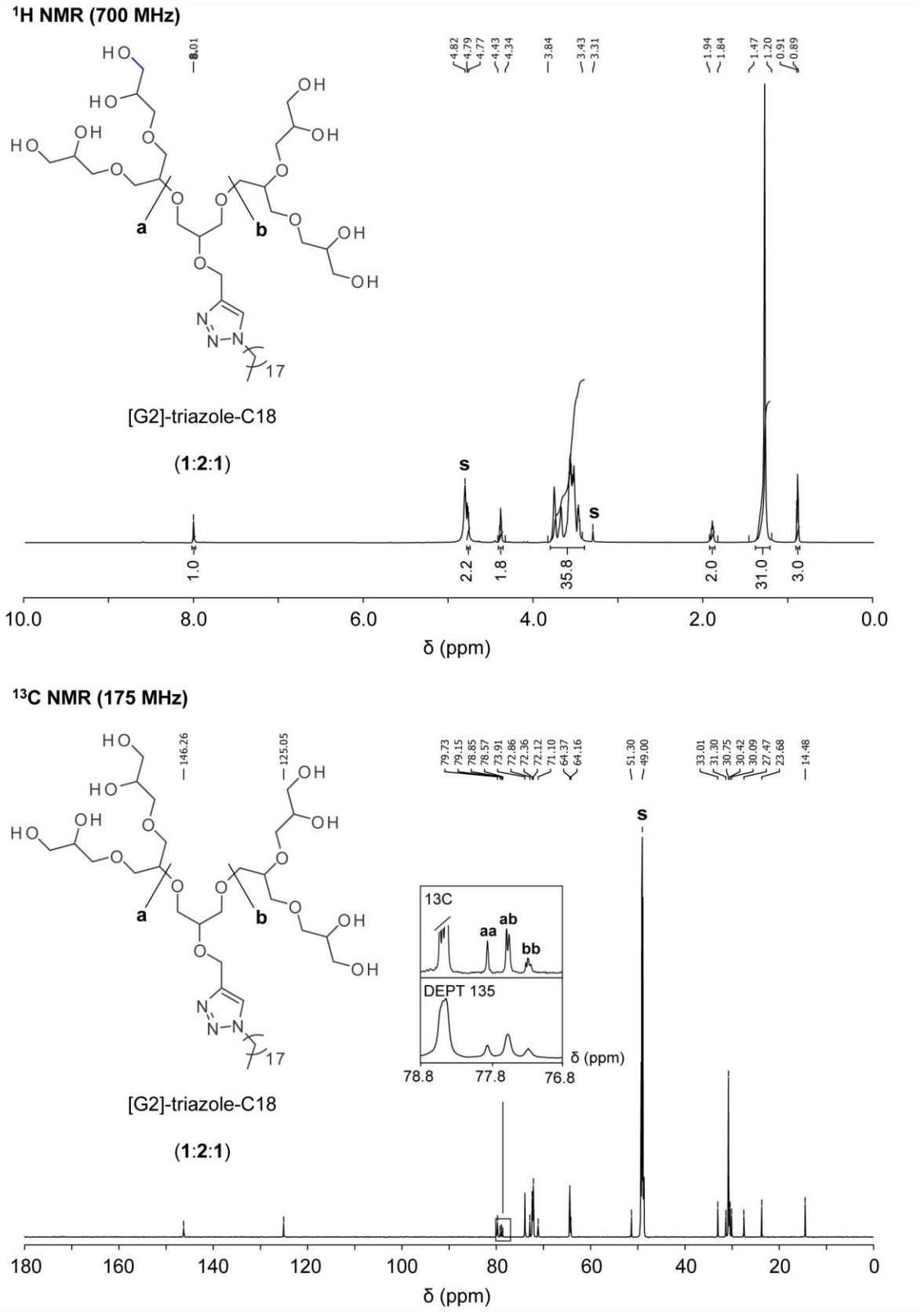

Figur 8.18: NMR Spectra of [G2]-triazole-C18 (**aa**:**ab**:**bb**, 1:2:1). The inset within the ^{13}C NMR Spectrum (bottom) shows ^{13}C and DEPT135 signals of the focal points, which are labeled with **aa**, **ab**, and **bb**, respectively. Solvent signals ([D_4] MeOH) are labeled with **s**.

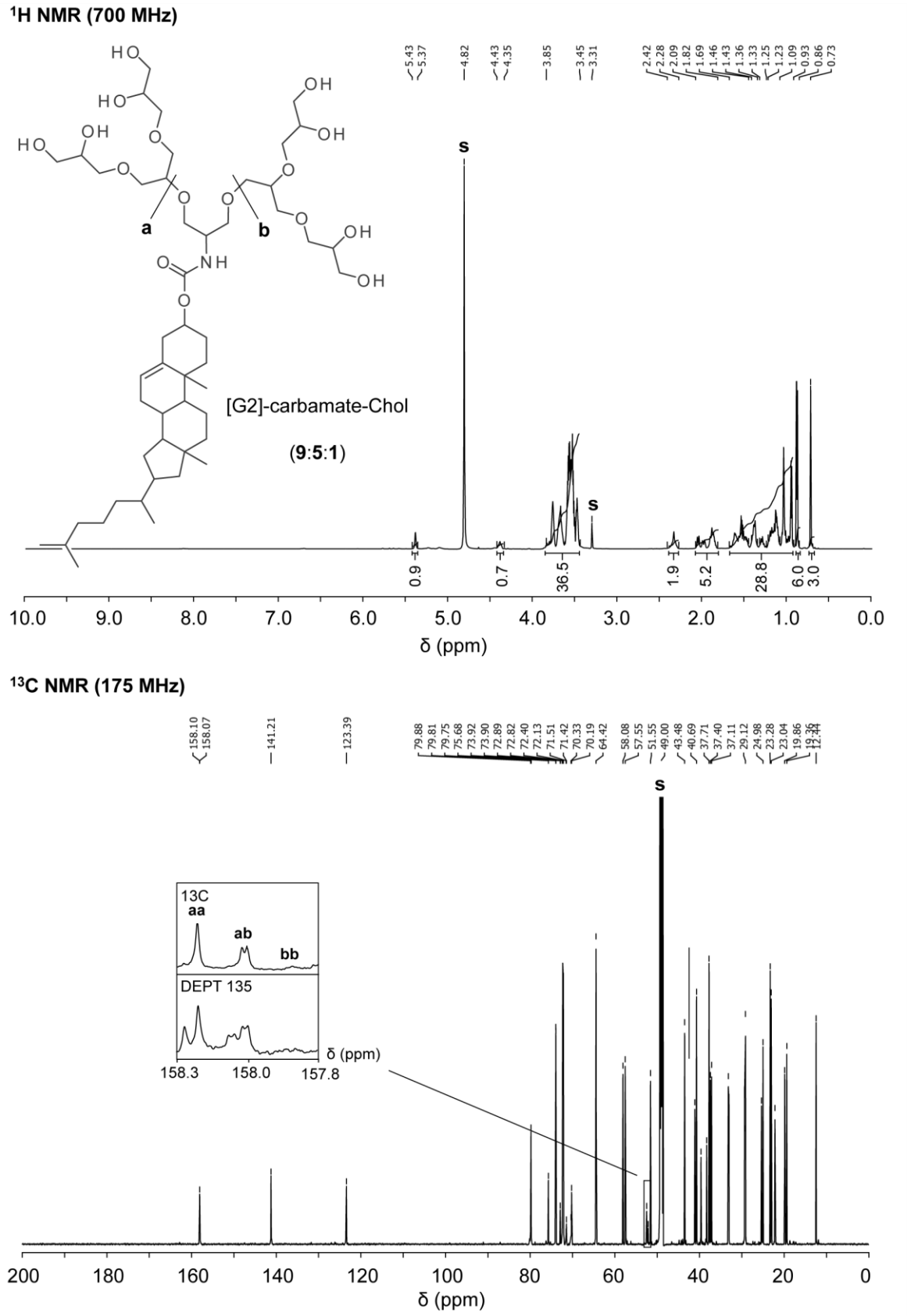

Figure 8.19: NMR Spectra of [G2]-carbamate-Chol (**aa**:**ab**:**bb**, 9:5:1). The inset within the ^{13}C NMR Spectrum (bottom) shows ^{13}C and DEPT135 signals of the focal points, which are labeled with **aa**, **ab**, and **bb**, respectively. Solvent signals ([D_4] MeOH) are labeled with **s**.

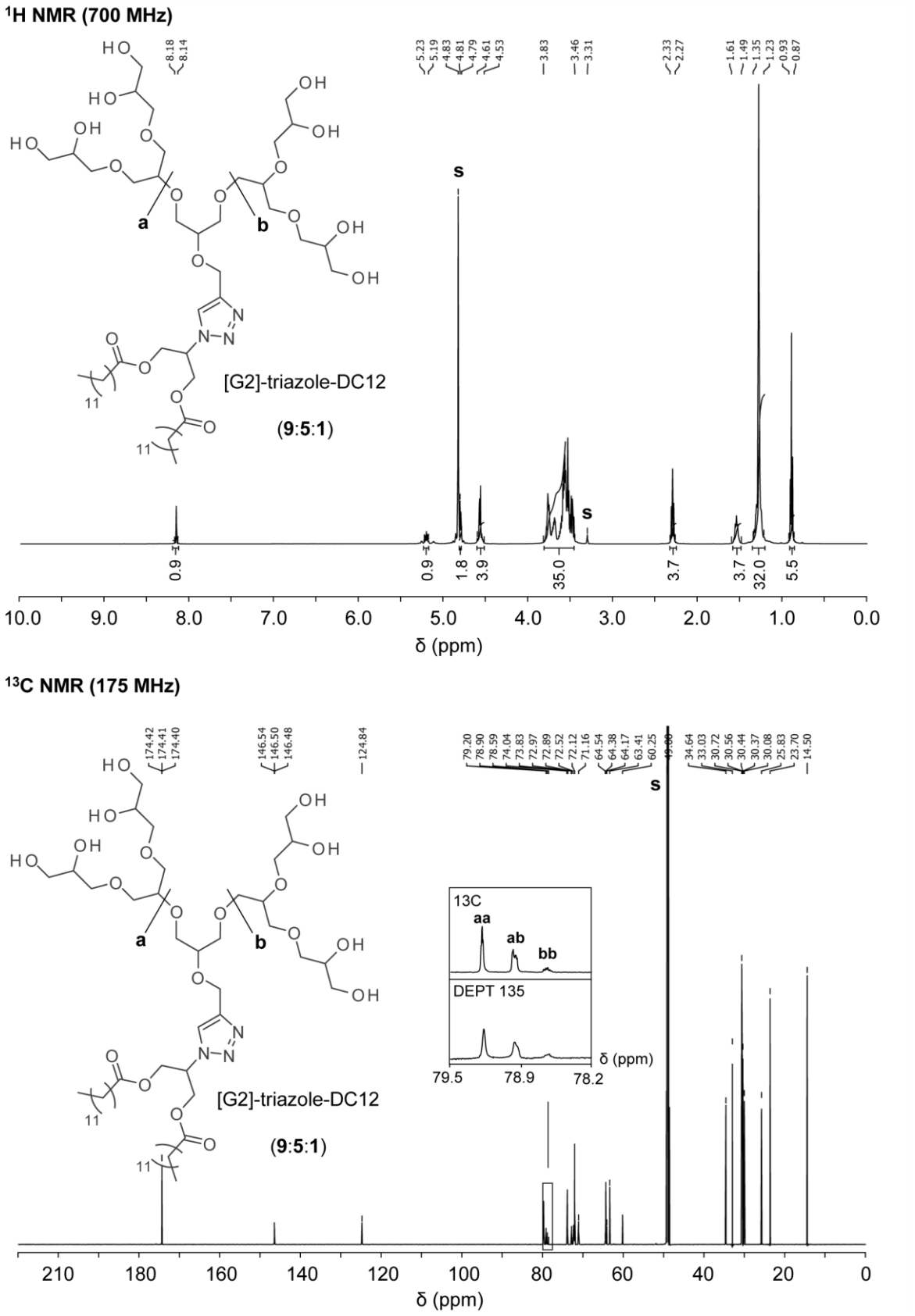

Figure 8.20: NMR Spectra of [G2]-triazole-DC12 (**aa**:**ab**:**bb**, 9:5:1). The inset within the ^{13}C NMR Spectrum (bottom) shows ^{13}C and DEPT135 signals of the focal points, which are labeled with **aa**, **ab**, and **bb**, respectively. Solvent signals ([D_4] MeOH) are labeled with **s**.

8.3 Chromatograms

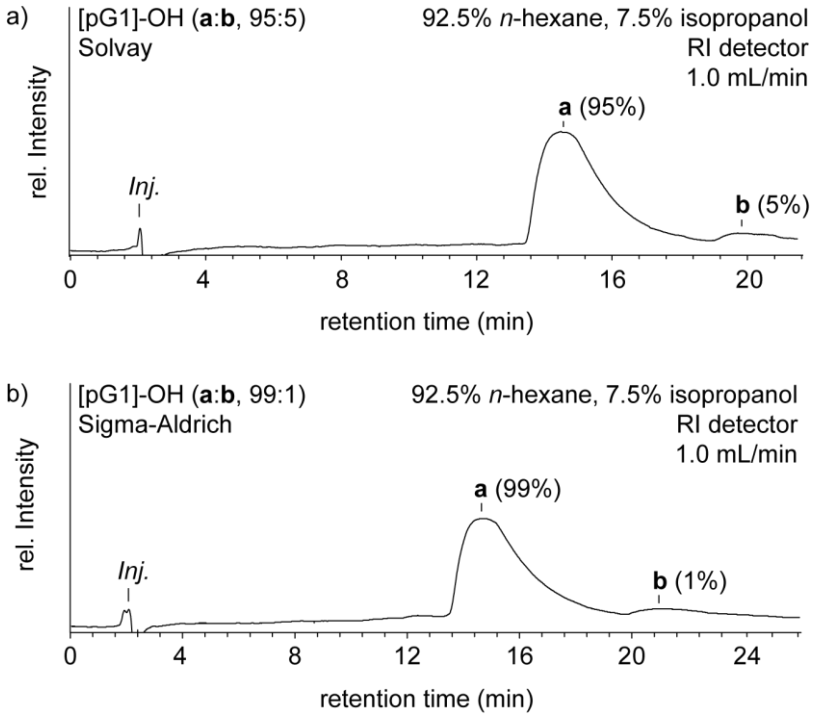

Figure 8.21: NP HPLC chromatograms of [pG1]-OH regioisomer mixtures, which were obtained from different technical oligoglycerol sources, *e.g.*, a) Solvay (product number: TM4516) or b) Sigma-Aldrich (product number: 17782 Aldrich). Information about the mobile phase composition (*n*-hexane, isopropanol), detection system (refractive index – RI detector), and flow rate (mL/min) are shown. The injection peak is labeled with *Inj.*

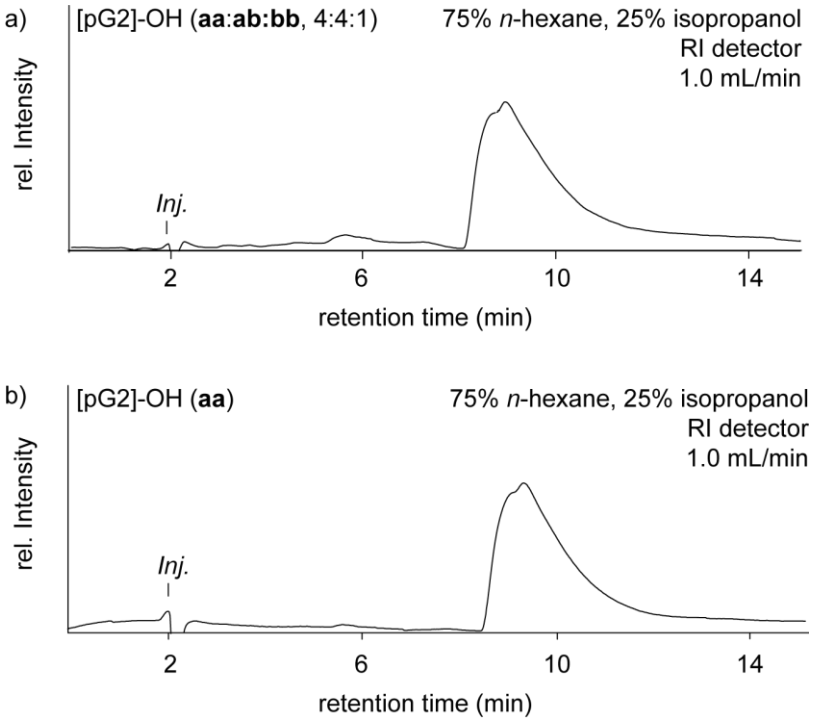

Figure 8.22: NP HPLC chromatograms taken from a) a [pG2]-OH regioisomer mixture (**aa**:**ab**:**bb**) and b) an individually synthesized regioisomer of [pG2]-OH (**aa**). Information about the mobile phase composition (*n*-hexane, isopropanol), detection system, and flow rate (mL/min) are shown. The injection peak is labeled with *Inj.*

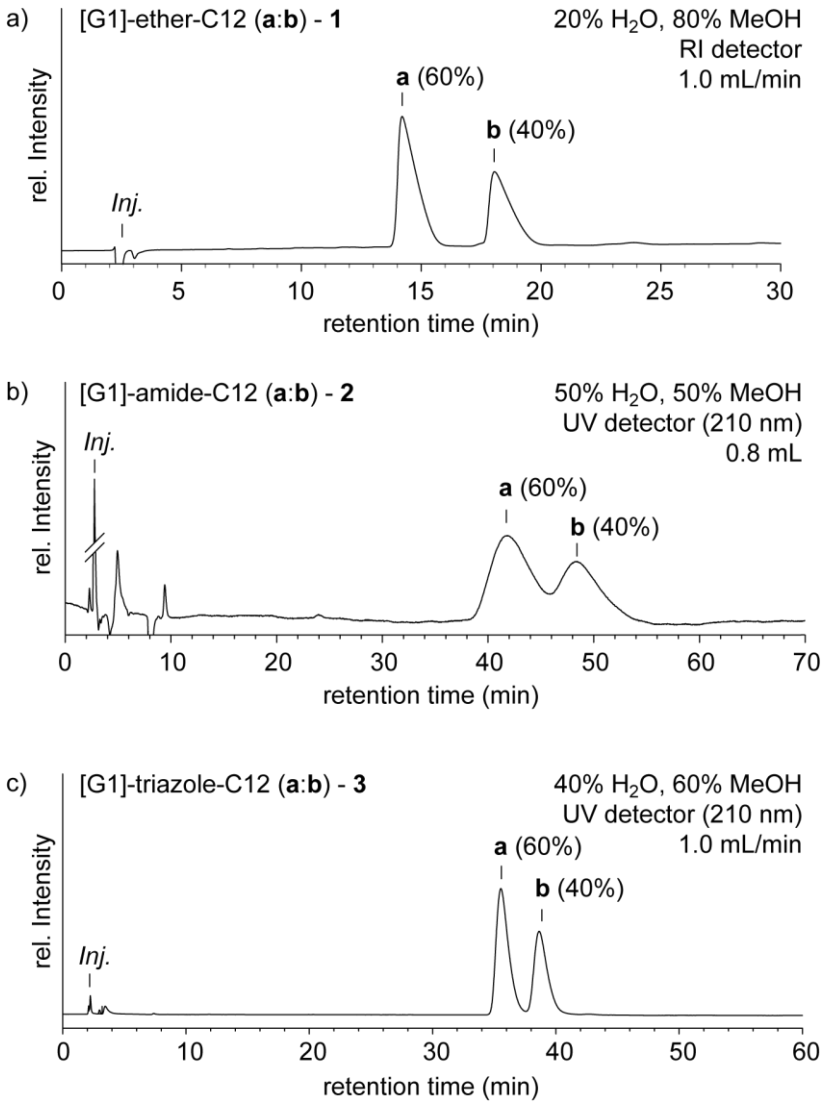

Figure 8.23: RP HPLC chromatograms obtained from different [G1] OGD mixtures: a) **1**, b) **2**, and c) **3**. The regioisomer proportions are similar in all [G1] OGD mixtures (**a**:**b**, 6:4). Information about the mobile phase composition (H_2O, MeOH), detector system, *e.g.*, UV detector or RI detector, and flow rate (mL/min) are given. The injection peak is labeled with *Inj.*

8.4 Dynamic Light Scattering Data

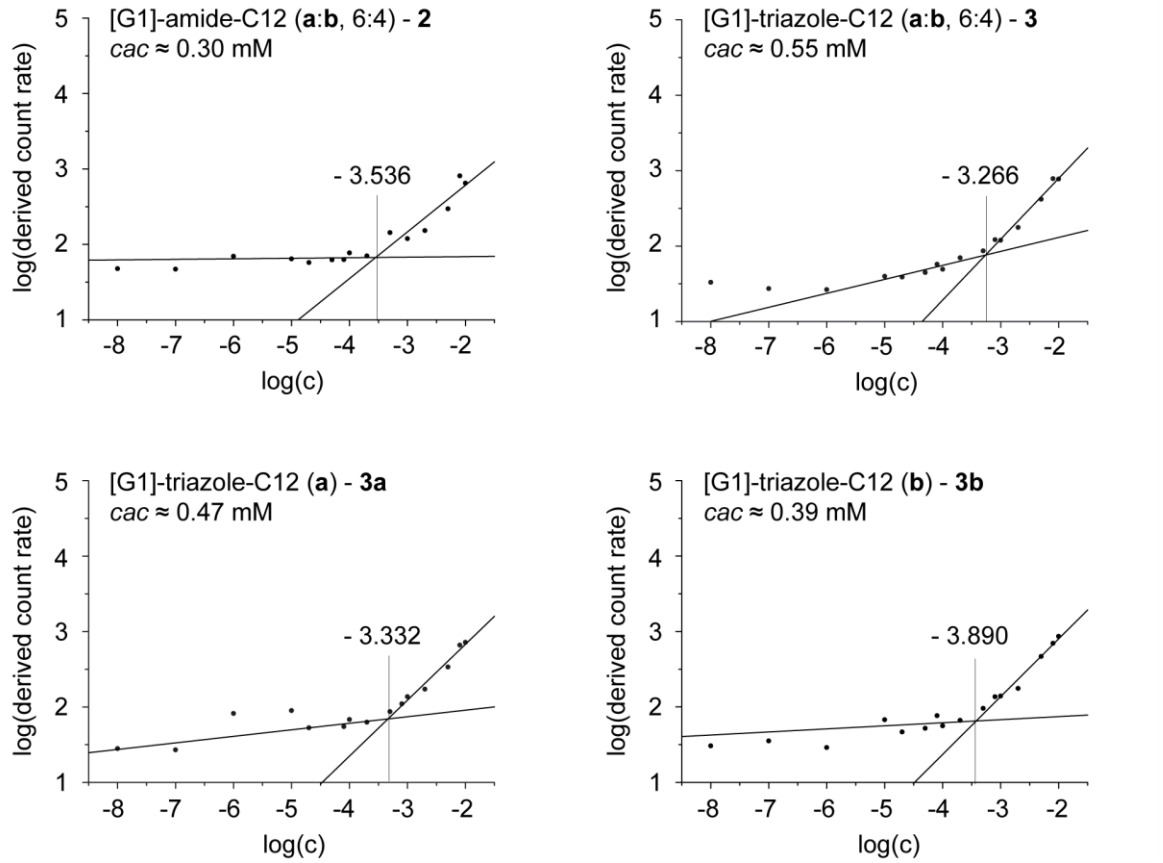

Figure 8.24: Double logarithmic plots of the derived count rate average against the OGD concentration obtained from different [G1] OGD mixtures and [G1] OGDs. The intersection between the linear fits (x-value) was taken as the *cac*.

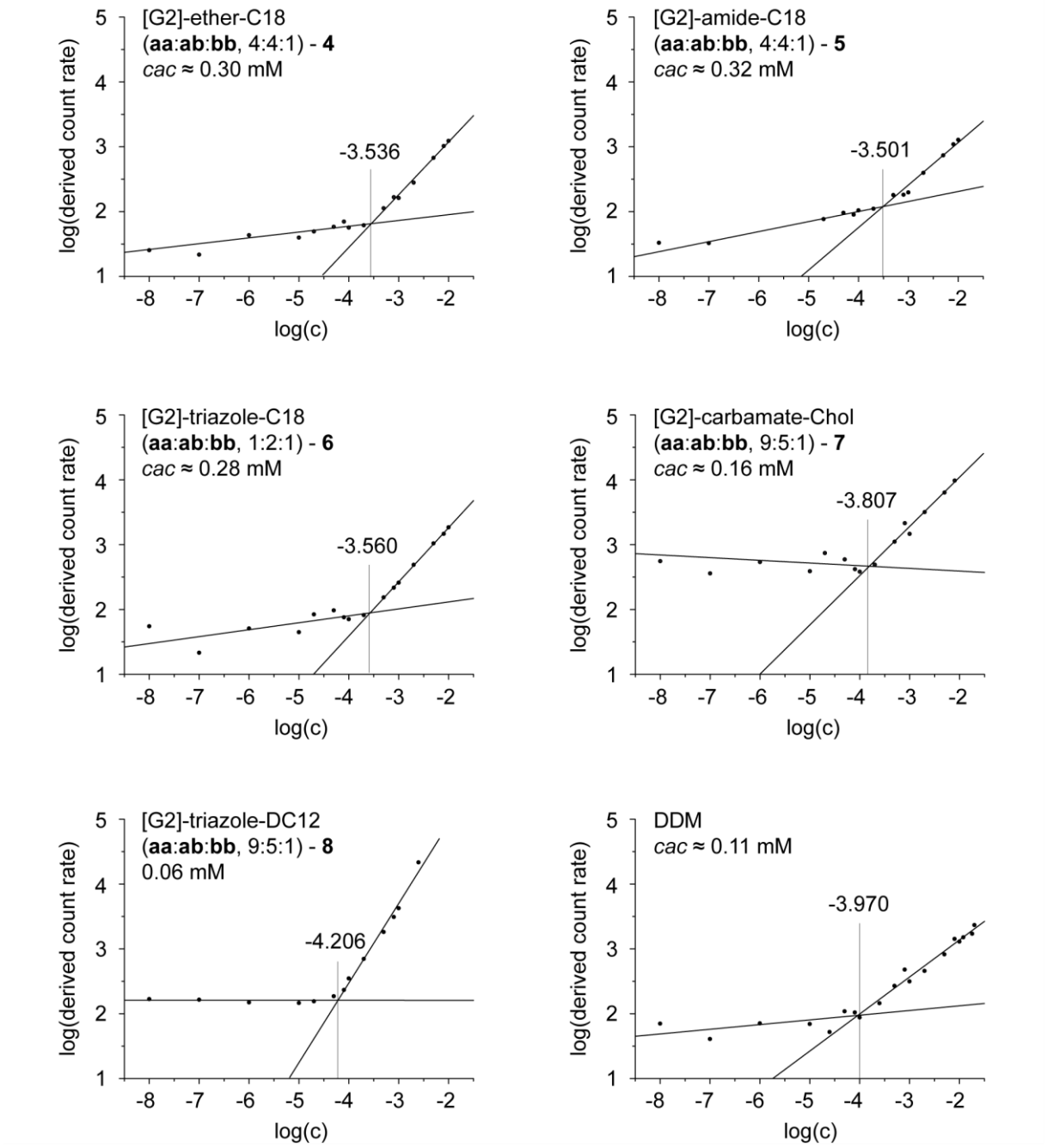

Figure 8.25: Double logarithmic plots of the derived count rate average against the OGD concentration obtained from different [G2] OGD mixtures and DDM. The intersection between the linear fits (x-value) was taken as the *cac*.

8.5 Average Charge States and Ligand Masses

Table 8.1: Charge states (*z*) obtained from mixtures of ubiquitin, myoglobin, and BLG during nESI-MS analysis (positive mode) with the [G1] OGD mixture **1**. Spectral intensities of the ligand-free forms (I_{apo}) were extracted from the mass spectra and normalized to the most abundant value.

ubiquitin		myoglobin		BLG	
z	I_{apo}	***z***	I_{apo}	***z***	I_{apo}
6	0.40	9	0.22	10	0.10
5	1.00	8	1.00	9	0.76
4	0.19	7	0.43	8	0.96
3	0.09	6	0.07	7	0.65
-	-	-	-	6	0.33

Table 8.2: Charge states (*z*) obtained from OmpF upon detergent exchange and nESI-MS analysis (positive mode) with [G1] OGD mixture **1** and [G2] OGD mixture **4**. Spectral intensities of the ligand-free forms (I_{apo}) were extracted from the mass spectra and normalized to the most abundant value.

[G1]-ether-C12 (**a**:**b**, 6:4)		[G2]-ether-C18 (**aa**:**ab**:**bb**, 4:4:1)	
z	I_{apo}	***z***	I_{apo}
22	0.09	22	0.06
21	0.42	21	0.36
20	0.72	20	0.96
19	1.00	19	1.00
18	0.69	18	0.85
17	0.50	17	0.47
16	0.25	16	0.23
15	0.12	15	0.06

Table 8.3: Charge states (*z*) obtained from OmpF upon detergent exchange and nESI-MS analysis (positive mode) with [G1] OGD mixture **3** and OG. Spectral intensities of the ligand-free forms (I_{apo}) were extracted from the mass spectra and normalized to the most abundant value.

[G1]-triazole-C12 (**a**:**b**, 6:4)		OG	
z	I_{apo}	***z***	I_{apo}
17	0.12	22	0.13
16	0.50	21	0.70
15	1.00	20	1.00
14	0.16	19	0.74
13	0.05	18	0.37
-	-	17	0.21
-	-	16	0.05
-	-	15	0.13

Table 8.4: Charge states (*z*) obtained from AqpZ-GFP upon extraction and nESI-MS analysis (positive mode) with [G1] OGD mixtures **1** and **3**. Spectral intensities of the ligand-free forms (I_{apo}) were extracted from the mass spectra and normalized to the most abundant value.

[G1]-ether-C12 (**a**:**b**, 6:4)		[G1]-triazole-C12 (**a**:**b**, 6:4)	
z	I_{apo}	***z***	I_{apo}
33	0.21	28	0.54
32	0.53	27	0.70
31	0.85	26	0.82
30	1.00	25	0.85
29	0.89	24	1.00
28	0.67	23	0.70
27	0.36	22	0.55
26	0.15	21	0.53

Table 8.5: Charge states (z) obtained from AqpZ-GFP upon extraction and nESI-MS analysis (positive mode) with [G2] OGD mixtures **7** and **8**. Spectral intensities of the ligand-free forms (I_{apo}) were extracted from the mass spectra and normalized to the most abundant value.

[G2]-carbamate-Chol (**aa**:**ab**:**bb**, 9:5:1)		[G2]-triazole-DC12 (**aa**:**ab**:**bb**, 9:5:1)	
z	I_{apo}	***z***	I_{apo}
33	0.63	30	0.57
31	0.36	29	0.68
30	1.00	28	1.00
29	0.79	27	0.95
28	0.59	26	0.72
27	0.38	25	0.51
-	-	24	0.33

Table 8.6: Charge states (*z*) obtained from AmtB-MBP upon extraction and nESI-MS analysis (positive mode) with [G1] OGD mixtures **1** and **3**. Spectral intensities of the ligand-free forms (I_{apo}) were extracted from the mass spectra and normalized to the most abundant value.

[G1]-ether-C12 (**a**:**b**, 6:4)		[G1]-triazole-C12 (**a**:**b**, 6:4)			
z	I_{apo}	***z***	I_{apo}	***z***	I_{apo}
36	0.12	43	0.13	33	0.30
35	0.23	42	0.33	32	0.24
34	0.38	41	0.54	31	0.41
33	0.72	40	0.73	30	0.55
32	1.00	39	0.94	29	0.73
31	0.82	38	1.00	28	0.74
30	0.52	37	0.97	27	0.58
29	0.26	36	0.81	26	0.26
28	0.09	35	0.62	25	0.04
-	-	34	0.50		

Table 8.7: Charge states (*z*) obtained from AmtB-MBP upon extraction and nESI-MS analysis (positive mode) with [G2] OGDs **7** and **8**. Spectral intensities of the ligand-free forms (I_{apo}) were extracted from the mass spectra and normalized to the most abundant value.

[G2]-carbamate-Chol (**aa**:**ab**:**bb**, 9:5:1)		[G2]-triazole-DC12 (**aa**:**ab**:**bb**, 9:5:1)			
z	I_{apo}	***z***	I_{apo}	***z***	I_{apo}
52	0.32	43	0.20	33	0.36
51	0.57	42	0.26	32	0.64
50	0.83	41	0.33	31	0.83
49	0.87	40	0.42	30	1.00
48	0.93	39	0.43	29	0.80
47	1.00	38	0.42	28	0.34
46	0.58	37	0.36	-	-
45	0.68	36	0.26	-	-
44	0.31	35	0.23	-	-
--	-	34	0.30	-	-

Table 8.8: Charge states (*z*) obtained from MATE-GFP upon extraction and nESI-MS analysis (positive mode) with [G1] OGD mixture **1** and [G2] OGD mixture **7**. Spectral intensities of the ligand-free forms (I_{apo}) were extracted from the mass spectra and normalized to the most abundant value.

[G1]-ether-C12 (**a**:**b**, 6:4)		[G2]-carbamate-Chol (**aa**:**ab**:**bb**, 9:5:1)	
z	I_{apo}	***z***	I_{apo}
19	0.07	19	0.20
18	0.26	18	0.39
17	0.60	17	0.72
16	1.00	16	1.00
15	0.61	15	0.83
14	0.12	14	0.66
-	-	13	0.48
-	-	12	0.42
-	-	11	0.19

Table 8.9: Charge states (*z*) obtained from NTSR1 upon detergent exchange and nESI-MS analysis (positive mode) with [G1] OGD mixture **1** and [G2] OGD mixture **7**. Spectral intensities of the ligand-free forms (I_{apo}) were extracted from the mass spectra and normalized to the most abundant value.

[G1]-ether-C12 (**a**:**b**, 6:4)		[G2]-carbamate-Chol (**aa**:**ab**:**bb**, 9:5:1)	
z	I_{apo}	***z***	I_{apo}
12	0.09	12	0.19
11	0.44	11	0.34
10	1.00	10	0.77
9	0.52	9	1.00
8	0.12	8	0.15

Table 8.10: Ligand masses that were extracted from mass spectra of AqpZ-GFP upon extraction and nESI-MS analysis (positive mode) with [G2] OGD mixtures **7** and **8**. The average masses (± SD) are summarized in Table 6.2.

[G2]-carbamate-Chol (**aa**:**ab**:**bb**, 9:5:1)		[G2]-triazole-DC12 (**aa**:**ab**:**bb**, 9:5:1)	
DEPC – $\Delta(m/z)\cdot z$	CDL – $\Delta(m/z)\cdot z$	CDL – $\Delta(m/z)\cdot z$	-
941.16	1454.52	1307.61	-
860.87	1362.47	1319.92	-
896.83	1368.96	1430.46	-
891.30	1498.85	1447.68	-
884.70	1392.60	1351.75	-
930.90	1426.50	-	-

Table 8.11: Ligand masses that were extracted from mass spectra of AmtB-MBP upon extraction and nESI-MS analysis (positive mode) with [G2] OGD mixtures **7** and **8**. The average masses (± SD) are summarized in Table 6.2.

[G2]-carbamate-Chol (**aa**:**ab**:**bb**, 9:5:1)		[G2]-triazole-DC12 (**aa**:**ab**:**bb**, 9:5:1)	
PI – $\Delta(m/z)\cdot z$	CDL – $\Delta(m/z)\cdot z$	CDL – $\Delta(m/z)\cdot z$	-
900.99	1380.21	1401.92	-
1016.61	1407.28	1372.52	-
987.47	1410.17	1393.76	-
988.08	1390.26	1403.68	-
994.08	1413.60	1407.95	-
1007.93	1396.01	1381.20	-

Table 8.12: Ligand masses that were extracted from mass spectra of MATE-GFP upon extraction and nESI-MS analysis (positive mode) with [G1] OGD mixtures **1** and [G2] OGD mixture **7**. The average masses (± SD) are summarized in Table 6.2.

[G1]-ether-C12 (**a**:**b**, 6:4)		[G2]-carbamate-Chol (**aa**:**ab**:**bb**, 9:5:1)	
CDL – $\Delta(m/z)\cdot z$	-	CDL – $\Delta(m/z)\cdot z$	-
1414.08	-	1435.50	-
1403.69	-	1387.00	-
1406.72	-	1400.63	-
1405.46	-	1395.70	-
1402.80	-	1407.20	-
-	-	1414.14	-

8.6 Mass Spectra

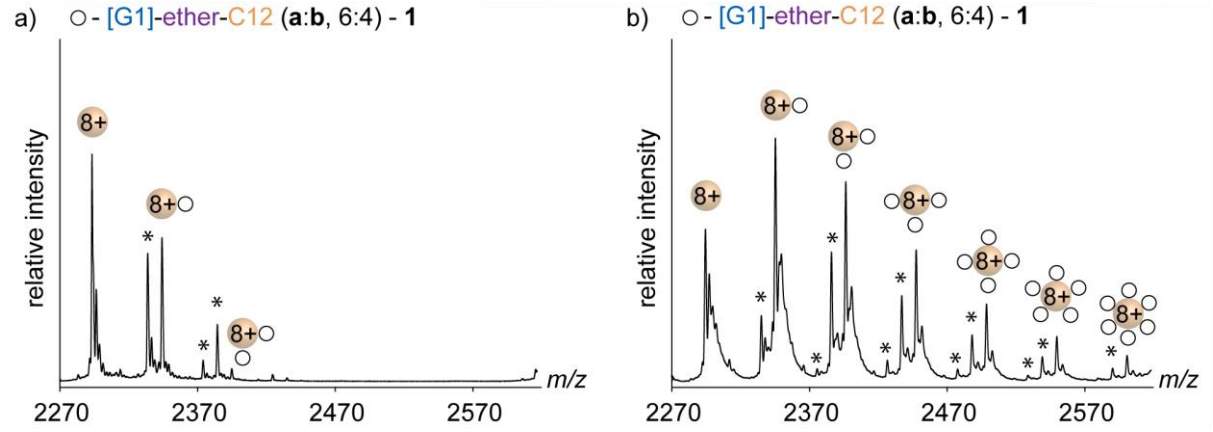

Figure 8.26: Zoom into MS spectrum of BLG at charge state 8+ is shown. The PDCs were obtained from mixtures between BLG and **1**, which were analysed by nESI-MS using different detergent concentrations: a) 50 µM and b) 500 µM. The intensity profile among free BLG and its PDCs obtained from mixture b) can be described by a Poisson distribution, which indicates that non-specific contacts between BLG and OGD **1** during the nESI process contribute significantly to the formation of PDCs. Lactosylated forms of BLG and PDCs are labelled with an asterisk.

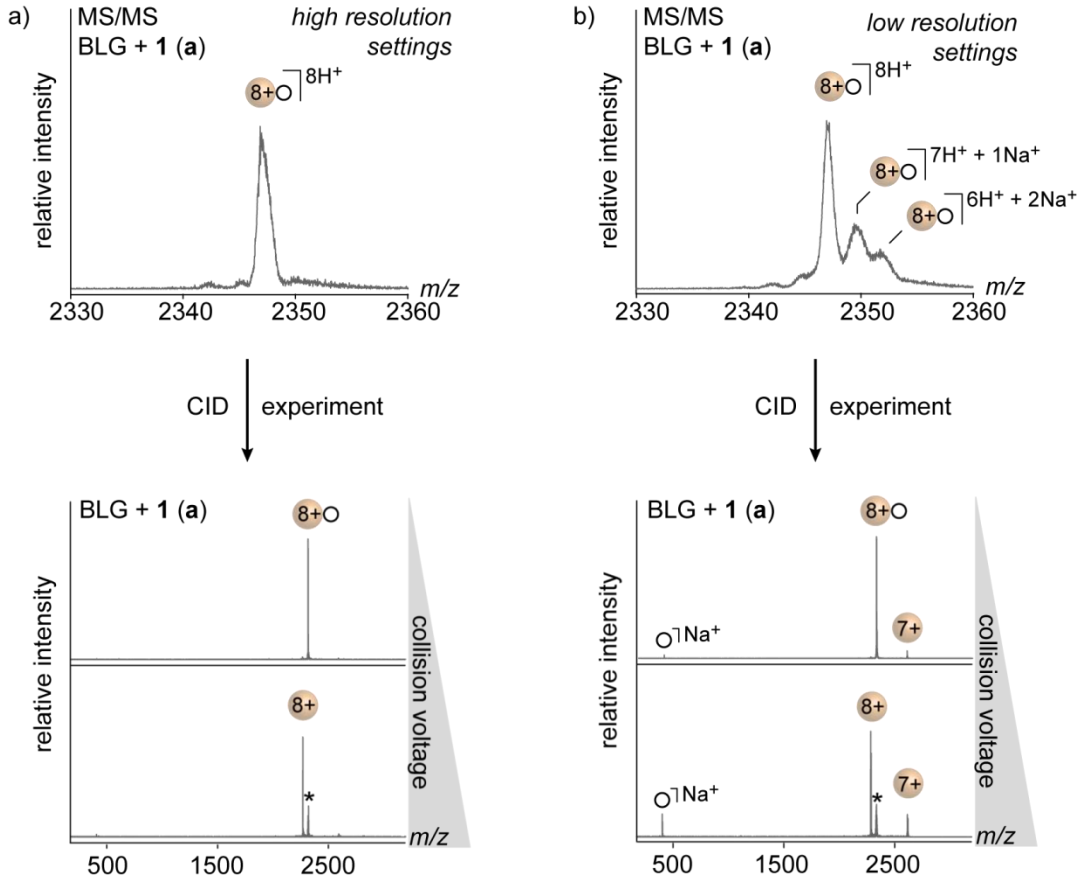

Figure 8.27: MS/MS experiments on PDC ions formed by BLG and [G1] OGD **1** (**a**). a) Zoom into PDC spectrum at charge state (z = 8+) upon m/z selection with a) high- or b) low resolution quadrupole settings (top) and MS/MS spectra before and after complete dissociation of the selected parent ion populations (bottom, collision voltage range: 2 - 30 V). Samples were analysed by nESI-MS from ammonium acetate buffer (10 mM) and sodium chloride (500 µM).

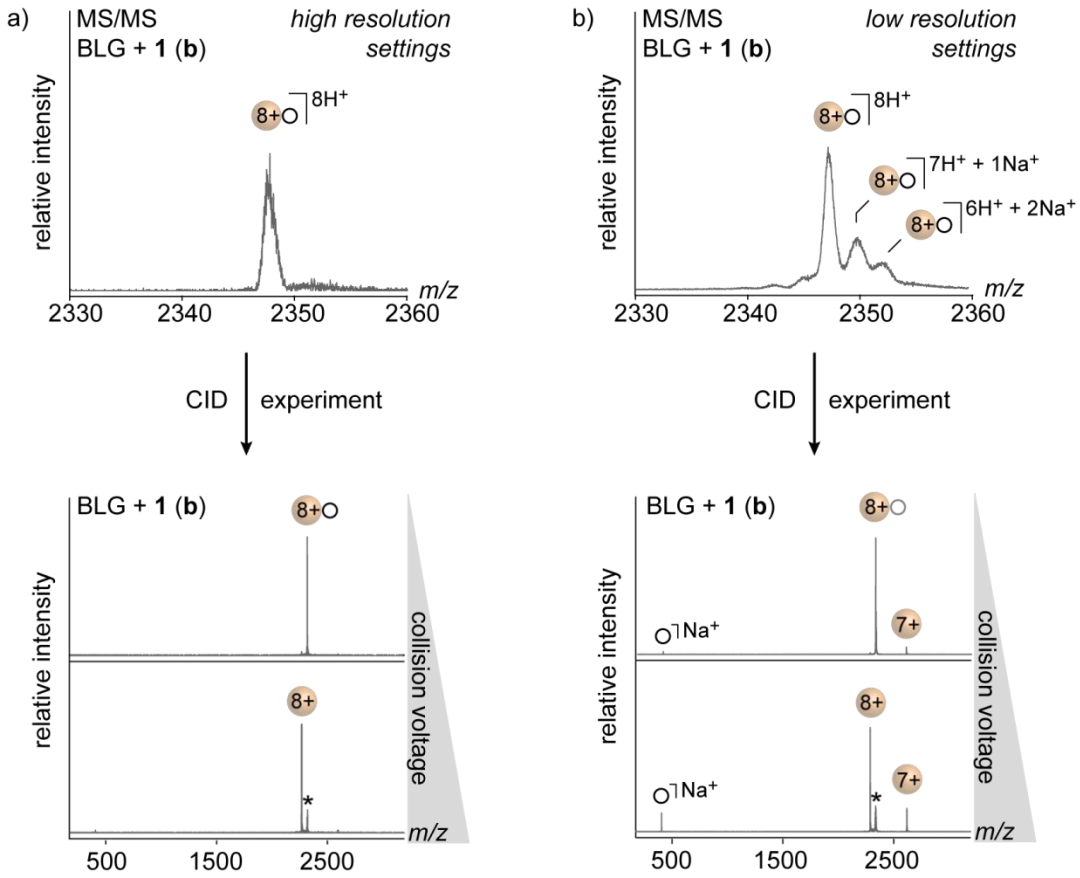

Figure 8.28: MS/MS experiments on PDC ions formed by BLG and [G1] OGD **1** (**b**). a) Zoom into PDC spectrum at charge state (z = 8+) upon m/z selection with a) high- or b) low resolution quadrupole settings (top) and MS/MS spectra before and after complete dissociation of the selected parent ion populations (bottom, collision voltage range: 2 - 30 V). Samples were analysed by nESI-MS from ammonium acetate buffer (10 mM) and sodium chloride (500 µM).

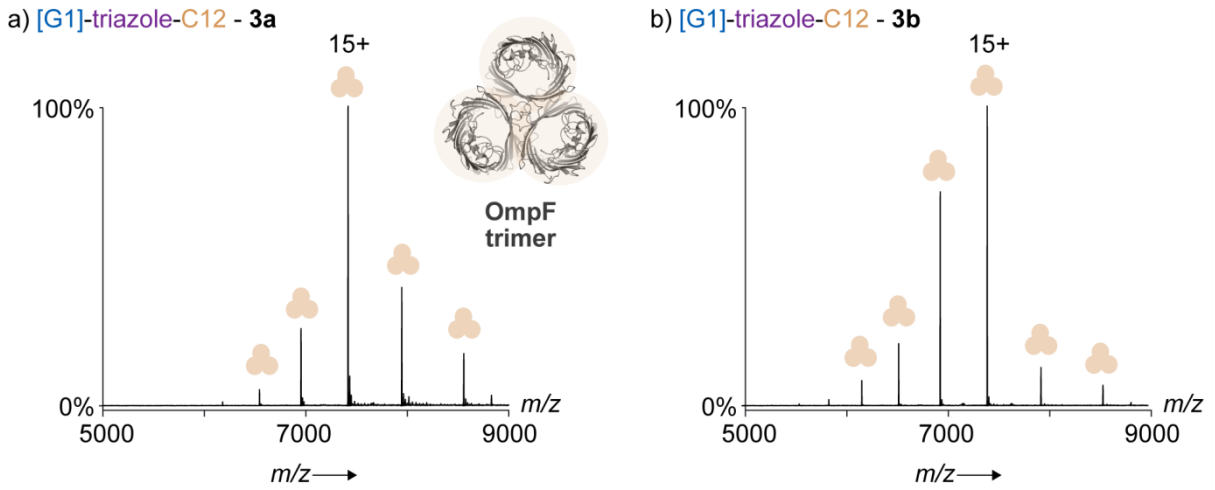

Figure 8.29: nESI-MS analysis of OmpF upon detergent exchange from OG to [G1] OGDs **3a** and **3b**.

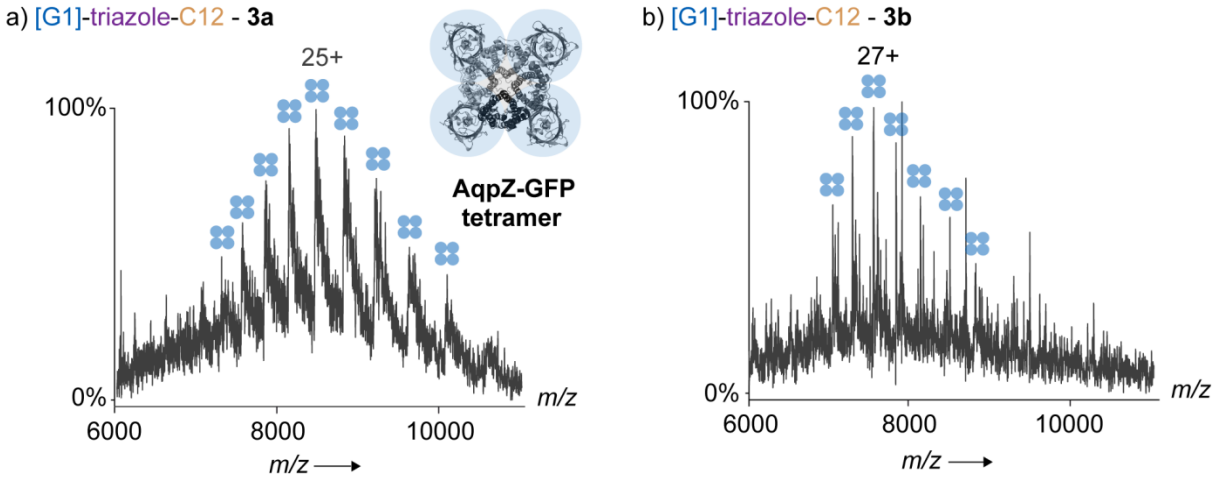

Figure 8.30: nESI-MS analysis of AqpZ-GFP upon extraction and IMAC with [G1] OGDs **3a** and **3b**.

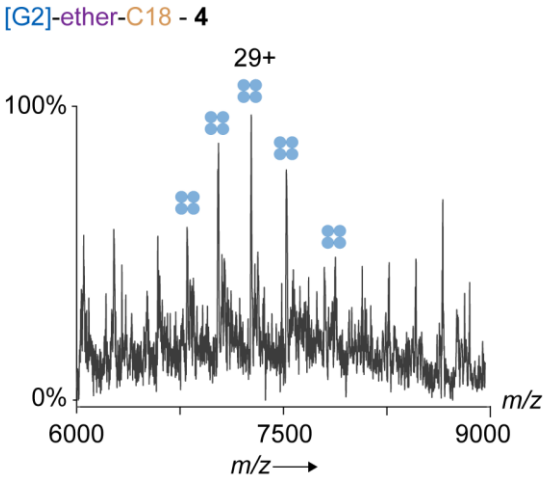

Figure 8.31: nESI-MS analysis of AqpZ-GFP upon extraction and IMAC with [G2] OGD mixture **4**.

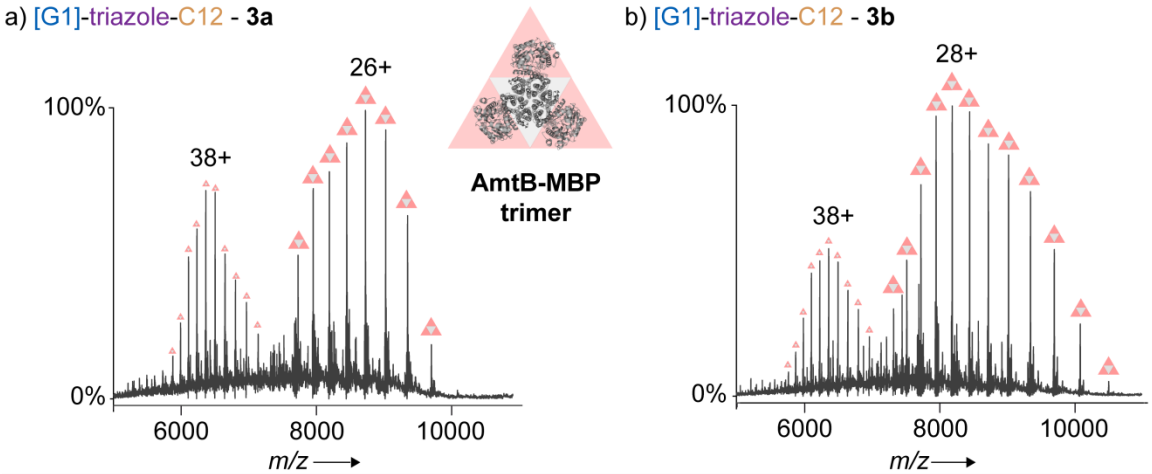

Figure 8.32: nESI-MS analysis of AmtB-MBP upon extraction and IMAC with [G1] OGDs **3a** and **3b**.

9. Curriculum Vitae

Personal Details

Name	M. Sc. Leonhard Hagen Urner
Address	Freie Universität Berlin Institute of Chemistry and Biochemistry Takustraße 3 14195 Berlin Germany
Email	leonhard.urner@fu-berlin.de
Birthday	3rd of June, 1990
Place of Birth	Berlin (Buch), Germany

Education

Since 05/2015	**Doctoral candidate** in the group of Prof. Dr. Kevin Pagel, Freie Universität Berlin, Institute of Chemistry and Biochemistry
04/2013 – 03/2015	**Master in Chemistry**, thesis in the group of Prof. Dr. Rainer Haag, Freie Universität Berlin, Institute of Chemistry and Biochemistry, grade: 1.0 (very good)
04/2010 – 04/2013	**Bachelor in Chemistry**, thesis in the group of Prof. Dr. Rainer Haag, Freie Universität Berlin, Institute of Chemistry and Biochemistry, grade: 1.0 (very good)
2009	**Abitur**, Heinrich-Schliemann-Gymnasium Berlin, grade: 2.0 (good)

Honors and Awards

10/2017 – 10/2018	Fellowship of the Nanoscale Focus Area of the Freie Universität Berlin
10/2015 – 10/2017	Fellowship of the Fonds der Chemischen Industrie (FCI)
04/2015 – 04/2016	Research Grant of the Nanoscale Focus Area of the Freie Universität Berlin (30.000 €)
2015	Teaching Award of the Freie Universität Berlin (10.000 €) for the lecture: “Translation of Project- and Research-Ideas into Start-up Companies”
2014	Poster award of the Berliner Chemie Symposium for the best scientific conference poster
2009	Book award of the Deutsche Physikalische Gesellschaft (DPG) for excellent achievements in the subject physics

Honorary Office

02/2016 – 02/2018	Vice president of the Reichsbanner Schwarz-Rot-Gold (promoting democracy for general public of Germany)
12/2013 – 02/2018	Board member of the Reichsbanner Schwarz-Rot-Gold
12/2016 – 12/2017	President of the JungChemikerForum of the German Chemical Society (GDCh) in Berlin (supporting young chemists with trainings in career planning, soft skills, team management, and by organizing conferences)
12/2014 – 12/2017	Board member of the JungChemikerForum of the German Chemical Society (GDCh) in Berlin

9.1 List of Publications

Urner, L. H.; Maier, Y. B.; Haag, R.; Pagel, K.; Exploring the Potential of Dendritic Oligoglycerol Detergents for Protein Mass Spectrometry, *JASMS* **2018**, *accepted*.

Schröder, H. V.; Mekic, A.; Hupatz, H.; Sobottka, S.; Witte, F.; Urner, L. H.; Gaedke; M.; Pagel, K.; Sarkar, B.; Paulus, B.; Schalley, C. A.; A molecular friction clutch, *Nanoscale* **2018**, *submitted*.

Huth, K.; Heek, T.; Achazi, K.; Kühne, C.; Urner, L. H.; Pagel, K.; Dernedde, J.; Haag, R.; Noncharged and Charged Monodendronised Perylene Bisimides as Highly Fluorescent Labels and their Bioconjugates, *Chem. Eur. J.* **2017**, DOI: 10.1002/chem.201605847.

Thota, B. N. S.; Urner, L. H.; Haag, R.; Supramolecular Architectures of Dendritic Amphiphiles in Water, *Chem. Rev.* **2016**, DOI: 10.1021/acs.chemrev.5b00417.

Urner, L. H.; Thota, B. N. S.; Nachtigall, O.; Warnke, S.; von Helden, G.; Haag, R.; Pagel, K.; Online monitoring the isomerization of an azobenzene-based dendritic bolaamphiphile using ion mobility-mass spectrometry, *Chem. Commun.* **2015**, DOI: 10.1039/c5cc01488c.

Nachtigall, O.; Kördel, C.; Urner, L. H., Haag, R.; Photoresponsive Switches at Surfaces Based on Supramolecular Functionalization with Azobenzene Oligoglycerol Conjugates, *Angew. Chem. Int. Ed.* **2014**, DOI: 10.1002/anie.201403331.